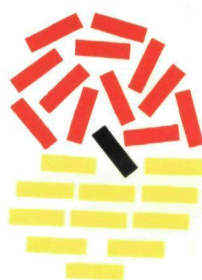


RENAL CLEARANCE OF ANIONIC DRUGS

mechanisms and interactions of
organic anion transport in dog kidney

FRANS G.M. RUSSEL



RENAL CLEARANCE OF ANIONIC DRUGS

**mechanisms and interactions of
organic anion transport in dog kidney**

RENAL CLEARANCE OF ANIONIC DRUGS

mechanisms and interactions of
organic anion transport in dog kidney

een wetenschappelijke proeve op het gebied van
de geneeskunde en tandheelkunde

PROEFSCHRIFT

ter verkrijging van de graad van doctor
aan de Katholieke Universiteit te Nijmegen,
volgens besluit van het college van decanen
in het openbaar te verdedigen
op vrijdag 15 januari 1988
des namiddags te 1.30 uur precies

door

François Gérard Marie Russel

geboren op 2 juli 1957
te Tegelen

Druk: SSN, Nijmegen

Promotor: Prof. Dr. C.A.M. van Ginneken

The investigations described in this thesis were carried out in the Department of Pharmacology (Head: Prof. Dr. C.A.M. van Ginneken), University of Nijmegen, Nijmegen, The Netherlands, and were supported by the Dutch Foundation for Medical Research MEDIGON.

To my parents,
who always encouraged me,
and to Eeke,
for her continuous loving support

Paranimfen: Drs. Arjen F.J. Geerts
Dr. Maikel Raghoebar

CIP-DATA KONINKLIJKE BIBLIOTHEEK, DEN HAAG

Russel, François Gérard Marie

Renal clearance of anionic drugs: mechanisms and
interactions of organic anion transport in dog kidney /
François Gérard Marie Russel. - [S.l. : s.n.]

(Nijmegen : SSN)

Thesis Nijmegen. - With ref. - With summary in Dutch.

ISBN 90-9001953-7

SISO 593 UDC 591.14:599.742(043.3)

Subject headings: organic anions / drugs / renal clearance.

Cover design: Eeke A. Faber

Frans G.M. Russel

Financial support by the Dr. Saal van Zwanenbergstichting for the publication of this thesis is gratefully acknowledged.

CONTENTS

Preface	9
Abbreviations	10
PART I INTRODUCTION	
1 Renal Handling of Organic Anions	15
2 Quantitative Urine Collection in Renal Clearance Studies in the Dog	45
PART II PHYSIOLOGICALLY BASED KIDNEY MODEL	
3 Renal Clearance of Phenolsulfonphthalein and the Interaction with Probenecid and Salicyluric Acid	65
4 Renal Clearance of Salicyluric Acid and the Interaction with Phenolsulfonphthalein	91
5 Renal Clearance of Iodopyracet and the Interaction with Probenecid	113
PART III SUBSTITUTED HIPPURATES	
6 Renal Clearance of Substituted Hippurates. I. Benzoylglycine (Hippurate) and Methyl-Substituted Benzoylglycines	135
7 Renal Clearance of Substituted Hippurates. II. 4-Amino-benzoylglycine and Hydroxy-Substituted Benzoylglycines	157

8	Renal Clearance of Substituted Hippurates. III. Methoxy-Substituted Benzoylglycines	173
---	---	-----

PART IV ISOLATED MEMBRANE VESICLES

9	Na^+ and H^+ Gradient-Dependent Transport of p-Aminohippurate in Membrane Vesicles from Dog Kidney Cortex	189
10	Effect of Substituted Benzoates on p-Aminohippurate Transport in Dog Renal Membrane Vesicles	213
11	Effect of Substituted Benzoylglycines (Hippurates) and Phenylacetylglycines on p-Aminohippurate Transport in Dog Renal Membrane Vesicles	231
	Summary and Conclusions	249
	Samenvatting en Conclusies (Summary and Conclusions in Dutch)	257
	Dankwoord (Acknowledgements)	265
	Curriculum Vitae	268

PREFACE

This thesis deals with a fundamental study on the mechanisms and interactions of organic anion transport in the dog kidney. The clinical importance of the renal organic anion transport system has been recognized for many years. A large number of drugs, many of which are used frequently in daily practice, are actively removed from the body by this secretory system. Accordingly, knowledge of the fundamental processes underlying renal anionic drug secretion is of value in drug development and essential for a rational pharmacotherapy.

The thesis is divided into four parts. Part I contains a general introduction into the state of the art, and a description of the clearance technique which was used throughout the *in vivo* investigations. Part II presents a physiologically based modeling approach to the renal clearance of anionic drugs. Special attention is paid to drug interactions at the level of tubular secretion. Part III deals with the specificity of organic anion secretion *in vivo*. The renal clearance of a series of monosubstituted hippurates was studied, and analyzed with the physiologically based kidney model described in Part II. Part IV examines the molecular mechanisms and specificity of p-aminohippurate transport in renal plasma membrane vesicles isolated from dog kidney cortex.

This study has a fundamental character, but I hope it will contribute to a better insight into the mechanisms by which anionic drugs are cleared by the kidney, especially in those situations where two or more drugs are administered concurrently, and that this may eventually lead to a more rational management of pharmacotherapy.

Accomplishing this study would not have been possible without the dedicated support of my family, friends and colleagues, whom I all gratefully acknowledge at the end of the thesis. In writing this thesis, I have benefited greatly from one of the old and profound 'Principles of Chinese Writing':

"Were I to await perfection, my book
would never be finished"

Tai T'ung (13th century)

Frans Russel

ABBREVIATIONS

AUC	Area under the plasma concentration-time curve ($\mu\text{g}\cdot\text{min}/\text{ml}$)
AUMC	Area under the first moment of the plasma concentration-time curve ($\mu\text{g}\cdot\text{min}^2/\text{ml}$)
AUR _R	Area under the renal excretion rate-time curve (mg)
AUMR _R	Area under the first moment of the renal excretion rate-time curve (mg.min)
BBMV	Brush border membrane vesicles
BLMV	Basolateral membrane vesicles
C _i	Total drug concentration in compartment i ($\mu\text{g}/\text{ml}$)
Cu _i	Unbound drug concentration in compartment i ($\mu\text{g}/\text{ml}$)
C _I	Plasma concentration of inhibitor ($\mu\text{g}/\text{ml}$)
CL	Total plasma drug clearance (ml/min)
CL _{int}	Intrinsic (secretion) clearance of drug (ml/min)
CLu _{int}	Intrinsic (secretion) clearance of unbound drug (ml/min)
CL _{NR}	Nonrenal plasma clearance of drug (ml/min)
CL _R	Renal plasma clearance of drug (ml/min)
D	Dose (mg)
D _{ur}	Fraction of the dose excreted unchanged into the urine in infinite time (%)
DISSPLA	Display Integrated Software System and Plotting Language, a computer program that was used for fitting the spline functions and for drawing the figures presented in this thesis
EGTA	Ethylene glycol-bis-(β aminoethyl ether)N,N'-tetraacetic acid
fu	Ratio of unbound to total drug concentrations in plasma
GF(R)	Glomerular filtration rate (ml/min)
HA	Hippuric acid (benzoylglycine)
HEPES	4-(2-Hydroxyethyl)-1-piperazine ethane sulfonic acid

I	Inhibitor concentration in the membrane vesicle experiments (mM)
IP	Iodopyracet
I.S.	Internal standard
i.v.	Intravenous
K_d	Dissociation constant for the binding of drug to protein ($\mu\text{g/ml}$)
$K_{I(i)}$	Inhibition constant ($\mu\text{g/ml}$ or mM)
k_{ij}	First-order rate constant associated with movement of drug from compartment i to compartment j (min^{-1})
K_m	Michaelis-Menten constant (mM)
K_T	Michaelis-Menten constant of the tubular secretion system ($\mu\text{g/ml}$)
$\log k'$	Logarithm of the capacity factor in liquid chromatography
$\log k_w$	Logarithm of the capacity factor in liquid chromatography obtained by extrapolation of retention data from binary eluents to 100% water
MES	2-(N-morpholino)-ethanesulfonic acid
MRT	Mean residence time calculated from the plasma concentration-time curve (min)
MRT_R	Mean residence time calculated from the renal excretion rate-time curve (min)
NONLIN	Computer program for nonlinear least-squares parameter estimation based on the Gauss-Newton method
P	Total concentration of sites on protein available for binding drug ($\mu\text{g/ml}$)
PAH	p-Aminohippurate (4-aminobenzoylglycine)
Prob	Probenecid
PSP	Phenolsulfonphthalein (phenol red)
Q_{GF}	Glomerular filtration (ml/min)
Q_R	Renal plasma flow (ml/min)
Q_{ur}	Urine flow (ml/min)
R_R	Renal excretion rate of drug ($\mu\text{g/min}$)
S	Substrate concentration in the membrane vesicle experiments (mM)
SUA	Salicyluric acid (2-hydroxybenzoylglycine)

T_M	Maximum transport capacity of the tubular secretion mechanism ($\mu\text{g}/\text{min}$ or mg/min)
t_R	Retention time of a retained solute in liquid chromatography (min)
t_0	Retention time of an unretained solute in liquid chromatography; the mobile phase hold-up time (min)
$t_{\frac{1}{2},p}$	Half-life of drug in plasma (min)
$t_{\frac{1}{2},ur}$	Half-life of drug in urine (min)
Tris	Tris(hydroxymethyl)aminomethane
TS	Tubular secretion
v	Rate of specific substrate transport into membrane vesicles (pmol/mg protein, 15 sec)
v'	Rate of specific substrate transport into membrane vesicles in presence of inhibitor (pmol/mg protein, 15 sec)
V_i	Volume of compartment i (ml or l)
V_{max}	Maximum rate of substrate transport into membrane vesicles (nmol/mg protein, 15 sec)
V_{ss}	Volume of distribution at steady state (ml or l)
Δt	Renal delay time (min)
λ	Detector wavelength (nm)
$\lambda_{z,ur}$	Elimination rate constant of the terminal exponential phase of drug in urine (min^{-1})

PART I

INTRODUCTION

Facilius natura intellegitur quam
enarratur

(Nature is easier understood than
explained)

Lucius Annaeus Seneca

RENAL HANDLING OF ORGANIC ANIONS

Frans G.M. Russel and Cees A.M. van Ginneken

Abstract - The kidney is the principal route for the elimination of drugs and their metabolites from the body. The processes that determine net drug excretion are closely related to the physiological events occurring in the functional units of the kidney, i.e., the nephrons. The proximal tubular cells are an important site for the carrier-mediated secretion of anionic drugs. Organic anions are actively transported at the basolateral membrane, concentrated intracellularly, and subsequently transported from the cell into the tubular lumen by mediated (facilitated) diffusion. The organic anion secretory system accepts a wide variety of compounds which may compete with each other for transport. This may have important clinical implications.

1.1 INTRODUCTION

The study of the mechanisms by which the kidney excretes foreign anions has traditionally belonged to the field of renal physiology. It was only many years after Marshall and coworkers in 1923 obtained the first conclusive proof of active secretion with phenolsulfonphthalein [82], that pharmacologists recognized the clinical importance of the renal organic anion transport system. The primary function of the organic anion system appears to be the facilitated elimination of endogenous metabolites and exogenous compounds, which are not easily degraded by the body, and which might be toxic if allowed to accumulate. In accordance with this vast task, the transport system accepts a wide variety of organic anions, having in common only a negative charge and a hydrophobic backbone.

Many organic cations are also actively secreted by the kidney [39,108,110,155], but the transport system for these compounds is clearly distinct from the organic anion system and it operates at a different cellular site [52,69,86,132].

In the past decade considerable progress has been made in the elucidation of the mechanisms involved in the tubular secretion of organic ions. These advances are inextricably linked to the advances in techniques for studying kidney function, e.g., isolated perfused kidney, isolated perfused tubules, microperfusion methods, cultured renal cells, isolated membrane vesicles [139].

The renal organic anion transport system has been the subject of a number of excellent reviews [39,41,46,90,106,110,131,144,154,155]. The purpose of the present paper is to summarize shortly the current knowledge on the renal handling of organic anions as an introduction to the investigations described in this thesis.

1.2 RENAL EXCRETION OF DRUGS

Physiology

Apart from its excretory function, the kidney plays a dominant role in the regulation of the constancy of the volume and composition of the internal environment. To perform this task, it is an organ of a high functional selectivity, capable of reabsorbing the necessary valuable substances and excreting waste products and undesirable excess of exogenous compounds taken into the body.

The action of the kidney is intimately related to its anatomical structure. The functional units of the kidney are the nephrons, of which there are about 1.5 million per kidney in the human. A schematic drawing of a nephron with the associated vascular supply in the cortex is given in Fig. 1.1. The basic components of the nephron are the glomerulus, surrounded by a Bowman's capsule, the proximal tubule, the loop of Henle, the distal tubule and the collecting tubule. A single layer of epithelial cells lines the lumen of the nephron throughout its entire length, and a close network of arterial and venous capillaries provide a tight contact between the blood circulation and these cells. The glomeruli receive the

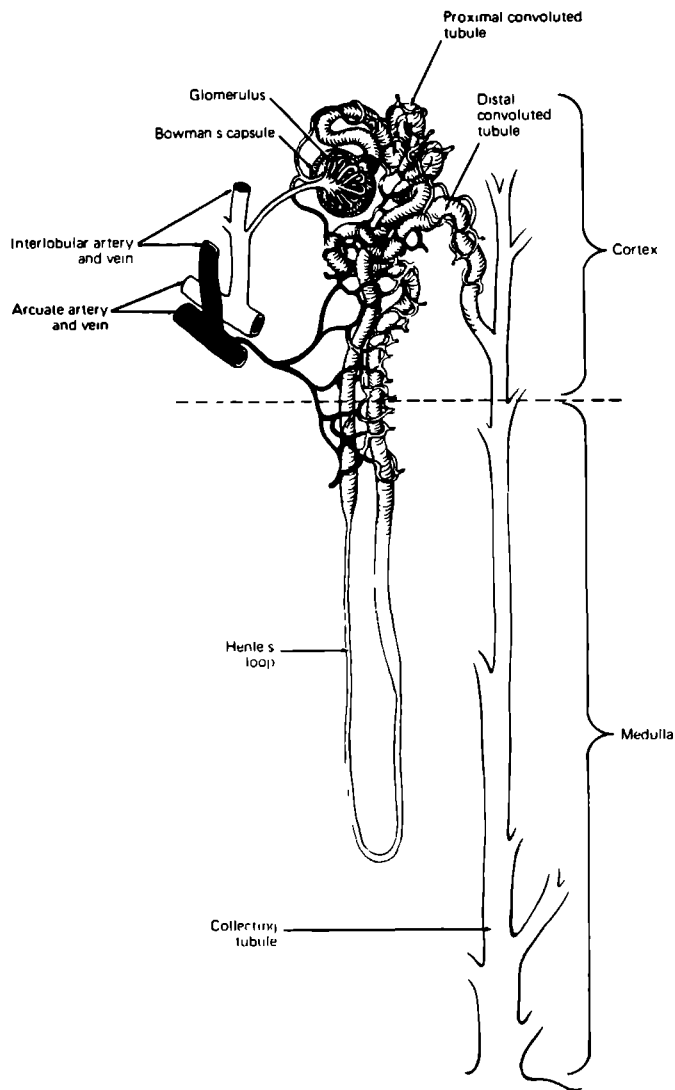


Fig. 1.1 The functional nephron with representative blood supply in the cortical region [From reference 63 with permission].

arterial blood first, and the glomerular filtrate passes down the tubule where electrolyte transport takes place and where most of the water is reabsorbed. Less than only 1% of the water in the initial ultrafiltrate

leaves the kidney as urine. The blood that has passed the glomerular capillary bed is transported via an efferent arteriole to a second network of capillaries that perfuses the proximal and distal portions of the tubules. More than 80% of the arterial blood flows to the cortex, while a fraction of the total blood supply reaches the medullary parts of the nephron.

The renal mechanisms which account for the formation and final composition of urine also determine the rate and extent by which drugs appear in the urine. Four different processes are the main determinants of drug excretion, viz., glomerular filtration, passive reabsorption, active tubular secretion, and active tubular reabsorption.

Glomerular Filtration and Passive Reabsorption

In man, about 25% of the cardiac output (1200 - 1500 ml/min) reaches the kidney, and of this volume about 10% is filtered at the glomeruli. The energy required for filtration is supplied by the hydrostatic pressure of the blood, which must overcome both the intracapsular pressure and the osmotic pressure of the plasma proteins. Compounds with a molecular weight of approximately 40,000 or less and a diameter up to 20Å are filtered by the glomerulus. Larger molecules are restricted from the filtrate, particularly those molecules which are negatively charged like, for example, albumin. Since most drugs are small enough to be filtered, only drug molecules bound to plasma proteins are excluded from the glomerular filtrate. From a kinetic point of view this implies that the effective clearance of a drug by glomerular filtration is equal to the glomerular filtration rate of an unbound substance (e.g., inulin, mannitol) times the fraction of drug not bound to plasma proteins.

The effective renal clearance may be further decreased by passive diffusion of the drug from the tubular fluid back into the blood stream. As nearly all the water of the filtrate is reabsorbed, steep concentration gradients of drug between the tubular fluid and the blood may exist all over the nephron. This situation strongly favors the movement of drug out of the tubular lumen, and in accordance with their physicochemical properties, drug molecules will passively diffuse back into the renal blood circulation. As usual when permeation of biological membranes by non-active mechanisms is concerned, back-diffusion is only possible for drug

molecules which are sufficiently lipophilic in nature. This practically always means that the drug should be unionized in urine. Therefore, the pK_a of the drug and the pH of the tubular urine determine the extent and rate of passive drug reabsorption.

The urinary pH can vary between 4.0 and 8.0 during its formation, depending on several metabolic factors. Normally, the urine is somewhat acidic as a result of the secretion of protons along the tubule. The acidification of urine facilitates the nonionic back-diffusion of weak acids, such as salicylic acid. Conversely, alkalization of the urine promotes the renal excretion of salicylic acid. For weak basic drugs obviously the opposite holds true. This principle is, for instance, used clinically in the treatment of salicylate poisoning by administration of sodium bicarbonate to produce an alkaline urine, which accelerates the elimination of drug.

Another important factor in the process of back-diffusion is the urine flow. When less water is reabsorbed more urine will be produced and less concentration of drug in the tubular fluid will occur. Clearly, this means a smaller concentration gradient and consequently, less back-diffusion.

Tubular Secretion

A number of substances are excreted from the capillaries surrounding the renal tubules into the luminal fluid by a carrier-mediated process (tubular secretion). With several experimental techniques it has been shown independently that many organic compounds are actively secreted by the proximal tubular cells of the nephron [90]. The pathways for organic anions and cations appear to be separate, but both transport systems are characterized by a broad specificity. Tubular secretion is an active carrier-mediated process in that it is concentration-, temperature-, and energy-dependent and susceptible to competition by similar substrates.

The characteristics of the renal organic anion transport system have been extensively studied with p-aminohippurate (PAH). Most of our knowledge about the exact anatomical location of PAH secretion derives from studies with isolated perfused rabbit tubules. The proximal tubule can be divided functionally into three segments, viz., S_1 , S_2 , and S_3 (Fig. 1.2). The highest rate of PAH secretion is seen in the S_2 segment of both the superficial and juxtamedullary nephrons of the rabbit kidney

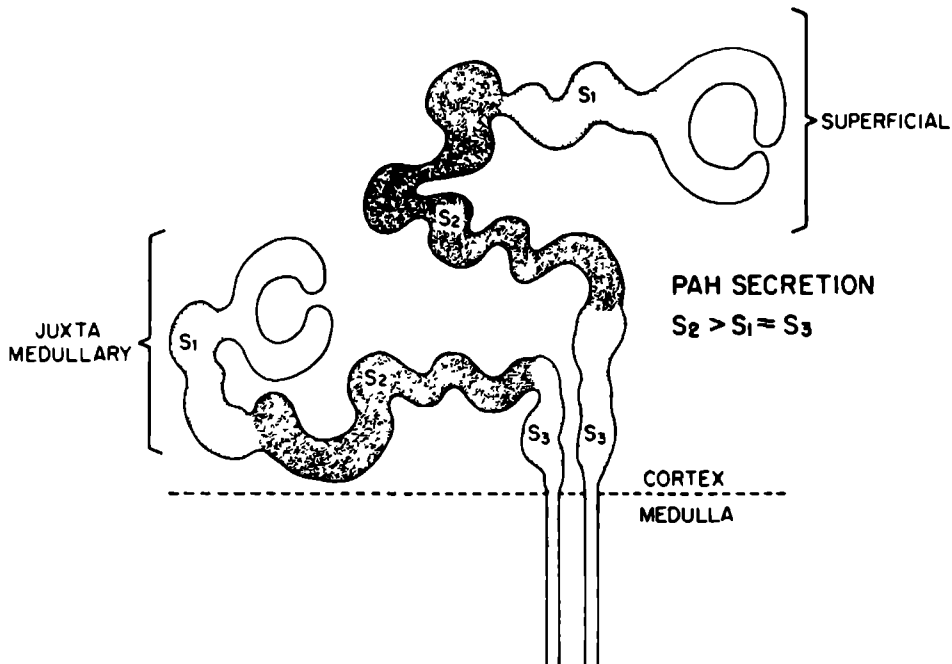


Fig. 1.2 Heterogeneity of PAH transport in rabbit proximal tubules. PAH is secreted in all parts of the tubule but most avidly in the S_2 segment [From reference 39 with permission].

[83,136,160]. Shimomura et al. [121] showed that the K_m values of the three segments were the same, while the maximal transport rate (V_{max}) in the S_2 segment was 5 to 6 times greater than in the other segments. They suggested that heterogeneity of PAH secretion along the proximal tubule is a result of an unequal distribution of transporters with common affinity. However, this pattern of heterogeneity is probably not representative for all mammalian species. For example in the pig, the S_1 segment is the predominant site of PAH secretion [117].

Whereas protein binding always decreases the extent of glomerular filtration, the tubular secretion of most organic anions seems to be unaffected, presumably due to the high dissociation rate of the drug-protein complex relative to its exposure time to the secretory system. Of course,

also the affinity of the carrier system has to be high enough to compete effectively with the plasma-protein molecules. However, these conditions are not universal as there are examples of drugs for which protein binding impedes tubular secretion [17,48,65,96].

Active Reabsorption

Carrier-mediated reabsorption from the tubular fluid occurs for many endogenous compounds which are indispensable to the body, e.g., glucose, amino acids, and some vitamins. The physicochemical properties of these nutrients preclude their effective return to the circulation by passive back-diffusion. Glucose, for example, is under physiological conditions not present in the voided urine because it is completely reabsorbed from the glomerular filtrate in the proximal tubules. Only when the amounts delivered to the kidney exceed the transport capacity of the carrier system, glucose appears in the urine.

Renal excretion of most organic anions is dominated by tubular secretion. Reabsorption, if any, takes usually place by simple diffusion. However, some compounds are known to be transported by tubular secretion as well as active reabsorption. Urate is an interesting example of an endogenous anion that undergoes bidirectional active transport [75,109]. The combined action of oppositely operating transport mechanisms explains the paradoxical effects of drugs like salicylate, probenecid, and phenylbutazone on urate excretion. In low doses they act as hyperuricemic drugs by inhibiting tubular urate secretion, whereas with high doses they exert a hypouricemic effect by inhibiting tubular urate reabsorption [44,124,162,163].

Exogenous organic anions for which active bidirectional transport has been reported are m-hydroxybenzoate [84,85], nicotinate [24], and pyrazinoate [153]. The transport systems which are involved in the specific secretion and reabsorption of these compounds are still not completely characterized, but there is evidence that they are, at least in part, different from the urate system [155].

1.3 RENAL CLEARANCE

Clearance

The concept of clearance was originally developed by renal physiologists as a means to measure kidney function in health and disease [131]. In pharmacokinetics, clearance is now generally considered as the most useful parameter for the evaluation of an elimination mechanism [111,135,158].

The renal clearance (CL_R) of a drug may be viewed as the volume of plasma from which drug is completely removed per unit time by the kidney. It is often defined as the rate of renal drug excretion at time t ($R_R = dA_e/dt$) divided by its plasma concentration at time t (C):

$$CL_R = R_R / C$$

In practice it is of course impossible to determine the momentaneous renal excretion rate of a drug. Therefore, urine is collected over a finite period and the mean excretion rate is divided by the plasma concentration measured at the midpoint of the collection interval [112].

Inulin

The rate at which a drug will be excreted in the urine is the net result of the four renal processes: glomerular filtration, passive back-diffusion, and active tubular reabsorption and secretion. If a drug does not undergo active reabsorption and secretion, its renal excretion rate will be linearly related to its plasma concentration and the renal clearance will be constant over a wide plasma concentration range. When the drug is furthermore not protein bound and not subject to passive reabsorption (for example inulin) its clearance will be equivalent to the glomerular filtration rate (Fig. 1.3).

Glucose and PAH

The processes of tubular secretion and active reabsorption are principally nonlinear in nature. Only at relatively low drug concentrations these mechanisms can be represented by a constant concentration-independent clearance. The classical examples of active tubular reabsorption and

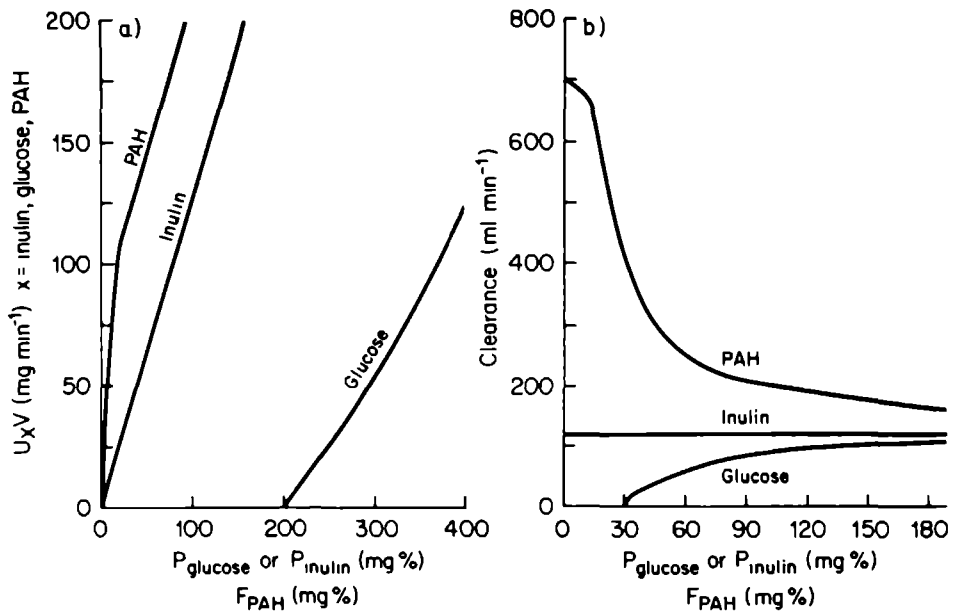


Fig. 1.3 Renal excretion rates (a) and corresponding clearances (b) of PAH, inulin, and glucose as a function of plasma concentrations in humans [From reference 119 with permission].

secretion are the clearance patterns of glucose and PAH, respectively (Fig. 1.3).

Usually no glucose is present in the urine, but when the plasma glucose concentration (P_{glucose}) is elevated above about 2 mg/ml , the so-called threshold value, glucose appears in the urine. As P_{glucose} is further raised, tubular reabsorption becomes increasingly saturated until the maximum rate of reabsorptive transport is reached. From this point the clearance is constant and equal to the glomerular filtration rate, since glucose is practically not bound to plasma proteins.

It is apparent from Fig. 1.3 that the renal excretion rate and clearance of PAH at low plasma concentrations are much greater than those of inulin, i.e., PAH undergoes net secretion. In fact, tubular secretion is so efficient under these conditions that nearly all PAH is removed from the blood as it passes through the kidney. In man, the clearance is 600 -

700 ml/min and approximately 90% of the total renal plasma flow. Correction of this value for hematocrit gives the effective renal blood flow. Although PAH is hardly bound to plasma proteins, extraction is never complete since always some blood passes directly from the glomerular capillaries into the medulla, thus escaping from clearance in the proximal tubules [95]. As the plasma concentration of PAH in plasma is increased the secretory system becomes saturated and renal clearance falls toward the level of the glomerular filtration rate. Ideally, the renal clearance of PAH can be described in terms of concomitant glomerular filtration and tubular secretion. However, there is evidence that PAH may undergo some tubular reabsorption [4,23], and in several species, including man, PAH is metabolized during transit through the kidney [35,45,80]. Intrarenal metabolism should always be taken into consideration, because it can have far-reaching consequences for the excretory pattern of the parent compound.

1.4 MECHANISMS OF ANION SECRETION

Experimental Techniques

From renal clearance studies an overall impression of the occurrence and kinetics of carrier transport can be obtained. Interaction studies may also provide evidence for the existence of carrier transport. In this respect special reference should be made to probenecid, a drug developed almost forty years ago to inhibit penicillin secretion, because of the scarce availability of the antibiotic in those days [13]. Ever since, probenecid has been the standard inhibitor in studies directed at the tubular secretion of anionic drugs.

For more detailed studies on the selectivity, localization, and energetics of the carrier systems obviously more sophisticated experimental methods are required. A number of *in vivo* and *in vitro* techniques [139] has been employed to study the sequence of movement of organic anions through the proximal tubular cells. Especially the relatively new technique of isolated renal plasma membrane vesicles has proven to be of great value for the study of transport mechanisms at specific membrane sites. Most studies have been carried out with a prototype of secreted anions, i.e., PAH

[106]. The picture of transtubular organic anion transport that emerged from these investigations is summarized in Fig. 1.4.

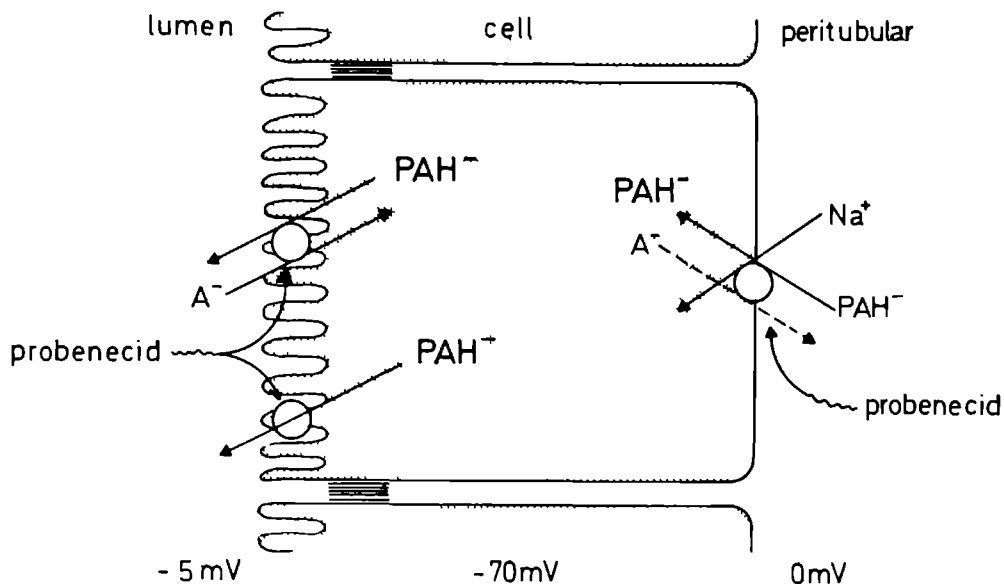


Fig. 1.4 Schematic model for proximal tubular transport of p-aminohippurate (PAH). PAH is actively transported at the basolateral membrane by a sodium gradient-dependent anion exchange mechanism. The high intracellular PAH concentration provides a driving force for the facilitated diffusion across the brush border membrane. This step occurs either via an anion exchange mechanism or a (gated) channel. PAH transport across both membranes is probenecid-sensitive.

Membrane Transport

The initial step in tubular secretion involves the carrier-mediated uptake of PAH from the interstitial fluid across the peritubular (basolateral) membrane into the proximal tubular cell. This transport step is active since PAH is taken up against an electrochemical gradient to achieve intracellular concentrations up to 30 times higher than those in the extracellular fluid. There is abundant evidence to indicate that PAH

transport is coupled to the transmembrane sodium gradient. However, recent studies with basolateral membrane vesicles have shown that this sodium-coupled mechanism can be stimulated additionally by an opposing anion gradient, suggesting a sodium gradient-stimulated anion exchange mechanism [33,67,115].

The movement of PAH out of the cell across the brush border membrane into the tubular lumen occurs by carrier-mediated (facilitated) diffusion, a process which can be considered as passive in the sense that the substance is transported down its electrochemical gradient. Recent studies strongly support the involvement of an anion exchange mechanism in the brush border membrane, but there are also indications for a (gated) channel that mediates the movement of PAH out the cell [55,64,106,110]. At present it is not clear whether both types of transport proceed via a single carrier or whether distinct carriers are involved.

The PAH transport system in the brush border membrane has a lower affinity but higher capacity than the transport system in the basolateral membrane. Both transport systems are competitively inhibited by probenecid, but the basolateral membrane system is more susceptible to inhibition [69,115].

1.5 KINETIC MODELING OF TUBULAR SECRETION

Classical Pharmacokinetics

In classical pharmacokinetics renal clearance is considered as a process operating directly from the central compartment. It is assumed implicitly that an equilibrium exists between the concentrations of drug in plasma and urine. However, this assumption is only valid in some special cases. Especially when carrier-mediated transcellular transport is involved, a simple equilibrium between plasma and urine is unlikely on theoretical grounds. For example, experiments on plasma kinetics and renal excretion of iodopyracet in the dog revealed that the classical Michaelis-Menten approach is unable to cover the pharmacokinetic profile of this compound. The main reason is that the equilibrium assumption is not valid for iodopyracet and other drugs that are eliminated by tubular secretion so rapidly that at low plasma concentrations the rate of excretion becomes limited by the renal plasma flow.

Physiologically Based Modeling

The limitations of classical pharmacokinetics have led to the need for a more physiological approach. Recently, a prototype of a new generation of physiologically based pharmacokinetic models was proposed, in which the kidney is set apart as a subsystem containing several compartments, e.g., plasma, glomerular, tubular as well as luminal compartments [49,50]. With such a model the transport systems can be accommodated at the exact site where they are operating. By using this type of kinetic modeling it appeared possible to describe the excretion kinetics of iodopyracet in a consistent way. It has been shown that the flow-dependent profile is just a limiting case of this general approach, whereas also the Michaelis-Menten equilibrium state follows directly from the model [49]. Furthermore, the models appeared to be useful in the characterization of drug interactions at the level of tubular secretion [50,113,114].

1.6 SPECIFICITY OF ORGANIC ANION SECRETION

One of the remarkable characteristics of the renal organic anion system is that it accepts compounds with a tremendous diversity in chemical structure. A wide variety of drugs and their metabolites as well as numerous endogenous substrates are excreted by the kidney by tubular secretion. A list with a number of representative compounds is given in Table 1.1.

A considerable effort has been made, particularly by Despopoulos [27] and Møller and Sheikh [90], to elucidate the structural features necessary for transport. However, none of these attempts have led to a comprehensive model accounting for all the structures that are accepted by the anion system. Recently, Ullrich and coworkers [141,142] showed that an organic backbone and a negative charge are in fact sufficient for affinity to the PAH transport system in the basolateral membrane. It has been suggested that this apparent lack of substrate specificity, which is unusual for carrier-mediated processes, stems from multiple transport systems with overlapping structural specificities [8,51,140]. However, at the present time evidence for this hypothesis is not conclusive.

Table 1.1 Examples of compounds which are excreted by the renal organic anion transport system.

Endogenous Compounds	Drug Metabolites
Aromatic amino acids [159]	Acetylated sulfonamides [1,120, 145,146]
Bile salts [9,165]	N-Acetylcysteine conjugates [59,91, 94,118,127]
Bilirubin [4]	Gentisate [152]
Cyclic AMP [15,25]	Glucuronide conjugates [78,87, 116,133]
Cyclic GMP [15,25]	Glutathione conjugates [74,76, 91,94]
Fatty acids [6,7]	Glycine conjugates [72,73,92, 130,161]
Hydroxyindoleacetate [47]	Pyrazinoate [34,153]
Oxalate [40,156]	Sulfate conjugates [30,149]
Prostaglandins [14,60,107]	
Urate [75,104,105]	
Drugs	
Acyclovir [89]	Iodipamide [12,88]
Acetazolamide [150]	Iothalamate [100]
Azidothymidine [71]	Methotrexate [16,79]
p-Aminohippurate [46,106]	Nitrofurantoin [102,148]
p-Aminosalicylate [56]	Penicillins [10,11,31,65,125]
Benzoates [152]	Phenolsulfonphthalein [37,96]
Bumethanide [107,128]	Phenylbutazone [43,152]
Cephalosporins [58,65,70,138]	Piretanide [99]
Captopril [28,29,123]	Probenecid [26,151]
Cisplatin [22,61]	Quinolones [147]
Diatrizoate [93]	Salicylate [15,42,116]
Diflunisal [3]	Saccharin [38]
Diodrast [93]	Sulfinpyrazone [77,103]
Ethacrynic acid [98]	Sulfonamides [53,65,101]
Furosemide [17,97,98]	Thiazides [157]
Gossypol [36]	Thymidine [164]
Hippuran [88,129]	Trimethoprim [20,21]
Ibuprofen [143]	
Indomethacin [2,126]	

1.7 CLINICAL IMPLICATIONS OF ANION SECRETION

Tubular secretion is an important process in the renal handling of many drugs, and may therefore be the basis of a variety of clinical implications. The presence of tubular secretion is often a vital link in the disposition and response of drugs with an intratubular site of action (e.g., diuretics, uricosurics, some antibiotics), especially when these drugs are highly bound to plasma proteins [19,39].

The organic anion transport system may also play a role in the development of nephrotoxicity with compounds that are highly accumulated in the proximal tubular cells, thereby exerting a direct toxic effect. A clinically important example is cephaloridine [137], and it has been suggested that the acute renal failure that is sometimes seen with renal contrast agents, is also a consequence of very high intracellular drug concentrations [57].

Since carrier-mediated processes are involved in organic anion secretion, there will be the potential problems of saturation and competition. Saturation of tubular secretion invariably leads to a decrease of the total body drug clearance and consequently, to a risk of unwanted drug accumulation in the body [18]. Drug interactions at the level of tubular secretion have been described many times. In principle, all compounds listed in Table 1.1 have the potential to compete with each others tubular secretion. For instance, it has been reported that several drugs are able to increase the half-life of penicillin in man [66]. An interaction with life-threatening consequences has been described recently between methotrexate and non-steroidal anti-inflammatory drugs [68,81,122,134]. Also interactions between drugs and endogenous substances may have clinical consequences, e.g., the interaction with urate transport.

Evidently, a proper understanding of the processes of tubular secretion and the renal handling of drugs in general, is a prerequisite for well-considered drug prescribing.

1.8 REFERENCES

1. Arita T, Hori R, Takada M, Akuzu S, and Misawa A: Transformation and excretion of drugs in biological systems. VII. Effect of biotransformation in renal excretion of sulfonamides. *Chem. Pharm. Bull.* 20: 570-580 (1972).
2. Baber N, Halliday L, Sibeon R, Littler T, and Orme ML'E: The interaction between indomethacin and probenecid. *Clin. Pharmacol. Ther.* 24: 298-307 (1978).
3. Baer JE, Breault GO, and Russo HF: Diflunisal renal clearance in anesthetized dogs. Effect of probenecid, urine flow and urine pH. *Arch. Int. Pharmacodyn. Ther.* 235: 204-210 (1978).
4. Baines AD, Gottschalk CW and Lassier WE: Microinjection study of p-aminohippurate excretion in rat kidneys. *Am. J. Physiol.* 214: 703-709 (1968).
5. Balant L, Dayer P, and Auckenthaler R: Clinical pharmacokinetics of the third generation cephalosporins. *Clin. Pharmacokinet.* 10: 101-143 (1985).
6. Barac-Nieto M and Cohen JJ: Non-esterified fatty acid uptake by dog kidney. Effects of probenecid and chlorothiazide. *Am. J. Physiol.* 215: 98-107 (1968).
7. Barac-Nieto M: Renal uptake of p-aminohippuric acid in vitro. Effects of palmitate and L-carnitine. *Biochim. Biophys. Acta* 233: 446-452 (1971).
8. Bárány EH: Selectivity of probenecid congeners for different organic acid transport systems in rabbit renal cortex. *Acta Pharmacol. Toxicol.* 35: 309-316 (1974).
9. Bárány EH: In vitro uptake of bile acids by choroid plexus, kidney cortex and anterior uvea. I. The iodipamide-sensitive transport systems in the rabbit. *Acta Physiol. Scand.* 93: 250-268 (1975).
10. Barza M, Bruschi J, Bergeron MG, Kemmotsu O, and Weinstein L: Extraction of antibiotics from the circulation by liver and kidney: Effect of probenecid. *J. Infect. Dis.* 131: 586-597 (1975).
11. Bergan T: Pharmacokinetics of beta-lactam antibiotics. *Scand. J. Infect. Dis.* 42: 83-98 (1984).

12. Berndt WO and Mudge GH: Renal excretion of iodipamide. Comparative study in the dog and rabbit. *Invest. Radiol.* 3: 414-426 (1968).
13. Beyer KH, Russo HF, Tillson EK, Miller AK, Verwey WF, and Gass SR: Benemid (di-n-propylsulfamyl)-benzoic acid: its renal affinity and its elimination. *Am.J. Physiol.* 166: 625-640 (1951).
14. Bito LZ, and Baroody RA: Comparison of renal prostaglandin and p-aminohippuric acid transport processes. *Am. J. Physiol.* 234: F80-88 (1978).
15. Blonde L, Wehmann RE, and Steiner AL: Plasma clearance rates and renal clearance of ³H-labeled cyclic AMP and ³H-labeled cyclic GMP in the dog. *J. Clin. Invest.* 53: 163-172 (1974).
16. Bourke RS, Chheda G, Bremer A, Watanabe O, and Tower DB:: Inhibition of renal tubular transport of methotrexate by probenecid. *Cancer Res.* 35; 110-116 (1975).
17. Bowman RH: Renal secretion of [³⁵S]furosemide and its depression by albumin binding. *Am. J. Physiol.* 229: 93-98 (1975).
18. Brater DC: The pharmacological role of the kidney. *Drugs* 19: 31-48 (1980).
19. Brater DC: Pharmacodynamic considerations in the use of diuretics. *Ann. Rev. Pharmacol. Toxicol.* 23: 45-62 (1983).
20. Cacini W and Myre SA: Uptake of trimethoprim by renal cortex. *Biochem. Pharmacol.* 19: 3483-3488 (1985).
21. Cacini W: In vivo renal tubular secretion of trimethoprim without metabolism. *Biochem. Pharmacol.* 36: 2693-2695 (1987).
22. Caterson R, Etheredge S, Snitch P, and Duggin G: Mechanisms of renal excretion of cisdichlorodiamine platinum. *Res. Commun. Chem. Pathol. Pharmacol.* 41: 255-264 (1983).
23. Cho KC and Cafruny EJ: Renal tubular reabsorption of p-aminohippuric acid (PAH) in the dog. *J. Pharmacol. Exp. Ther.* 173: 1-12 (1970).
24. Corr PB and May DG: Renal mechanisms for the excretion of nicotinic acid. *J. Pharmacol. Exp. Ther.* 192: 195-200 (1975).
25. Coulson R: Metabolism and excretion of exogenous adenosine 3',5'-monophosphate and guanosine 3',5'-monophosphate. Studies in the isolated perfused rat kidney and in the intact rat. *J. Biol. Chem.* 251: 4958-4967 (1976).

26. Dayton PG, Yü TF, Chen W, Berger L, West LA, and Gutman AB: The physiological disposition of probenecid, including renal clearance in man, studied by an improved method for its estimation in biological material. *J. Pharmacol. Exp. Ther.* 140: 278-286 (1963).
27. Despopoulos A: A definition of substrate specificity in renal transport of organic anions. *J. Theoret. Biol.* 8: 163-192 (1965).
28. Drummer OH, Thompson J, Hooper R, and Jarrott B: Effect of probenecid on the disposition of captopril and captopril dimer in the rat. *Biochem. Pharmacol.* 34: 3347-3351 (1985).
29. Drummer OH, Jarrott B: The disposition and metabolism of captopril. *Mec. Res. Rev.* 6: 75-97 (1986).
30. Duggin GG and Mudge GH: Renal tubular transport of paracetamol and its conjugates in the dog. *Br. J. Pharmacol.* 54: 359-366 (1975).
31. Eagle H and Newman E: The renal clearance of penicillins F, G, K and X. *J. Clin. Invest.* 26: 903-918 (1947).
32. Elias MM, Comin EJ, Ochoa JE, and Rodriguez Garay EA: Renal handling of bilirubin photoderivatives. *Experientia* 43: 875-878 (1987).
33. Eveloff J: p-Aminohippurate transport in basal-lateral membrane vesicles from rabbit renal cortex: stimulation by pH and sodium gradients. *Biochim. Biophys. Acta* 897: 474-480 (1979).
34. Fanelli GM Jr and Weiner IM: Pyrazinoate excretion in the chimpanzee: Relation to urate disposition and the actions of uricosuric drugs. *J. Clin. Invest.* 52: 1946-1957 (1973).
35. Girndt J, Mályusz M, Rumpf KW, Neubaur J, and Scheler F: Metabolism of p-aminohippurate and its relevance in man. *Nephron* 13: 138-144 (1974).
36. Goldinger JM, Lee SH, and Hong SK: Renal transport of gossypol in the rabbit. *Proc. Soc. Exp. Biol. Med.* 179: 50-54 (1985).
37. Goldring W, Clarke RW, and Smith HW: The phenol red clearance in normal man. *J. Clin. Invest.* 15: 221-228 (1936).
38. Goldstein RS, Hook JB, and Bond JT: Renal tubular transport of saccharin. *J. Pharmacol. Exp. Ther.* 204: 690-695 (1978).
39. Grantham JJ and Chonko AM: Renal handling of organic anions and cations; metabolism and excretion of uric acid. In: *The Kidney*, edited by BM Brenner and FC Rector, pp. 663-700, WB Saunders, Philadelphia (1986).

40. Greger L, Lang F, Oberleithner H, and Deetjen P: Handling of oxalate by the rat kidney. *Pflügers Arch.* 374: 243-248 (1978).
41. Greven J: Renal transport of drugs. In: *Renal transport of organic substances*, edited by R Greger, F Lang, and S Silbernagl, pp. 262-277, Springer Verlag, Berlin (1981).
42. Gutman AB, Yü TF, and Sirota JH: A study by simultaneous clearance techniques of salicylate excretion in man. Effect of alkalinization of the urine by bicarbonate administration; effect of probenecid. *J. Clin. Invest.* 34: 711-721 (1955).
43. Gutman AB, Dayton PG, Yü TF, Berger L, Chen W, Sicam LE, and Burns JJ: A study of the inverse relationship between pK_a and rate of renal excretion of phenylbutazone analogs in man and dog. *Am. J. Med.* 29: 1017-1033 (1960).
44. Gutman and Yü TF: A three-component system for regulation of renal excretion of uric acid in man. *Trans. Assoc. Am. Physicians* 74: 353-365 (1961).
45. Gyrd-Hansen N and Rasmussen F: Acetylation of p-aminohippuric acid in the kidney. Renal clearance of p-aminohippuric acid and N⁴-acetylated p-aminohippuric acid in pigs. *Acta Physiol. Scand.* 80: 249-283 (1970).
46. Häberle DA: Characteristics of p-aminohippurate transport in the mammalian kidney. In: *Renal transport of organic substances*, edited by R Greger, F Lang, and S Silbernagl, pp. 188-209, Springer Verlag, Berlin (1981).
47. Hakim R, Watrous WM, and Fujimoto JM: The renal tubular transport and metabolism of serotonin (5-HT) and 5-hydroxyindoleacetic acid (5-HIAA) in the chicken. *J. Pharmacol. Exp. Ther.* 175: 749-762 (1970).
48. Hall S and Rowland M: Influence of fraction unbound upon the renal clearance of furosemide in the isolated perfused rat kidney. *J. Pharmacol. Exp. Ther.* 232: 263-268 (1985).
49. Hekman P and Van Ginneken CAM: Kinetic modeling of the renal excretion of iodopyracet in the dog. *J. Pharmacokinet. Biopharm.* 10: 77-92 (1982).
50. Hekman P and Van Ginneken CAM: Simultaneous kinetic modelling of plasma levels and urinary excretion of salicyluric acid and the influ-

- ence of probenecid. *Eur. J. Drug Metab. Pharmacokinet.* 3: 239-249 (1983).
51. Hewitt WR, Wagner PA, Bostwick EF and Hook JB: Transport ontogeny and selective substrate stimulation as models for identification of multiple renal organic anion transport systems. *J. Pharmacol. Exp. Ther.* 202: 711-723 (1977).
 52. Holohan PD and Ross CR: Mechanisms of organic cation transport in kidney plasma membrane vesicles. 1. Countertransport studies. *J. Pharmacol. Exp. Ther.* 215: 191-197 (1980).
 53. Hori R, Sunayashiki K, and Kamiya A: Pharmacokinetic analysis of renal handling of sulfamethizole. *J. Pharm. Sci.* 65: 463-465 (1976).
 54. Hori R, Sunayashiki K, and Kamiya A: Tissue distribution and metabolism of drugs. I. Quantitative investigation on renal handling of phenolsulfonphthalein and sulfonamides in rabbits. *Chem. Pharm. Bull.* 26: 740-745 (1978).
 55. Hori R, Takano M, Okano T, Kitazawa S, and Inui KI: Mechanisms of p-aminohippurate transport by brush-border and basolateral membrane vesicles isolated from rat kidney cortex. *Biochim. Biophys. Acta* 692: 97-100 (1982).
 56. Huang KC, Moore KB, and Campbell PC Jr.: Renal excretion of para-aminosalicylic acid. A two-way transport system in the dog. *Am. J. Physiol.* 199: 5-8 (1960).
 57. Humes HB and Weinberg JM: Toxic nephropathies. In: *The Kidney*, edited by BM Brenner and FC Rector, pp. 1491-1532, Saunders, Philadelphia (1986).
 58. Ings RMJ, Reeves DS, White LO, Bax RP, Bywater MJ, and Holt HA: The human pharmacokinetics of cefotaxime and its metabolites and the role of renal tubular secretion on their elimination. *J. Pharmacokinet. Biopharm.* 13: 121-142 (1985).
 59. Inoue M, Okajima K, and Morino Y: Renal transtubular transport of mercapturic acid in vivo. *Biochim. Biophys. Acta* 641: 122-128 (1981).
 60. Irish JM: Secretion of prostaglandin E_2 by rabbit proximal tubules. *Am. J. Physiol.* 237: F268-273 (1979).
 61. Jacobs C, Kalman SM, Tretton M, and Weiner MW: Renal handling of cis-diaminedichloroplatinum(II). *Cancer Treat. Rep.* 64: 1223-1226 (1980).

62. Josephson B, Grieg A, Kakossaios G, and Kallas J: Renal tubular excretion from high plasma levels of paraaminohippurate (PAH) and diodrast (D) in unanesthetized rabbits. *Acta Physiol. Scand.* 30: 11-21 (1954).
63. Junquiera LC, Carneiro J, and Coutopoulos AN: Basic Histology. Urinary tract, pp. 354-371, Lange Medical Publications, Los Altos, California (1975).
64. Kahn AM, Branham S, and Weinman EJ: Mechanism of urate and p-aminohippurate transport in renal microvillus membrane vesicles. *Am. J. Physiol.* 245: F151-158 (1983).
65. Kamiya A, Okumura K, and Hori R: Quantitative investigation on renal handling of drugs in rabbits, dogs, and humans. *J. Pharm. Sci.* 72: 440-443 (1983).
66. Kampmann J, Hansen JM, Siersbaek-Nielsen K, and Laursen H: Effect of some drugs on penicillin half-life in blood. *Clin. Pharmacol. Ther.* 13: 516-519 (1972).
67. Kasher JS, Holohan PD, and Ross CR: Na^+ gradient-dependent p-aminohippurate (PAH) transport in rat basolateral membrane vesicles. *J. Pharmacol. Exp. Ther.* 227: 122-129 (1983).
68. King HW, Macfarlane AW, Graham RM, and Verbov JL: Near fatal drug interactions with methotrexate given for psoriasis. *Br. Med. J.* 295: 752-753 (1987).
69. Kinsella JL, Holohan PD, Pessah NI, and Ross CR: Transport of organic ions in renal cortical luminal and antiluminal membrane vesicles. *J. Pharmacol. Exp. Ther.* 209: 443-450 (1979).
70. Kirby WMM and Regamey C: Pharmacokinetics of cefazolin compared with four other cephalosporins. *J. Infect. Dis.* 128: S341-346 (1973).
71. Klecker RW, Collins JM, Yarchoan R, Thomas R, Jenkins JF, Broder S, and Myers CE: Plasma and cerebrospinal fluid pharmacokinetics of 3'-azido-3'-deoxythymidine: A novel pyrimidine analog with potential application for the treatment of patients with AIDS and related diseases. *Clin. Pharmacol. Ther.* 41: 407-412 (1987).
72. Knoefel PK and Huang KC: Biochemorphology of renal tubular transport: Hippuric acid and related substances. *J. Pharmacol. Exp. Ther.* 126: 296-303 (1959).

73. Knoefel PK, Huang KC, and Jarboe CH: Renal disposal of salicylic acid. *Am. J. Physiol.* 203: 6-10 (1962).
74. Kramer RA, Foureman G, Greene KE, and Reed DJ: Nephrotoxicity of S-(2-chloroethyl)glutathione in the Fischer rat: Evidence for γ -glutamyltranspeptidase-independent uptake by the kidney. *J. Pharmacol. Exp. Ther.* 242: 741-748 (1987).
75. Lang F: Renal handling of urate. In: *Renal transport of organic substances*, edited by R Greger, F Lang, and S Silbernagl, pp. 234-261, Springer Verlag, Berlin (1981).
76. Lash LH and Jones DP: Uptake of the glutathione conjugate S-(1,2-dichlorovinyl)glutathione by renal basolateral membrane vesicles and isolated kidney cells. *Mol. Pharmacol.* 28: 278-282 (1985).
77. Lentjes EWGM, Russel FGM, and Van Ginneken CAM: Renal clearance of sulphinpyrazone in man. *Eur. J. Clin. Pharmacol.* 31: 473-478 (1986).
78. Little JM, Chari MV, and Lester R: Excretion of cholate glucuronide. *J. Lipid Res.* 26: 583-592 (1985).
79. Lui CY, Lee MG, and Chiou WL: Urinary pH and urine flow independent renal clearance of methotrexate in dogs. *J. Pharmacokinet. Biopharm.* 13: 159-171 (1985).
80. Mályusz M, Girndt J, Mályusz G and Ochwaldt B: Die Metabolisierung von p-Aminohippurate in Nieren von normalen Ratten mit experimentellem Goldblatt-Hochdruck. *Pflugers Arch.* 333: 156-165 (1972).
81. Maiche AG: Acute renal failure due to concomitant action of methotrexate and indomethacin. *Lancet* jun 14: 1390 (1986).
82. Marshall EK, Vickers JL: The mechanism of the elimination of phenol-sulfonphthalein by the kidney; a proof of secretion by the convoluted tubules. *Bull. Johns Hopkins Hosp.* 34: 1-7 (1923).
83. Maunsbach AB: Ultrastructure of the proximal tubule. In: *Handbook of Physiology, Section 8: Renal Physiology*, edited by J Orloff and RW Berliner, pp. 31-79, American Physiological Society, Washington DC (1973).
84. May DG and Weiner IM: Bidirectional active transport of m-hydroxybenzoate in proximal tubule of dogs. *Am. J. Physiol.* 218: 430-436 (1970).

85. May DG and Weiner IM: The renal mechanisms for the excretion of m-hydroxybenzoic acid in Cebus monkey: Relationship to urate transport. *J. Pharmacol. Exp. Ther.* 176: 407-417 (1971).
86. McKinney TD: Heterogeneity of organic base secretion by proximal tubules. *Am. J. Physiol.* 243: F404-407 (1982).
87. Meffin PJ, Zilm DM, and Veenendaal JR: A renal mechanism for the clofibric acid-probenecid interaction. *J. Pharmacol. Exp. Ther.* 227: 739-742 (1983).
88. Milton A and Odilind B: Renal tubular accumulation of organic substances: A new in vivo method which differentiates between luminal and peritubular uptake. *Acta Physiol. Scand.* 123: 237-248 (1985).
89. deMiranda P, Good SS, Laskin OL, Krashny HC, Connor JD, and Lietman PS: Disposition of intravenous radioactive acyclovir. *Clin. Pharmacol. Ther.* 30: 662-672 (1981).
90. Møller JV and Sheikh MI: Renal organic anion transport system: Pharmacological, physiological, and biochemical aspects. *Pharmacol. Rev.* 34: 315-358 (1983).
91. Monks TJ and Lau SS: Renal transport processes and glutathione conjugate-mediated nephrotoxicity. *Drug Metab. Dispos.* 15: 437-441 (1987).
92. Mudge GH, Garlid K, and Weiner IM: Renal tubular secretion of o-acetylaminohippurate. *Am. J. Physiol.* 203: 881-885 (1962).
93. Mudge GH, Berndt WO, Saunders A, and Beattie B: Renal transport of diatrizoate in the rabbit, dog, and rat. *Nephron* 8: 156-172 (1971).
94. Newton JF, Hoefle D, Gemborys MW, Mudge GH, and Hook JB: Metabolism and excretion of a glutathione conjugate of acetaminophen in the isolated perfused rat kidney. *J. Pharmacol. Exp. Ther.* 237: 519-524 (1986).
95. Nissen OI: the extraction fraction of p-aminohippurate in the superficial and deep venous draining of the cat kidney. *Acta Physiol. Scand.* 73: 329-338 (1968).
96. Ochwaldt BK and Pitts RF: Disparity between phenol red and diodrast clearance in the dog. *Am. J. Physiol.* 187: 318-322 (1956).
97. Odilind B: Relation between tubular secretion of furosemide and its saluretic effect. *J. Pharmacol. Exp. Ther.* 208: 515-521 (1979).

98. Odlin B: Relation between tubular secretion and effects of five loop diuretics. *J. Pharmacol. Exp. Ther.* 211: 238-244 (1979).
99. Odlin B, Beermann B, Selén G, and Persson AEG: Renal tubular secretion of piretanide and its effects on electrolyte reabsorption and tubuloglomerular feedback mechanism. *J. Pharmacol. Exp. Ther.* 225: 742-746 (1983).
100. Odlin B, Hällgren R, Sohtell M, and Lindström B: Is ^{125}I iothalamate an ideal marker for glomerular filtration? *Kidney Int.* 27: 9-16 (1985).
101. Owada E, Takahashi K, Hori R, and Arita T: Transformation and excretion of drugs in biological systems. X. Renal excretion mechanisms of sulfonamides in rabbits. *Chem. Pharm. Bull.* 22: 594-600 (1974).
102. Paul MF, Bender RC, and Nohle EG: Renal excretion of nitrofurantoin (Furadantin). *Am. J. Physiol.* 197: 580-584 (1959).
103. Perel JM, Dayton PG, Snell MM, Yü TF, and Gutman AB: Studies of interactions among drugs in man at the renal level. Probenecid and sulfapyrazone. *Clin. Pharmacol. Ther.* 10: 834-840 (1969).
104. Poulsen H and Praetorius E: Tubular excretion of uric acid in rabbits. *Acta Pharmacol. Toxicol.* 10: 371-378 (1954).
105. Praetorius E and Kirk JE: Hypouricemia: With evidence for tubular elimination of uric acid. *J. Lab. Clin. Med.* 35: 856-868 (1950).
106. Pritchard JB: Luminal and peritubular steps in renal transport of p-aminohippurate. *Biochim. Biophys. Acta* 906: 295-308 (1987). (1950).
107. Rennick BR: Renal tubular transport of prostaglandins: Inhibition by probenecid and indomethacin. *Am. J. Physiol.* 233: F133-137 (1977).
108. Rennick BR: Renal tubule transport of organic cations. *Am. J. Physiol.* 240: F83-89 (1981).
109. Roch-Ramel F, Diezi-Chomety F, De Rougement D, Tellier M, Widmer J, and Peters G: Renal excretion of uric acid in the rat: A micropuncture and microperfusion study. *Am. J. Physiol.* 230: 768-776 (1976).
110. Ross CR and Holohan PD: Transport of organic anions and cations in isolated renal plasma membranes. *Ann. Rev. Pharmacol. Toxicol.* 23: 65-85 (1983).

- 111 Rowland M and Tozer TN Clinical Pharmacokinetics Concepts and Applications, pp 48-64, Lea & Febiger, Philadelphia (1980)
- 112 Russel FGM, Wouterse AC, Hekman P, Grutters G, and Van Ginneken CAM Quantitative urine collection in renal clearance studies in the dog J Pharmacol Methods 17 125-136 (1987)
- 113 Russel FGM, Wouterse AC, and Van Ginneken CAM Physiologically based pharmacokinetic model for the renal clearance of phenolsulfonphthalein and the interaction with probenecid and salicylic acid in the dog J Pharmacokinet Biopharm 15 349-368 (1987)
- 114 Russel FGM, Wouterse AC, and Van Ginneken CAM Physiologically based pharmacokinetic model for the renal clearance of salicylic acid and the interaction with phenolsulfonphthalein in the dog Drug Metab Dispos 15 695-701 (1987)
- 115 Russel FGM, Van der Linden PEM, Vermeulen WG, Heijn M, Van Os CH, and Van Ginneken CAM Na^+ and H^+ gradient-dependent transport of p-aminohippurate in membrane vesicles from dog kidney cortex Biochem Pharmacol submitted (1987)
- 116 Schachter D, and Manis JG Salicylate and salicylate conjugates Fluorimetric estimation, biosynthesis, and renal excretion in man J Clin Invest 37 800-807 (1958)
- 117 Schali C and Roch-Ramel F Uptake of ^3H -PAH and ^{14}C -urate into isolated proximal segments of the pig kidney Am J Physiol 241 F591-596 (1981)
- 118 Scheffer VH and Stevens JL Mechanism of transport for toxic cysteine conjugates in rat kidney cortex membrane vesicles Mol Pharmacol 32 293-298 (1987)
- 119 Schuster VL and Seldin DW Renal clearance In The Kidney Physiology and Pathophysiology, edited by DW Seldin and G Gebisch, pp 365-395, Raven Press, New York (1985)
- 120 Shimoda M, Kokue EI, Tanaka N, and Hayama T Contribution of renal active secretion in renal excretion of N^4 -acetylsulfamonomethoxine in conscious pigs J Pharmacobiodyn 9 865-870 (1986)
- 121 Shimomura A, Chonko AM, and Grantham JJ Basis for heterogeneity of para-aminohippurate secretion in rabbit proximal tubules Am J Physiol 240 F430-436 (1981)

122. Singh RR, Malaviya AN, Pandley JN, and Guleria JS: Fatal interaction between methotrexate and naproxen. *Lancet* jun 14: 1390 (1986).
123. Singhvi, SM, Duchin KL, Willard DA, McKinstry DW, and Migdalof BH: Renal handling of captopril: Effect of probenecid. *Clin. Pharmacol. Ther.* 32: 182-189 (1982).
124. Sirota JH, Yü TF, and Gutman AB: Effect of benemid (p-(di-n-propylsulfamyl)-benzoic acid) on urate clearance and other discrete renal functions in gouty subjects. *J. Clin. Invest.* 31: 692-701 (1952).
125. Sjövall J, Westerlund D, and Alván G: Renal excretion of intravenously infused amoxycillin and ampicillin. *Br. J. Clin. Pharmacol.* 19: 191-201 (1985).
126. Skeith MD, Sunkin PA, and Healey LA: Renal excretion of indomethacin and its inhibition by probenecid. *Clin. Pharmacol. Ther.* 9: 89-93 (1978).
127. Smith AG and Francis JE: Evidence for the active renal secretion of S-pentachlorophenyl-N-acetyl-L-cysteine by female rats. *Biochem. Pharmacol.* 32: 3797-3801 (1983).
128. Smith DE and Lau HSH: Determinants of bumethanide response in the dog: Effect of probenecid. *J. Pharmacokinet. Biopharm.* 11: 31-46 (1983).
129. Smith HW, Goldring W, and Chasis H: The measurement of the tubular excretory mass, effective blood flow and filtration rate in the normal human kidney. *J. Clin. Invest.* 17: 263-278 (1938).
130. Smith HW, Finkelstein N, Aliminos L, Crawford B, and Graber M: The renal clearances of substituted hippuric acid derivatives and other aromatic acids in dog and man. *J. Clin. Invest.* 24: 388-404 (1945).
131. Smith HW: *The Kidney: Structure and function in health and disease*, Oxford University Press, New York (1951).
132. Somogyi A: New insights into the renal secretion of drugs. *Trends Pharmacol. Sci.* 8: 354-357 (1987).
133. Sperber I: The excretion of some glucuronic acid derivatives and phenol sulfuric esters in the chicken. *Ann. R. Agric. Coll. Sweden* 15: 317-349 (1948).

134. Thyss A, Milano G, Kubar J, Namer M, and Schneider M: Clinical and pharmacokinetic evidence of a life-threatening interaction between methotrexate and ketoprofen. *Lancet* feb. 1: 256-258 (1986).
135. Tucker GT: Measurement of the renal clearance of drugs. *Br. J. Clin. Pharmac.* 12: 761-770 (1981).
136. Tune BM, Burg MB, and Patlak CS: Characteristics of p-aminohippurate transport in proximal renal tubules. *Am. J. Physiol.* 217: 1057-1063 (1969).
137. Tune BM, Fernhold M, and Schwartz A: Mechanism of cephaloridine transport in the kidney. *J. Pharmacol. Exp. Ther.* 191: 311-317 (1974).
138. Tune BM: Relationship between the transport and toxicity of cephalosporins in the kidney. *J. Infect. Dis.* 132: 189-194 (1975).
139. Ullrich KJ and Greger R: Approaches to the study of tubule transport functions. In: *The Kidney: Physiology and Pathophysiology*, edited by DW Seldin and G Giebisch, pp. 427-469, Raven Press, New York (1985).
140. Ullrich KJ, Rummrich G, Klöss, and Lang HJ: Contraluminal sulfate transport in the proximal tubule of the rat kidney. V. Specificity: phenolphthaleins, sulfonphthaleins, and other sulfo dyes, sulfamoyl-compounds and diphenylamine-2-carboxylates. *Pflügers Arch.* 404: 311-318 (1985).
141. Ullrich KJ, Rummrich G, Fritsch G, and Klöss S: Contraluminal para-aminohippurate (PAH) transport in the proximal tubule of the rat kidney. II. Specificity: aliphatic dicarboxylic acids. *Pflügers Arch.* 408: 38-45 (1987).
142. Ullrich KJ, Rummrich G, and Klöss S: Contraluminal para-aminohippurate (PAH) transport in the proximal tubule of the rat kidney. III. Specificity: monocarboxylic acids. *Pflügers Arch.* 409: 547-554 (1987).
143. Van Ginneken CAM: Pharmacokinetics of antipyretic and anti-inflammatory analgesics. pp. 109-119, PhD Thesis, Nijmegen (1976).
144. Van Ginneken CAM and Russel FGM: Carrier-mediated transport in the renal handling of drugs. In: *Topics in Pharmaceutical Sciences*, edited by DD Breimer and P Speiser, pp. 155-165, Elsevier, Amsterdam (1983).

145. Vree TB, Hekster CA, Braakman M, Janssen T, Oosterbaan M, Termond E, and Tjhuis M: Pharmacokinetics, acetylation-deacetylation, renal clearance, and protein binding of sulphamerazine, N_4 -acetylsulphamerazine, and N_4 -trideuteroacetylsulphamerazine in 'fast' and 'slow' acetylators. *Biopharm. Drug Dispos.* 4: 271-291 (1983).
146. Vree TB, Hekster YA, Tjhuis MW, Termond EFS, and Nouws JFM: Pharmacokinetics, metabolism and renal excretion of sulfatroxazole and its 5-hydroxy- and N_4 -acetylmetabolites in man. *Biopharm. Drug Dispos.* 7: 239-252 (1986).
147. Vree TB, Wijnands WJA, Guelen PJM, Baars AM, and Hekster YA: Pharmacokinetics: metabolism and renal excretion of quinolones in man. *Pharm. Weekbl. (Sci.)* 8: 29-34 (1986).
148. Watari N, Aizawa K, and Kaneniwa N: Dose- and time-dependent kinetics of the renal excretion of nitrofurantoin in the rabbit. *J. Pharm. Sci.* 74: 165-170 (1985).
149. Watrons WM, May DG, and Fujimoto JM: Mechanism of the renal tubular transport of morphin and MES in the chicken. *J. Pharmacol. Exp. Ther.* 172: 224-229 (1970).
150. Weiner IM, Washington JA II, and Mudge GH: Studies on the renal excretion of salicylate in the dog. *Bull. Johns Hopkins Hosp.* 105: 284-297 (1959).
151. Weiner IM, Washington JA II, and Mudge GH: On the mechanism of action of probenecid on renal tubular secretion. *Bull. Johns Hopkins Hosp.* 106: 333-346 (1960).
152. Weiner IM, Blanchard KC, and Mudge GH: Factors influencing renal excretion of foreign acids. *Am. J. Physiol.* 207: 953-963 (1964).
153. Weiner IM and Tinker JP: Pharmacology of pyrazinamide: Metabolic and renal function related to the mechanism of drug induced urate retention. *J. Pharmacol. Exp. Ther.* 180: 411-434 (1972).
154. Weiner IM: Transport of weak acids and bases. In: *Handbook of Physiology, Section 8: Renal Physiology*, edited by J Orloff and RW Berliner, pp. 521-554, American Physiological Society, Washington DC (1973).
155. Weiner IM: Organic acids and bases and uric acid. In: *The Kidney: Physiology and Pathophysiology*, edited by DW Seldin G Giebisch, pp. 1703-1724, Raven Press, New York (1985).

156. Weinman EJ, Frankfurt SJ, Ince A, and Samsom S: Renal tubular transport of organic acids. Studies with oxalate and para-aminohippurate in the rat. *J. Clin. Invest.* 61: 801-806 (1978).
157. Welling PG: Pharmacokinetics of the thiazide diuretics. *Biopharm. Drug Dispos.* 7: 501-535 (1986).
158. Wilkinson GR: Clearance approaches in pharmacology. *Pharmacol. Rev.* 39: 1-47 (1987).
159. Williams WM, and Huang KC: Structural specificity in the renal tubular transport of tyrosine. *J. Pharmacol. Exp. Ther.* 219: 69-74 (1981).
160. Woodhall PB, Tisher CC, Simonson CA, and Robinson RK: Relationship between para-aminohippurate secretion and cellular morphology in rabbit proximal tubules. *J. Clin. Invest.* 61: 1320-1329 (1978).
161. Wu H and Elliott HC: Urinary excretion of hippuric acid by man. *J. Appl. Physiol.* 16: 553-556 (1961).
162. Yü TF and Gutman AB: Paradoxical retention of uric acid by uricosuric drugs in low dosage. *Proc. Soc. Exp. Biol. Med.* 90: 542-547 (1955).
163. Yü TF and Gutman AB: Study of the paradoxical effects of salicylate in low, intermediate and high dosage on the renal mechanisms for excretion of urate in man. *J. Clin. Invest.* 38: 1298-1315 (1959).
164. Zaharko DS, Bolten BJ, Chinten D, and Wiernik PH: Pharmacokinetic studies during phase I trials of high-dose thymidine infusions. *Cancer Res.* 39: 4777-4781 (1979).
165. Zins GR, and Weiner IM: Bidirectional transport of taurocholate by the proximal tubule of the dog. *Am. J. Physiol.* 215: 840-845 (1968).

QUANTITATIVE URINE COLLECTION IN RENAL CLEARANCE
STUDIES IN THE DOG¹

Frans G.M. Russel, Alfons C. Wouterse, Peter Hekman, Gerry J. Grutters^ζ, and Cees A.M. van Ginneken

Abstract - A double-walled urinary catheter is described which allows rapid and quantitative urine collection at short time intervals. The catheter consists of a polyurethane outer cannula in which a small Teflon cannula is inserted. The essential of the catheter is that at the end of a collection period residual urine in the bladder can be collected completely via the outer cannula by flushing the bladder with physiological salt through the inner cannula. In this manner urine can be collected in a very reproducible way at intervals down to 5 min. The use of the catheter was illustrated in a study on the renal clearance of hippuric acid in the dog. Plasma concentration and renal excretion rate were followed after i.v. injection of 0.9 g sodium hippurate. In accordance with previous studies, it was found that the renal excretion of hippuric acid consisted of glomerular filtration and active tubular secretion. A large variability was observed in the tubular transport maximum (3800 - 11600 µg/min) and the Michaelis-Menten constant (22 - 190 µg/ml), which were used to characterize the secretory system. The interpretation and value of these transport parameters is discussed briefly.

¹Published in: J. Pharmacol. Methods 17, 125-136 (1987).

^ζCentral Animal Laboratory, University of Nijmegen

2.1 INTRODUCTION

Renal clearance is one of the major routes of elimination of drugs and their metabolites in the living organism. Especially when renal clearance contributes significantly to the total elimination of a drug, knowledge of the basic processes that determine transport is of great importance with relation to the duration and extent of effects and side-effects of the drug. The mechanisms that contribute to the renal excretion of a drug are directly related to the physiology of the kidney, but will also depend upon the plasma protein binding and upon the physicochemical properties of the substance. From a kinetic point of view four different transport processes can be distinguished, viz., glomerular filtration, passive back diffusion, active tubular secretion, and active tubular reabsorption [1]. Glomerular filtration and back diffusion can be considered as passive processes in which the transport rates are linearly related to the plasma drug concentration. Active secretion and active reabsorption are carrier-mediated processes; they are characterized by saturability and susceptibility to competition by structurally related compounds.

In pharmacokinetics the parameter clearance is used to describe the loss of drug across an eliminating organ. The kidney takes a privileged role in organ clearance studies in that it is the only organ that allows relatively easy and direct sampling at the site of excretion without invasive methods. The renal clearance of a drug is defined as the ratio of renal excretion rate over the plasma concentration at the same time. In practice urine is collected over a finite period and the mean excretion rate is estimated by dividing the amount excreted in the sample by the time interval. The appropriate plasma concentration is determined at the midpoint of the urine collection interval, assuming that the plasma concentration changes linearly with time. It is obvious that this will practically never be the case and that the assumption of linear change is only valid for small collection intervals. This implies that an accurate determination of the course of renal drug clearance, especially when carrier-mediated processes are involved, requires quantitative collection of the urine produced during short time intervals.

Several techniques were described for the collection of urine from mammals, including surgical procedures in which one or both ureters are can-

nulated [2-5] In the noninvasive methods urine is usually collected through a single-walled cannula that is brought into the bladder via the urethra A major disadvantage of such a catheter is that it can give rise to incomplete emptying of the bladder, especially when the sampling intervals need to be small This causes contamination of the urine sample with residual urine from the foregoing collection interval, and incorrect estimations of urine flow and renal excretion rate will be the result In this paper a double-walled urinary catheter is described which allows quantitative urine sampling at intervals down to 5 min During a collection period it is used as a conventional catheter through which the produced urine flows constantly via the outer cannula The essential point is that at the end of a collection period, the residual urine in the bladder now can be collected completely by rinsing the bladder with a measured amount of physiological salt through the inner cannula The usefulness of the catheter is demonstrated on the basis of a study on the renal clearance of hippuric acid in the dog

2.2 MATERIALS AND METHODS

Materials

The Braunule T cannulas were obtained from Braun (Melsungen, FRG), the double-walled urinary catheter (URO 90 009) from Talas (Ommen, The Netherlands) The infusion sets used were from Medica (Den Bosch, The Netherlands) and were equiped with a disposable Dial-a-flow from Abbott (Amstelveen, The Netherlands) to adjust the flow Urinary pH was measured with a Sensorex pH electrode, Sensorex (Westminster, USA) Blood was withdrawn into heparinized 10 ml Monovettes from Sarstedt (Eindhoven, The Netherlands) Sodium hippurate was purchased from British Drug Houses Ltd (Poole, England), LiChrosorb RP18 and salicyluric acid from Merck (Darmstadt, FRG), sodium pentobarbital from Apharma (Arnhem, The Netherlands), heparin from Organon (Oss, The Netherlands), atropine sulphate, mannitol and inulin from O P G (Utrecht, The Netherlands). Ilibitan[®] from ICI Holland (Rotterdam, The Netherlands), Albipen[®] from Gist Brocades (Delft, The Netherlands), Aqualuma plus from Lumac (Schaesberg, The Netherlands), [³H]inulin (1.59 Ci/mmol)

from The Radiochemical Centre, Amersham (Buckinghamshire, England), and Visking 8 dialysis tubing from Instrumentenhandel Z.H. (Den Haag, The Netherlands). All other chemicals were of analytical grade and were purchased from Merck (Darmstadt, FRG).

Analytical Methods

Hippuric acid (HA) was determined in plasma and urine by high performance liquid chromatography. A Hewlett Packard 1084B was used equipped with a variable wavelength detector, autosampler and terminal (HP 7850 LC). The stainless-steel column (150 × 4.6 mm I D.) was packed with LiChrosorb RP-18, particle size 5 µm. The mobile phase consisted of a mixture of methanol and twice-distilled water (30:70) containing 0.01 M citrate (pH 2.6) and was delivered at a rate of 1.0 ml/min. The column temperature was 40°C and the detector wavelength was set at 245 nm. Under these conditions the retention times of HA and the internal standard salicyluric acid were 3.3 and 5.5 min respectively.

Into a screw-capped extraction tube 1.0 ml plasma, 100 µl internal standard solution (500 µg/ml in methanol) and 5.0 ml methanol were pipetted. After shaking for 1 min, the tube was centrifuged for 15 min at 2000g. The supernatant was transferred into another test tube and evaporated to dryness at 30°C with dry filtered air. The residue was redissolved in 1.0 ml of the mobile phase and 10 µl was injected into the column. To 100 µl of the urine samples 100 µl internal standard and 800 µl mobile phase were added, after which 10 µl was injected into the HPLC system. The HA concentration in plasma and urine was determined by comparing the peak area ratio of HA and internal standard with a standard curve of peak area ratio versus HA concentrations spiked to blank plasma and urine. Linear calibration curves were obtained in all cases.

Concentrations of [³H]inulin in plasma and urine were estimated in a Packard 3370 liquid scintillation counter. Samples of 0.5 ml plasma or urine were placed in a 20 ml counting vial and 10 ml scintillation fluid (Aqualuma plus) was added. Quench correction of samples was carried out using the channels-ratio method.

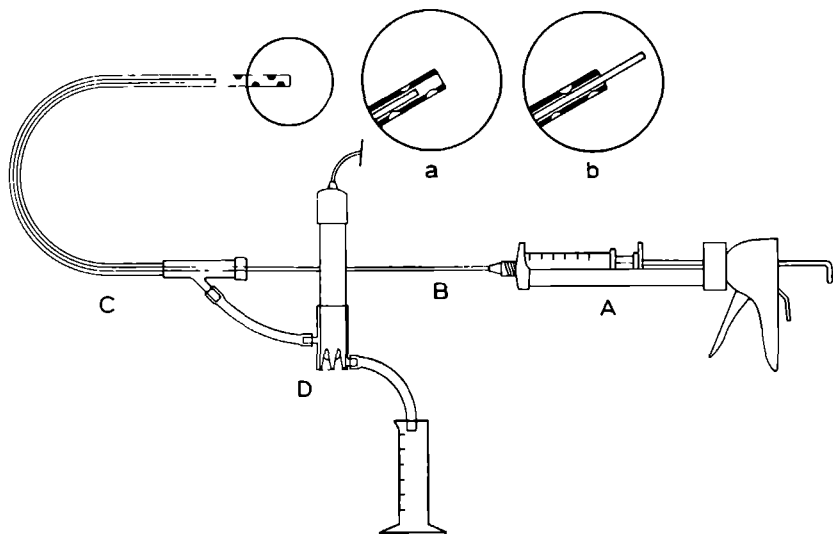


Fig. 2.1 Experimental setup for the quantitative collection of urine. The double-walled catheter (C) is provided at the tip with four perforations (a) to prevent obstruction by the bladder wall. When the catheter is brought into the bladder the inner cannula (B) is pushed forward, so that the tip sticks out of the outer cannula (b). Urine flows through the outer cannula via a perspex vial with a pH electrode (D) into a measuring glass. The bladder is flushed through the inner cannula with a plastic syringe placed in a hand-operated gun (A).

Urinary Catheter

For the quantitative collection of urine samples, a double-walled catheter was developed in our laboratory. The catheter consists of polyurethane outer tubing having a length of 45 cm (2 mm I.D. \times 3 mm O.D.) and a 70 cm long inner cannula of Teflon (0.5 mm I.D. \times 1.0 mm O.D.) (Fig. 2.1C). The outer cannula is provided at the tip, over a distance of 5 cm, with four perforations having a diameter of approximately 3 mm (Fig. 2.1a,b). In this manner variations in urine flow caused by obstruction of the catheter by the bladder wall is prevented. The inner cannula is attached to a 60 ml plastic syringe and is inserted in the outer cannula through an Y-shaped connection sealed with silicone rubber

(Fig. 2.1B). Through this cannula the bladder can be rinsed at the end of a urine collection period. To ease this flushing procedure the syringe is placed in a hand-operated gun, obtained from a local tool shop, which is usually used for the application of plastic sealant (Fig. 2.1A). The voided urine flows through the outer cannula in a perspex vial in which a pH electrode fits (Fig. 2.1D). Finally, the urine is collected and the volume is measured.

Clearance Experiments

Male Beagle dogs, weighing 12 to 16 kg, were fasted overnight and anesthetized by intravenous administration of 30 mg/kg of pentobarbital sodium. As premedication, atropine sulfate (0.5%, 1 ml i.v.) was given to prevent vagal inhibition of the heart and to reduce salivary and bronchial secretions. After induction of anesthesia, the dogs received endotracheal intubation and were ventilated with room air using a Harvard (model 607) ventilator. The cephalic veins of both forelegs were cannulated (Braunule T, length 50 mm, ϕ 1.0 \times 1.5 mm) for blood sampling and drug administration purposes. A constant infusion of 5% mannitol and 0.5% inulin (2 ml/min) was administered throughout the experiment in order to obtain a sufficiently high and constant urine flow. The pH of the voided urine was controlled by an infusion of 8.4% sodium bicarbonate at a rate (3-8 ml/min) such that the urinary pH remained at a level of 7.0 ± 0.5 .

Each dog received as an i.v. bolus a solution of 0.9 g sodium hippurate in 10 ml water, sterilized by filtration. At regular times throughout the experiment blood samples were taken into heparinized tubes. The first 0.5 ml of a blood sample were discarded in order to fill and rinse the dead volume of the cannula (approximately 0.2 ml). Plasma was separated by centrifugation for 20 min at 2000g and stored at -20°C until analysis. After a blood sample was taken, the collecting cannula was flushed with 0.5 ml heparin (50 U/ml) in physiological salt to prevent coagulation.

Urine was collected during the first 50 min of the experiment at 5 min intervals, and afterwards at 10 min intervals. The double-walled urinary catheter was introduced through the urethra into the bladder using a 1% chlorhexidine gluconate antiseptic cream (Hibitane[®]) as lubricant. While the catheter was inserted, care was taken that the tip of the inner can-

nula was just inside the outer cannula (Fig. 2.1a). Once inside the bladder, the inner cannula was pushed further into the outer cannula so that the tip stuck out for about 0.5 cm (Fig. 2.1b). Up to 90 sec before the end of a collection period, the produced urine flowed through the outer cannula and the urinary pH was constantly measured. At that time the bladder was rinsed in about 30 sec with exactly 15 ml of physiological salt via the inner cannula. In the remaining 60 sec, the diluted bladder content was allowed to flow from the bladder through the outer cannula. The volume of voided urine and physiological salt was registered, and a sample was stored at -20°C until analysis.

After the last blood and urine samples for the determination of HA were taken, the glomerular filtration rate was estimated by steady state inulin clearance during infusion of [^3H]inulin. The [^3H]inulin was added to the 5% mannitol and 0.5% inulin infusion resulting in an activity of 0.04 $\mu\text{Ci/ml}$. At the same time 1 ml of this solution, but with an activity of 3.3 μCi [^3H]inulin/ml, was rapidly injected. In this manner a constant plasma concentration of inulin (approximately 100 $\mu\text{g/ml}$) was obtained after about 15 min. During the following 40 min six blood samples were taken and urine was collected quantitatively every 5 min.

At the end of the experiment, the cannulas and the urinary catheter were removed, and the dog was allowed to recover. Ampicillin (Albipen[®] 15%, 0.1 ml/kg) was given subcutaneously to protect against infections. The dog was kept in quarantine until radioactivity of the voided urine was less than 1 pCi/ml. Before the dog was used for another experiment, at least 3 weeks of recovery were observed. In this way dogs could be used many times for an experiment.

Protein Binding

Plasma protein binding of HA was determined by ultrafiltration using Visking dialysis tubing (flat width, 10 mm; average pore, size 2.4 nm). The tubing was cut into pieces of 10 cm and soaked in distilled water for 1 hour. Excess of water was removed by gentle wiping. One end of the tube was knotted, and 2 ml of plasma were carefully pipetted into the open end. Then the open end was knotted and the tubes were folded in a U-shape into a centrifuge tube. First the water bound to the membrane was removed by precentrifugation for 10 min at 1000g. After that the

bags were transferred to another tube and centrifuged at 1000g for the time required to obtain 150-200 μ l ultrafiltrate (approximately 60 min). With this procedure, volume reduction of the plasma sample was less than 10%, leaving the protein binding equilibrium almost unaffected. No significant binding of HA was found to the dialysis membrane. Ultrafiltrates were treated and analyzed in the same way as urine samples were.

Pharmacokinetic Analysis

Plasma concentration and renal excretion rate curves were fitted separately to a linear open two compartment model. Applying statistical moments theory, basic pharmacokinetic parameters were estimated [6,7]. First the area under the plasma curve (AUC), the area under the first moment of the plasma curve (AUMC), and the area under the renal excretion rate curve (AUR_R) were calculated. Total plasma clearance (CL) was defined as the reciprocal of the AUC normalized for the dose (D):

$$CL = D/AUC \quad (2.1)$$

The mean residence time was determined as,

$$MRT = AUMC/AUC \quad (2.2)$$

and the volume of distribution at steady state (V_{ss}) was calculated from the product of clearance and mean residence time:

$$V_{ss} = CL \cdot MRT \quad (2.3)$$

Renal clearance (CL_R) was estimated by the total excretion method,

$$CL_R = CL \cdot \frac{AUR_R}{D} = \frac{AUR_R}{AUC} \quad (2.4)$$

where AUR_R equals the total amount of the compound excreted unchanged.

The renal excretion process of HA was analyzed in detail by fitting the renal excretion rate (R_R) as a function of the average plasma concentration (C) over each urine collection period according to the following equation:

$$R_R = (f_u \cdot GFR + \frac{T_M}{K_T + C}) \cdot C \quad (2.5)$$

where f_u is the fraction of unbound drug in plasma, GFR is the glomerular filtration rate determined by inulin clearance, T_M is the tubular transport maximum and K_T is the Michaelis-Menten constant of the secretion system [8,9].

Curve fitting was done by least-squares nonlinear regression analysis in which all data were equally weighted, using the computer program NONLIN [10]. All values are expressed as mean \pm standard deviation (SD).

2.3 RESULTS

The use of the urinary catheter in clearance experiments is shown schematically in Fig. 2.1. To prevent injury of the urethra the hard inner cannula was pulled back in the outer cannula while the catheter was brought into the bladder. After the catheter was placed in the bladder, the inner cannula was pushed forward to allow unhindered rinsing of the bladder. This flushing procedure takes not more than 90 sec, namely about 30 sec to bring in 15 ml of physiological salt and at most 60 sec to recover the saline and residual urine completely from the bladder. Until recently the double-walled catheter, which is easy to construct, was made by ourselves from the cannulas described. In the meanwhile, the catheter has become also commercially available from Talas (Ommen, The Netherlands).

To demonstrate the value of the catheter in clearance studies, the renal clearance of hippuric acid (HA) was studied in four dogs. Fig. 2.2 shows a representative example of the course of plasma concentration and renal excretion rate of HA after i.v. injection in one of the animals. The measured plasma and urine curves could be described well mathematically by a two-compartment open model. All curves were fitted separately to this model by nonlinear regression analysis. The relevant pharmacokinetic parameters obtained from these fits are given in Table 2.1. The HA was

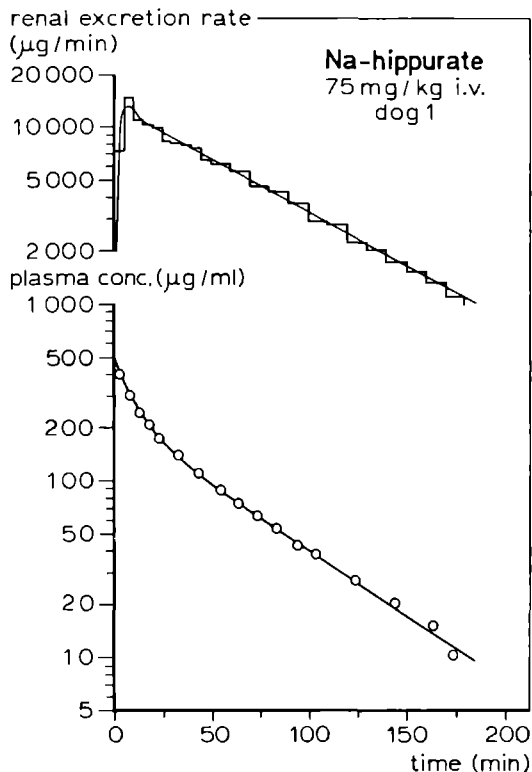


Fig. 2.2 Renal excretion rate and plasma concentration as a function of time after rapid i.v. injection of 0.93 g sodium hippurate into dog 1. The curves through the experimental data were obtained by fitting the plasma and urine data separately to a linear open two compartment model.

rapidly cleared from the circulation and excreted almost completely ($92.0 \pm 7.0\%$) into the urine. Endogenous HA levels were negligible compared to the concentrations obtained in plasma and urine after administration of exogenous HA. Deconjugation of the glycine moiety, as was described by Quick [11] in the nephrectomized dog, was not observed. Neither in plasma nor in urine could the uncoupled product benzoic acid be detected.

The glomerular filtration rate (GFR) of each dog was estimated by steady state $[^3\text{H}]$ inulin clearance directly after the HA experiment (Table 2.1). Preliminary studies, in which the inulin clearance was monitored

Table 2.1 Pharmacokinetic parameters characterizing the renal handling of hippuric acid.

Dog	Weight (kg)	Dose (g)	Urine flow ^a (ml/min)	Urine pH ^a	GFR ^b (ml/min)	fu ^b	MRT ^b (min)	CL ^b (ml/min)	CL _R ^b (ml/min)	V _{ss} ^b (ml)
1	12.4	0.93	0.87	7.0	42	0.66	50	60	59	3000
2	16.5	0.93	1.11	6.6	65	0.74	36	100	88	3600
3	12.0	0.93	0.89	7.0	31	0.79	63	54	52	3400
4	13.0	0.94	0.81	7.3	33	0.75	52	63	53	3300
Mean	13.5	0.93	0.92	7.0	43	0.74	50	69	63	3300
S.D.	2.1	0.01	0.13	0.3	16	0.05	11	21	17	300

^aWeighted average of all urine samples.

^bGFR = glomerular filtration rate determined by inulin clearance; fu = free fraction of the drug in plasma; MRT = mean residence time; CL = total plasma clearance; CL_R = overall renal clearance; and V_{ss} = volume of distribution at steady state.

during the entire experiment, revealed that the GFR remained constant throughout the experiment and was not different from the GFR determined after the last samples for HA analysis had been taken (Russel et al., unpublished results). Measurement of plasma protein binding demonstrated that the fraction of unbound HA was virtually constant over the concentration range of 5 - 450 $\mu\text{g/ml}$ with an average value of 0.74 (Table 2.1). Urine flow and urine pH were kept as constant as possible throughout the experiment. Average values of each experiment are given in Table 2.1. Fig. 2.3 shows a representative example of the course of urine flow and pH during one of the experiments.

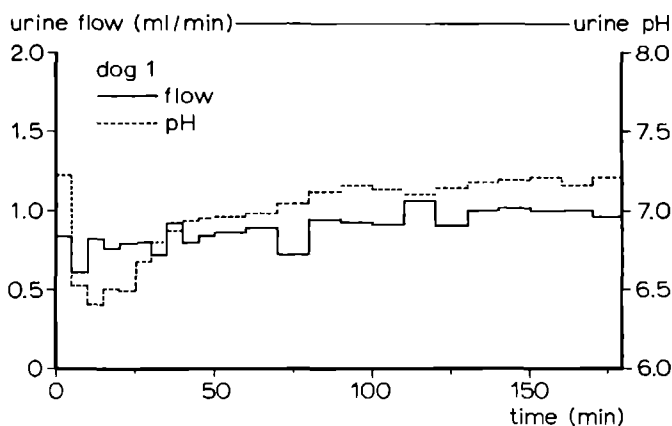


Fig. 2.3 Course of the urine flow and urine pH during the experiment shown in Fig. 2.2.

A plot of the renal excretion rate against the plasma concentration, the so-called tubular titration curve, is one of the best ways to examine the processes that determine the renal clearance of a drug. In Fig. 2.4 such a plot is shown for HA in one of the dogs. If only glomerular filtration would occur, the plot should yield a straight line representing the product of the inulin clearance and the fraction of unbound drug in plasma. However, it is clear from Fig. 2.4 that the renal excretion of HA exceeds by far the amount that enters the urine by glomerular filtration, which also indicates that tubular secretion occurs. The observed excretion profiles could be described by the summation of glomerular filtration and

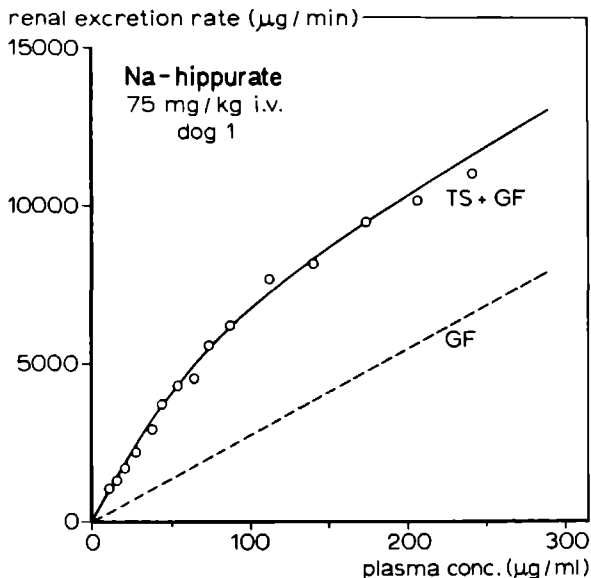


Fig. 2.4 Relationship between the renal excretion rate and the plasma concentration of sodium hippurate after i.v. administration of 0.93 g to dog 1. The renal excretion process can be described by a combination of glomerular filtration (GF) and tubular secretion (TS). The solid line represents the curve calculated after fitting the data to Eq. 2.5, the dotted line reflects the glomerular filtration of the drug.

active tubular secretion. Assuming that the tubular secretion of HA conforms Michaelis-Menten kinetics and is dependent on the total plasma drug concentration, the tubular titration curves were analyzed with NONLIN according to Eq. 2.5. The results of these fits are summarized in Table 2.2.

2.4 DISCUSSION

In studying the renal handling of drugs, it is of crucial importance that the urinary excretion of a drug be measured accurately. Errors may arise from incomplete emptying of the bladder after a collection period, or

Table 2.2 Tubular transport maximum (T_M) and Michaelis-Menten constant (K_T) characterizing the active renal secretion of hippuric acid.

Dog	T_M ($\mu\text{g}/\text{min}$)	K_T ($\mu\text{g}/\text{ml}$)
1	6800 \pm 500	80 \pm 14
2	4900 \pm 300	22 \pm 4
3	3800 \pm 400	39 \pm 13
4	11600 \pm 1300	190 \pm 33

Data are presented as means \pm SD

from too large collection intervals with relation to the changes in renal excretion rate. In this paper a double-walled catheter is described that makes it possible to collect urine quantitatively at short intervals in dog clearance experiments. The method appears to be highly reproducible and allows a very detailed study of the mechanisms that govern renal drug clearance. The dog was chosen for the in vivo model because of the good physiological resemblance between the human and dog kidney [12]. Also, a somewhat larger animal makes it possible to collect a relatively large amount of blood and urine samples. An additional advantage of the model is that because of the noninvasive methods the dogs can be used several times for different clearance experiments, so that, if desired, interindividual variations can be eliminated.

To illustrate the abilities of the in vivo model, the renal clearance of HA was studied. It can be concluded from the experiments that the excretion of HA is composed of at least two processes, i.e., glomerular filtration and active tubular secretion. These results are in good agreement with previous studies [13-15]. Passive reabsorption by nonionic diffusion is very unlikely under the experimental circumstances, because of the high urine flow and the high urinary pH compared to the dissociation constant of HA ($\text{pK}_a = 3.80$). The HA is cleared almost completely via the kidney without further metabolism. A small part of the dose is eliminated extrarenally, presumably via the liver. A possible deglycina-

tion reaction could not be detected and will be also very improbable, because such a reaction was only described to occur under very unphysiological conditions [11].

Quantitative analysis of the active tubular secretion of HA revealed that there is a considerable interindividual variability in affinity and transport capacity. The tubular transport maximum (T_M) ranged from 3800 to 11600 $\mu\text{g}/\text{min}$ (21 - 65 $\mu\text{mol}/\text{min}$) and the Michaelis-Menten constant (K_T) from 22 to 190 $\mu\text{g}/\text{ml}$ (0.12 - 1.06 mM). Comparable intersubject variations were also observed by Knoefel and Huang [13]. In this context, it should be emphasized that the characterization of the excretion process of HA by Eq. 2.5 is merely an operational one. Several factors that are of influence on the carrier-mediated transport, e.g., protein binding, actual drug concentration at the site of transport, cellular retention etc., are not taken into consideration in this approach [16]. Therefore, the parameters T_M and K_T found in this way have to be looked upon as apparent constants. In order to account for all the typical features concerning the renal handling of drugs, more physiologically based pharmacokinetic models are required [17,18]. In a forthcoming paper attention will be paid to the use of these models to come to a comprehensive understanding of renal transport mechanisms of drugs in the described dog model.

2.5 REFERENCES

1. Weiner, I.M. (1973) Transport of weak acids and bases. In: Handbook of Physiology (Orloff, J., Berliner, R.W., eds.), pp. 521-554, American Physiological Society, Washington DC.
2. Domer, F.R. (1971) Animal Experiments in Pharmacological Analysis. pp. 529-564, Charles C. Thomas, Springfield Illinois.
3. White, W.A. (1971) A technic for urine collection from anesthetized male rats. Lab. Anim. Sci. 21, 401-402.
4. Lloyd, W.E., Buck, W.B. (1971) Technique for semipermanent cannulation of ureters in bovine, ovine, porcine, and canine species. Am. J. Vet. Res. 32, 817-821.

5. Staskin, D.R., Parsons, K.F., Levin, R.M., Wein, A.J. (1981) A new technique for chronic catheterization of female dogs. *Invest. Urol.* 19, 109-110.
6. Yamaoka, K., Nakagawa, T., Uno, T. (1978) Statistical moments in pharmacokinetics. *J. Pharmacokinet. Biopharm.* 6, 547-558.
7. Benet, L.Z., Galeazzi, R.L. (1979) Noncompartmental determination of the steady-state volume of distribution. *J. Pharm. Sci.* 68, 1071-1074.
8. Hori, R., Sunayashiki, K., Kamiya, A. (1976) Pharmacokinetic analysis of the renal handling of sulfamethizole. *J. Pharm. Sci.* 65, 463-465.
9. Garrett, E.R. (1978) Pharmacokinetics and clearances related to renal processes. *Int. J. Clin. Pharmacol.* 16, 155-172.
10. Metzler, C.M., Elfring, G.L., McEwen, A.J. (1974) A package of computer programs for pharmacokinetic modeling. *Biometrics* 30, 562-563.
11. Quick, A.J. (1932) The site of synthesis of hippuric acid and phenylaceturic acid in the dog. *J. Biol. Chem.* 90, 73-82.
12. Kessler, R.H. (1962) Clinical pharmacology of chlorothiazide compounds. *Clin. Pharmacol. Ther.* 3, 109-118.
13. Knoefel, P.K., Huang, K.C. (1959) Biochemorphology of renal tubular transport: hippuric acid and related substances. *J. Pharmacol. Exp. Ther.* 126, 296-303.
14. Elliott, H.C., Walker, A.A. (1964) Fluorometric microanalysis of plasma hippuric acid and comparison of hippurate with p-aminohippurate clearances in dogs. *Proc. Soc. Exp. Biol. Med.* 116, 268-270.
15. Wan, S.H., Riegelman, S. (1972) Renal contribution to overall metabolism of drugs I: Conversion of benzoic acid to hippuric acid. *J. Pharm. Sci.* 61, 1278-1284.
16. Van Ginneken, C.A.M., Russel, F.G.M. (1983) Carrier-mediated transport in the renal handling of drugs. In: *Topics in Pharmaceutical Sciences* (Breimer, D.D., Speiser, P., eds.), pp. 155-165, Elsevier, Amsterdam.
17. Hekman, P., Van Ginneken, C.A.M. (1982) Kinetic modeling of the renal excretion of iodopyracet in the dog. *J. Pharmacokinet. Biopharm.* 10, 77-92.

18. Gerlowski, L.E., Jain, R.H. (1983) Physiologically based pharmacokinetic modeling: principles and applications. J. Pharm. Sci. 72, 1103-1127.

PART II

PHYSIOLOGICALLY BASED KIDNEY MODEL

A picture of reality drawn in a few sharp lines cannot be expected to be adequate to the variety of all its shades. Yet even so the draftsman must have the courage to draw the lines firm.

Hermann Weyl

RENAL CLEARANCE OF PHENOLSULFONPHTHALEIN AND THE
INTERACTION WITH PROBENECID AND SALICYLURIC ACID¹

Frans G.M. Russel, Alfons C. Wouterse, and Cees A.M. van Ginneken

Abstract - Plasma kinetics and renal excretion of intravenous phenolsulfonphthalein (PSP, 1.0 g), with and without concomitant administration of probenecid or salicyluric acid (SUA), were studied in the Beagle dog. Pharmacokinetic analysis revealed that tubular secretion is the predominant route of excretion, and that secretion is inhibited by probenecid and SUA. A physiologically based kidney model was developed that incorporates the functional characteristics of the kidney that determine the excretion of PSP, i.e., renal plasma flow, urine flow, nonlinear protein binding, glomerular filtration, tubular secretion and tubular accumulation. The model enabled an accurate description and analysis of the measured plasma levels and renal excretion rates. The interaction with probenecid and SUA could be adequately described with the model by inhibition of the carrier-mediated uptake of PSP into the proximal tubular cells. However, both compounds clearly differed in their inhibitory action. Whereas probenecid showed simple competitive inhibition, for SUA a considerably more complex interaction (two-site competitive system) had to be taken into consideration. Especially in the interaction experiments, only satisfactory fits to the model were obtained when secretion was assumed to be dependent on unbound PSP concentrations. Model calculations showed that in the control experiments tubular secretion was accompanied by a pronounced accumulation of PSP within the proximal tubular cells, which was

¹Published in: J. Pharmacokinet. Biopharm. 15, 349-368 (1987).

clearly diminished in presence of probenecid or SUA. The predicted accumulation ratios were in good agreement with previous studies.

3.1 INTRODUCTION

Phenolsulfonphthalein (PSP) is an indicator dye that is actively secreted by the proximal tubules of the kidney. Ever since evidence was obtained for its tubular secretion [1], PSP has been studied extensively as a model substrate for the renal organic anion transport system. The first step in secretion involves active transport at the basolateral membrane into the tubule cell, followed by a less efficient transport across the brush-border membrane into the tubular fluid. The slower transfer to the lumen consequently contributes to transient intracellular accumulation and retention of the compound.

Binding of PSP to plasma albumin has been reported to limit the extent of secretion [2-4]. This is one reason that, compared to p-aminohippurate (PAH), a smaller fraction of PSP is extracted at low concentrations from renal plasma during a single passage through the kidney. Also a less efficient interaction with the tubular secretory system and a possible reabsorptive component, observed in experiments with rabbits [5], may contribute to the lower extractability of the dye.

Renal excretion of PSP is susceptible to inhibition by other organic anions such as PAH [6], iodopyracet [7], and probenecid [8]. On the other hand, PSP has little influence on the tubular secretion of PAH and iodopyracet [6]. How these findings should be interpreted is still not clear, but they certainly suggest a functional heterogeneity of the organic anion transport system. This hypothesis is further supported by the observation that kidney tubules of *Necturus* are unable to transport PSP whereas they readily excrete PAH [9].

It is well established that the primary site of inhibition of secretion of one organic acid by another is at the level of active uptake across the basolateral membrane. But detailed information on the precise nature of inhibition is scarce and not always in common agreement. For instance, probenecid is generally regarded as a competitive inhibitor of organic

anion secretion [10]. However, for its effect on PSP excretion competitive [8] as well as noncompetitive inhibition [11] was reported. Furthermore, in a previous study on the effect of probenecid on the secretion of salicyluric acid (SUA) we observed also a noncompetitive type of interaction [12].

The purpose of the present study was twofold. First, to develop a physiologically based model, as accurate but also as simple as possible, that is able to quantify the relevant processes of renal PSP excretion. This kidney model, based on previous described models [12,13], incorporates the important features of transtubular transport and nonlinear protein binding. Second, to characterize the interaction of probenecid and salicyluric acid on PSP excretion with the aid of this model.

3.2 MATERIALS AND METHODS

Materials

The Braunule T cannulas were obtained from Braun (Melsungen, FRG), the double-walled urinary catheter (URO 90.009) from Talas (Ommen, The Netherlands). Blood was withdrawn into heparinized 10 ml Monovettes from Sarstedt (Eindhoven, The Netherlands). Phenolsulfonphthalein, salicyluric acid, indole-3-acetic acid, and LiChrosorb RP18 were from Merck (Darmstadt, FRG), probenecid from Sigma (St. Louis, Mo., USA), sodium pentobarbital from Apharma (Arnhem, The Netherlands), heparin from Organon (Oss, The Netherlands), atropine sulphate, mannitol, and inulin from O.P.G. (Utrecht, The Netherlands). Albipen[®] from Gist Brocades (Delft, The Netherlands), and Visking 8 dialysis tubing from Instrumentenhandel Z.H. (Den Haag, The Netherlands). All other chemicals were of analytical grade and were purchased from Merck (Darmstadt, FRG).

Clearance Experiments

Male Beagle dogs, weighing 10 to 16 kg, were fasted overnight and anesthetized by intravenous administration of 30 mg/kg of pentobarbital sodium. As premedication atropine sulphate (0.5%, 1 ml i.v.) was given. The dogs were intubated and ventilated using a Harvard (model 607) ven-

tilator. The cephalic vein of both forelegs was cannulated (Braunule T, length 50 mm, ϕ 1.0 \times 1.5 mm) for blood sampling and drug administration purposes. A constant infusion of 5% mannitol and 0.5% inulin (2 ml/min) was administered throughout the experiment in order to obtain a sufficiently high and constant urine flow. In this way the pH of the voided urine remained fairly constant at a level of 7.0 ± 0.8 . Each dog received as an i.v. bolus a sterile solution of 1.0 g PSP dissolved in 15 ml water containing an equimolar amount of sodium bicarbonate. In a second experiment, using the same dogs, 1.0 g PSP was given after SUA or probenecid preadministration. In case of SUA treatment the dogs received 30 min prior to injection of PSP a priming dose of 300 mg (5% in aqueous sodium bicarbonate, 6 ml i.v.) followed by a constant infusion of a 2.5% solution at a rate of 3 ml/hr (dogs 2 and 3) or a 5% solution at 5 ml/hr (dog 1). Probenecid treatment (dogs 4, 5, and 6) involved a priming dose of 75 mg (2.5% in aqueous sodium bicarbonate, 3 ml i.v.) at $t = -30$ min, followed by constant infusion of a 0.5% solution at a rate of 5 ml/hr. At regular times throughout the experiment blood samples were taken into heparinized tubes. Plasma was separated by centrifugation for 20 min at 2000g and stored at -20°C until analysis. Urine was collected quantitatively with a double-walled urinary catheter [14] at 5 min intervals during the first 100 min of the experiment, and afterwards at 10 min intervals. The diluted urine samples were stored at -20°C until analysis. At the end of the experiment the cannulas and the urinary catheter were removed, and the dog was allowed to recover. Ampicillin (Albipen[®] 15%, 0.1 mg/kg) was given subcutaneously to protect against infections. Before the dog was used for the second experiment at least 3 weeks of recovery were observed.

Spectrophotometric Assay

Concentrations of PSP were determined in plasma and urine according to the method of Ochwaldt and Pitts [2]. Plasma samples (500 μl) were extracted with 2.0 ml acetone by shaking for 15 min. After centrifugation for 10 min at 2000g, 0.2 ml 1N sodium hydroxide solution was added to 2.0 ml of the clear supernatant, and absorbance was read at 546 nm. The diluted urine samples could be measured directly after alkalization with sodium hydroxide as described above. Inulin was assayed according to the

method of Heyrovski [15]. After hydrolysis to fructose and reaction with indole-3-acetic acid in hydrochloric acid (32% w/w) absorbance was measured at 515 nm.

HPLC Assay

SUA and probenecid were determined by high-performance liquid chromatography (HPLC). Both procedures were described in detail previously [12,16]. A Hewlett Packard 1084B was used equipped with a variable wavelength detector, autosampler and terminal (HP 7850 LC). The stainless-steel column (150 × 4.6 mm I.D.) was packed with LiChrosorb RP-18, particle size 5 µm. Peak area ratios using an internal standard were calculated for calibration and quantification purposes.

Protein Binding

Plasma protein binding of PSP was determined by ultrafiltration using Visking dialysis tubing (flat width 10 mm, average pore size 2.4 nm). Plasma (2.0 ml) was pipetted into the tubes that were folded in a U-shape into a centrifuge tube. Membrane-bound water was removed by precentrifugation for 10 min at 1000g. After that, the bags were transferred to another tube and centrifuged at 1000g for 60 min, yielding about 150 µl ultrafiltrate. Binding of PSP to the dialysis membrane was negligible. The ultrafiltrates were treated and analyzed in the same way as the urine samples. Assuming one class of binding site plasma protein binding was analyzed with the aid of the computer program NONLIN [17] according to the following equations, derived from the mass-action law:

$$C = C_u + P \cdot C_u / (K_d + C_u) \quad (3.1)$$

$$C_u = f_u C \quad (3.2)$$

where C is the total plasma drug concentration, C_u the unbound drug concentration in plasma, f_u is the fraction of drug in plasma unbound, P is the total concentration of protein binding sites, and K_d is the dissociation constant of the drug-protein complex. Average values are expressed as mean ± standard deviation (SD).

Pharmacokinetic Analysis

Plasma concentration time curves could be fitted well to the sum of two exponential equations (NONLIN), whereas renal excretion rate-time curves were analyzed employing the log-trapezoidal rule [18]. Applying statistical moments theory, basic pharmacokinetic parameters were calculated [19,20]. The area under the plasma curve (AUC) was calculated by direct integration. The area under the renal excretion rate curve (AUR_R), and the area under the first moment of this curve ($AUMR_R$) were estimated from 0 to time t by means of the log-trapezoidal rule and extrapolation to infinity using the terminal phase of the plot

$$AUR_R = \int_0^t R_R dt + \frac{R_R(t)}{\lambda_{z,ur}} \quad (3.3)$$

$$AUMR_R = \int_0^t t \cdot R_R dt + \frac{t \cdot R_R(t)}{\lambda_{z,ur}} + \frac{R_R(t)}{(\lambda_{z,ur})^2} \quad (3.4)$$

where $R_R(t)$ is the last measured renal excretion rate at time t and $\lambda_{z,ur}$ is the terminal elimination constant determined by least squares regression analysis from the log-linear terminal phase of the curve. Half-lives of PSP in plasma ($t_{1/2,p}$) and urine ($t_{1/2,ur}$) were obtained from their respective terminal elimination rate constants. Total plasma clearance (CL) and initial volume of distribution (V_1) were calculated using standard equations [21]. The mean residence time was determined from the moments of the renal excretion rate curve as

$$MRT_R = AUMR_R / AUR_R \quad (3.5)$$

Renal clearance (CL_R) was estimated by the total excretion method,

$$CL_R = CL \cdot \frac{AUR_R}{D} = \frac{AUR_R}{AUC} \quad (3.6)$$

where AUR_R represents the total amount of PSP excreted in infinite time into urine

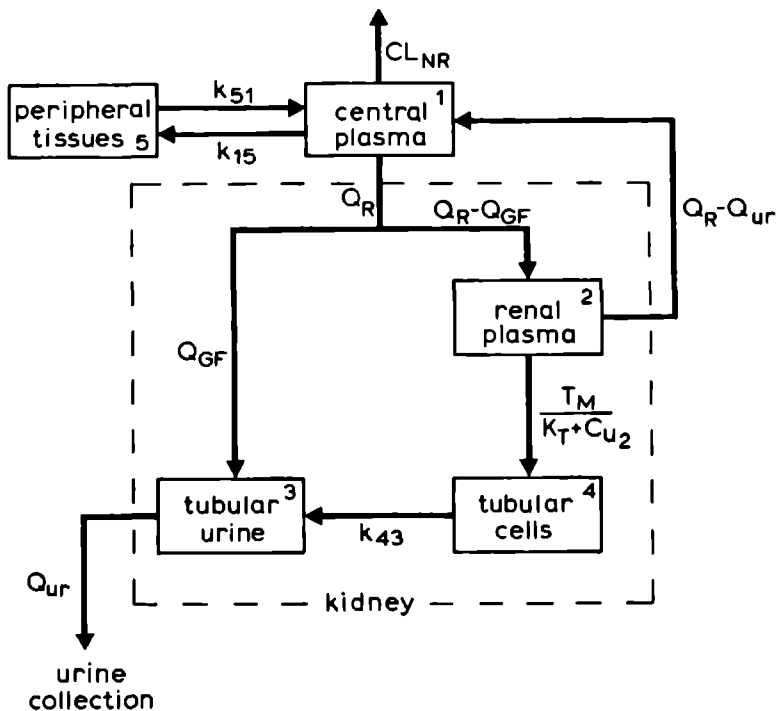


Fig. 3.1 Physiologically based pharmacokinetic model for the renal clearance of PSP. See Materials and Methods for explanation of symbols.

Kidney Model

The physiologically based model for the renal excretion of PSP is illustrated by the diagram in Fig. 3.1. Transport processes and compartmental concentrations of the drug can be described by the following set of equations:

Central plasma

$$V_1 \frac{dC_1}{dt} = (Q_R - Q_{ur})C_2 + k_{51}V_5C_5 - (Q_R + CL_{NR} + k_{15}V_1)C_1 \quad (3.7)$$

Renal plasma

$$V_2 \frac{dC_2}{dt} = Q_R C_1 - Q_{GF} C_{u1} - (Q_R - Q_{ur}) C_2 - \frac{T_M C_{u2}}{K_T + C_{u2}} \quad (3.8)$$

Tubular urine

$$V_3 \frac{dC_3}{dt} = Q_{GF} C_{u1} + k_{43} V_4 C_4 - Q_{ur} C_3 \quad (3.9)$$

Tubular cells

$$V_4 \frac{dC_4}{dt} = \frac{T_M C_{u2}}{K_T + C_{u2}} - k_{43} V_4 C_4 \quad (3.10)$$

Peripheral tissues

$$V_5 \frac{dC_5}{dt} = k_{15} V_1 C_1 - k_{51} V_5 C_5 \quad (3.11)$$

where,

- V_i = volume of compartment i (ml)
- C_i = total drug concentration in compartment i ($\mu\text{g/ml}$)
- C_{u_i} = unbound drug concentration in compartment i ($\mu\text{g/ml}$)
- k_{ij} = first-order rate constant associated with movement of drug from compartment i to compartment j (min^{-1})
- Q_R = renal plasma flow (ml/min)
- Q_{GF} = glomerular filtration (ml/min)
- Q_{ur} = urine flow (ml/min)
- CL_{NR} = nonrenal plasma clearance (ml/min)
- T_M = maximum transport capacity of the tubular secretion mechanism ($\mu\text{g/min}$)
- K_T = Michaelis-Menten constant of the tubular secretion mechanism ($\mu\text{g/ml}$)

The renal excretion rate ($\mu\text{g/min}$) in this model is represented by

$$R_R = Q_{ur} \cdot C_3 \quad (3.12)$$

and the unbound drug concentration in compartment i can be calculated after rearrangement of equations 3.1 and 3.2:

$$Cu_i = \frac{1}{2}[-(P + K_d - C_i) + \sqrt{(P + K_d - C_i)^2 + 4K_d C_i}] \quad (3.13)$$

The experimentally observed plasma concentration and renal excretion rate curves were simultaneously analyzed with the model described above with the aid of the computer program NONLIN. Several weighting factors were tested, in most cases $1/C^2$ gave the best fits. The goodness of fit to the plasma concentration and renal excretion rate data was evaluated through the deviations between observations and model-predicted values expressed as $R^2 = 1 - \Sigma(\text{Obs})^2 / \Sigma(\text{Dev})^2$, where $\Sigma(\text{Obs})^2$ is the corrected sum of squared observations and $\Sigma(\text{Dev})^2$ the sum of squared deviations.

3.3 RESULTS

Protein Binding

Over the concentration range measured (5 - 450 $\mu\text{g/ml}$) nonlinear plasma protein binding of PSP was observed, the fraction unbound increasing from 15 - 40% (Fig. 3.2). Neither probenecid (40 - 120 $\mu\text{g/ml}$) nor SUA (20 - 125 $\mu\text{g/ml}$) interfered with the binding of PSP. Interindividual variation in binding was very small. Therefore, all data ($n=74$) were pooled and analyzed according to Eq. 3.1. The binding parameters obtained from this fit were $441 \pm 31 \mu\text{g/ml}$ and $123 \pm 14 \mu\text{g/ml}$ for total concentration of protein binding sites (P) and dissociation constant (K_d), respectively.

Pharmacokinetic Analysis

Representative examples of plasma disappearance and renal excretion rate of intravenous administered PSP with or without simultaneous infusion of SUA or probenecid are shown in Fig. 3.3. Plasma and urinary data were analyzed separately by statistical moment theory. The results of these calculations are summarized in Table 3.1. Steady-state concentrations of the inhibitors are given in Table 3.2.

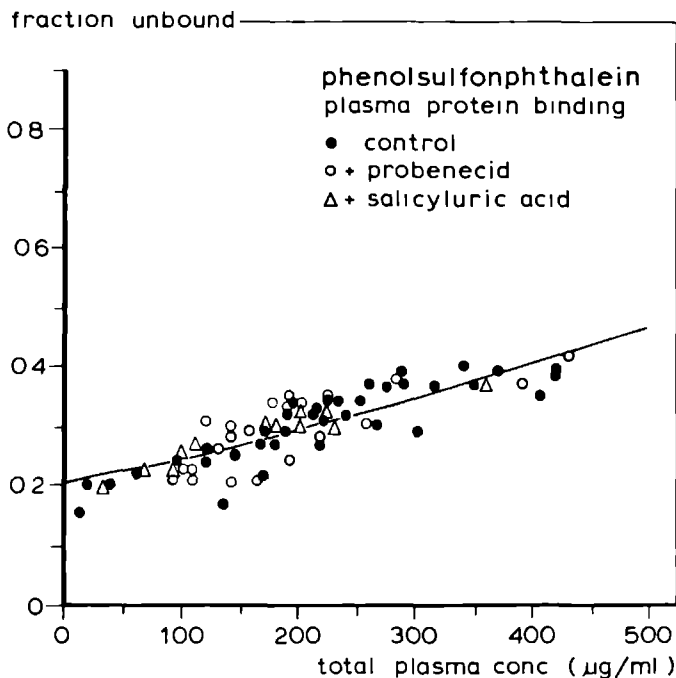


Fig. 3.2 Effect of probenecid and salicylic acid on the plasma protein binding of PSP. The line through the data is calculated by Eq. 3.1.

In the control experiments $66 \pm 10\%$ of the administered dose was excreted unchanged into urine at a renal clearance of 40 ± 7 ml/min. Assuming an average protein binding of about 30% it could be calculated from the product with glomerular filtration (Table 3.2) that the contribution of drug filtration to the total renal clearance was about 9 ml/min. Hence, it was obvious that active tubular secretion was the predominant route of renal excretion at the given dose. Treatment with probenecid or with SUA resulted in a clear reduction of renal clearance. Because glomerular filtration and protein binding remained unaffected this effect could be fully accounted for by inhibition of tubular secretion. The extraction ratio of PSP at low plasma concentrations as calculated from the ratio of CL_R and renal plasma flow (Table 3.2) was 0.46 ± 0.08 . This value reduced in presence of SUA or probenecid to 0.12 ± 0.05 or 0.20 ± 0.03 , respectively.

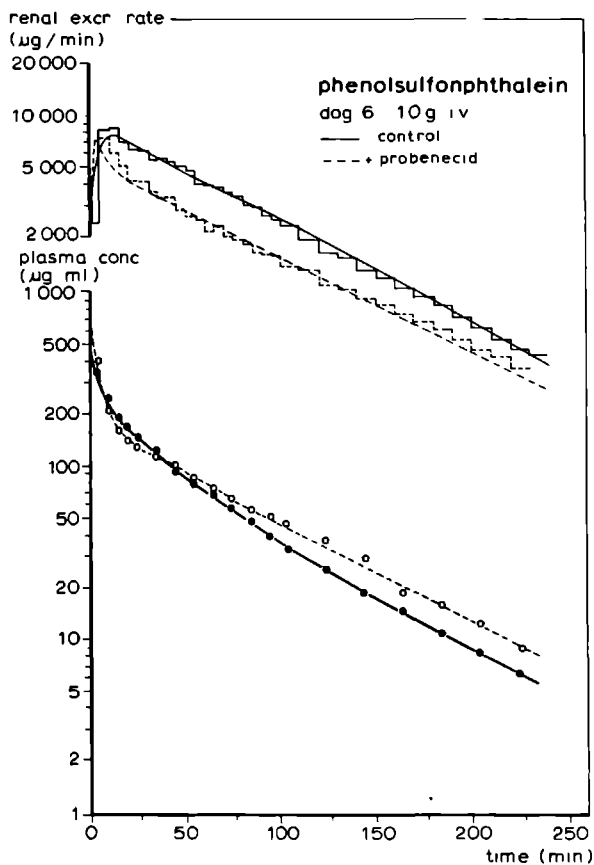


Fig. 3.3A Renal excretion rate and plasma concentration as function of time after rapid i.v. administration of 1.0 gram PSP with or without concomitant infusion of probenecid. The solid and broken lines in the figures represent the results of data analysis according to the kidney model.

The terminal half-lives in plasma and urine were both clearly extended under influence of probenecid or SUA. The MRT_R , calculated from the renal excretion rate curve, was also increased, although less pronounced. It is important to notice that under conditions of nonlinear kinetics, which is obviously the case for PSP, the MRT_R only represents the mean residence time of those drug molecules that are excreted via the kidney. Although the MRT_R can be calculated irrespective of whether the drug has nonlinear disposition kinetics or is eliminated peripherally, it is only

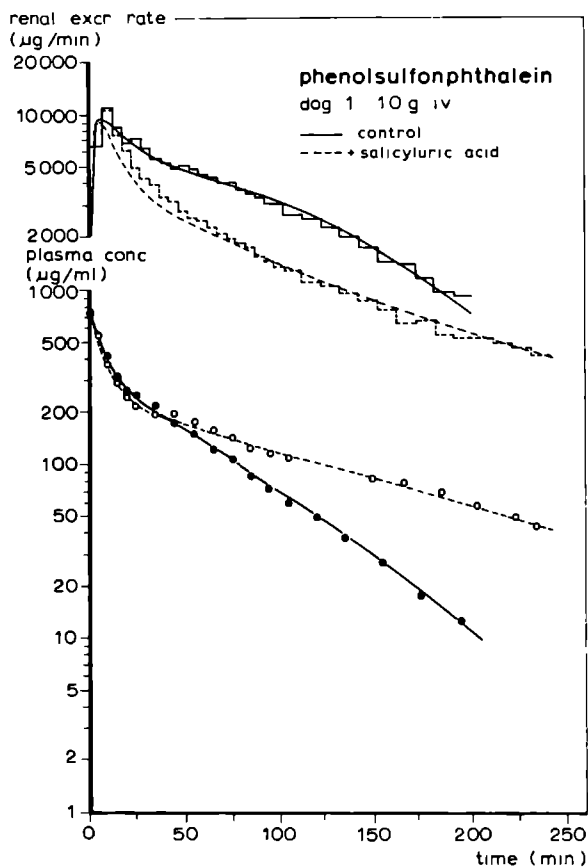


Fig. 3.3B Renal excretion rate and plasma concentration as function of time after rapid i.v. administration of 1.0 gram PSP with or without concomitant infusion of SUA. The solid and broken lines in the figures represent the results of data analysis according to the kidney model.

for linear pharmacokinetic systems that it equals the total mean residence time in the body.

Kidney Model

In order to come to a comprehensive understanding of the relation between plasma and renal excretion kinetics of PSP a physiologically based pharmacokinetic model was proposed. Starting from previously described models for the active renal secretion of iodopyracet [13] and SUA [12]

Table 3.1 Basic pharmacokinetic parameters of PSP after rapid i.v. injection of 1.0 gram with or without concomitant administration of salicyluric acid (SUA) or probenecid (Prob).

Dog	Inhibitor	plasma			urine		
		$t_{\frac{1}{2},p}$ (min)	CL (ml/min)	V_1 (l)	$t_{\frac{1}{2},ur}$ (min)	MRT_R (min)	CL_R (ml/min)
1	-	40	42	1.2	60	87	32
	SUA	99	27	1.4	78	86	14
2	-	46	46	1.5	60	84	32
	SUA	66	44	1.6	90	112	27
3	-	46	55	1.9	58	86	41
	SUA	83	36	1.7	83	108	24
4	-	44	75	2.5	54	70	39
	Prob	54	62	2.4	47	67	37
5	-	42	78	2.5	38	56	44
	Prob	66	52	2.0	60	76	26
6	-	48	74	2.6	52	80	49
	Prob	54	67	1.4	61	83	30

the features of nonlinear protein binding and tubular drug retention were incorporated. A schematic representation of the model is given in Fig. 3.1. The kidney is set apart as a subsystem consisting of a plasma, tubular cell and tubular urine compartment. Active transport of unbound PSP takes place from renal plasma into the tubular cell compartment according to Michaelis-Menten kinetics, subsequently followed by first-order transport into the tubular urine compartment. Although in the control experiments active transport was also proportional to total PSP concentrations, unbound concentrations were used because in the interaction experiments with probenecid and SUA only satisfactory fits were

Table 3.2 Physiological and experimentally found parameters used as constants in the kidney model.

Dog	Weight (kg)	Inhibitor	C_I ($\mu\text{g/ml}$)	Q_{GF} (ml/min)	Q_{ur} (ml/min)	Q_R^a (ml/min)	V_3 (ml)
1	10.0	-	-	28 \pm 4	0.77 \pm 0.05	110	1.16 \pm 0.08
	13.6	SUA	122 \pm 6	32 \pm 4	1.14 \pm 0.25	150	1.71 \pm 0.38
2	12.2	-	-	26 \pm 3	0.83 \pm 0.05	134	1.24 \pm 0.07
	13.0	SUA	32 \pm 9	28 \pm 2	0.79 \pm 0.10	143	1.18 \pm 0.15
3	13.9	-	-	30 \pm 2	0.95 \pm 0.10	153	1.42 \pm 0.15
	15.0	SUA	22 \pm 5	34 \pm 4	1.25 \pm 0.20	165	1.88 \pm 0.30
4	13.7	-	-	41 \pm 3	0.92 \pm 0.38	151	1.38 \pm 0.57
	13.6	Prob	59 \pm 3	43 \pm 4	1.05 \pm 0.39	150	1.58 \pm 0.59
5	13.2	-	-	33 \pm 4	0.84 \pm 0.26	145	1.26 \pm 0.39
	12.5	Prob	120 \pm 5	35 \pm 5	0.93 \pm 0.93	138	1.40 \pm 0.29
6	15.4	-	-	32 \pm 2	0.68 \pm 0.19	169	1.02 \pm 0.28
	15.7	Prob	45 \pm 4	33 \pm 3	0.98 \pm 0.19	173	1.47 \pm 0.28

aQ_R is directly estimated from the body weight (see text), therefore no SD.

obtained when the tubular secretion was assumed to be dependent on unbound concentrations. Glomerular filtration was considered to be dependent on unbound drug concentration in the central plasma compartment. To describe the plasma kinetics of PSP completely a tissue compartment was allocated to the central compartment and a first-order clearance constant was introduced which represented the extra-renal clearance pathway.

Table 3.2 lists some of the parameters used as constants in the model. Q_{GF} was determined by steady-state inulin clearance. For Q_R a value of 11 ml/min,kg was taken [22]. The volume of the tubular urine compartment (V_3) was considered to be dependent on urine flow and renal delay

time [23]. Assuming a constant renal delay time (Δt) of 1.5 min V_3 was calculated as follows:

$$V_3 = Q_{ur} \cdot \Delta t \quad (3.14)$$

The values for V_1 were taken from Table 3.1 and for V_5 an arbitrary value of 1 l was chosen. The remaining constants were estimated from literature, e.g., for V_2 a value of 10 ml [24] and for V_4 a value of 30 ml [25].

The model was fitted to the experimental data of the control experiments using NONLIN. The results of these calculations are listed in Table 3.3 and are also represented by the solid lines through the datapoints in Figs. 3.3, 3.4 and 3.5. R^2 was better than 0.95 in most cases. Figs. 3.4 and 3.5 are so-called tubular titration curves, in which a direct representation of the relationship between renal excretion rate and plasma concentration at the midpoint of a urine collection period is given. There were no indications for passive reabsorption of PSP, probably due to the relatively high urine flows resulting from the infusion with mannitol.

Effect of Probenecid

Administration of probenecid resulted in a clear reduction of PSP clearance (Table 3.1, Fig. 3.4). As was mentioned before, this could be attributed to inhibition of tubular secretion. In accordance with the findings of Sheikh [8] the effect of probenecid was adequately described by competitive inhibition of the active uptake of PSP into the tubular cells. To quantify this interaction the Michaelis-Menten term in the kidney model, which describes the carrier-mediated transport from renal plasma into the tubular cell compartment, was modified as follows:

$$\frac{T_M Cu_2}{K_T(1 + C_I/K_I) + Cu_2} \quad (3.15)$$

where C_I is the plasma concentration of the inhibitor, in this case probenecid, and K_I the inhibition constant for probenecid. Steady-state probenecid plasma concentrations that were reached are given in Table

Table 3.3 Model parameters characterizing the renal handling of PSP and the effect of probenecid and SUA^a.

Dog	Inhibitor	T_M (mg/min)	K_T (μ g/ml)	K_I (μ g/ml)	CL_{NR} (ml/min)	k_{43} (min ⁻¹)	k_{15} (min ⁻¹)	k_{51} (min ⁻¹)
1	-	4.4±0.5	8±3	-	10±2	0.19±0.13	0.069±0.004	0.054±0.005
	SUA	6.5±2.5	16±5	3±2	14±2	0.19±0.24	0.071±0.009	0.057±0.003
2	-	5.3±0.7	18±6	-	14±2	0.22±0.11	0.047±0.003	0.045±0.004
	SUA	5.3±3.5	30±27	14±12	22±3	0.23±0.21	0.111±0.009	0.077±0.008
3	-	6.3±1.1	15±7	-	14±2	0.19±0.10	0.049±0.004	0.050±0.007
	SUA	6.5±3.6	18±12	5±3	12±3	0.20±0.15	0.079±0.004	0.063±0.005
4	-	7.4±1.2	19±7	-	31±2	0.18±0.06	0.020±0.002	0.031±0.002
	Prob	9.6±5.6	25±20	29±23	31±2	0.17±0.09	0.028±0.002	0.042±0.003
5	-	7.7±1.4	17±7	-	40±2	0.20±0.08	0.014±0.002	0.030±0.002
	Prob	12.0±4.0	26±10	25±10	33±2	0.20±0.14	0.062±0.007	0.050±0.002
6	-	8.5±1.6	18±7	-	24±2	0.17±0.06	0.033±0.002	0.039±0.003
	Prob	8.7±4.3	18±13	17±12	37±2	0.16±0.09	0.187±0.007	0.080±0.004

^aStandard deviations were calculated for the situation in which plasma concentration data were reciprocally weighted ($1/C^2$) and renal excretion rate data were equally weighted.

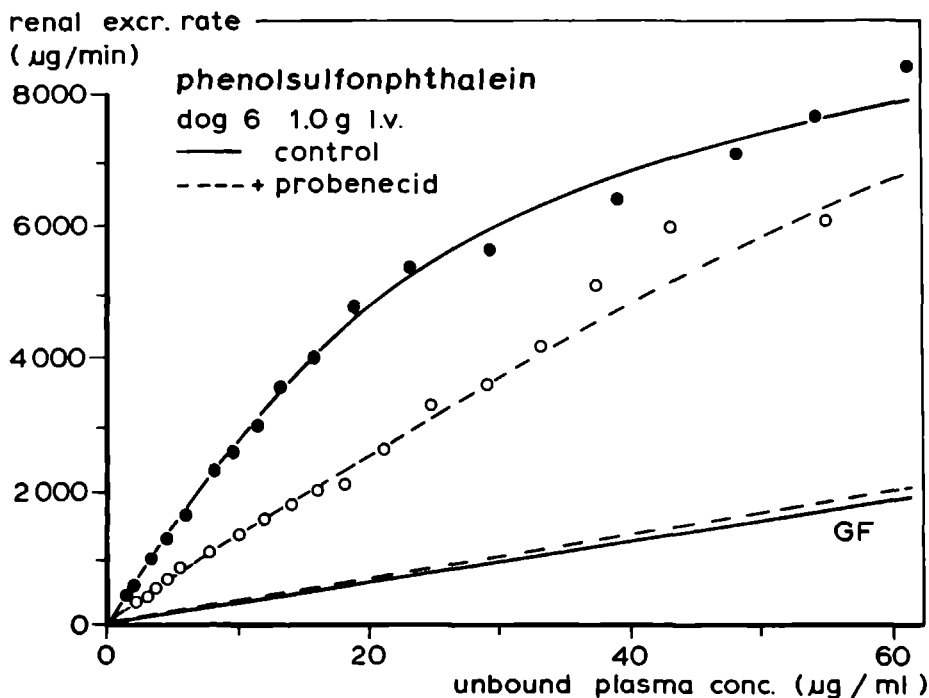


Fig. 3.4 Tubular titration curve representing the relationship between the renal excretion rate and the unbound plasma concentration after i.v. administration of PSP with or without probenecid. The lines through the data points are calculated according to the kidney model. GF represents the clearance by glomerular filtration of PSP.

3.2. Eq. 3.15 was incorporated in the differential equations 3.8 and 3.10 and the model thus obtained was used to analyze the data of the probenecid interaction experiments. Results are summarized in Table 3.3 and represented by the dotted lines in Figs. 3.3A and 3.4.

Effect of Salicylic Acid

SUA also clearly interfered with tubular secretion of PSP (Table 3.1), but the concave tubular titration curves that were observed (Fig. 3.5) could not be described in terms of simple inhibition kinetics. A more complex type of interaction had to be taken into consideration. A two-site competitive system, known from enzyme kinetics as ligand exclusion model

[26], was successfully used to describe the interaction of SUA with PSP. In this system it is assumed that binding of the inhibitor to a single site prevents the substrate from binding to either of two identical sites.

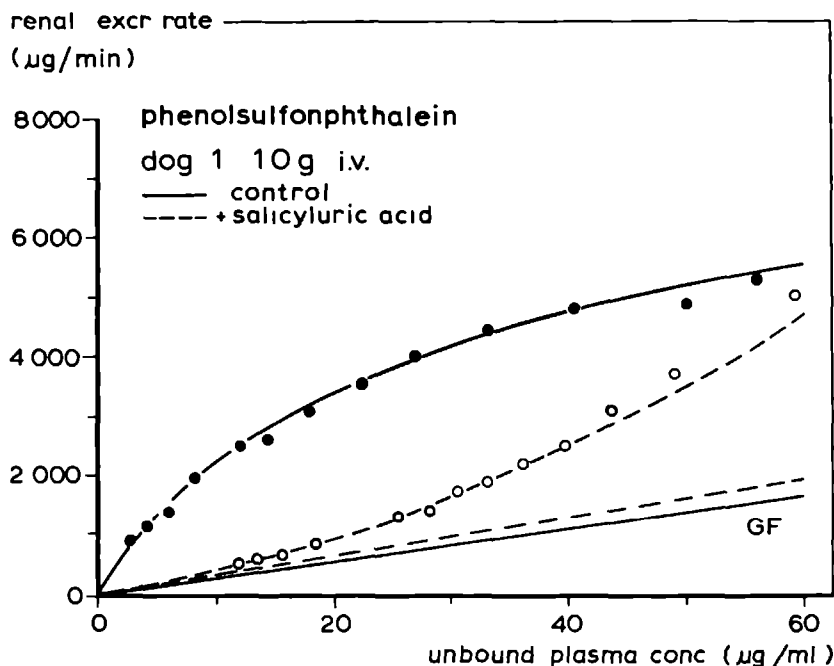


Fig. 3.5 Tubular titration curve representing the relationship between the renal excretion rate and the unbound plasma concentration after i.v. administration of PSP with or without SUA. The lines through the data points are calculated according to the kidney model. GF represents the clearance by glomerular filtration of PSP.

This interaction is described by the following equation:

$$\frac{T_M(C_{u2}/K_T + C_{u2}^2/K_T^2)}{1 + 2C_{u2}/K_T + C_{u2}^2/K_T^2 + C_I/K_I} \quad (3.16)$$

where C_I and K_I are the plasma concentration of SUA (Table 3.2) and the inhibition constant, respectively. In absence of the inhibitor Eq. 3.16

reduces to the normal Michaelis-Menten equation which was also used to describe PSP kinetics in the control experiments. Experimental data were analyzed after Eq. 3.16 was incorporated into equations 3.8 and 3.10. Results are summarized in Table 3.3 and represented by the dotted lines in Figs. 3.3B and 3.5.

3.4 DISCUSSION

The most important step in the renal clearance of PSP and a wide variety of other organic anions is the transepithelial transport from renal plasma into urine [27]. Several studies have confirmed that the cells of the proximal tubules are responsible for the secretion of these compounds [28]. Active tubular secretion is almost always accompanied with transient accumulation and retention of the substrate in the cells [29,30]. The degree of accumulation is determined by the extent at which these compounds are actively transported across the basolateral membrane into the cells and the ease at which they can be transported out of the cells into the tubular lumen.

The separate pharmacokinetic analyses of plasma and renal excretion data provide an overall impression of the renal clearance of PSP. The results clearly show that active secretion is the predominant route of renal elimination and that this transport step can be inhibited by probenecid and SUA. However, the parameters obtained from this analysis are mainly of qualitative merit. Because of the nonlinear kinetics of PSP all parameters are a function of the administered dose and are dependent on factors that influence the nonlinearity of the system.

In order to account for the processes that govern the renal excretion of PSP in a quantitative and more meaningful manner, a physiologically based kidney model was used. New features of the present model are that it incorporates nonlinear protein binding and a compartment that represents the cells of the proximal tubules. The use of this model enables us to describe and analyze the plasma kinetics and renal excretion process of PSP in a comprehensive way. Furthermore, the model appears to be very useful in the characterization of drug interactions at the level of tubular secretion.

It is a striking observation that in the interaction experiments only satisfactory fits were obtained when tubular secretion was considered to be proportional to unbound PSP concentrations, whereas in control experiments it did not seem to matter much whether bound or unbound concentrations were used. The role of protein binding in renal secretion is still poorly understood. For several compounds, including PSP, it was reported that protein binding retards tubular secretion to a certain extent [2-4,31-33]. On the other hand, there are examples of other compounds for which protein binding is not a limitation in secretion [7,34,35]. The determining factors in this respect are the rate of dissociation of the drug-protein complex, the transit time through the peritubular capillaries, diffusion into the cortical interstitium, and the affinity for the transport system. Apparently, the affinity of PSP for the secretory system relative to the other factors is not large enough to give a complete extraction from the plasma in a single passage through the kidney. The extraction ratio of PSP at low plasma concentrations was about 0.5. This is in agreement with previously reported values of 0.7 [36] and 0.5 [37] in the dog. Although the extraction is not complete it seems likely that the affinity is sufficient to clear more than only the unbound fraction of PSP, which explains why in the control experiments comparable fits were obtained for bound and unbound concentrations. However, in the interaction experiments the apparent affinity of the transport system is, due to competitive inhibition by probenecid and SUA, thus far decreased that dissociation of bound PSP becomes very unlikely. Under these conditions it is understandable that secretion is proportional to the unbound plasma concentration.

It can be concluded from the results in Table 3.3 that in the control experiments a considerable accumulation of PSP within the tubular cells takes place. The cellular uptake of PSP, expressed as the intrinsic unbound secretion clearance $CL_{u,int} = T_M/K_T$ is 430 ± 86 ml/min, whereas the clearance out of the cells into the lumen, represented by $V_4 \cdot k_{43}$, is only 5.8 ± 0.5 ml/min. In Fig. 3.6 the cellular concentration of PSP is simulated, using the model parameters calculated from the experiments in dog 1 (Table 3.3). The course of the simulated curves can be explained as follows: In the beginning of the experiment PSP concentrations in renal plasma are so high that the active uptake system is saturated and oper-

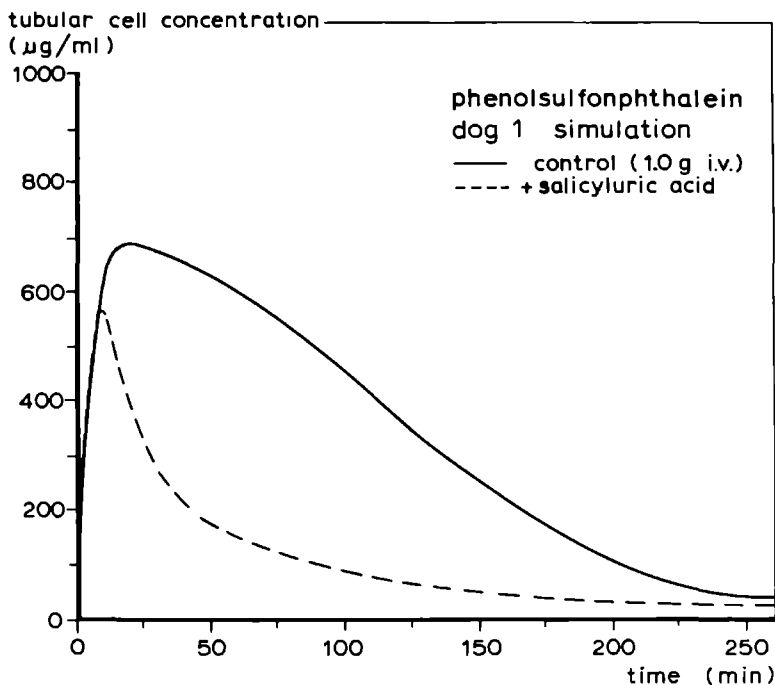


Fig. 3.6 Course of the proximal tubular cell concentration of PSP with or without the presence of SUA. The parameters used for this simulation were obtained from the analysis of plasma and urine curves of dog 1 according to the kidney model.

ates at its transport maximum. Since T_M is not affected by SUA the initial uptake rate into the cells is the same as in the control experiment. As the plasma concentration gradually falls, the rate of uptake into the cells in presence of SUA eventually lags behind as a result of the reduced apparent affinity of the transport system. Because the clearance out of the cells was not influenced by SUA, cellular concentrations were lower and decreased more rapidly. Comparison of Fig. 3.3B and Fig. 3.6 shows that the concentration in the control substantially exceeds the plasma concentration, the concentration ratio tubular cells to plasma ranging from approximately 4 at high plasma concentrations to approximately 10 at lower concentrations. In presence of SUA PSP accumulation is substantially decreased. In this situation the cell to plasma ratio does not exceed a

value of 1.5. A similar pattern was observed for the interaction with probenecid (not shown). These simulated accumulation values are in good agreement with in vitro observations [30].

The interaction with probenecid could be described well with the model when a competitive inhibition of active uptake of PSP into the tubular cells was assumed (Eq. 3.15). Studies with isolated membrane vesicles have shown that the transport step from cell to lumen is also a potential site of interaction [38], but no evidence for such an interference was obtained. The interaction with SUA is considerably more complicated. The pronounced concave shape of the tubular titration curves (Fig. 3.5) pointed to a special kind of interaction. The possibilities for such an interaction are limited because without inhibitor active PSP transport has to obey straightforward Michaelis-Menten kinetics. A type of interaction that meets this requirement is when the inhibitor reacts directly with the substrate, thus preventing it from being transported. However, binding between PSP and SUA is very unlikely. The most attractive explanation is to consider a system for PSP consisting of two identical transport sites, in which SUA can act as a pure competitive inhibitor (Eq. 3.16). The special thing about this interaction is that competition of SUA for a single site prevents transport of PSP via either of the two sites. SUA may overlap or utilize part of each PSP binding site or may cause steric hindrance or distortion in both sites by binding to one of the sites. Although this explanation is somewhat tentative it provides a useful operational relation for the characterization of the interaction between PSP and SUA. Further studies, for instance, with isolated membrane vesicles, are necessary to clarify the precise mechanism of this interaction. Anyway, the clear difference in inhibitory action between SUA and probenecid furnishes supporting evidence for a supposed heterogeneity of the organic anion transport system.

In conclusion, the kidney model described in this paper is able to adequately describe and account for the plasma kinetics and renal excretion of PSP and the interaction with two competing drugs. The model incorporates the functional characteristics of the kidney that are of importance in the renal handling of PSP. In future, other mechanisms such as passive or active reabsorption, urine flow and pH dependency, and renal effects of drugs that are cleared by the kidney (e.g., diuretics, uricosuric

agents, anti-inflammatory analgesics) have to be incorporated to make the model applicable to different types of drugs and several clinically relevant situations. However, much fundamental research is still needed to fit in all these features in a sound way.

3.5 REFERENCES

1. E.K. Marshall and J.L. Vickers. The mechanism of the elimination of phenolsulfonphthalein by the kidney; a proof of secretion by the convoluted tubules. *Bull. Johns Hopkins Hosp.* 34:1-7 (1923).
2. B.K. Ochwaldt and R.F. Pitts. Disparity between phenol red and diodrast clearances in the dog. *Am. J. Physiol.* 187:318-322 (1956).
3. A. Heidland and E. Riedl. Renaler Phenolsulfonphthalein-Transport nach Sulfonamidbedingter Entkoppelung der Farbstoff-Plasmabindung. *Klin. Wochenschr.* 15:816-820 (1968).
4. R. Iiori, K. Sunayashiki, and A. Kamiya. Tissue distribution and metabolism of drugs. I. Quantitative investigation on renal handling of phenolsulfonphthalein and sulfonamides in rabbits. *Chem. Pharm. Bull.* 26:740-745 (1978).
5. U. Gerdes, J. Kristensen, J.V. Møller, and M.I. Sheikh. Renal handling of phenol red. III. Bidirectional transport. *J. Physiol.* 227:115-129 (1975).
6. H.W. Smith. The kidney: Structure and function in health and disease, Oxford University Press, New York, Oxford 1951.
7. H.W. Smith, W. Goldring, and H. Chasis. The measurement of the tubular excretory mass, effective blood flow and filtration rate in the normal human kidney. *J. Clin. Invest.* 17:263-278 (1938).
8. M.I. Sheikh. Renal handling of phenol red. I. A comparative study on the accumulation of phenol red and p-aminohippurate in rabbit kidney tubules in vitro. *J. Physiol.* 227:565-590 (1972).
9. G.A. Tanner, P.K. Carmines, and W.B. Kinter. Excretion of phenol red by the Necturus kidney. *Am. J. Physiol.* 236:F442-447 (1979).
10. I.M. Weiner, J.A. Washington, and G.H. Mudge. On the mechanism of action of probenecid on renal tubular secretion. *Bull. Johns Hopkins Hosp.* 106:333-346 (1972).

11. W. Braun. Zum Mechanismus der gegenseitigen Hemmung von Phenolrot, Paraaminohippursäure und Probenecid. *Arch. Exp. Path. Pharmacol.* 239:400-409 (1960).
12. P. Hekman and C.A.M. Van Ginneken. Simultaneous kinetic modelling of plasma levels and urinary excretion of salicylic acid and the influence of probenecid. *Eur. J. Drug Metab. Pharmacokinet.* 3:239-249 (1983).
13. P. Hekman and C.A.M. Van Ginneken. Kinetic modelling of the renal excretion of iodopyracet in the dog. *J. Pharmacokinet. Biopharm.* 10:77-92 (1982).
14. F.G.M. Russel, A.C. Wouterse, P. Hekman, G.J. Grutters, and C.A.M. Van Ginneken. Quantitative urine collection in renal clearance studies in the dog. *J. Pharmacol. Methods* 17:125-136 (1987).
15. A. Heyrovski. A new method for the determination of inulin in plasma and urine. *Clin. Chim. Acta* 1:470-474 (1956).
16. P. Hekman, P.A.T.W. Porskamp, H.C.J. Ketelaars, and C.A.M. Van Ginneken. Rapid high-performance liquid chromatographic method for the determination of probenecid in biological fluids. *J. Chrom.* 182:252-256 (1980).
17. C.M. Metzler, G.L. Elfring, and A.J. McEwen. A package of computer programs for pharmacokinetic modeling. *Biometrics* 30:562-563 (1974).
18. W.L. Chiou. Critical evaluation of potential error in pharmacokinetic studies using the linear trapezoidal rule method for the calculation of the area under the plasma level-time curve. *J. Pharmacokinet. Biopharm.* 6:539-546 (1978).
19. K. Yamaoka, T. Nakagawa, and T. Uno. Statistical moments in pharmacokinetics. *J. Pharmacokinet. Biopharm.* 6:547-558 (1978).
20. L.Z. Benet and R.L. Galeazzi. Noncompartmental determination of the steady-state volume of distribution. *J. Pharm. Sci.* 68:1071-1074 (1979).
21. M. Gibaldi and D. Perrier. *Pharmacokinetics*, Marcell Dekker Inc., New York 1982.
22. B.H. Ewald. Renal function tests in normal Beagle dogs. *Am. J. Vet. Res.* 28:741-749 (1967).

23. E. Bojesen. The function of the urinary tract as dead space in renal clearance experiments. *Scand. J. Clin. Lab. Invest.* 1:290-294 (1949).
24. F.P. Chinard. Comparative renal excretion of glomerular substances following instantaneous injection into a renal artery. *Am. J. Physiol.* 180:617-619 (1955).
25. M.S. Dunnill and W. Halley. Some observations on the quantitative anatomy of the kidney. *J. Pathol.* 110:113-121 (1973).
26. I.H. Segel. *Enzyme kinetics, Behavior and Analysis of Rapid Equilibrium and Steady-State Enzyme Systems*, John Wiley & Sons, New York, 1975.
27. J.V. Møller and M.I. Sheikh. Renal organic anion transport system: pharmacological, physiological, and biochemical aspects. *Pharmacol. Rev.* 34:315-358 (1983).
28. I.M. Weiner. Transport of weak acids and bases. In: *Handbook of Physiology*, J. Orloff and R.W. Berliner (eds.), American Physiological Society, Washington DC, 1973, pp. 521-554.
29. R.P. Forster and J.H. Copenhaver. Intracellular accumulation as an active process in a mammalian renal transport system in vitro. *Am. J. Physiol.* 186:167-171 (1956).
30. M.I. Sheikh and J.V. Møller. Renal handling of phenol red. IV. Tubular localization in rabbit and rat kidney in vivo. *Am. J. Physiol.* 238:F159-165 (1980).
31. R.H. Bowman. Renal secretion of [³⁵S]-furosemide and its depression by albumin binding. *Am. J. Physiol.* 229:93-98 (1975).
32. S. Hall and M. Rowland. Influence of fraction unbound upon the renal clearance of furosemide in the isolated perfused rat kidney. *J. Pharmacol. Exp. Ther.* 232:263-268 (1985).
33. A. Kamiya, K. Okumura, and R. Hori. Quantitative investigation on renal handling of drugs in rabbits, dogs, and humans. *J. Pharm. Sci.* 72:440-443 (1983).
34. J.H. Gustafson and L.Z. Benet. Saturable kinetics of intravenous chlorothiazide in the rhesus monkey. *J. Pharmacokinet. Biopharm.* 9:461-476 (1981).
35. I. Bekersky, A.C. Popick, and W.A. Colburn. Influence of protein binding and metabolic interconversion on the disposition of sulfisoxa-

- zole and its N⁴-acetyl metabolite by the isolated perfused rat kidney. *Drug Metab. Dispos.* 12:607-613 (1984).
36. E. Marshall. The secretion of phenol red by the mammalian kidney. *Am. J. Physiol.* 99:77-86 (1931).
37. H.L. Sheehan. The renal elimination of phenol red in the dog. *J. Physiol.* 87:237-253 (1936).
38. C.K. Ross and P.D. Holohan. Transport of organic anions and cations in isolated renal plasma membranes. *Ann. Rev. Pharmacol. Toxicol.* 23:65-85 (1983).

RENAL CLEARANCE OF SALICYLURIC ACID AND THE INTERACTION
WITH PHENOLSULFONPHTHALEIN¹

Frans G.M. Russel, Alfons C. Wouterse, and Cees A.M. van Ginneken

Abstract - Plasma kinetics and renal excretion of salicyluric acid (SUA, 0.8 g) administered iv, with and without concomitant administration of phenolsulfonphthalein (PSP), were studied in the beagle dog. Pharmacokinetic analysis revealed that tubular secretion is the predominant route of excretion, and that secretion is inhibited by PSP. A physiologically based kidney model is presented comprising all the functional characteristics of the kidney that determine the excretion of SUA, i.e., renal plasma flow, urine flow, nonlinear protein binding, glomerular filtration, tubular secretion and tubular accumulation. The model enabled an accurate description and analysis of the measured plasma levels and renal excretion rates. The interaction with PSP could be adequately described with the model by noncompetitive inhibition of the carrier-mediated uptake of SUA into the tubular cells. Furthermore, a small but significant reduction in nonrenal SUA clearance was observed. Model calculations showed that, in the control experiments tubular secretion was accompanied by a pronounced accumulation of SUA within the cells, which was clearly diminished in the presence of PSP. The predicted accumulation ratios were in good agreement with previously reported in vitro values.

¹Published in: Drug Metab. Dispos. 15, 695-701 (1987).

4.1 INTRODUCTION

Active renal secretion is an important elimination route for a wide variety of organic anionic drugs and metabolites. Several studies have confirmed that the cells of the proximal tubules are responsible for the transport of these compounds. The initial step in tubular secretion involves active uptake at the basolateral membrane, resulting in intracellular accumulation of the drug and subsequent, probably facilitated, diffusion across the brush-border membrane into the luminal fluid [1,2].

Most of the characteristics of this system have been determined by studying the tubular transport of compounds like phenolsulfonphthalein (PSP), iodopyracet, and, in particular, p-aminohippurate (PAH). Especially from competition experiments, there is now increasing evidence suggesting that the renal secretory system consists of several overlapping subsystems with different affinities for the large diversity of compounds transported [1,3].

The present study concerns the renal clearance of salicyluric acid (SUA), the major metabolite of salicylic acid. SUA is largely eliminated from the general circulation via the kidney by glomerular filtration and active tubular secretion. Despite its considerable binding to plasma proteins, renal clearance at low plasma concentrations is the same as PAH clearance [4]. The lipophilic nature of SUA, as a result of internal hydrogen bonding, may lead to a substantial passive back diffusion under conditions of high tubular load in combination with a low urinary flow and pH. Tubular secretion of SUA is, as are almost all organic anions susceptible to inhibition by probenecid, but whereas probenecid generally acts as a competitive inhibitor, a noncompetitive type of interaction with SUA was observed [5]. Furthermore, in a study on the effect of probenecid and SUA on the renal clearance of PSP, probenecid showed simple competitive inhibition, while for SUA a considerably more complex type of interaction (two-site competitive system) had to be taken into consideration [6]. We therefore wondered what the influence of PSP on the renal clearance of SUA would be.

Previously, we showed the usefulness of physiologically based modeling in characterizing renal drug clearance and interactions at the level of tubular secretion [5,7]. In this paper, we propose an extension of these

models, by incorporating the important features of transtubular transport and nonlinear protein binding. The aim of the present study was to quantify all the relevant processes of renal SUA excretion and the effect of PSP with the aid of this extended physiologically based kidney model.

4.2 MATERIALS AND METHODS

Materials.

Salicyluric acid, phenolsulfonphthalein, indole-3-acetic acid, and LiChrosorb RP18 were from Merck (Darmstadt, FRG). Braunule T cannulas were obtained from Braun (Melsungen, FRG), the double-walled urinary catheter (URO 90.009) from Talas (Ommen, The Netherlands), and Visking 8 dialysis tubing from Instrumentenhandel Z.H. (Den Haag, The Netherlands). All other materials and chemicals were described previously [8].

Clearance Experiments.

The experiments were done in male beagle dogs, weighing 12 to 17 kg, as was described in detail previously [8]. In summary, the dogs were fasted overnight and anesthetized with sodium pentobarbital (30 mg/kg, iv). As premedication, atropine sulfate (0.5%, 1 ml iv) was given. A cannula (Braunule T) was inserted into the cephalic vein of each foreleg for blood sampling and drug administration. A constant infusion of 5% mannitol and 0.5% inulin (2 ml/min) was administered throughout the experiment. In this way, a sufficiently high urine flow and constant pH (7.0 ± 0.8) were obtained. Each dog received as an iv bolus a sterile solution of 0.8 g of SUA dissolved in 15 ml of water containing an equimolar amount of sodium bicarbonate. In a second experiment, the same dogs received a priming dose of 200 mg of PSP (2.5% in aqueous sodium bicarbonate, 8 ml iv) 30 min prior to injection of 0.8 g of SUA, followed by a constant infusion of the same solution at a rate of 5 ml/hr. At regular times throughout the experiment, blood samples were taken into heparinized tubes. Plasma was separated by centrifugation for 20 min at 2000g. Urine was collected quantitatively with a double-walled urinary catheter at 5 min intervals during the first 100 min of the experiment,

and afterwards at 10 min intervals. Plasma and urine samples were stored at -20°C until analysis. Before the dog was used for the second experiment, at least 3 weeks of recovery were observed.

Analytical Methods.

SUA was determined in plasma and urine by HPLC. as was described previously [5]. A Hewlett Packard 1084B chromatograph was used equipped with a variable wavelength detector, autosampler and terminal (HP 7850 LC). The stainless-steel column (150 × 4.6 mm I.D.) was packed with LiChrosorb RP-18, particle size 5 µm.

Concentrations of PSP were determined by a spectrophotometric assay [9]. Plasma samples (500 µl) were treated with 2.0 ml of acetone by shaking for 15 min to precipitate plasma proteins. After centrifugation for 10 min at 2000g, 0.2 ml of 1N NaOH solution was added to 2.0 ml of the clear supernatant, and the absorbance was measured at 546 nm.

Inulin was assayed according to the method of Heyrovski [10]. After hydrolysis to fructose and reaction with indole-3-acetic acid in hydrochloric acid (32% w/w), the absorbance was measured at 515 nm.

Protein Binding.

Plasma protein binding of SUA was determined by ultrafiltration using Visking dialysis tubing [8]. The ultrafiltrates were treated and analyzed in the same way as urine samples were. Assuming one class of binding sites, the plasma protein binding was analyzed according to the following equations, derived from the mass-action law:

$$C = fuC + P \cdot fuC / (K_d + fuC) \quad (4.1)$$

$$C_u = fuC \quad (4.2)$$

where C is the total plasma drug concentration, C_u the unbound drug concentration in plasma, fu is the fraction of drug in plasma unbound, P is the total concentration of protein binding sites, and K_d is the dissociation constant of the drug-protein complex.

Pharmacokinetic Analysis.

Basic pharmacokinetic parameters were calculated from the plasma concentration-time curves and renal excretion rate-time curves, applying statistical moments theory [11,12]. The data points were interpolated using a cubic spline method [13], as it was impossible to fit the typical nonlinear semilogarithmic plots to the usual multiexponential equations. The area under the plasma curve was calculated by numerical integration after extrapolation of the rapid distribution phase to time 0, and the terminal phase of the plot to infinity. In a similar way, the area under the renal excretion rate curve and the area under the first moment of this curve were estimated after extrapolation to infinity using the terminal phase of the plot. Using standard equations, total plasma clearance (CL) and initial volume of distribution (V_1) were calculated [14]. The mean residence time was determined from the renal excretion rate curve (MRT_R), dividing the area under the first moment curve by the area under the curve. Renal clearance (CL_R) was estimated by the total excretion method, in which the total amount of SUA excreted in infinite time into urine was calculated from the area under the renal excretion rate curve. The nonrenal clearance (CL_{NR}) was determined by subtracting the renal clearance from the total plasma clearance.

Kidney Model.

The physiologically based model for the renal excretion of SUA is illustrated by the diagram in Fig. 4.1. Transport processes and compartmental concentrations of the drug can be described by the following set of equations.

Central plasma

$$V_1 \frac{dC_1}{dt} = (Q_R - Q_{ur})C_2 + k_{51}V_5C_5 - (Q_R + CL_{NR} + k_{15}V_1)C_1 \quad (4.3)$$

Renal plasma

$$V_2 \frac{dC_2}{dt} = Q_R C_1 - Q_{GF}C_{u1} - (Q_R - Q_{ur})C_2 - \frac{T_M C_2}{K_T + C_2} \quad (4.4)$$

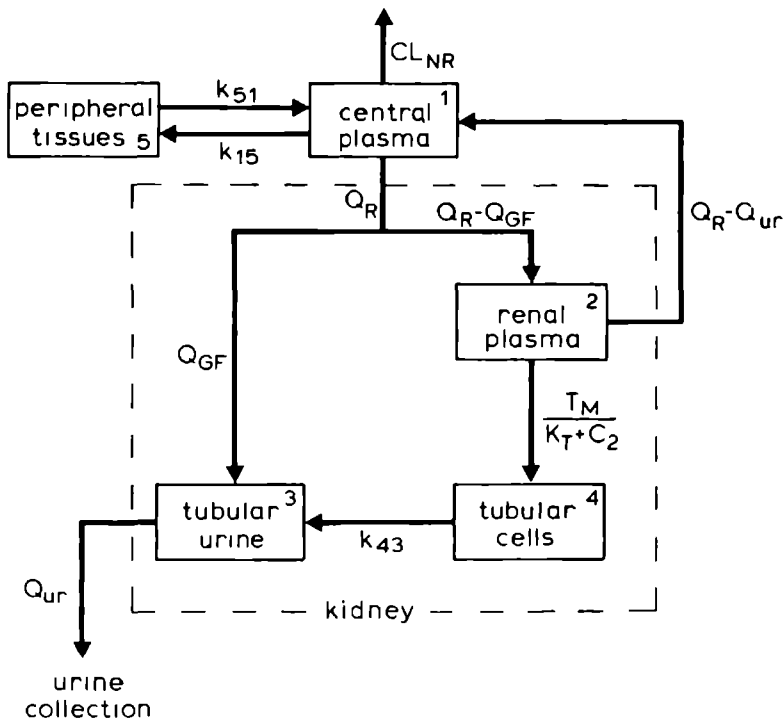


Fig. 4.1 Physiologically based pharmacokinetic model for the renal clearance of SUA. See Materials and Methods for explanation of symbols.

Tubular urine

$$V_3 \frac{dC_3}{dt} = Q_{GF} C_{u1} + k_{43} V_4 C_4 - Q_{ur} C_3 \quad (4.5)$$

Tubular cells

$$V_4 \frac{dC_4}{dt} = \frac{T_M C_2}{K_T + C_2} - k_{43} V_4 C_4 \quad (4.6)$$

Peripheral tissues

$$V_5 \frac{dC_5}{dt} = k_{15} V_1 C_1 - k_{51} V_5 C_5 \quad (4.7)$$

where,

- V_i = volume of compartment i (ml)
- C_i = total drug concentration in compartment i ($\mu\text{g/ml}$)
- C_{u1} = unbound drug concentration in compartment 1 ($\mu\text{g/ml}$)
- k_{ij} = first-order rate constant associated with movement of drug from compartment i to compartment j (min^{-1})
- Q_R = renal plasma flow (ml/min)
- Q_{GF} = glomerular filtration (ml/min)
- Q_{ur} = urine flow (ml/min)
- CL_{NR} = nonrenal plasma clearance (ml/min)
- T_M = maximum transport capacity of the tubular secretion mechanism ($\mu\text{g/min}$)
- K_T = Michaelis-Menten constant of the tubular secretion mechanism ($\mu\text{g/ml}$)

The renal excretion rate ($\mu\text{g/min}$) in this model is represented by

$$R_R = Q_{ur} \cdot C_3 \quad (4.8)$$

and the unbound drug concentration in compartment 1 can be calculated after rearrangement of equations 4.1 and 4.2:

$$C_{u1} = \frac{1}{2} [-(P + K_d - C_1) + \sqrt{(P + K_d - C_1)^2 + 4K_d C_1}] \quad (4.9)$$

The experimentally observed plasma concentration and renal excretion rate curves were simultaneously fitted to the model described above.

Data Analysis.

The spline functions were fitted to the equally weighted data with the rational spline interpolation routine of the DISSPLA computer package [15]. DISSPLA was also used for drawing the figures presented in this study. All other data were analyzed with the aid of the computer program NONLIN [16]. Plasma protein data were weighted equally. For the kidney model, several weighting factors were tested; in most cases, the reciprocal weighting procedure gave the best fits. In order to make the

standard deviations of experiments in which different weighting factors were used comparable to each other, all standard deviations were calculated for one set of weighting factors, e g , plasma concentration data were reciprocally weighted ($1/C^2$) and renal excretion rate data were equally weighted. The goodness of fit to the plasma concentration and renal excretion rate data was evaluated through the deviations between observed and model-predicted values as $R^2 = 1 - \Sigma(\text{Obs})^2 / \Sigma(\text{Dev})^2$, where $\Sigma(\text{Obs})^2$ is the corrected sum of squared observations and $\Sigma(\text{Dev})^2$ the sum of squared deviations. Statistical differences between means were established using Student's t-test for paired samples. Average values are expressed as mean \pm SD.

4.3 RESULTS

Protein Binding.

Concentration-dependent plasma protein binding of SUA was observed, the fraction unbound ranging from 30-60% (Fig 4 2). PSP did not interfere with protein binding of SUA. Because interindividual variation in binding was found to be small, data of all experiments ($n=46$) were pooled and analyzed according to Eq 4 1. The results of this fit were 222 ± 26 $\mu\text{g/ml}$ and 96 ± 19 $\mu\text{g/ml}$ for total concentration of protein binding sites (P) and dissociation constant (K_d), respectively.

Pharmacokinetic Analysis.

A representative example of plasma disappearance and renal excretion rate after intravenous administration of SUA with or without simultaneous infusion of PSP is shown in Fig 4 3. The pronounced nonlinear shape of these curves indicated that at least one capacity-limited process is involved in the kinetics of SUA. Plasma and urinary data were analyzed separately after cubic spline interpolation of the data points and extrapolation of the terminal phase to infinity, assuming log-linear decline. Although linear extrapolation may overestimate the area under the curve in cases of nonlinear elimination, the contribution of this residual area was only small, not exceeding 5% for any of the curves. The parameters calculated are summarized in Table 4 1. Steady state concentrations of PSP that were reached are given in Table 4 2.

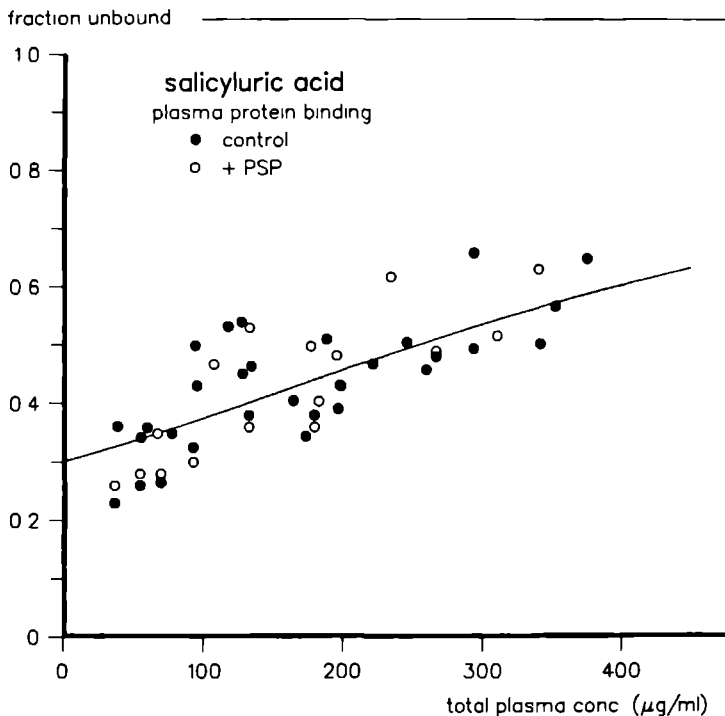


Fig. 4.2 Plasma protein binding of SUA with or without the presence of PSP. The line through the data is calculated by Eq. 4.1.

Total plasma clearance of SUA was significantly reduced from 56 ± 5 ml/min to 48 ± 8 ml/min ($p < 0.05$), during PSP administration. The fraction of the dose excreted unchanged into the urine (D_{ur}) remained unaffected, namely $75 \pm 6\%$ in the control experiments and $77 \pm 6\%$ in presence of PSP. As a result, renal clearance, calculated from the product of total clearance and the fraction of the dose excreted, decreased from 42 ± 2 ml/min to 37 ± 6 ml/min in presence of PSP, although the difference failed to reach the 5% level of statistical significance. The decrease in renal clearance could not account fully for the reduction in total plasma clearance, therefore it is likely that PSP also interferes with the nonrenal clearance of SUA. Assuming an average protein binding of approximately 45%, it could be calculated from the product with glomerular filtration (Table 4.2) that the contribution of filtration to the total renal clearance

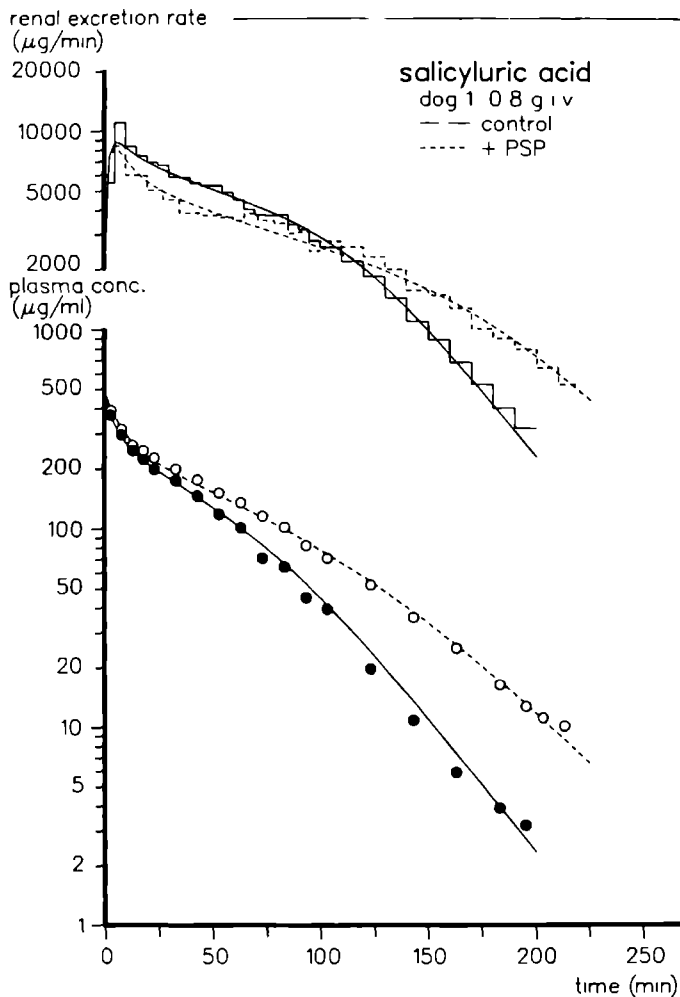


Fig. 4.3 Renal excretion rate and plasma concentration as function of time after rapid i.v. administration of 0.8 gram SUA with or without concomitant infusion of PSP. The solid and broken lines in the figure represent the results of data analysis according to the kidney model.

of SUA was about 16 ml/min. Obviously, active tubular secretion accounted for the greater part of renal clearance. The decrease in renal clearance could be ascribed to an effect of PSP on the tubular secretion of SUA, as glomerular filtration and protein binding remained unchanged.

Table 4.1 Basic pharmacokinetic parameters of SUA after rapid iv injection of 0.8 gram with or without concomitant administration of PSP.

Dog	Inhibitor	plasma			urine		
		CL (ml/min)	CL _{NR} (ml/min)	V ₁ (l)	MRT _R (min)	CL _R (ml/min)	D _{ur} (%)
1	-	52	10	1.84	62	42	80
	PSP	38	9	1.71	82	29	76
2	-	63	20	1.87	69	43	67
	PSP	57	15	1.59	87	42	73
3	-	55	16	1.71	62	39	72
	PSP	51	13	1.74	71	38	74
4	-	55	11	1.55	65	44	79
	PSP	45	6	1.86	90	39	86
Mean	-	56	14	1.74	64	42	75
±SD		5	5	0.15	3	2	6
Mean ^a	PSP	48 [*]	11 [*]	1.73	82 ^{**}	37	77
±SD		8	4	0.14	8	6	6

^aMean values compared to control levels (paired t-test; *p<0.05, **p<0.02).

The MRT_R of SUA, calculated from the renal excretion rate curve, increased significantly from 64 ± 4 min to 82 ± 8 min (p<0.02) as a result of concomitant PSP infusion (Table 4.1). It should be noticed that the MRT_R can be calculated irrespective of whether the drug has nonlinear disposition kinetics or is eliminated peripherally. However, due to the evident nonlinear renal elimination of SUA, the MRT_R is not equal to the total mean residence time in the body, but only represents the mean residence time of those drug molecules that are excreted via the renal path-

Table 4.2 Physiological and experimentally found parameters used as constants in the kidney model^b.

Dog	Weight (kg)	PSP conc. (μ g/ml)	Q_{GF} (ml/min)	Q_{ur} (ml/min)	Q_R^c (ml/min)	V_3 (ml)
1	12.0	—	32 \pm 3	1.13 \pm 0.06	132	1.70 \pm 0.09
	12.4	45 \pm 5	30 \pm 4	1.43 \pm 0.15	136	2.14 \pm 0.22
2	16.8	—	32 \pm 4	1.08 \pm 0.05	185	1.62 \pm 0.08
	16.9	35 \pm 4	33 \pm 4	1.02 \pm 0.04	186	1.53 \pm 0.06
3	14.8	—	30 \pm 2	0.83 \pm 0.12	163	1.24 \pm 0.18
	14.2	40 \pm 5	50 \pm 4	0.81 \pm 0.21	156	1.22 \pm 0.32
4	16.5	—	50 \pm 3	0.85 \pm 0.09	182	1.28 \pm 0.14
	15.0	24 \pm 4	39 \pm 3	0.81 \pm 0.07	165	1.22 \pm 0.11
Mean	15.0	—	36	0.97	165	1.46
\pm SD	2.2		9	0.15	24	0.23
Mean	14.6 ^a	36	38 ^a	1.02 ^a	161 ^a	1.53 ^a
\pm SD	1.9	9	9	0.29	20	0.43

^aNo significant differences with controls (paired t-test; $p > 0.3$).

^bThe other constants were obtained as follows: V_1 was taken from table 1, for V_5 an arbitrary value of 1 l was chosen, V_2 and V_4 were estimated from literature as 10 ml (20) and 30 ml (21), respectively.

^c Q_R was directly estimated from the body weight (see text), therefore no SD.

way. No significant difference was observed for the initial volume of distribution term V_1 .

Kidney Model.

The physiologically based pharmacokinetic model for the renal clearance of SUA presented in this study is an extension of previously described models for iodopyracet [7] and SUA (5). New elements of the model are

that it accounts for nonlinear protein binding and that it incorporates a compartment representing the proximal tubular cells of the kidney. These cells are the main anatomical site for the active secretion of a wide variety of compounds. A schematic representation of the model is given in Fig. 4.1. The kidney is set apart as a subsystem divided into a plasma, tubular cell, and tubular urine compartment. Active transport of SUA takes place from renal plasma into the tubular cell compartment via a capacity-limited pathway obeying Michaelis-Menten kinetics, subsequently followed by first-order transport into the tubular urine compartment.

The most satisfactory fits to the model were obtained when tubular secretion was assumed to be dependent on total concentrations, rather than on unbound concentrations. The average goodness of fits, $R^2_{\text{plasma}} = 0.993 \pm 0.008$ and $R^2_{\text{urine}} = 0.979 \pm 0.013$ (Table 4.4), were significantly better than the values obtained when unbound concentrations were used, e.g., $R^2_{\text{plasma}} = 0.904 \pm 0.044$ ($p < 0.005$) and $R^2_{\text{urine}} = 0.896 \pm 0.034$ ($p < 0.005$). Therefore, active tubular secretion of SUA was considered to be dependent on the total concentration in renal plasma. Naturally, glomerular filtration was a function of the unbound drug concentration, operating directly from the central compartment into the tubular urine compartment.

To describe the plasma kinetics of SUA completely, a peripheral tissue compartment was allocated to the central compartment and a first-order clearance constant was introduced, representing the extrarenal clearance pathway. In Table 4.2, the parameters used as constants in the model are listed. Q_{GF} was determined by steady state inulin clearance. For Q_R a value of 11 ml/min/kg was taken [17]. The volume of the tubular urine compartment (V_3) was considered to be dependent on urine flow and renal delay time [18]. Assuming a constant renal delay time (Δt) of 1.5 min [19], V_3 was calculated as $V_3 = Q_{ur} \cdot \Delta t$.

Plasma concentration and renal excretion rate data of each experiment were simultaneously fitted to the model using NONLIN. The results of these calculations are listed in Tables 4.3 and 4.4 and are also represented by the solid and broken lines through the data points in Figs. 4.3 and 4.4. The tubular titration curves in Fig. 4.4 are linear plots of renal excretion rate against plasma concentration at the midpoint of a urine collection interval. They give a good impression of the processes that deter-

Table 4.3 Model parameters characterizing the renal handling of SUA and the effect of PSP.

Dog	Inhibitor	T_M (mg/min)	K_T (μ g/ml)	CL_{NR} (ml/min)	k_{43} (min ⁻¹)	k_{15} (min ⁻¹)	k_{51} (min ⁻¹)
1	—	4.1 \pm 0.4	19 \pm 7	11 \pm 4	0.33 \pm 0.30	0.058 \pm 0.031	0.118 \pm 0.051
	PSP	2.3 \pm 0.3	20 \pm 4	9 \pm 2	0.38 \pm 0.71	0.046 \pm 0.008	0.082 \pm 0.012
2	—	3.6 \pm 0.4	28 \pm 10	20 \pm 1	0.31 \pm 0.15	0.045 \pm 0.003	0.055 \pm 0.008
	PSP	3.2 \pm 0.6	28 \pm 15	14 \pm 4	0.29 \pm 0.30	0.061 \pm 0.011	0.052 \pm 0.010
3	—	4.8 \pm 0.5	29 \pm 8	16 \pm 4	0.10 \pm 0.03	0.065 \pm 0.022	0.121 \pm 0.033
	PSP	3.8 \pm 0.3	31 \pm 6	13 \pm 2	0.10 \pm 0.04	0.070 \pm 0.010	0.108 \pm 0.014
4	—	4.7 \pm 0.9	47 \pm 15	10 \pm 3	0.07 \pm 0.03	0.088 \pm 0.013	0.109 \pm 0.015
	PSP	3.9 \pm 1.7	48 \pm 32	8 \pm 6	0.08 \pm 0.09	0.055 \pm 0.019	0.086 \pm 0.029
Mean	—	4.3	31	14	0.20	0.064	0.101
\pm SD		0.6	5	3	0.14	0.018	0.031
Mean ^a	PSP	3.3 [*]	32	11 [*]	0.21	0.058	0.082
\pm SD		0.7	12	3	0.15	0.010	0.023

^aMean values compared to control levels (paired t-test; *p<0.05).

Table 4.4 Goodness of fit of the kidney model to the observed plasma concentration and renal excretion rate data of SUA.

Dog	Inhibitor	R ² plasma	R ² urine
1	—	0.999	0.995
	PSP	0.998	0.977
2	—	0.978	0.969
	PSP	0.982	0.961
3	—	0.998	0.992
	PSP	0.997	0.987
4	—	0.996	0.988
	PSP	0.997	0.965

mine the renal clearance of SUA and the effect of PSP. It appears from Fig. 4.4 that SUA undergoes net tubular secretion which becomes saturated at high plasma levels. In that situation, the final part of the titration curve parallels the glomerular filtration (GF) curve. Because of concentration-dependent protein binding, this line is not straight but has a somewhat concave shape, for glomerular filtration always operates on the fraction of the drug that is not protein bound. The effect of PSP manifests itself in a decreased renal excretion rate of SUA over the whole plasma concentration range measured. Evaluation of the curves with the kidney model revealed that this effect could be characterized consistently by a noncompetitive inhibition of the active transport step from renal plasma into the tubular cells (Table 4.3). The maximum transport rate (T_M) was significantly reduced from 4.3 ± 0.6 mg/min to 3.3 ± 0.7 mg/min ($p < 0.05$), whereas the Michaelis-Menten constant (K_T) remained unaltered (31 ± 5 μ g/ml vs. 32 ± 12 μ g/ml). Furthermore, a small but signif-

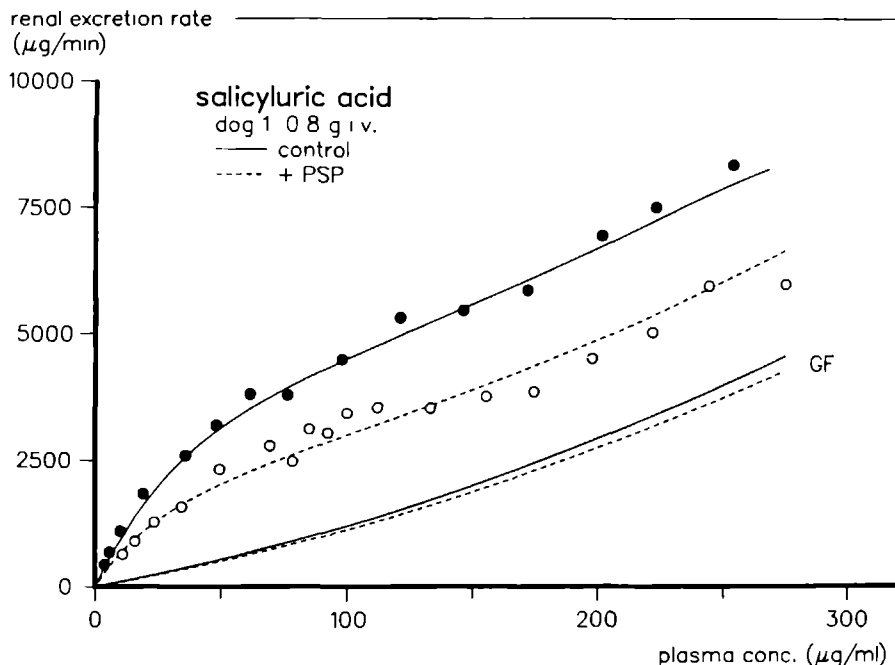


Fig. 4.4 Tubular titration curves representing the relationship between the renal excretion rate and the plasma concentration after i.v. administration of SUA with or without PSP. The lines through the data points are calculated according to the kidney model. GF represents the clearance by glomerular filtration of SUA.

ificant effect on the nonrenal clearance (CL_{NR}) of SUA was calculated (14 ± 3 ml/min vs. 11 ± 3 ml/min; $p < 0.05$). Under the experimental conditions, passive reabsorption appeared to be negligible, presumably due to the mannitol induced diuresis and the high urinary pH (7.0 ± 0.8) as compared to the dissociation constant of SUA ($pK_a = 3.6$) [22].

4.4 DISCUSSION

The physiologically based model presented provides an overall representation of the renal secretory system, comprising all the functional characteristics of the kidney that are involved in the excretion of SUA. New

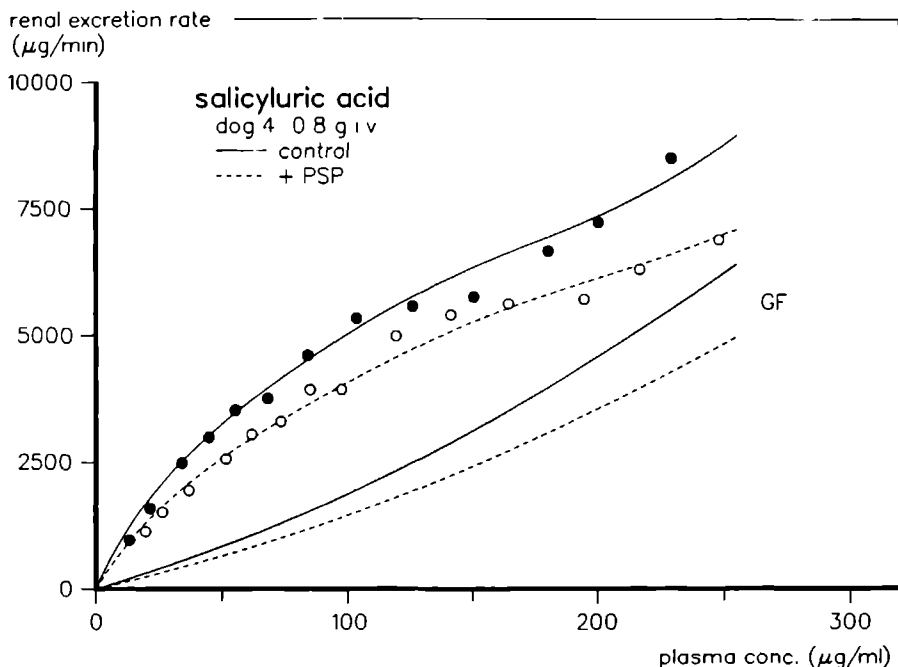


Fig. 4.4 Continued.

features of the model are that it accounts for nonlinear plasma protein binding and carrier-mediated transport through the cells of the proximal tubules. The latter process plays an important role in the renal clearance of SUA and a large number of other organic anions.

The role of plasma protein binding is appreciably less understood. It has been suggested that for compounds cleared with a high affinity for the secretory system, protein binding does not limit the extent of tubular secretion, whereas for drugs that are secreted with a relatively low affinity renal clearance will be dependent on the fraction unbound [23]. Obviously, there will be more determining factors in this respect, like the rate of dissociation of the drug-protein complex, the transit time through the peritubular capillaries and diffusion into the cortical interstitium. Since the renal clearance of SUA equals the PAH clearance at low plasma

concentrations [4], the affinity for the secretory system appears to be large enough, relative to other factors, to give a complete extraction from the plasma in a single passage through the kidney. This is in agreement with our findings that the best fits to the model were obtained when tubular secretion was considered to be proportional to the total plasma concentration of SUA.

Active secretion of organic anions is usually associated with accumulation and retention of the drug within the proximal tubular cells [24]. From the results in Table 4.3, it can be concluded that SUA substantially accumulates within the tubular cells. The cellular uptake of SUA in the control experiments, expressed as the intrinsic secretion clearance $Cl_{int} = T_M/K_T$ is 152 ± 50 ml/min. This value surpasses many times the clearance out of the cells into the lumen, represented by $V_4 \cdot k_{43}$, being 6 ± 4 ml/min. In Fig. 4.5, the cellular concentration of SUA is simulated, using the model parameters calculated from the experiments in dog 1 (Table 4.3). The cellular SUA concentration without PSP exceeds the plasma concentration considerably, the concentration ratio of tubular cells to plasma ranging from approximately 2 at high plasma concentrations to approximately 8 at lower concentrations. These simulated accumulation values are in close accordance with observations in the isolated perfused rat kidney [25]. In the presence of PSP, accumulation of SUA was reduced as a result of interference with the active cellular uptake. In this situation, the cell to plasma ratio ranged from approximately 0.8 at high plasma concentrations to 4.5 at lower concentrations. Although uptake was decreased, the extent of retention within the cells was apparently not influenced by PSP, as judged from the profile of the cellular concentration curve (Fig. 4.5).

SUA is known to have a renal clearance considerably less than that of PAH at high plasma concentrations [26]. This was attributed to passive tubular reabsorption occurring to an increasing extent with increased tubular loading. Dependent on urine flow and urinary pH, even transition from net secretion to net reabsorption was observed, resulting from the fact that tubular secretion is saturable while back-diffusion is a passive process without limitations [4,27]. However, our results clearly show that, under conditions where passive back-diffusion is negligible the maximal rate of tubular transport of SUA, 4.3 ± 0.6 mg/min (Table 4.3), is

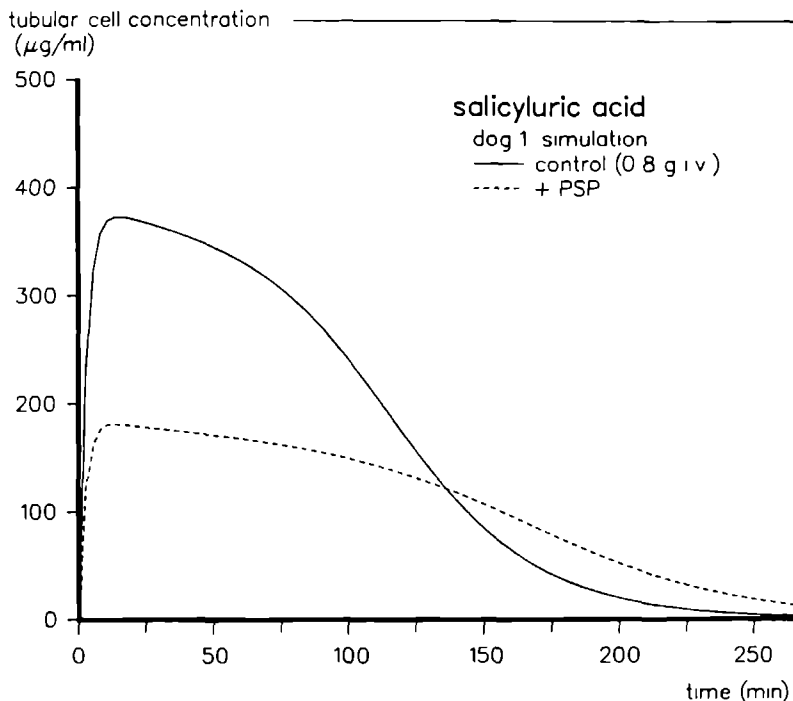


Fig. 4.5 Course of the proximal tubular cell concentration of SUA with or without the presence of PSP. The parameters used for this simulation were obtained from the analysis of plasma and urine curves of dog 1 according to the kidney model.

still much lower than the value of 15 ± 2 mg/min reported for PAH [28]. It can be concluded that, although passive reabsorption may contribute under certain conditions to a less efficient clearance, the limited capacity of the secretory system for SUA is the main reason for the restricted excretion at high plasma concentrations.

Analysis with the kidney model showed that PSP behaved like a noncompetitive inhibitor of the active uptake of SUA into the tubular cells. A similar type of interaction was described previously for the effect of probenecid on SUA secretion [5]. PSP reduced to a lesser degree the extrarenal clearance of SUA, presumably by interfering with hepatic elimination, a transport pathway that bears a certain resemblance with the renal secretory system [29]. The question of how the mechanism of the

PSP interaction should be interpreted at a molecular level cannot be answered directly from this study. In view of the hypothesis of multiple transport systems, it can be speculated that PSP and SUA bind to distinct transport sites in which binding of PSP to its site prevents SUA from binding to the other site by steric hindrance or distortion. When SUA has little or no affinity for the "PSP"-site, the interaction will manifest itself as noncompetitive. Clearly, detailed in vitro work focused on the concept of multiplicity of the organic anion transport system will be necessary to elucidate the actual mechanism of this interaction.

4.5 REFERENCES

1. J.V. Møller and M.I. Sheikh: Renal organic anion transport system: pharmacological, physiological, and biochemical aspects. *Pharmacol. Rev.* **34**,315-358 (1983).
2. I.M. Weiner: Organic acids and bases and uric acid. In "The Kidney: Physiology and Pathophysiology" (D.W. Seldin and G. Giebisch eds.), pp. 1703-1724. Raven Press, New York, 1985.
3. K.J. Ullrich, G. Rumrich, S. Klöss, and H.-J. Lang: Contraluminal sulfate transport in the proximal tubule of the rat kidney.V.Specificity: phenolphthaleins, sulfonphthaleins, and other sulfo dyes, sulfamoyl-compounds and diphenylamine-2-carboxylates. *Pflügers Arch.* **404**,311-318 (1985).
4. P.K. Knoefel, K.C. Huang, and C.H. Jarboe: Renal disposal of salicyluric acid. *Am. J. Physiol.* **203**,6-10 (1962).
5. P. Hekman and C.A.M. Van Ginneken: Simultaneous kinetic modelling of plasma levels and urinary excretion of salicyluric acid and the influence of probenecid. *Eur. J. Drug Metab. Pharmacokinet.* **3**,239-249 (1983).
6. F.G.M. Russel, A.C. Wouterse, and C.A.M. Van Ginneken: Physiologically based pharmacokinetic model for the renal clearance of phenolsulfonphthalein and the interaction with probenecid and salicyluric acid in the dog. *J. Pharmacokinet. Biopharm.*, **15**,349-368 (1987).
7. P. Hekman and C.A.M. Van Ginneken: Kinetic modelling of the renal excretion of iodopyracet in the dog. *J. Pharmacokinet. Biopharm.* **10**,77-92 (1982).

8. F.G.M. Russel, A.C. Wouterse, P. Hekman, G.J. Grutters, and C.A.M. Van Ginneken: Quantitative urine collection in renal clearance studies in the dog. *J. Pharmacol. Methods*, **17**,125-136 (1987).
9. B.K. Ochwaldt and R.F. Pitts: Disparity between phenol red and diodrast clearances in the dog. *Am. J. Physiol.* **187**,318-322 (1956).
10. A. Heyrovski: A new method for the determination of inulin in plasma and urine. *Clin. Chim. Acta* **1**,470-474 (1956).
11. K. Yamaoka, T. Nakagawa, and T. Uno: Statistical moments in pharmacokinetics. *J. Pharmacokinet. Biopharm.* **6**,547-558 (1978).
12. L.Z. Benet and R.L. Galeazzi: Noncompartmental determination of the steady-state volume of distribution. *J. Pharm. Sci.* **68**,1071-1074 (1979).
13. K.C. Yeh and K.C. Kwan: A comparison of numerical integrating algorithms by trapezoidal, lagrange, and spline approximation. *J. Pharmacokinet. Biopharm.* **6**,79-98 (1978).
14. M. Gibaldi and D. Perrier: *Pharmacokinetics*. Marcell Dekker Inc., New York, 1982.
15. DISSPLA user's manual: Display Integrated Software System and Plotting Language, Version 9.2. Integrated Software Systems Corporation. San Diego Ca., 1984.
16. C.M. Metzler, G.L. Elfring, and A.J. McEwen: A package of computer programs for pharmacokinetic modeling. *Biometrics* **30**,562-563 (1974).
17. B.H. Ewald: Renal function tests in normal beagle dogs. *Am. J. Vet. Res.* **28**,741-749 (1967).
18. E. Bojesen: The function of the urinary tract as dead space in renal clearance experiments. *Scand. J. Clin. Lab. Invest.* **1**,290-294 (1949).
19. P.A. Morales, C.H. Crowder, A.P. Fishman, M.H. Maxwell, and D.M. Gomez: Measurement and significance of urinary appearance time in the dog. *Am. J. Physiol.* **163**,454-460 (1950).
20. F.P. Chinard: Comparative renal excretion of glomerular substances following instantaneous injection into a renal artery. *Am. J. Physiol.* **180**,617-619 (1955).
21. M.S. Dunnill and W. Halley: Some observations on the quantitative anatomy of the kidney. *J. Pathol.* **110**,113-121 (1973).

22. H.W. Smith, N. Finkelstein, L. Aliminosa, B. Crawford, and M. Graber: The renal clearances of substituted hippuric acid derivatives and other aromatic acids in dog and man. *J. Clin. Invest.* **24**,388-404 (1945).
23. G.T. Tucker: Measurement of the renal clearance of drugs. *Br. J. Clin. Pharmacol.* **12**,761-770 (1981).
24. R.P. Forster and J.H. Copenhaver: Intracellular accumulation as an active process in a mammalian renal transport system in vitro. *Am. J. Physiol.* **186**,167-171 (1956).
25. I. Bekersky and N. Olejnik: Effect of probenecid on the renal tubular secretion of salicylic acid by the isolated perfused rat kidney. *Drug Metab. Dispos.* **13**,630-633 (1985).
26. P.K. Knoefel and K.C. Huang: Biochemorphology of renal tubular transport: hippuric acid and related substances. *J. Pharmacol. Exp. Ther.* **126**,296-303 (1959).
27. I.M. Weiner, K.D. Garlid, J.A. Romeo, and G.H. Mudge: Effects of tubular secretion and reabsorption on titration curves of tubular transport. *Am. J. Physiol.* **200**,393-399 (1961).
28. D. Schachter and N. Freinkel: Self-depression of Tm_{PAH} in the dog at high plasma PAH levels and its reversibility by acetate. *J. Clin. Invest.* **167**,531-538 (1951).
29. E.H. Bárány: The liver-like anion transport system in rabbit kidney, uvea and choroid plexus. II. Efficiency of acid drugs and other anions as inhibitors. *Acta Physiol. Scand.* **88**,491-504 (1973).

RENAL CLEARANCE OF IODOPYRACET AND THE INTERACTION WITH PROBENECID¹

Frans G.M. Russel, Alfons C. Wouterse and Cees A.M. van Ginneken

Abstract - Plasma kinetics and renal excretion of iodopyracet (3.0 g, administered i.v.) with and without concomitant administration of probenecid were studied in the beagle dog. Pharmacokinetic analysis revealed that tubular secretion is the predominant route of excretion, and that secretion is inhibited by probenecid. A physiologically based kidney model is proposed comprising all the functional characteristics of the kidney that determine the excretion of iodopyracet, i.e. renal plasma flow, urine flow, protein binding, glomerular filtration, tubular secretion and tubular accumulation. The model enabled an accurate description and analysis of the measured plasma levels and renal excretion rates. Renal clearance of iodopyracet is characterized by supply-limited elimination at low plasma concentrations and capacity-limited elimination at high plasma levels. The interaction with probenecid could be adequately described with the model by competitive inhibition of the carrier-mediated uptake of iodopyracet into the tubular cells. Model calculations showed that in the control experiments tubular secretion was accompanied by a pronounced accumulation of iodopyracet within the cells, which was clearly diminished in presence of probenecid.

¹Biopharm. Drug Dispos., in press

5.1 INTRODUCTION

The renal clearance of iodopyracet (Diodrast), a radiographic contrast agent, has historically received a lot of attention as a means to estimate tubular function and plasma flow through the kidney. Its renal excretion pattern strongly resembles that of the prototypic anion p-aminohippurate (PAH). Transport of iodopyracet into the urine occurs very rapidly by glomerular filtration and extensive tubular secretion. At low plasma concentrations the rate of excretion is so high that the renal clearance approaches the renal plasma flow and becomes flow-limited [1]. Under these circumstances extraction from the plasma in a single passage through the kidney is virtually complete [2], implying that plasma protein binding of iodopyracet, which amounts to about 30% [3], does not form any hindrance to tubular secretion. It also implies that at low plasma levels reabsorption from the tubular urine is negligible. Passive pH-dependent reabsorption is very unlikely to occur for iodopyracet, even at high tubular loading, considering the low pK_a of 2.7 [4], compared with the usual urinary pH.

It has been well documented that the renal secretion of iodopyracet, and in general of organic anions, is confined to the proximal tubular cells. The sequence of transport through these cells is active uptake across the basolateral membrane, intracellular accumulation, followed by diffusion (probably facilitated) across the brush-border membrane into the tubular fluid. Intracellular accumulation is highly dependent on the efficiency of the active transport step across the basolateral membrane. In case of iodopyracet the extent of accumulation in the cells and urine will determine its visibility as a renal contrast agent, thus providing an estimate of the functional viability of the proximal tubular cells in health and disease. The extent of tubular accumulation may also play an important part in the pathogenesis of radiocontrast agent-induced acute renal failure [5], as a result of a direct toxic effect on the tubular cells.

In a previous study we showed the usefulness of physiologically based modeling in characterizing the flow-dependent renal kinetics of iodopyracet [6]. However, the model described did not account for the phenomenon of intracellular accumulation. The purpose of the present study was to incorporate this important feature of transtubular transport, and

to quantify the relevant processes of renal iodopyracet excretion with this extended model. Furthermore, the kidney model was used to describe the interaction with the standard inhibitor probenecid, in order to get more insight in the mechanisms and effects of drug interactions at the level of tubular secretion.

5.2 MATERIALS AND METHODS

Materials

Iodopyracet was obtained from Dagra NV (Diemen, The Netherlands), probenecid from Sigma (St. Louis, Mo., USA), indole-3-acetic acid and LiChrosorb RP18 were from Merck (Darmstadt, FRG). Braunule T cannulas were obtained from Braun (Melsungen, FRG), the double walled urinary catheter (URO 90.009) from Talas (Ommen, The Netherlands), and Visking 8 dialysis tubing from Instrumentenhandel Z.H. (Den Haag, The Netherlands). All other materials and chemicals were described previously [7].

Clearance Experiments

The experiments were done in male Beagle dogs, weighing 11 to 15 kg, as was described in detail previously [7,8]. In summary, the dogs were fasted overnight and anesthetized with sodium pentobarbital (30 mg/kg, i.v.). As premedication atropine sulfate (0.5%, 1 ml i.v.) was given. A cannula (Braunule T) was inserted into the cephalic veins of both forelegs for blood sampling and drug administration. A constant infusion of 5% mannitol and 0.5% inulin (2 ml/min) was administered throughout the experiment. In this way, a sufficiently high urine flow and constant pH (7.0 ± 0.8) was obtained. Each dog received as an i.v. bolus a sterile solution of 3.0 g iodopyracet dissolved in 20 ml water containing an equimolar amount of sodium bicarbonate. In case of probenecid treatment the dogs received 30 min prior to injection of iodopyracet a priming dose of 75 mg probenecid (2.5% in aqueous sodium bicarbonate, 3 ml i.v.), followed by a constant infusion of a 0.5% solution at a rate of 2.5 ml/hr (dogs 1 and 3) or 5 ml/hr (dogs 2 and 4). At regular times throughout the experiment blood samples were taken into heparinized tubes. Plasma

was separated by centrifugation for 20 min at 2000g. Urine was collected quantitatively with a double walled urinary catheter at 5 min intervals during the first 100 min of the experiment, and afterwards at 10 min intervals. Plasma and urine samples were stored at -20°C until analysis. Before the dog was used for the second experiment at least three weeks of recovery were observed.

Analytical Methods

Iodopyracet was determined in plasma and urine and probenecid was determined in plasma by high-performance liquid chromatography (HPLC). Both procedures were described previously [9,10]. A Hewlett Packard 1084B chromatograph was used equipped with a variable wavelength detector, autosampler and terminal (HP 7850 LC). The stainless-steel column (150 × 4.6 mm I.D.) was packed with LiChrosorb RP-18, particle size 5 µm.

Inulin was assayed by a spectrophotometric method [11]. After hydrolysis to fructose and reaction with indole-3-acetic acid in hydrochloric acid (32% w/w) absorbance was measured at 515 nm.

Protein Binding

Plasma protein binding of iodopyracet was determined by ultrafiltration [6] using Visking dialysis tubing (flat width 10 mm, average pore size 2.4 µm). Plasma (2.0 ml) was pipetted into the tubes, precentrifuged (10 min at 1000g) to remove membrane bound water, and subsequently centrifuged for 60 min at 1000g yielding about 150 µl ultrafiltrate. Binding of iodopyracet to the dialysis membrane was found to be negligible. The ultrafiltrates were treated and analyzed in the same way as urine samples were.

Pharmacokinetic Analysis

Plasma concentration-time curves and renal excretion rate-time curves were fitted separately to the usual multiexponential equations. Basic pharmacokinetic parameters were calculated from these fits applying statistical moments theory [12,13]. The area under the plasma curve was calculated by direct integration after extrapolation of the terminal phase of the plot to infinity. In the same way the area under the renal excretion rate

curve as well as the area under the first moment of this curve were calculated. Half-lives of iodopyracet in plasma ($t_{1/2,p}$) and urine ($t_{1/2,ur}$) were obtained from their respective terminal elimination rate constants. Using standard equations [14], total plasma clearance (CL) was calculated as the dose divided by the area under the plasma curve, and the initial volume of distribution (V_1) as the dose divided by the extrapolated zero-time plasma concentration. The mean residence time was determined from the renal excretion rate curve (MRT_R), dividing the area under the first moment curve by the area under the curve. The total amount of iodopyracet excreted in infinite time into urine was directly obtained from the area under the renal excretion rate curve. Renal clearance (CL_R) was calculated as the product of total plasma clearance and fraction of the dose excreted unchanged in the urine (D_{ur}), and the nonrenal clearance (CL_{NR}) was determined by subtracting the renal clearance from the total plasma clearance.

Kidney Model

The physiologically based model for the renal excretion of iodopyracet is illustrated by the diagram in Fig. 5.1. Transport processes and compartmental concentrations of the drug can be described by the following set of equations:

Central plasma

$$V_1 \frac{dC_1}{dt} = (Q_R - Q_{ur})C_2 + k_{51}V_5C_5 - (Q_R + CL_{NR} + k_{15}V_1)C_1 \quad (5.1)$$

Renal plasma

$$V_2 \frac{dC_2}{dt} = Q_R C_1 - Q_{GF}C_{u1} - (Q_R - Q_{ur})C_2 - \frac{T_M C_2}{K_T + C_2} \quad (5.2)$$

Tubular urine

$$V_3 \frac{dC_3}{dt} = Q_{GF}C_{u1} + k_{43}V_4C_4 - Q_{ur}C_3 \quad (5.3)$$

Tubular cells

$$V_4 \frac{dC_4}{dt} = \frac{T_M C_2}{K_T + C_2} - k_{43} V_4 C_4 \quad (5.4)$$

Peripheral tissues

$$V_5 \frac{dC_5}{dt} = k_{15} V_1 C_1 - k_{51} V_5 C_5 \quad (5.5)$$

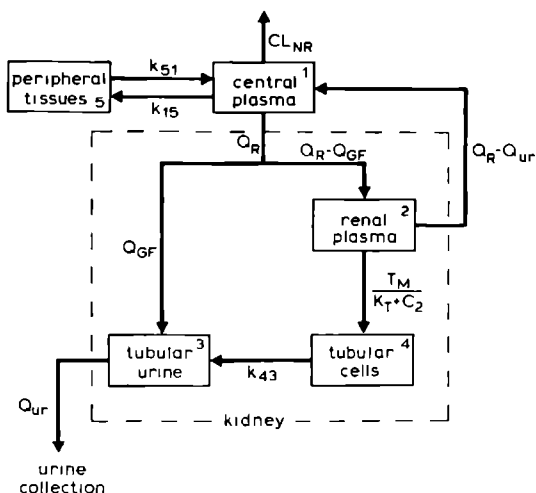


Fig. 5.1 Physiologically based pharmacokinetic model for the renal clearance of iodopyracet. See Materials and Methods for explanation of symbols.

where,

- V_i = volume of compartment i (ml)
- C_i = total drug concentration in compartment i ($\mu\text{g/ml}$)
- C_{u1} = unbound drug concentration in compartment 1 ($\mu\text{g/ml}$)
- k_{ij} = first-order rate constant associated with movement of drug from compartment i to compartment j (min^{-1})
- Q_R = renal plasma flow (ml/min)
- Q_{GF} = glomerular filtration (ml/min)
- Q_{ur} = urine flow (ml/min)

- CL_{NR} = nonrenal plasma clearance (ml/min)
 T_M = maximum transport capacity of the tubular secretion mechanism ($\mu\text{g}/\text{min}$)
 K_T = Michaelis-Menten constant of the tubular secretion mechanism ($\mu\text{g}/\text{ml}$)

The renal excretion rate ($\mu\text{g}/\text{min}$) is represented by

$$R_R = Q_{ur} \cdot C_3 \quad (5.6)$$

The experimentally observed plasma concentration and renal excretion rate curves were simultaneously analyzed with the model described above.

Data Analysis

Curve-fitting was done with the aid of the computer program NONLIN [15]. In the exponential fits data were weighted reciprocally. For the kidney model several weighting factors were tested, in most cases best fits were obtained when plasma data were weighted reciprocally ($1/C^2$) and renal excretion rate data were weighted equally. In order to make the standard deviations (SD) obtained from fits in which different weighting factors were used comparable to each other, all SD were calculated for the above-mentioned set of weighting factors. The goodness of fit to the plasma concentration and renal excretion rate data was evaluated through the deviations between observed and model-predicted values as $R^2 = 1 - \Sigma(\text{Obs})^2 / \Sigma(\text{Dev})^2$, where $\Sigma(\text{Obs})^2$ is the corrected sum of squared observations and $\Sigma(\text{Dev})^2$ the sum of squared deviations. Statistical differences between means were established using Student's t-test for paired samples. Average values are expressed as mean \pm SD. The figures presented in this study were drawn with the DISSPLA computer package [16].

5.3 RESULTS

Protein Binding

Plasma protein binding of iodopyracet was determined in each experiment in at least five different samples. Over the concentration range measured (10-1000 $\mu\text{g/ml}$) binding was virtually constant. Therefore, binding data of each experiment were averaged. Results are presented in Table 5.2. The mean fraction unbound in the control experiments was 0.72 ± 0.03 . Probenecid (14-58 $\mu\text{g/ml}$) had no effect on the protein binding of iodopyracet, the fraction unbound remaining 0.74 ± 0.04 ($p>0.3$).

Pharmacokinetic Analysis

Fig. 5.2 depicts a representative example of plasma disappearance and renal excretion rate of intravenous administered iodopyracet with or without simultaneous infusion of probenecid. Pharmacokinetic parameters were determined from plasma and urinary data separately and the results of these calculations are summarized in Table 5.1.

Total plasma clearance of iodopyracet was significantly reduced from 88 ± 23 ml/min to 73 ± 14 ml/min ($p<0.02$), while the fraction of the dose excreted unchanged into the urine remained unaffected ($89 \pm 8\%$ vs. $88 \pm 6\%$, $p>0.8$). As a result, renal clearance, calculated from the product of plasma clearance and fraction of the dose excreted, decreased from 79 ± 25 ml/min to 62 ± 15 ml/min ($p<0.05$). The decrease in renal clearance fully accounted for the reduction in total plasma clearance, indicating that probenecid had no effect on the nonrenal clearance of iodopyracet (Table 5.1). The contribution of glomerular filtration to the total renal clearance of iodopyracet in the controls was 25 ± 7 ml/min, as calculated from the product of the fraction unbound and the glomerular filtration rate (Table 5.2). From these results it is clear that tubular secretion of iodopyracet is the most important route of renal excretion at the given dose. The decrease in renal clearance by probenecid could be fully ascribed to inhibition of tubular secretion, since glomerular filtration and protein binding remained unchanged (Table 5.2).

Administration of probenecid resulted in a significant increase of the MRT_R and the terminal half-lives of iodopyracet in plasma and urine, whereas no significant difference was observed for the initial volume of

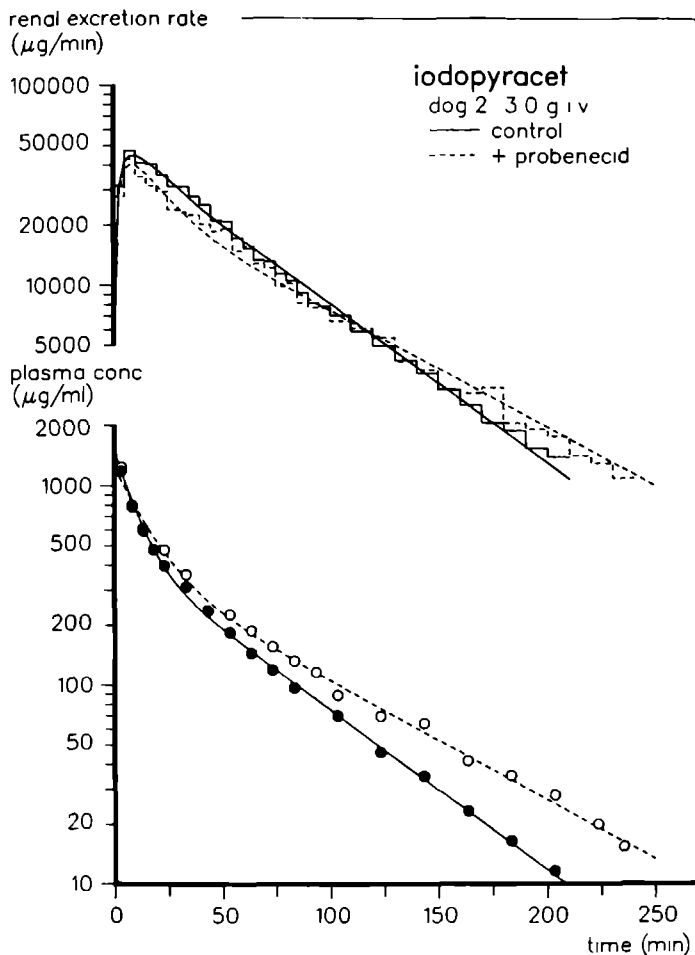


Fig. 5.2 Renal excretion rate and plasma concentration as function of time after rapid i.v. administration of 3.0 gram iodopyracet with or without concomitant infusion of probenecid. The solid and broken lines in the figure represent the results of data analysis according to the kidney model.

distribution term V_1 . The mean residence time was calculated from the renal excretion rate curve as this parameter, contrary to the mean residence time obtained from the moments of the plasma concentration curve, does not suffer from the assumptions of linear disposition kinetics and elimination from the central compartment. However, it should be empha-

Table 5.1 Basic pharmacokinetic parameters of IP after rapid i.v. injection of 3.0 gram with or without concomitant administration of probenecid (Prob).

Dog	Inhibitor	plasma				urine			
		$t_{1/2,p}$ (min)	CL (ml/min)	CL _{NR} (ml/min)	V ₁ (l)	$t_{1/2,ur}$ (min)	MRT _R (min)	CL _R (ml/min)	D _{ur} (%)
1	—	30	122	7	2.25	52	56	115	94
	Prob	40	94	11	2.05	57	68	83	88
2	—	37	81	2	1.99	44	58	79	98
	Prob	51	68	9	2.26	53	67	59	87
3	—	44	80	15	2.92	58	66	65	81
	Prob	55	67	14	2.42	62	70	53	95
4	—	43	71	9	2.11	59	78	58	82
	Prob	48	63	6	2.18	67	86	51	81
Mean	—	38	88	9	2.32	53	66	79	89
±SD		6	23	6	0.42	7	8	25	8
Mean ^a	Prob	48 ^{***}	73 ^{***}	12	2.23	60 ^{**}	73 ^{***}	62 [*]	88
±SD		6	14	2	0.15	6	9	15	6

^aMean values compared to control levels (paired t-test; *p<0.05, **p<0.02).

Table 5.2 Physiological and experimentally found parameters used as constants in the kidney model^b.

Dog	Weight (kg)	Prob conc. ($\mu\text{g/ml}$)	fu	Q_{GF} (ml/min)	Q_{ur} (ml/min)	V_3 (ml)
1	14.5	—	0.72 ± 0.07	44 ± 4	0.61 ± 0.16	0.92 ± 0.24
	13.6	14 ± 2	0.74 ± 0.02	32 ± 2	1.09 ± 0.27	1.64 ± 0.41
2	12.3	—	0.68 ± 0.04	31 ± 2	0.92 ± 0.14	1.38 ± 0.21
	13.0	54 ± 4	0.71 ± 0.04	34 ± 2	0.85 ± 0.09	1.28 ± 0.14
3	12.2	—	0.74 ± 0.03	32 ± 2	1.40 ± 0.28	2.10 ± 0.42
	12.3	19 ± 3	0.72 ± 0.02	38 ± 3	0.88 ± 0.12	1.32 ± 0.18
4	11.3	—	0.76 ± 0.08	21 ± 2	0.72 ± 0.15	1.08 ± 0.22
	11.3	58 ± 4	0.80 ± 0.04	32 ± 3	0.86 ± 0.13	1.29 ± 0.19
Mean	12.6	—	0.72	32	0.91	1.37
$\pm\text{SD}$	1.4		0.03	9	0.35	0.52
Mean	12.6^a	36	0.74^a	34^a	0.92^a	1.38^a
$\pm\text{SD}$	1.0	23	0.04	3	0.11	0.17

^aNo significant differences with controls (paired t-test; $p > 0.3$).

^bThe other constants were obtained as follows: V_1 and CL_{NR} were taken from Table 1, for V_5 an arbitrary value of 1 l was chosen, V_2 and V_4 were estimated from literature as 10 ml [17] and 30 ml [18], respectively.

sized that only for linear pharmacokinetics the MRT_{R} equals the total mean residence time in the body. Due to the obvious nonlinear renal elimination of iodopyracet the MRT_{R} merely represents the mean residence time of those drug molecules that are excreted by the kidney.

Kidney Model

A schematic representation of the physiologically based kidney model is given in Fig. 5.1. In the model the kidney is set apart as a subsystem

divided into a renal plasma, tubular cell and tubular urine compartment. Active transport of iodopyracet takes place from renal plasma into the tubular cell compartment via a capacity-limited pathway obeying Michaelis-Menten kinetics, subsequently followed by first-order transport into the tubular urine compartment. Active tubular secretion was assumed to be dependent on the total iodopyracet concentration in renal plasma. Glomerular filtration was considered to be a function of the unbound drug concentration, operating directly from the central compartment into the tubular urine compartment. For a complete description of iodopyracet kinetics a peripheral tissue compartment was allocated to the central compartment and a nonrenal clearance pathway was introduced. In Table 5.2 the parameters used as constants in the model are listed. Q_{GF} was determined by steady-state inulin clearance. The volume of the tubular urine compartment (V_3) was considered to be dependent on urine flow and renal delay time [19]. Assuming a constant renal delay time (Δt) of 1.5 min [20], V_3 was calculated as $V_3 = Q_{ur} \cdot \Delta t$.

The kidney model was fitted to the plasma concentration and renal excretion rate data of the control experiments using NONLIN. Estimates of the model parameters are given in Table 5.3 and the results are also represented by the solid lines through the datapoints in Figs. 5.2 and 5.3. The average goodness of fit between the observed and model-predicted plasma concentration and renal excretion rate data were $R^2_{\text{plasma}} = 0.993 \pm 0.005$ and $R^2_{\text{urine}} = 0.984 \pm 0.012$, respectively. The tubular titration curves in Fig. 5.3 give a direct representation of the relationship between renal excretion rate and plasma concentration at the midpoint of a urine collection interval. It appears from these plots that iodopyracet undergoes net tubular secretion which becomes saturated at high plasma levels. In that situation the titration curve parallels the glomerular filtration curve, indicating that passive reabsorption was negligible under the experimental conditions. Fig. 5.3 also shows that in the controls the initial part of the titration curve is almost a straight line which clearly differs from the usual Michaelis-Menten profile. The reason for this deviation is that iodopyracet is cleared so rapidly by tubular secretion that at low plasma concentrations extraction from the renal plasma is almost complete and the rate of excretion becomes flow-limited [2,6]. This means that the renal clearance of iodopyracet at low plasma levels practically approaches

Table 5.3 Model parameters characterizing the renal handling of IP and the effect of probenecid (Prob).

Dog	Inhibitor	T_M (mg/min)	K_T (μ g/ml)	K_I (μ g/ml)	Q_R (ml/min)	k_{43} (min ⁻¹)	k_{15} (min ⁻¹)	k_{51} (min ⁻¹)
1	—	39±2	31±4	—	160±6	0.27±0.05	0.063±0.004	0.057±0.003
	Prob	38±7	32±13	4±2	150±24	0.29±0.10	0.063±0.005	0.046±0.004
2	—	32±2	26±9	—	109±10	0.29±0.05	0.055±0.003	0.046±0.002
	Prob	33±11	28±17	7±4	109±29	0.28±0.14	0.027±0.003	0.031±0.002
3	—	31±10	41±21	—	83±23	0.29±0.14	0.018±0.002	0.026±0.002
	Prob	33±11	38±31	8±6	92±12	0.29±0.14	0.024±0.003	0.031±0.003
4	—	24±4	44±32	—	88±13	0.33±0.20	0.055±0.004	0.052±0.003
	Prob	25±14	40±35	11±9	88±17	0.32±0.21	0.060±0.015	0.062±0.005
Mean	—	32	36	—	110	0.30	0.048	0.045
±SD		6	8		35	0.03	0.020	0.014
Mean	Prob	32 ^a	34 ^a	8	110 ^a	0.30 ^a	0.044 ^a	0.042 ^a
±SD		5	6	3	28	0.02	0.021	0.015

^aNo significant differences with controls (paired t-test; $p>0.2$).

the renal plasma flow. Indeed, the extraction ratio of iodopyracet as determined from the ratio of the renal clearance at low plasma concentrations ($<100 \mu\text{g/ml}$) and the model-calculated Q_R (Table 5.3) was 1.01 ± 0.02 . Administration of probenecid resulted in a significant reduction of this value to 0.74 ± 0.10 ($p < 0.02$).

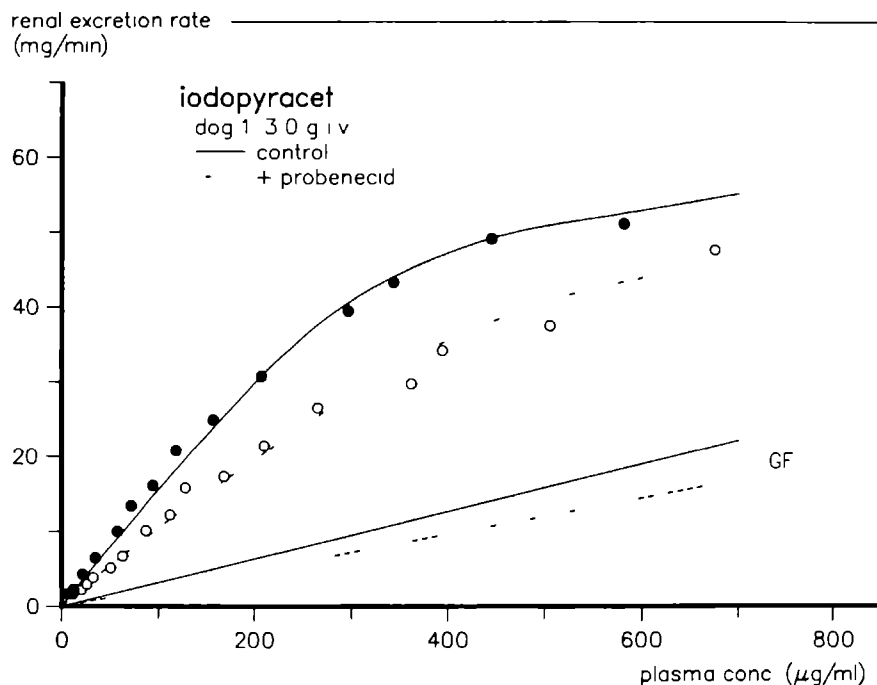


Fig. 5.3 Tubular titration curves representing the relationship between the renal excretion rate and the plasma concentration after i.v. administration of iodopyracet with or without probenecid. The lines through the data points are calculated according to the kidney model. GF represents the clearance by glomerular filtration of iodopyracet.

The effect of probenecid could be adequately described with the kidney model by competitive inhibition of the carrier-mediated transport of iodopyracet from renal plasma into the tubular cell compartment. To quantify this interaction the Michaelis-Menten constant of the tubular secretion mechanism (K_T) in Eq. 5.2 and 5.4 was substituted by the following expression for competitive inhibition $K_T(1 + C_I/K_I)$, where C_I represents

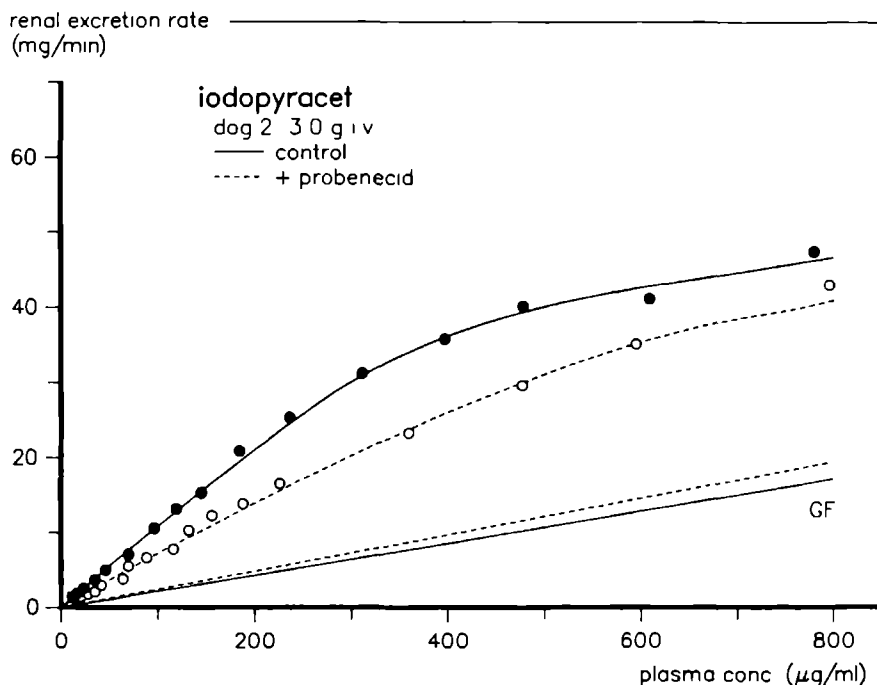


Fig. 5.3 Continued.

the plasma concentration of probenecid and K_I the inhibition constant of probenecid. Steady-state plasma concentrations of probenecid that were reached are given in Table 5.2. Results of the model calculations in presence of probenecid are summarized in Table 5.3 and represented by the dotted lines in Figs. 5.2 and 5.3.

In order to get an impression of the extent of tubular accumulation of iodopyracet, the time course of the concentration in the tubular cell compartment was simulated with the model (Fig. 5.4), using the parameters obtained from the experiments in dog 2 (Table 5.3). Comparison of the simulated concentrations (Fig. 5.4) with the corresponding plasma concentrations (Fig. 5.2) shows that in the control the cellular iodopyracet levels are considerably higher than the levels in plasma. The concentration ratio tubular cells to plasma increased from 5.4 at the highest cell con-

centration of 3360 $\mu\text{g/ml}$ ($t=14$ min) to a constant value of approximately 10.0 at cell concentrations lower than 1000 $\mu\text{g/ml}$ ($t>85$ min). In presence of probenecid cellular concentrations were lower and accumulation was clearly reduced. At the highest cell concentration of 2400 $\mu\text{g/ml}$ ($t=11$ min) the cell to plasma ratio was 3.6, which thereafter slowly increased to a value of 5.7 at a cell concentration of 200 $\mu\text{g/ml}$ ($t=175$ min).

5.4 DISCUSSION

The results of the pharmacokinetic analysis of plasma and renal excretion data separately clearly showed that iodopyracet is rapidly cleared from the circulation, largely by renal clearance. At the given dose, active tubular secretion is the major pathway of renal elimination. This transport step can be inhibited by probenecid resulting in a reduced renal clearance and a retarded elimination of iodopyracet.

In order to account for the processes that govern the renal clearance of iodopyracet in a more meaningful manner a physiologically based kidney model was developed that enabled the simultaneous analysis of both the plasma and the renal excretion data. The model incorporates all the functional characteristics of the kidney that are involved in the excretion of iodopyracet, including the important feature of carrier-mediated transport through the cells of the proximal tubules.

It appears from the tubular titration curves in Fig. 5.3 that the renal clearance of iodopyracet is characterized by supply-limited elimination at low plasma concentrations and capacity-limited elimination at high plasma levels. It follows directly from the results in Table 5.3 that in the controls the maximum clearance capacity of the secretory system, expressed as the intrinsic secretion clearance $CL_{\text{int}} = T_M/K_T = 950 \pm 350$ ml/min, is many times higher than the renal plasma flow ($Q_R = 110 \pm 35$ ml/min). CL_{int} is so high that at plasma levels up to the level at which tubular secretion begins to be saturated, elimination is perfusion rate-limited, in which case the limiting value of clearance is the renal plasma flow. Obviously, the saturation kinetics of iodopyracet are masked by this flow limitation. As a consequence, the estimates for K_T are necessarily rough, since the only information on this parameter can be derived from the small

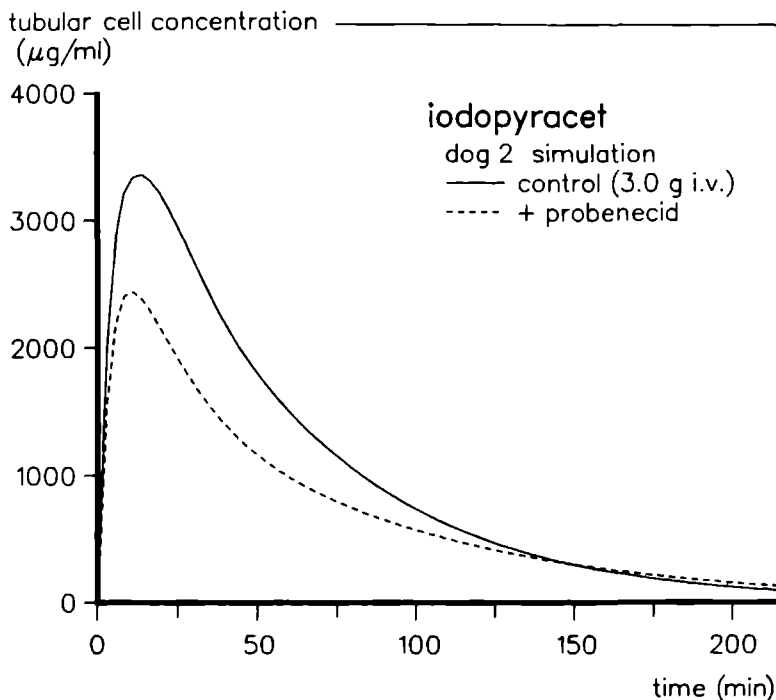


Fig. 5.4 Course of the proximal tubular cell concentration of iodopyracet with or without the presence of probenecid. The parameters used for this simulation were obtained from the analysis of plasma and urine curves of dog 2 according to the kidney model.

part of the tubular titration curve in which the initial linear course branches off to the point where the maximum transport rate is reached. The flow-dependency of renal clearance practically abolished in presence of probenecid. As a result of the competitive inhibition of the secretory system the CL_{int} , now expressed as $T_M/[K_T(1 + C_I/K_I)]$ strongly decreased to a value of 190 ± 80 ml/min.

In calculating Q_R it is implicitly assumed that any iodopyracet present in erythrocytes is not available for filtration or secretion in the kidney. This assumption is based on experiments which have shown that, although some iodopyracet penetrates the erythrocytes, extraction from erythrocytes during passage through the kidney is negligible [2,21]. It must be

recognized that the value obtained for Q_R is only an approximation of the true renal plasma flow. Q_R is merely an operational parameter, characterizing the plasma flow that perfuses the functional parts of the kidney tubules. Because iodopyracet is secreted by the proximal tubules it seems certain that virtually all extraction occurs in the cortex and that plasma directly entering the medulla (5-10 % of total renal plasma flow) [22] does not contribute to excretion. Therefore, it is likely that Q_R reflects the cortical plasma flow and as such underestimates the total renal plasma flow.

In accordance with in vitro observations [23], the simulation study with the kidney model showed that iodopyracet substantially accumulates within the proximal tubular cells prior to excretion (Fig. 5.4). It can be concluded from the results in Table 5.3 that cellular accumulation results directly from the very efficient active uptake across the basolateral membrane into the cells compared with the much slower transport out of the cells into the tubular lumen. The cellular uptake of iodopyracet in the control experiments, which as mentioned before practically approaches the renal plasma flow (110 ± 35 ml/min), strongly exceeds the clearance out of the cells, represented by the term $V_4 \cdot k_{43}$, being only 9 ± 1 ml/min. In presence of probenecid accumulation of iodopyracet was reduced as a result of interference with the active cellular uptake.

In summary, the physiologically based kidney model enabled a comprehensive description of the flow-dependent and capacity-limited renal clearance of iodopyracet. The interaction with probenecid could be adequately described with the model by competitive inhibition of the active uptake of iodopyracet into the tubular cells. Model simulation predicted a pronounced cellular accumulation within the proximal tubules, which was reduced in presence of probenecid. Finally, the kidney model described in this paper has also proven to be useful in a study on the renal clearance of phenolsulfonphthalein [8]. The physiologically based modeling approach may serve to get further insight in the mechanisms and implications of carrier-mediated drug transport in the kidney. Future work has to be focused on incorporating the mechanisms of active and passive drug reabsorption and on scaling-up the model to the human situation.

5.5 REFERENCES

1. I.M. Weiner, in *The Kidney: Physiology and Pathophysiology*, D.W. Seldin and G. Giebisch (Eds.), Raven Press, New York, 1985, pp. 1703-1724.
2. H.W. Smith, *The Kidney: Structure and Function in Health and Disease*, Oxford University Press, New York, 1951, pp. 148-162.
3. W.W. Smith and H.W. Smith, *J. Biol. Chem.*, **124**, 107 (1938).
4. H.W. Smith, N. Finkelstein, L. Aliminosa, B. Crawford and M. Graber, *J. Clin. Invest.*, **24**, 388 (1945).
5. H.B. Humes and J.M. Weinberg, in *The Kidney*, third ed., vol. II, B.M. Brenner and F.C. Rector (Eds.), Saunders, Philadelphia, 1986, pp. 1491-1532.
6. P. Hekman and C.A.M. van Ginneken, *J. Pharmacokinet. Biopharm.*, **10**, 77 (1982).
7. F.G.M. Russel, A.C. Wouterse and C.A.M. van Ginneken, *J. Pharmacol. Methods*, **17**, 125 (1987).
8. F.G.M. Russel, A.C. Wouterse and C.A.M. van Ginneken, *J. Pharmacokinet. Biopharm.*, **15**, 349 (1987).
9. P. Hekman and C.A.M. van Ginneken, *J. Chromatogr. Biomed. Appl.*, **182**, 492 (1980).
10. P. Hekman P.A.T.W. Porskamp, H.C.J. Ketelaars and C.A.M. van Ginneken, *J. Chromatogr. Biomed. Appl.*, **182**, 252 (1980).
11. A. Heyrovski, *Clin. Chim. Acta.*, **1**, 470 (1956).
12. K. Yamaoka, T. Nakagawa and T. Uno, *J. Pharmacokinet. Biopharm.*, **6**, 547 (1978).
13. L.Z. Benet and R.L. Galeazzi, *J. Pharm. Sci.*, **68**, 1071 (1979).
14. M. Gibaldi and D. Perrier, *Pharmacokinetics*, Marcell Dekker, New York, 1982.
15. C.M. Metzler, G.L. Elfring and A.J. McEwen, *Biometrics*, **30**, 562 (1974).
16. DISSPLA user's manual, Display Integrated Software System and Plotting Language, Version 9.2, Integrated Software Systems Corporation, San Diego Ca., 1984.
17. F.P. Chinard, *Am. J. Physiol.*, **180**, 617 (1955).
18. M.S. Dunnill and W. Halley, *J. Pathol.*, **110**, 113 (1973).
19. E. Bojesen, *Scand. J. Clin. Lab. Invest.*, **1**, 290 (1949).

20. P.A. Morales, C.H. Crowder, A.P. Fishman, M.H. Maxwell and D.M. Gomez, *Am. J. Physiol.*, **163**, 454 (1950).
21. H.A. Fozzard, *Am. J. Physiol.*, **206**, 309 (1964).
22. G.D. Thorburn, H.H. Kopald, J.A. Herd, M. Hollenberg, C.C.C. O'Morchoe and A.C. Barger, *Circ. Res.*, **8**, 290 (1963).
23. M.B. Burg and P.F. Weller, *Am. J. Physiol.*, **217**, 1053 (1969).

PART III

SUBSTITUTED HIPPURATES

Models are to be used,
but not to be believed

Henri Theil

RENAL CLEARANCE OF SUBSTITUTED HIPPURATES.
 I. BENZOYLGLYCINE (HIPPURATE) AND METHYL-SUBSTITUTED
 BENZOYLGLYCINES¹

Frans G M Russel, Alfons C Wouterse, and Cees A M van Ginneken

Abstract - Plasma kinetics and renal excretion of benzoylglycine (hippurate) and methyl-substituted benzoylglycines were studied in three Beagle dogs, after rapid intravenous administration of about 1 gram of glycine conjugate. Benzoylglycine and the 3- and 4-methyl analogs showed non-linear plasma protein binding varying between 20 and 80% over a concentration range of 5 - 450 µg/ml. For 2-methylbenzoylglycine an extremely high protein binding, practically approaching 100%, was observed at low plasma levels (<50 µg/ml). All conjugates were largely cleared via the kidney (>80% of the dose) and, except for the 2-methyl analog, rapidly eliminated from plasma. Plasma concentration and renal excretion rate data were analyzed simultaneously with a previously developed physiologically based kidney model. Tubular secretion appeared to be a function of the total drug concentration in renal plasma, except for 2-methylbenzoylglycine, presumably due to its tight protein binding. The average values of the parameters characterizing the tubular transport maximum (T_M in mg/min) and the apparent affinity for the secretory system (K_T in µg/ml) were: benzoylglycine $T_M = 5.5 \pm 0.8$, $K_T = 40 \pm 5$, 3-methylbenzoylglycine $T_M = 7.1 \pm 3.3$, $K_T = 49 \pm 1$, 4-methylbenzoylglycine $T_M = 8.0 \pm 1.6$, $K_T = 14 \pm 6$. Secretion of 2-methylbenzoylglycine was not saturated. Accordingly, only the ratio $T_M/K_T = 163 \pm 54$ ml/min could be calculated. An inter-

¹J Pharmacol Exp Ther, submitted. Partly published as an abstract in: Naunyn-Schmiedeberg's Arch Pharmacol 330, R32 (1985)

esting observation was the partial deconjugation of 4-methylbenzoylglycine to its corresponding benzoate. 4-Methylbenzoate was only found in plasma and not in urine, indicating that the benzoate was either cleared extrarenally, or completely metabolized during transfer through the kidney.

6.1 INTRODUCTION

Because of their high renal clearance, hippurate analogs traditionally are considered as prototypical substrates of the organic anion transport system present in the proximal tubules of the kidney [Møller and Sheikh, 1983]. Hippurate (benzoylglycine) itself is an endogenous substance that is excreted in large amounts in normal urine [Grantham and Chenko, 1986]. Well-known exogenous hippurates are salicylurate (2-hydroxybenzoylglycine), the major metabolite of salicylic acid, o-iodohippurate (Hippuran), a renal contrast agent, and p-aminohippurate (PAH). The latter two have been primarily used as a means to estimate renal plasma flow and tubular function in normal and disease states [Smith, 1951]. Hippuran is still used for clinical purposes, whereas PAH has become the anion of choice in the experimental characterization of the renal organic anion system in vivo and in vitro [Møller and Sheikh, 1983; Grantham and Chenko, 1986].

Studies with PAH have shown that the principal step in transtubular secretion of organic anions is active carrier-mediated transport from peritubular fluid to cytoplasm across the basolateral membrane, resulting in high intracellular concentrations. The anion is subsequently transported down its concentration gradient into the tubular lumen by a mediated process in the brush border membrane [Weiner, 1985].

The substrate specificity of the renal organic anion system has been the subject of many investigations. In the fifties and early sixties extensive analyses were performed on structure analogs of hippurate to determine the minimal requirements for carrier-mediated transport. Despopoulos [1965] concluded that the carbonyl and carboxylate group are essential in the secretion of hippurates. Later on, attention was shifted from the

hippurates to other classes of organic anions in an attempt to come to a comprehensive characterization of the chemical structures required for mediated transport. Recently, it has been proposed that the great variety of secreted anions, having in common only a negative charge and a hydrophobic backbone, are not transported by a single uniform carrier system but by several parallel systems with overlapping specificities [Häberle, 1981; Møller and Sheikh, 1983].

In this, and two accompanying papers we examined the renal clearance of a series of mono-substituted benzoylglycines (hippurates) in the dog. The purpose of these studies was to determine systematically the influence of ring substitution on the excretory characteristics of benzoylglycine. Previously, we proposed a physiologically based pharmacokinetic model for the saturable renal clearance of organic anions [Russel et al., 1987a,b]. This kidney model was applied to quantify the relevant processes that are involved in the renal excretion of the benzoylglycines. In the present study plasma and renal excretion kinetics of benzoylglycine and methyl-substituted benzoylglycines were investigated. The renal handling of these compounds is of special interest as they are the major metabolites of toluene and xylenes. These organic solvents are widely used in industry and concentrations of the metabolites in urine of workers are generally regarded as a quantitative measure of exposure to these solvents [Ogata et al., 1986].

6.2 MATERIALS AND METHODS

Chemicals

Benzoylglycine (hippurate) and salicyluric acid were commercially available from British Drug Houses Ltd. (Poole, England) and Merck (Darmstadt, FRG), respectively. The methyl-substituted benzoylglycines were prepared by chemical synthesis as described below. Glycine was obtained from Merck, o-, m- and p-toluylochloride were from Aldrich (Brussel, Belgium), sodium pentobarbital from Apharma (Arnhem, The Netherlands), atropine sulfate, mannitol and inulin from O.P.G. (Utrecht, The Netherlands). [^3H]inulin (2.03 Ci/mmol) was from Amersham (Buckinghamshire, England). All other chemicals were purchased from Merck.

Preparation of the Methyl-Benzoylglycines

The methyl-substituted benzoylglycines were prepared according to the Schotten-Baumann method from the corresponding acylchlorides by reaction with glycine in the presence of a slight excess of sodium hydroxide [Vogel, 1978]. The compounds were purified by recrystallization from boiling water. The identity and purity were checked by comparing melting points with available literature values [Beilstein, 1926] and by TLC and HPLC. TLC was performed on silicagel GF₂₅₄ plates (Merck, Darmstadt, FRG) with a mobile phase of chloroform:methanol:acetic acid (80:20:3). Spots were detected under UV light and by immersing the plates in a saturated iodine solution in carbon tetrachloride. The HPLC method is described under analytical methods.

Clearance Experiments

The experiments were done in three male beagle dogs, weighing 11 to 15 kg, as was described in detail previously [Russel et al., 1987c]. The dogs were fasted overnight and anesthetized by intravenous administration of sodium pentobarbital (30 mg/kg). As premedication atropine sulfate (0.5%, 1 ml i.v.) was given. After anesthesia occurred, the dogs were artificially respirated with room air using a Harvard (model 607) ventilator. The cephalic vein of both forelegs was provided with a Braunule T cannula (Braun, Melsungen, FRG) for blood sampling and drug administration. A constant infusion of 5% mannitol and 0.5% inulin was administered at a rate of 2 ml/min throughout the experiment to obtain a sufficiently high and constant urine flow. The urinary pH was controlled by an infusion of 8.4% sodium bicarbonate at a rate (3-8 ml/min) such that the pH remained at a level of 7.0 ± 0.6 .

Each dog received as an intravenous bolus a sterile solution of the substituted benzoylglycine dissolved in about 15 ml of water containing an equimolar amount of sodium bicarbonate. At regular times throughout the experiment, blood samples were taken into heparinized tubes. Plasma was separated by centrifugation for 20 min at 2000g. Urine was collected quantitatively with a double-walled urinary catheter (URO 90.009 from Talas, Ommen, The Netherlands) by rinsing the bladder with 15 ml physiological saline. During the first 50 min of the experiment urine was collected every 5 min and afterwards every 10 min. The plasma and diluted urine samples were stored at -20°C until analysis.

At the end of the experiment, the glomerular filtration rate was estimated by steady-state [^3H]inulin clearance. The [^3H]inulin was added to the mannitol-inulin infusion (0.04 $\mu\text{Ci/ml}$) and concomitantly 1 ml of this solution, but with an activity of 3.3 $\mu\text{Ci/ml}$, was rapidly injected. During the following 40 min, six blood samples were taken and urine was collected every 5 min. Before the dog was used for the next experiment, at least three weeks of recovery were observed.

Analytical Methods

The substituted benzoylglycines were determined in plasma and urine by reversed phase HPLC, according to a previously described method [Russel et al., 1987c]. A Hewlett Packard 1084B was used equipped with a variable wavelength detector, autosampler, and terminal (HP 7850 LC). The stainless-steel column (150 \times 4.6 mm I.D.) was packed with LiChrosorb RP-18, particle size 5 μm (Merck, Darmstadt, FRG). The mobile phase consisted of a mixture of methanol and twice-distilled water (30:70) containing 0.01 M citrate (pH 2.6). The column temperature was 35°C and the eluent was delivered at a flow rate of 1.0 ml/min. Operating values of the wavelength detector (λ) and retention times (t_R) of the compounds were: benzoylglycine λ = 245 nm, t_R = 4.1 min; 2-methylbenzoylglycine λ = 228 nm, t_R = 5.5 min; 3-methylbenzoylglycine λ = 235 nm, t_R = 8.3 min; 4-methylbenzoylglycine λ = 238 nm, t_R = 7.9 min. Salicyluric acid (2-hydroxybenzoylglycine, t_R = 6.2 min) was used as internal standard in the assay of benzoylglycine, 2-methylbenzoylglycine as internal standard of 3-methylbenzoylglycine and benzoylglycine as internal standard of 3- and 4-methylbenzoylglycine.

Concentrations in plasma and urine were determined by comparing the peak area ratio of compound and internal standard with a calibration curve of peak area ratio versus compound concentrations spiked to blank plasma and urine. Linear correlations ($r^2 > 0.98$) were found over the compound concentration range 1 - 700 $\mu\text{g/ml}$ for plasma and 10 - 7000 $\mu\text{g/ml}$ for urine. The coefficient of variation over the examined concentration ranges for plasma and urine was less than 5%.

Plasma and urine were checked for the presence of the corresponding acid derivative, resulting from a possible *in vivo* deglycination reaction. For this purpose the samples were run in a mobile phase consisting of

methanol:water (0.01 M citrate pH 2.6) in a ratio of 50:50, with the detector wavelength set at 254 nm. In the experiments with 4-methylbenzoylglycine, 4-methylbenzoic acid ($t_R = 5.4$ min) was found in plasma and concentrations were quantified in the same way as described above.

Concentrations of [^3H]inulin in plasma and urine were estimated using standard liquid scintillation techniques after dissolution of 0.5 ml plasma or urine in 10 ml Aqualuma plus (Lumac, Schaesberg, The Netherlands).

Protein Binding

Plasma protein binding of the substituted benzoylglycines was determined by ultrafiltration [Russel et al., 1987c], using Visking 8 dialysis tubing (Instrumentenhandel Z.H., Den Haag, The Netherlands). The ultrafiltrates were treated and analyzed in the same way as urine samples were. No significant binding of any of the benzoylglycines to the dialysis membrane was found. Assuming one class of binding site, plasma protein binding was analyzed according to the following equations

$$C = C_u + P \cdot C_u / (K_d + C_u) \quad (6.1)$$

$$C_u = f_u C \quad (6.2)$$

where C is the total plasma drug concentration, C_u the unbound drug concentration in plasma, f_u is the fraction of drug in plasma unbound, P is the total concentration of protein binding sites and K_d is the dissociation constant of the drug-protein complex.

Pharmacokinetic Analysis

Basic pharmacokinetic parameters were calculated from the plasma-concentration time curves and renal excretion rate-time curves, applying statistical moments theory [Yamaoka et al., 1978]. Plasma curves could be fitted well to the sum of two exponential equations, while renal excretion rate curves were analyzed using a cubic spline interpolation method [Yeh and Kwan, 1978], as it was often impossible to fit the typical non-linear semilogarithmic plots to the usual multiexponential equations. The area under the plasma curve was calculated by direct integration after

extrapolation of the terminal phase of the plot to infinity. The area under the renal excretion rate curve and the area under the first moment of this curve were estimated by numerical integration of the interpolated data points from time 0 to the last measured excretion rate and by subsequent extrapolation of the log-linear terminal phase of the curve to infinity.

Half-lives in plasma ($t_{1/2,p}$) and urine ($t_{1/2,ur}$) were obtained from the respective terminal elimination rate constants. Using standard equations, total plasma clearance (CL) and initial volume of distribution (V_1) were calculated [Gibaldi and Perrier, 1982]. The mean residence time was determined from the renal excretion rate curve (MRT_R), dividing the area under the first moment curve by the area under the curve. The total amount excreted in infinite time into urine was directly obtained from the area under the renal excretion rate curve. Renal clearance (CL_R) was calculated as the product of total plasma clearance and the fraction of the dose excreted unchanged in the urine (D_{ur}).

Kidney Model

The physiologically based model that was used to analyze the renal excretion of the substituted benzoylglycines is shown in Fig. 6.1. The model was described in detail earlier [Russel et al., 1987a,b], therefore only a brief description is given.

Transport processes and compartmental concentrations of the drug are described by the following set of equations:

$$V_1 \frac{dC_1}{dt} = (Q_R - Q_{ur})C_2 + k_{51}V_5C_5 - (Q_R + CL_{NR} + k_{15}V_1)C_1 \quad (6.3)$$

$$V_2 \frac{dC_2}{dt} = Q_R C_1 - Q_{GF}C_{u1} - (Q_R - Q_{ur})C_2 - \frac{T_M C_2}{K_T + C_2} \quad (6.4)$$

$$V_3 \frac{dC_3}{dt} = Q_{GF}C_{u1} + k_{43}V_4C_4 - Q_{ur}C_3 \quad (6.5)$$

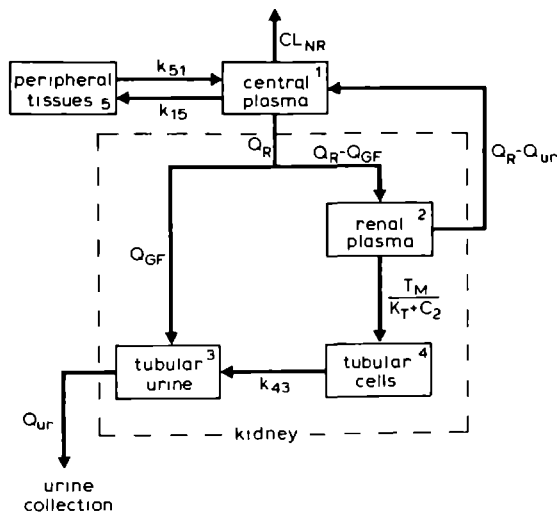


Fig. 6.1 Physiologically based pharmacokinetic model for the renal clearance of substituted benzoylglycines. See Materials and Methods for explanation of symbols.

$$V_4 \frac{dC_4}{dt} = \frac{T_M C_2}{K_T + C_2} - k_{43} V_4 C_4 \quad (6.6)$$

$$V_5 \frac{dC_5}{dt} = k_{15} V_1 C_1 - k_{51} V_5 C_5 \quad (6.7)$$

$$R_R = Q_{ur} \cdot C_3 \quad (6.8)$$

where V_i = volume of compartment i (ml); C_i = total drug concentration in compartment i ($\mu\text{g/ml}$); C_{u1} = unbound drug concentration in compartment 1 ($\mu\text{g/ml}$); k_{ij} = first-order rate constant associated with movement of drug from compartment i to compartment j (min^{-1}); Q_R = renal plasma flow (ml/min); Q_{GF} = glomerular filtration (ml/min); Q_{ur} = urine flow (ml/min); CL_{NR} = nonrenal plasma clearance (ml/min); T_M = maximum

transport capacity of the tubular secretion mechanism ($\mu\text{g}/\text{min}$); K_T = Michaelis-Menten constant of the tubular secretion mechanism ($\mu\text{g}/\text{ml}$); R_R = renal excretion rate ($\mu\text{g}/\text{min}$).

The unbound drug concentration (C_u) can be expressed as a function of C after rearrangement of equations 6.1 and 6.2. The parameters Q_R , Q_{GF} , Q_{ur} and all compartmental volumes (V_i) were used as constants in the model. They were either experimentally found or taken from literature [Russel et al., 1987b]. Q_{GF} , Q_{ur} and V_1 were experimentally determined. For Q_R a value of 11 ml/min per kg body weight was taken. Under the assumption of a constant renal delay time (Δt) of 1.5 min, V_3 was calculated as $V_3 = Q_{ur} \cdot \Delta t$. For V_2 and V_4 literature values of 10 ml and 30 ml, respectively, were taken, while an arbitrary value of 1 liter was chosen for V_5 . The remaining parameters, viz., T_M , K_T , CL_{NR} , k_{43} , k_{15} and k_{51} were estimated by fitting the experimentally observed plasma concentration and renal excretion rate curves simultaneously to the kidney model.

Data Analysis

The spline functions were fitted to the equally weighted renal excretion rate data with the rational spline interpolation routine of the DISSPLA computer package [DISSPLA, 1984]. DISSPLA was also used for drawing the figures presented in this study. All other data were analyzed with the aid of the computer program NONLIN [Metzler et al., 1974]. Plasma protein data were weighted equally and in the exponential fits data were weighted reciprocally ($1/C^2$). In most cases best fits to the kidney model were obtained when plasma data were reciprocally weighted and renal excretion rate data were weighted equally. The goodness of fit was evaluated through the deviations between observed and model-predicted values as $R^2 = 1 - \Sigma(\text{Obs})^2 / \Sigma(\text{Dev})^2$, where $\Sigma(\text{Obs})^2$ is the corrected sum of squared observations and $\Sigma(\text{Dev})^2$ the sum of squared deviations. Average values are expressed as mean \pm SD.

6.3 RESULTS

Experimental Conditions and Protein Binding

The experimental conditions of the clearance studies are given in Table 6.1. The glomerular filtration was determined by measuring the steady state [^3H]inulin clearance and ranged from 17 to 43 ml/min. The urine flow, induced by mannitol, varied between 0.8 and 1.3 ml/min and the urinary pH was controlled with sodium bicarbonate between pH 6.9 and 7.6.

Table 6.1 Experimental conditions of the clearance studies with methyl-substituted benzoylglycines.

Dog	Weight (kg)	Substituent	Dose (mg)	Q_{GF} (ml/min)	Q_{ur} (ml/min)	pH_{ur}
1	12.4	H	930	42 ± 2	0.87 ± 0.11	6.95 ± 0.26
	12.3	2- CH_3	1000	25 ± 2	1.33 ± 0.65	7.54 ± 0.15
	12.5	3- CH_3	860	42 ± 2	0.97 ± 0.17	6.95 ± 0.22
	12.8	4- CH_3	990	27 ± 1	1.17 ± 0.37	7.35 ± 0.06
2	12.0	H	930	31 ± 2	0.89 ± 0.26	7.01 ± 0.15
	11.5	2- CH_3	990	23 ± 1	0.76 ± 0.40	7.49 ± 0.21
	11.5	3- CH_3	860	17 ± 1	1.19 ± 0.28	7.58 ± 0.08
	12.0	4- CH_3	990	24 ± 1	0.92 ± 0.22	7.22 ± 0.15
3	13.0	H	940	33 ± 2	0.81 ± 0.33	7.30 ± 0.25
	13.3	2- CH_3	1010	23 ± 1	0.85 ± 0.23	7.27 ± 0.11
	14.8	3- CH_3	1880	43 ± 2	0.97 ± 0.52	7.09 ± 0.23
	13.3	4- CH_3	990	29 ± 2	0.85 ± 0.26	7.20 ± 0.18

Plasma protein binding of benzoylglycine and the methyl-substituted analogs is shown in Fig. 6.2. Interindividual variation in protein binding was small, therefore for each compound data of all three dogs were pooled and analyzed according to Eq. 6.1. The results of these calculations are given in Table 6.2. The plasma protein binding of benzoylglycine was fairly constant (0.68 - 0.82) over the concentration range measured,

whereas the methyl-substituted analogs clearly showed concentration-dependent protein binding. An unusual binding profile was observed for 2-methylbenzoylglycine. At plasma concentrations below 100 $\mu\text{g/ml}$ the fraction unbound decreased dramatically, which is expressed by the very low dissociation constant (Table 6.2). Extrapolation of the binding curve predicted a fraction unbound of practically zero for concentrations lower than 30 $\mu\text{g/ml}$ (Fig. 6.2).

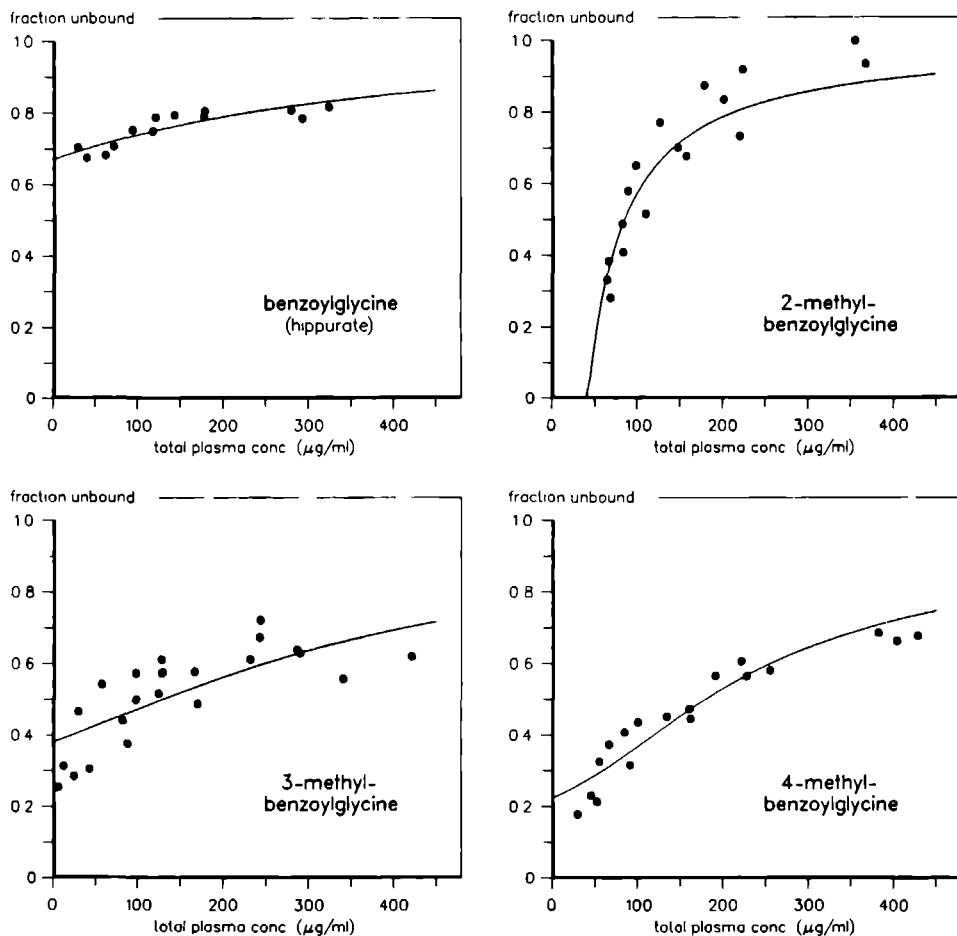


Fig. 6.2 Plasma protein binding of benzoylglycine and methyl-substituted benzoylglycines.

Table 6.2 Plasma protein binding of methyl-substituted benzoylglycines.

Substituent	n	P ($\mu\text{g/ml}$)	K_d ($\mu\text{g/ml}$)
H	13	92 ± 16	187 ± 46
2-CH ₃	17	43 ± 5	0.01 ± 4
3-CH ₃	25	167 ± 31	103 ± 30
4-CH ₃	18	126 ± 10	36 ± 7

Pharmacokinetic Analysis

Representative examples of the plasma concentration and renal excretion rate after intravenous administration of benzoylglycine and methyl-substituted benzoylglycines are shown in Fig. 6.3. Basic pharmacokinetic parameters were determined from plasma and urinary data separately by statistical moment analysis and the results are presented in Table 6.3.

At the given doses, all conjugates were largely eliminated from the general circulation by renal clearance ($D_{ur} > 80\%$). Taking the plasma protein binding into consideration, it is apparent that the total renal clearance (CL_R) of each of the benzoylglycines exceeded the clearance of the unbound fraction by glomerular filtration, indicating that all compounds were actively secreted by the kidney. All conjugates were rapidly eliminated from plasma, except for the 2-methyl analog. Compared to the others, 2-methylbenzoylglycine had a low plasma clearance (43 ± 3 ml/min) and a long terminal half-life in plasma (149 ± 48 min), which was more than two times higher than the corresponding value in urine (61 ± 28 min). It seems likely that the extremely high protein binding at low plasma concentrations accounted for the slow terminal elimination of this compound. It should be noticed that all parameters listed in Table 6.3 are not of absolute value but, due to the evident nonlinear processes of saturable protein binding and active renal secretion, they are dependent on the administered dose.

In all experiments plasma and urine samples were checked for the presence of the corresponding benzoate derivative, as it has been reported

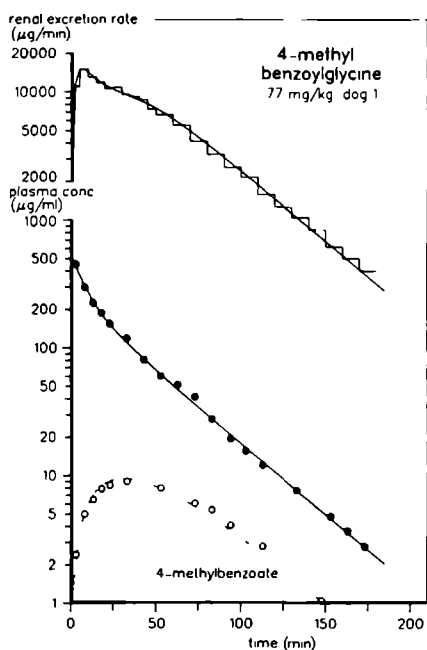
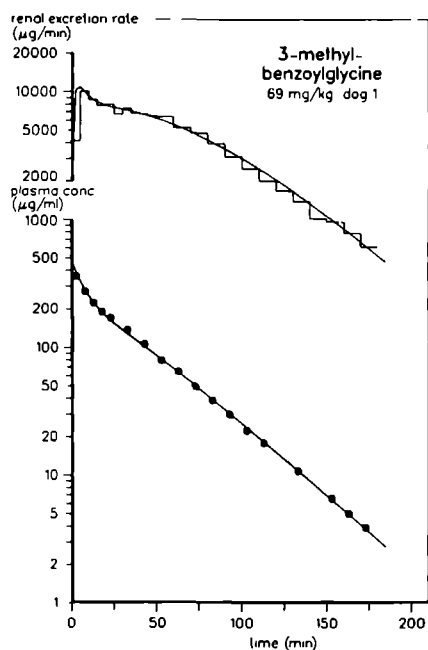
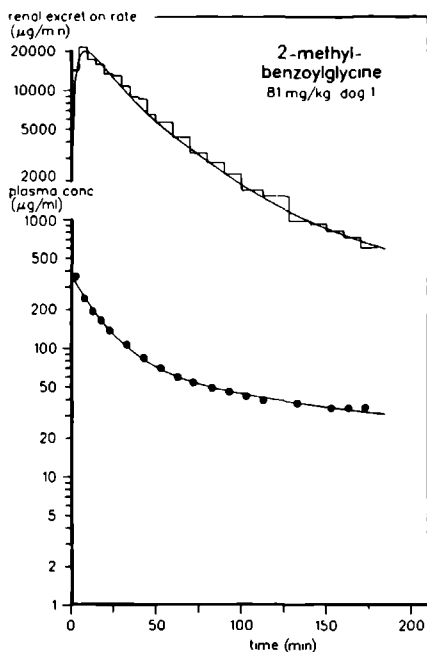
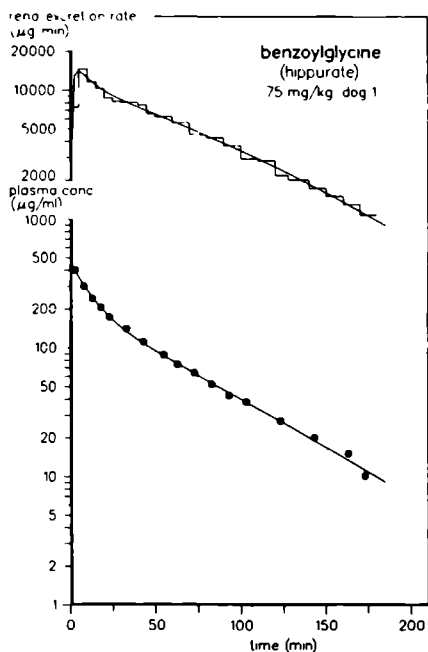


Fig. 6.3 Renal excretion rate and plasma concentration of benzoylglycine and methyl-substituted benzoylglycines. The solid lines through the data points represent the results of data analysis according to the kidney model.

Table 6.3 Basic pharmacokinetic parameters of methyl-substituted benzoylglycines after rapid intravenous injection.

Substituent	Dog	plasma			urine			
		$t_{\frac{1}{2},p}$ (min)	CL (ml/min)	V_1 (l)	$t_{\frac{1}{2},ur}$ (min)	MRT_R (min)	CL_R (ml/min)	D_{ur} (%)
H	1	40	60	1.97	50	73	59	98
	2	46	54	2.17	69	101	52	97
	3	49	63	2.02	48	72	56	89
	Mean(SD)	45(5)	59(5)	2.05(0.10)	56(12)	82(16)	56(4)	95(5)
2-CH ₃	1	186	45	2.74	92	59	40	88
	2	95	43	2.65	50	73	40	92
	3	167	40	2.77	40	58	35	88
	Mean(SD)	149(48)	43(3)	2.72(0.06)	61(28)	63(8)	38(3)	89(2)
3-CH ₃	1	28	67	1.76	40	65	56	83
	2	48	36	1.29	75	109	31	85
	3	34	71	1.62	46	68	57	80
	Mean(SD)	37(10)	58(19)	1.56(0.24)	54(19)	81(25)	48(15)	83(3)
4-CH ₃	1	27	83	1.79	31	49	72	87
	2	37	62	1.90	50	78	52	83
	3	32	80	2.06	39	57	66	82
	Mean(SD)	32(5)	75(11)	1.92(0.14)	40(10)	61(15)	63(10)	84(3)

that some benzoylglycines may be deglycinated in the organism [Quick, 1932; Mályusz et al., 1972; Bekersky et al., 1980]. Only in the experiments with 4-methylbenzoylglycine deconjugation could be detected. The deconjugation product, 4-methylbenzoate, was found in plasma and not in urine (Fig. 6.3), indicating that the acid either is metabolized completely within the kidney, or is reabsorbed unchanged into the general circulation and cleared or metabolized elsewhere. Metabolism in the kidney may involve reconjugation with glycine or other routes, of which glucuronidation is most likely. The voided urine was not examined for the presence of glucuronides. Plasma concentration data of 4-methylbenzoate were fitted to two exponentials; the half-life of the ascending phase was 23 ± 10 min and of the descending phase 33 ± 10 min. The maximum plasma concentration (± 10 $\mu\text{g/ml}$) was reached in about 30 min, after which concentrations up to 25% of the parent compound were observed. Since the volume of distribution of 4-methylbenzoate is not known, no information can be obtained on clearance values and absolute quantities formed.

Kidney Model

The physiologically based kidney model for the renal excretion of the glycine conjugates is depicted in Fig. 6.1. The model is composed of a series of lumped compartments representing the kidney, the central plasma pool and the peripheral tissues. The drug is introduced in the central plasma compartment by i.v. injection and can be distributed from there to the kidney and peripheral tissues or be eliminated by nonrenal clearance. The kidney compartment is subdivided into a renal plasma, tubular cell and tubular urine compartment. Clearance by glomerular filtration is considered to be dependent on unbound drug concentration in the central plasma compartment. Active transport takes place from renal plasma into the tubular cell compartment according to Michaelis-Menten kinetics, followed by first-order transport into the tubular urine compartment. Tubular secretion was assumed to be a function of total drug concentration in renal plasma, except for 2-methylbenzoylglycine. At low plasma concentrations, the renal extraction ratio of the 2-methyl analog was nearly zero, whereas renal clearance of the other benzoylglycines approached the renal plasma flow, indicating that plasma protein binding does not hinder the active renal secretion of these compounds.

Table 6.4 Model parameters characterizing the renal handling of methyl-substituted benzoylglycines.

Substituent	Dog	T_M (mg/min)	K_T (μ g/ml)	CL_{NR} (ml/min)	k_{43} (min^{-1})	k_{15} (min^{-1})	k_{51} (min^{-1})
H	1	5.8 ± 2.1	46 ± 38	0 ± 2	0.07 ± 0.03	0.033 ± 0.020	0.043 ± 0.006
	2	4.6 ± 0.7	38 ± 12	4 ± 2	0.08 ± 0.04	0.047 ± 0.003	0.063 ± 0.006
	3	6.2 ± 1.1	37 ± 20	5 ± 3	0.27 ± 0.17	0.027 ± 0.002	0.026 ± 0.002
	Mean(SD)	5.5(0.8)	40(5)	3(3)	0.14(0.11)	0.036(0.010)	0.044(0.019)
2-CH ₃ ^a	1	216 ^b		1 ± 5	0.31 ± 0.17	0.023 ± 0.005	0.035 ± 0.003
	2	109		10 ± 6	0.33 ± 0.39	0.026 ± 0.004	0.046 ± 0.006
	3	164		10 ± 7	0.16 ± 0.12	0.026 ± 0.007	0.033 ± 0.003
	Mean(SD)	163(54)		7(5)	0.27(0.09)	0.025(0.002)	0.038(0.007)
3-CH ₃	1	8.2 ± 1.9	48 ± 25	7 ± 2	0.05 ± 0.01	0.053 ± 0.007	0.083 ± 0.014
	2	3.4 ± 1.2	49 ± 21	10 ± 4	0.16 ± 0.23	0.071 ± 0.007	0.070 ± 0.008
	3	9.6 ± 1.6	50 ± 20	11 ± 4	0.07 ± 0.04	0.084 ± 0.008	0.071 ± 0.008
	Mean(SD)	7.1(3.3)	49(1)	9(2)	0.09(0.06)	0.069(0.016)	0.075(0.007)
4-CH ₃	1	9.5 ± 0.3	8 ± 2	10 ± 3	0.53 ± 0.20	0.054 ± 0.004	0.053 ± 0.003
	2	6.3 ± 1.6	18 ± 19	7 ± 5	0.14 ± 0.12	0.042 ± 0.005	0.043 ± 0.009
	3	8.2 ± 0.5	17 ± 4	13 ± 2	0.37 ± 0.12	0.041 ± 0.003	0.043 ± 0.002
	Mean(SD)	8.0(1.6)	14(6)	10(3)	0.35(0.20)	0.046(0.007)	0.046(0.006)

^aTubular secretion was considered dependent on unbound plasma concentrations.

^bSince secretion was not saturated estimates of T_M and K_T were very inaccurate (SD > 200%), therefore only the ratio T_M/K_T (ml/min) is given.

Plasma concentration and renal excretion rate data of each experiment were simultaneously fitted to the model and the results are listed in Table 6.4 and are also represented by the solid lines through the data points in Figs. 6.3 and 6.4. The goodness of fit between the observed and model-predicted plasma concentration and renal excretion rate data was in all cases: $R^2_{\text{plasma}} > 0.990$ and $R^2_{\text{urine}} > 0.982$. In Fig. 6.4, the renal excretion rate is plotted linearly against the plasma concentration at the midpoint of a urine collection interval. These so-called tubular titration curves clearly show that all compounds undergo net tubular secretion over the concentration range measured. The lines representing the glomerular filtration are slightly curved as a result of the nonlinear protein binding. With the exception of 2-methylbenzoylglycine, the titration curves paralleled the glomerular filtration line at high concentrations, indicating that tubular secretion was saturated. Because saturation was not reached for 2-methylbenzoylglycine, the estimates of the parameters describing active transport (T_M and K_T) were inevitably crude and highly correlated, therefore only the ratio T_M/K_T , the intrinsic unbound secretion clearance (CL_{int}), is given (Table 6.4).

There were no indications to suggest that active or passive reabsorption were involved in the renal clearance of the benzoylglycines. Non-ionic back-diffusion is very unlikely to occur, considering the high urine flow and the high urinary pH as compared to the dissociation constants of the compounds ($pK_a < 4.5$).

6.4 DISCUSSION

The results of the present study show that the renal excretion of benzoylglycine and methyl-substituted derivatives is dominated by tubular secretion. The plasma concentration and renal excretion rate curves could be adequately described with the physiologically based kidney model in terms of concomitant glomerular filtration and active secretion, despite the considerable differences in kinetics.

All substances showed concentration-dependent plasma protein binding which affected their renal clearance to a greater or lesser degree. Obviously, the excretion by glomerular filtration was influenced in all cases,

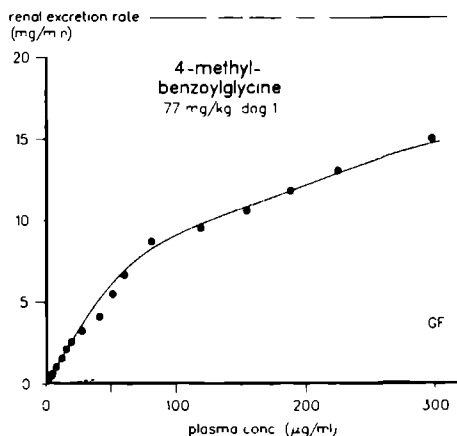
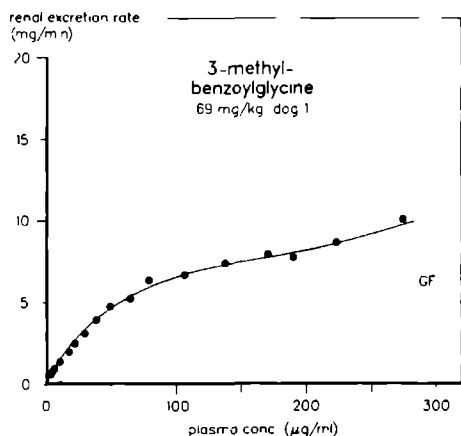
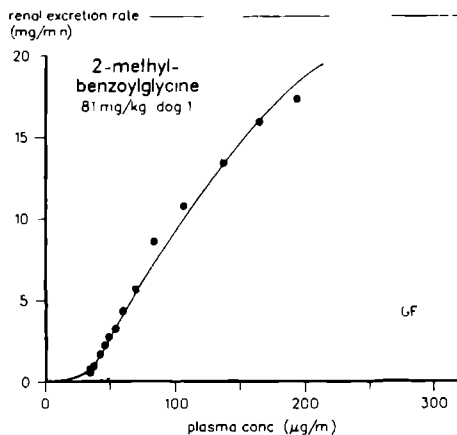
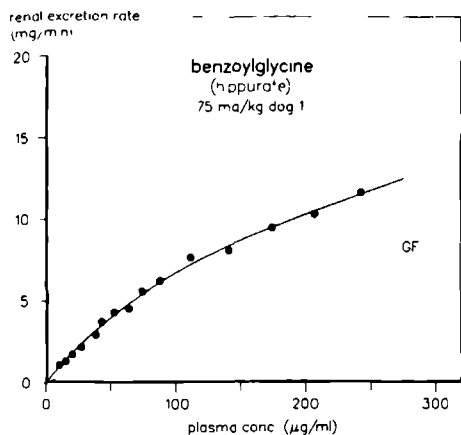


Fig. 6.4 Tubular titration curves representing the relationship between renal excretion rate and plasma concentration of benzoylglycine and methyl-substituted benzoylglycines. The solid lines through the data points are calculated according to the kidney model. GF represents the clearance by glomerular filtration.

for only the unbound concentration in plasma is available for filtration. Plasma protein binding did not directly affect the tubular secretion of benzoylglycine and 3- and 4-methylbenzoylglycine, presumably due to a rapid dissociation of the drug-protein complex relative to the affinity for the secretory system. However, in case of 2-methylbenzoylglycine the very low dissociation constant of the complex apparently prevented the

protein bound fraction from being secreted. As a result of the extremely high protein binding at low plasma concentrations, elimination from plasma was strongly retarded and renal excretion was almost completely inhibited at concentrations below 30 $\mu\text{g/ml}$. However, it should be mentioned that although evidence for the inhibitory effect of tight protein binding on tubular secretion of 2-methylbenzoylglycine is plausible, there remains a theoretical possibility of saturable tubular reabsorption being responsible for the lack of renal excretion at plasma levels below 30 $\mu\text{g/ml}$.

Apart from the variable effects of protein binding on renal clearance, the excretory profiles of the benzoylglycines varied also as a result of differences in their kinetic interaction with the tubular secretory system. The lowest tubular transport maximum (T_M) was observed for benzoylglycine, followed by 3- and 4-methylbenzoylglycine, while the clearance capacity of 2-methylbenzoylglycine was apparently too high to estimate its T_M at the given dose (Table 6.4). This hampered also the calculation of the apparent affinity constant for tubular secretion (K_T) of the 2-methyl analog. The K_T of benzoylglycine and 3-methylbenzoylglycine were about the same value and the lowest value was found for the 4-methyl isomer. Taken these results together, it follows that the maximum clearance capacity of the secretory system, expressed as the intrinsic secretion clearance $CL_{\text{int}} = T_M/K_T$, was largest for 4-methylbenzoylglycine ($CL_{\text{int}} = 570 \pm 180 \text{ ml/min}$). As this value surpasses the renal plasma flow several times, renal elimination is perfusion-rate limited up to plasma concentrations at which tubular secretion starts to get saturated. This is expressed by the initial linear part in the tubular titration curve of 4-methylbenzoylglycine, the slope of which is an estimate of the renal plasma flow. The rate constants describing transport from tubular cell to lumen (k_{43}) were in the same range for all compounds (Table 6.4). Although this transport step is in principle also saturable, it is known from in vitro studies with PAH [Kinsella et al., 1979] that it is characterized by a very high capacity and low affinity ($K_m > 3.5 \text{ mM}$), thus it seems justified to approximate the transfer from cell to lumen by a first-order process.

An interesting finding of the present study is the conversion of 4-methylbenzoylglycine into 4-methylbenzoate. The absence of 4-methylbenzoate from urine indicated that the compound was either

cleared extrarenally, or completely metabolized during transit through the kidney. It is important to notice that the renal clearance of 4-methylbenzoylglycine may have been influenced by the presence of 4-methylbenzoate. If both compounds share the same secretory transport system, it is possible that tubular secretion was partially inhibited. On the other hand, renewed glycine conjugation within the kidney and subsequent excretion could lead to an overestimation of tubular secretion.

A commonly used test of exposure to toluene and xylenes is based on the excretion of benzoylglycine and methyl-benzoylglycines in urine [Ogata et al., 1986]. It is generally assumed that the tubular secretory capacity for benzoylglycines is so high that it precludes renal excretion as the rate-limiting step in disposition [Riihimäki and Hänninen, 1987]. However, if the results of the present study may be extrapolated to the human situation, the differences in excretory profiles demonstrate that this assumption may not always hold true. For instance, exposure to o-xylene is not noticed until plasma levels of its metabolite have exceeded a certain threshold value. Clearly, an adequate evaluation of biological exposure to xenobiotics by monitoring the urinary excretion of their final metabolites is not possible without a thorough knowledge of the basic processes that determine the renal excretion of the metabolites involved.

Acknowledgements

The authors are indebted to Mr. H. van Deelen and Dr. A.J. Beld for the preparation of the glycine conjugates.

6.5 REFERENCES

- Beilstein's Handbuch der Organischen Chemie, Vierte Auflage, Band IX, pp. 465, 477 and 487, Julius Springer, Berlin, 1926.
- Bekersky, I., Colburn, W.A., Fishman, L. and Kaplan, S.A.: Metabolism of salicylic acid in the isolated perfused rat. Interconversion of salicyluric and salicylic acids. Drug Metab. Dispos. 8, 319-324, 1980.

- Despopoulos, A.: A definition of substrate specificity in renal transport of organic anions. *J. Theoret. Biol.* 8, 163-192, 1965.
- DISSPLA User's Manual: Display Integrated Software System and Plotting Language, Version 9.2. Integrated Software Systems Corp., San Diego, CA, 1984.
- Gibaldi, M. and Perrier, D.: Pharmacokinetics, pp. 45-111, Marcel Dekker Inc., New York, 1982.
- Grantham, J.J. and Chenko, A.M.: Renal handling of organic anions and cations; Metabolism and excretion of uric acid. In *The Kidney*, ed. by B.M. Brenner and F.C. Rector, pp. 663-700, W.B. Saunders, Philadelphia, 1986.
- Häberle, D.A.: Characteristics of p-aminohippurate transport in the mammalian kidney. In *Renal transport of organic substances*, ed. by R. Greger, F. Lang and S. Silbernagel, pp. 189-209, Springer-Verlag, Berlin, 1981.
- Kinsella, J.L., Holohan, P.D., Pessah, N.I. and Ross, C.R.: Transport of organic ions in renal cortical luminal and antiluminal membrane vesicles. *J. Pharmacol. Exp. Ther.* 209, 443-450, 1979.
- Mályusz, M., Girndt, J., Mályusz, G. and Ochwaldt, B.: Die Metabolisierung von p-Aminohippurat in Nieren von normalen Ratten und Ratten mit experimentellen Goldblatt-Hochdruck. *Pflügers Arch.* 333, 156-165, 1972.
- Metzler, C.M., Elfring, G.L. and McEwen, A.J.: A package of computer programs for pharmacokinetic modeling. *Biometrics* 30, 562-563, 1974.
- Møller, J.V. and Sheikh, M.I.: Renal organic anion transport system: pharmacological, physiological, and biochemical aspects. *Pharmacol. Rev.* 34, 315-358, 1983.
- Ogata, M. and Taguchi, T.: Quantitative analysis of urinary glycine conjugates by high performance liquid chromatography: excretion of hippuric acid and methylhippuric acids in the urine of subjects exposed to vapours of toluene and xylenes. *Int. Arch. Occup. Environm. Health* 58, 121-129, 1986.
- Quick, A.J.: The site of the synthesis of hippuric acid and phenylacetic acid in the dog. *J. Biol. Chem.* 90, 73-82, 1932.

- Riihimäki, V. and Hänninen, O.: Xylenes. In Ethel Browning's Toxicity and Metabolism of Industrial Solvents, 2nd edition, Vol. 1: Hydrocarbons, ed. by R. Snyder, pp. 64-84, Elsevier Science Publishers, Amsterdam, 1987.
- Russel, F.G.M., Wouterse, A.C. and van Ginneken, C.A.M.: Physiologically based pharmacokinetic model for the renal clearance of phenolsulfonphthalein and the interaction with probenecid and salicyluric acid in the dog. *J. Pharmacokinet. Biopharm.* 15, 349-368, 1987a.
- Russel, F.G.M., Wouterse, A.C. and van Ginneken, C.A.M.: Physiologically based pharmacokinetic model for the renal clearance of salicyluric acid and the interaction with phenolsulfonphthalein in the dog. *Drug Metab. Dispos.* 15, 695-701, 1987b.
- Russel, F.G.M., Wouterse, A.C., Hekman, P., Grutters, G.J. and van Ginneken, C.A.M.: Quantitative urine collection in renal clearance studies in the dog. *J. Pharmacol. Methods* 17, 125-136, 1987c.
- Smith, H.W.: The Kidney: Structure and function in health and disease, pp. 143-168, Oxford University Press, New York, 1951.
- Vogel, A.: Vogel's practical organic chemistry, p. 885, Longman, London, 1978.
- Weiner, I.M.: Organic acids and bases and uric acid. In The Kidney: Physiology and pathophysiology, ed. by D.W. Seldin and G. Giebisch, pp. 1703-1724, Raven Press, New York, 1985.
- Yamaoka, K. Nakagawa, T. and Uno, T.: Statistical moments in pharmacokinetics. *J. Pharmacokinet. Biopharm.* 6, 547-558, 1978.
- Yeh, K.C. and Kwan, K.C.: A comparison of numerical integrating algorithms by trapezoidal, lagrange and spline approximation. *J. Pharmacokinet. Biopharm.* 6, 79-98, 1978.

RENAL CLEARANCE OF SUBSTITUTED HIPPURATES.
 II. 4-AMINOBENZOYLGLYCINE AND HYDROXY-SUBSTITUTED
 BENZOYLGLYCINES¹

Frans G.M. Russel, Alfons C. Wouterse, and Cees A.M. van Ginneken

Abstract - Plasma kinetics and renal excretion of 4-aminobenzoylglycine (p-aminohippurate) and hydroxy-substituted benzoylglycines were studied in three Beagle dogs after rapid intravenous administration of about 1 gram. Plasma protein binding of 4-amino-, 3-hydroxy-, and 4-hydroxybenzoylglycine was low (<15%) and practically constant over a concentration range of 5 - 450 µg/ml, while the 2-hydroxy analog showed concentration-dependent protein binding ranging from 40 - 80%. The excretory patterns of the 4-amino, 3- and 4-hydroxy analogs were essentially the same; rapid elimination from plasma into urine (>80% of the dose), mainly by very efficient supply-limited tubular secretion. Conversely, the excretion of 2-hydroxybenzoylglycine was characterized by a lower plasma clearance and total renal excretion (64% of the dose), and a limited capacity of the tubular secretory system. Plasma concentration and renal excretion rate data were analyzed simultaneously according to a physiologically based kidney model. The kinetic parameters characterizing the tubular secretion of 2-hydroxybenzoylglycine were, $T_M = 4.4 \pm 0.9$ mg/min and $K_T = 23 \pm 8$ µg/ml. Since secretion of the other compounds was not saturated, only the intrinsic secretion clearance ($CL_{int} = T_M/K_T$), could be estimated; 4-amino- $CL_{int} = 145 \pm 50$ ml/min, 3-hydroxy- $CL_{int} = 194 \pm 21$ ml/min, and 4-hydroxybenzoylglycine $CL_{int} = 153 \pm 23$ ml/min.

¹J. Pharmacol. Exp. Ther., submitted

7.1 INTRODUCTION

In the present study, the second in a series of three on the renal handling of substituted hippurates, the excretory characteristics of 4-aminobenzoylglycine (p-aminohippurate) and hydroxy-substituted benzoylglycines were investigated. 4-Aminobenzoylglycine was chosen by renal physiologists many years ago as a model compound to study the properties of the renal organic anion system [Smith et al., 1938; Smith et al., 1945]. Preference for this compound emanated from its very efficient renal clearance, weak binding to plasma proteins, limited reabsorption, and convenience to be analyzed chemically in biological fluids. At low plasma concentrations, renal clearance of 4-aminobenzoylglycine approaches the renal plasma flow, since extraction from plasma during a single passage of blood through the kidney is almost complete. In fact, its renal clearance was used for a long time as a measure of renal plasma flow, but it has been shown that it is not under all conditions a reliable parameter [Aukland and Løyning, 1970; Lote et al., 1985]. Furthermore, in man and some animal species 4-aminobenzoylglycine is metabolized to a certain extent during passage through the kidney from blood to urine [Setchell and Blanch, 1961; Mályusz et al., 1972; Girndt et al., 1974].

Among the hydroxy-substituted benzoylglycines, the kinetics and renal excretion of the 2-hydroxy analog (salicylurate) have received most attention, because it is the major metabolite of salicylic acid. Although 2-hydroxybenzoylglycine is bound considerably to plasma proteins, its renal clearance equals the 4-aminobenzoylglycine clearance at low plasma concentrations, indicating that protein binding does not limit the extent of secretion [Knoefel et al., 1962]. At high plasma concentrations, 2-hydroxybenzoylglycine showed renal excretory transport to a small degree in comparison with 4-aminobenzoylglycine [Knoefel and Huang, 1959]. It was suggested that because of the high hydrophobicity, as a result of internal hydrogen bonding, passive reabsorption accounted for the lower tubular excretory transport rather than a limited capacity of the secretory system [Knoefel et al., 1962]. However, recently we showed that under circumstances where passive back-diffusion is negligible, the maximal rate of tubular transport of 2-hydroxybenzoylglycine is considerably less than that described for 4-aminobenzoylglycine [Russel et al., 1987].

The renal excretory characteristics of 4-hydroxybenzoylglycine were found to resemble those of its 4-amino analog. At high plasma concentrations ($>200 \mu\text{g/ml}$) 4-hydroxybenzoylglycine saturated the tubular transport system and underwent tubular excretory transport at a maximal rate such as found with the 4-amino analog. The compound had a low hydrophobicity and accordingly little tendency to undergo passive tubular reabsorption [Knoefel et al., 1962].

The renal clearance of 3-hydroxybenzoylglycine has been studied only at low plasma concentrations ($<5 \mu\text{g/ml}$). Under these conditions its renal clearance was essentially identical to that of its 4-hydroxy and 4-amino analogs [Smith et al., 1945].

In the foregoing paper we investigated the renal handling of benzoylglycine and methyl-substituted benzoylglycines in the dog [Russel et al., 1988a]. The aim of the present study was to determine under exactly the same circumstances the excretory characteristics of 4-amino- and 2-, 3-, and 4-hydroxybenzoylglycine.

7.2 MATERIALS AND METHODS

Chemicals

4-Aminobenzoylglycine (p-aminohippuric acid) and 2-hydroxybenzoylglycine (salicyluric acid) were commercially available from Merck (Darmstadt, FRG). The 3- and 4-hydroxy-substituted benzoylglycines were prepared by chemical synthesis as described below. The preparation of 4-methoxybenzoylglycine is described elsewhere [Russel et al., 1988b]. Glycine, 3- and 4-hydroxybenzoic acid and dioxane were obtained from Merck, N-hydroxysuccinimide and N,N'-dicyclohexylcarbodiimide were from Janssen Chimica (Beerse, Belgium). All other chemicals are described elsewhere [Russel et al., 1988a].

Preparation of 3- and 4-Hydroxybenzoylglycine

The active ester method, as described by Van Brussel and Van Sumere [1978], was used to synthesize 3- and 4-hydroxybenzoylglycine. An activated ester was prepared by reaction of the corresponding hydroxybenzoate with N-hydroxysuccinimide in presence of N,N'-dicyclohexylcarbo-

diimide in dry dioxane. The ester was separated by filtration and subsequently added to a slight alkaline glycine solution to yield the hydroxy-substituted benzoylglycine. The compounds were purified by recrystallization from boiling water. The identity and purity were checked by comparing melting points with available literature values [Van Brussel and Van Sumere, 1978] and by TLC and HPLC, the methods of which are described elsewhere [Russel et al., 1988a].

Clearance Experiments

The experiments were done in the same three male Beagle dogs that were used in the foregoing study, under exactly the same conditions [Russel et al., 1988a]. Each dog received as a rapid intravenous injection a sterile solution of about 1 gram of 4-amino- or hydroxy-substituted benzoylglycine dissolved in about 15 ml water containing an equimolar amount of sodium bicarbonate. At regular times throughout the experiment blood samples were taken and urine was collected quantitatively. At the end of each experiment the glomerular filtration rate was estimated by measuring the steady-state [^3H]inulin clearance.

Analytical Methods

The 4-amino- and hydroxy-substituted benzoylglycines were determined in plasma and urine according to the elsewhere described HPLC method [Russel et al., 1988a], with slight modifications. The mobile phase consisted of a varying mixture of methanol and twice-distilled water containing 0.01 M citrate (pH 2.6). The methanol-water ratio was 10:90 in the determination of 4-aminobenzoylglycine, 20:80 for 3-hydroxybenzoylglycine, and 30:70 for 2- and 4-hydroxybenzoylglycine. Operating values of the wavelength detector (λ), retention times (t_R) and internal standards (I.S.) were: 4-aminobenzoylglycine $\lambda = 254$ nm, $t_R = 3.0$ min, I.S. = 4-methoxybenzoylglycine ($t_R = 16.0$ min); 2-hydroxybenzoylglycine $\lambda = 245$ nm, $t_R = 6.2$ min, I.S. = benzoylglycine ($t_R = 4.1$ min); 3-hydroxybenzoylglycine $\lambda = 238$ nm, $t_R = 3.4$ min, I.S. = 4-methylbenzoylglycine ($t_R = 11.0$ min); 4-hydroxybenzoylglycine $\lambda = 240$ nm, $t_R = 2.0$ min, I.S. = 4-methylbenzoylglycine ($t_R = 7.9$ min).

Plasma and urine samples were checked for the presence of the corresponding acid derivative, resulting from a possible in vivo deglycination

reaction. In the plasma samples of the experiments with 4-hydroxybenzoylglycine, chromatographed under the same conditions as described above, a small amount of 4-hydroxybenzoate ($t_R = 5.8$ min) was found. Concentrations were, however, too low (<1 $\mu\text{g/ml}$) to be quantified accurately.

The determination of plasma protein binding and [^3H]inulin concentrations in plasma and urine were the same as described in the foregoing paper.

Kinetic Analysis

Plasma concentration and renal excretion rate curves were analyzed separately by statistical moment theory and basic pharmacokinetic parameters were calculated. Plasma curves were fitted to the sum of two exponentials, except for the nonlinear semilogarithmic plots of 2-hydroxybenzoylglycine. These curves were fitted using a cubic spline interpolation method in combination with extrapolation of the initial distribution phase of the plot to time 0, and the terminal phase of the plot to infinity. The renal excretion rate curves of all experiments were analyzed in the same way.

In order to come to a comprehensive analysis of the processes that determine the renal excretion of the compounds, plasma concentration and renal excretion rate data of each experiment were analyzed simultaneously according to a physiologically based kidney model. Equations, calculation methods and computer programs are described in detail elsewhere [Russel et al., 1988a]. Average values are expressed as means \pm SD.

7.3 RESULTS

Experimental Conditions and Protein Binding

The parameters describing the experimental circumstances of the clearance studies are given in Table 7.1. The glomerular filtration rate (Q_{GF}), measured by steady state [^3H]inulin clearance, ranged from 22 - 38 ml/min, the mannitol induced urine flow (Q_{ur}) varied from 0.6 - 1.3 ml/min and the urinary pH from 7.0 - 7.7.

Table 7.1 Experimental conditions of the clearance studies with 4-amino- and hydroxy-substituted benzoylglycines.

Dog	Weight (kg)	Substituent	Dose (mg)	Q_{GF} (ml/min)	Q_{ur} (ml/min)	pH_{ur}
1	13.0	4-NH ₂	1060	27 ± 3	0.83 ± 0.22	7.67 ± 0.16
	13.5	2-OH	970	38 ± 4	0.94 ± 0.31	7.15 ± 0.31
	13.0	3-OH	980	30 ± 1	0.63 ± 0.25	7.54 ± 0.11
	13.7	4-OH	1130	31 ± 1	1.21 ± 0.41	7.53 ± 0.12
2	13.3	4-NH ₂	1050	22 ± 4	1.04 ± 0.22	7.37 ± 0.13
	13.5	2-OH	980	27 ± 3	0.69 ± 0.20	7.24 ± 0.16
	12.8	3-OH	980	28 ± 3	0.64 ± 0.19	7.35 ± 0.12
	13.5	4-OH	1160	28 ± 1	0.89 ± 0.51	7.46 ± 0.10
3	15.0	4-NH ₂	1060	34 ± 3	1.05 ± 0.25	7.19 ± 0.14
	14.8	2-OH	980	30 ± 1	0.83 ± 0.28	7.05 ± 0.24
	14.8	3-OH	960	34 ± 1	0.95 ± 0.28	7.26 ± 0.16
	15.2	4-OH	1090	32 ± 1	1.26 ± 0.45	7.42 ± 0.14

Plasma protein binding of 4-aminobenzoylglycine and the hydroxy-substituted benzoylglycine is shown in Fig. 7.1. Protein binding data of all experiments were pooled for each compound, since differences in the extent of binding were small between the dogs. Over the plasma concentration range measured (5 - 450 µg/ml), the fraction unbound was virtually constant for 4-amino- (0.95 ± 0.05 , $n=13$), 3-hydroxy- (0.89 ± 0.06 , $n=9$) and 4-hydroxybenzoylglycine (0.91 ± 0.05 , $n=14$). The plasma protein binding of 2-hydroxybenzoylglycine was concentration-dependent, the fraction unbound varying from 0.2 - 0.6, and the data ($n=30$) were analyzed according to a one site binding model as described in the foregoing paper. The results of these calculations were 218 ± 24 µg/ml for total concentration of protein binding sites (P) and 92 ± 18 µg/ml for the dissociation constant (K_d) of the drug-protein complex.

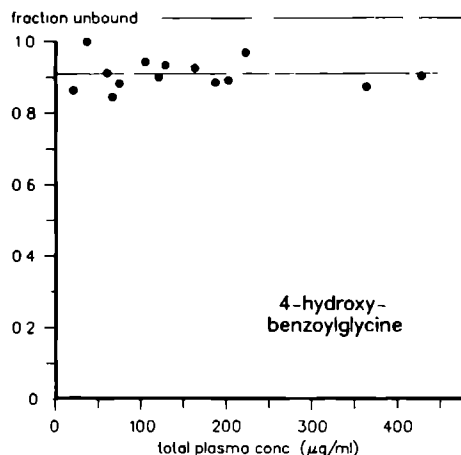
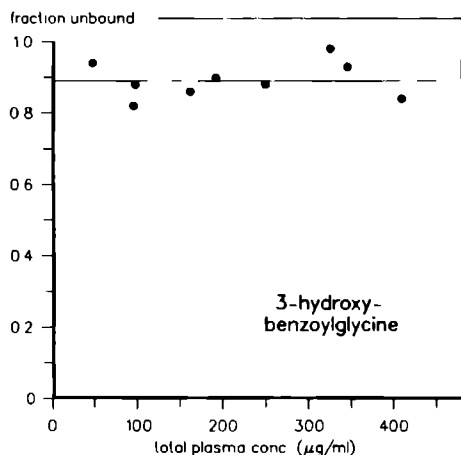
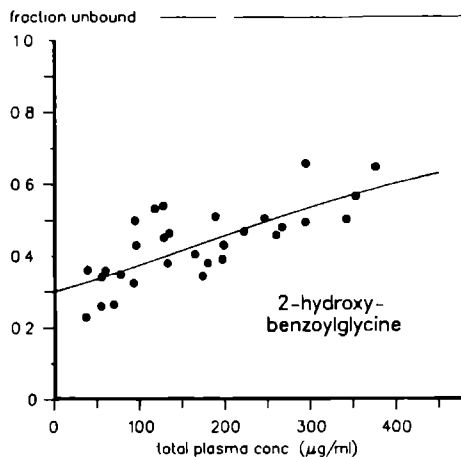
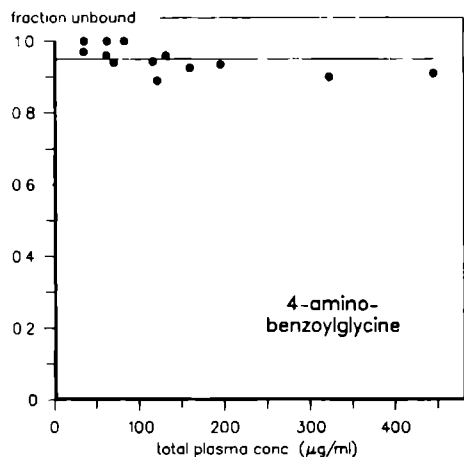


Fig. 7.1 Plasma protein binding of 4-aminobenzoylglycine and hydroxy-substituted benzoylglycines.

Pharmacokinetic Analysis

Representative examples of plasma concentration and renal excretion rate after intravenous administration of 4-aminobenzoylglycine and hydroxy-substituted benzoylglycines are shown in Fig. 7.2. Plasma and renal excretion data were analyzed separately and basic pharmacokinetic parameters are given in Table 7.2. The results show that 4-amino-, 3-hydroxy- and 4-hydroxybenzoylglycine were rapidly eliminated from

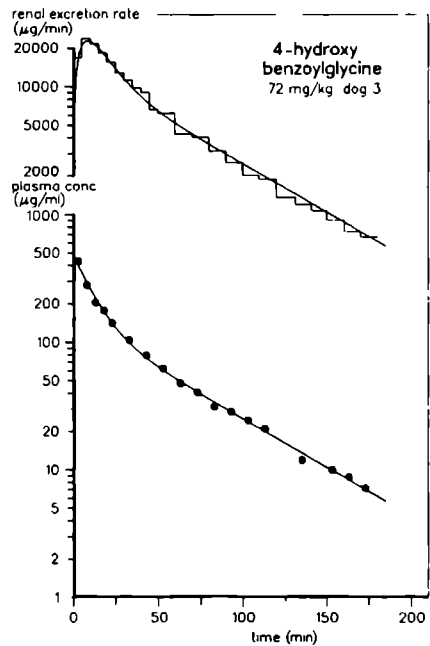
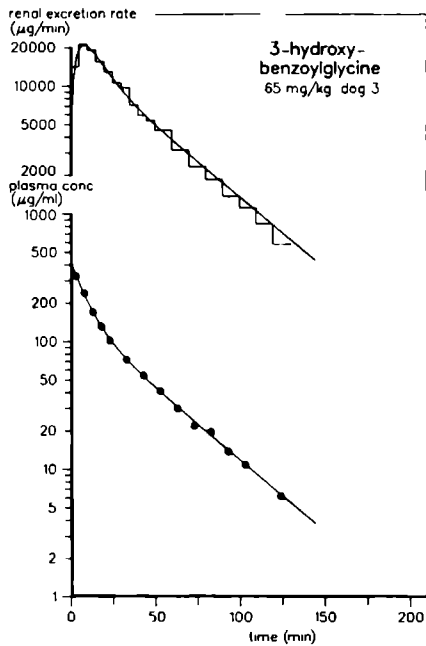
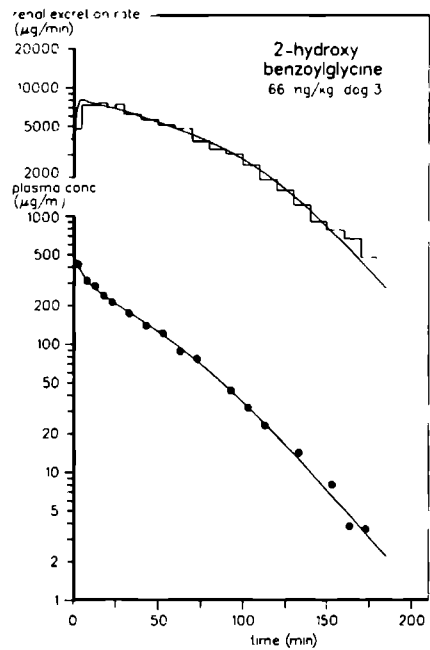
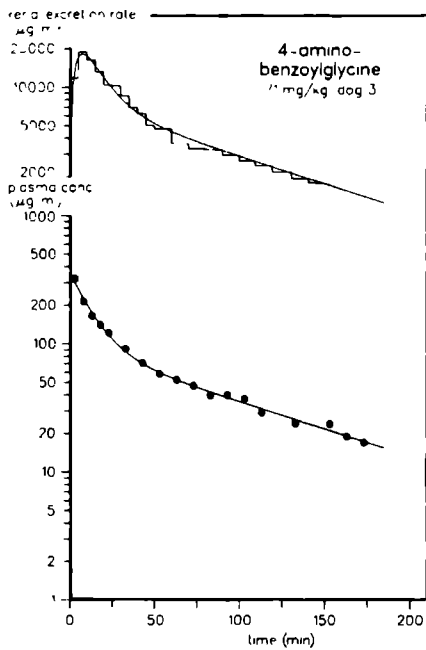


Fig. 7.2 Renal excretion rate and plasma concentration of 4-aminobenzoylglycine and hydroxy-substituted benzoylglycines. The solid lines through the data points represent the results of data analysis according to the kidney model.

Table 7.2 Basic pharmacokinetic parameters of 4-amino- and hydroxy-substituted benzoylglycines after rapid intravenous injection.

Substituent	Dog	plasma			urine			
		$t_{1/2,p}$ (min)	CL (ml/min)	V_1 (l)	$t_{1/2,ur}$ (min)	MRT _R (min)	CL _R (ml/min)	D _{ur} (%)
4-NH ₂	1	36	90	1.45	64	52	79	88
	2	42	73	1.95	43	62	67	92
	3	71	82	2.96	53	58	70	85
	Mean(SD)	50(19)	82(9)	2.12(0.77)	53(11)	57(5)	72(6)	88(4)
2-OH	1	20	69	1.90	23	57	46	66
	2	25	50	2.11	35	73	31	63
	3	20	61	1.95	30	63	39	63
	Mean(SD)	22(3)	60(10)	1.99(0.11)	29(6)	64(8)	39(8)	64(2)
3-OH	1	23	120	1.78	35	35	97	81
	2	29	96	2.24	28	40	79	83
	3	27	116	2.31	23	33	91	78
	Mean(SD)	26(3)	111(13)	2.11(0.30)	29(6)	36(4)	89(9)	81(3)
4-OH	1	37	98	2.38	38	40	92	94
	2	33	71	1.46	37	57	62	88
	3	40	90	2.26	43	48	87	97
	Mean(SD)	37(4)	86(14)	2.03(0.50)	39(3)	48(9)	80(16)	93(5)

plasma, largely by renal excretion ($D_{ur} > 80\%$). The high total renal clearance of these compounds as compared to the clearance that would be observed by glomerular filtration alone, is indicative for avid tubular secretion.

The pharmacokinetic profile of 2-hydroxybenzoylglycine differed clearly from its hydroxy isomers and 4-amino analog. Its plasma clearance was much lower and only $64 \pm 2\%$ of the administered dose was excreted in the urine. Accordingly, renal clearance was also substantially lower. However, taking an average protein binding of 40 - 50% into account, it can be calculated that the total renal clearance was still twice the value attributable to glomerular filtration, showing that 2-hydroxybenzoylglycine is also cleared by tubular secretion.

Since splitting of the glycine moiety from 4-amino- and 2-hydroxybenzoylglycine has been described in the rat [Mályusz et al., 1972; Bekersky et al., 1980], we checked all plasma and urine samples for the presence of the corresponding benzoates. Only in case of 4-hydroxybenzoylglycine, small amounts of its benzoate ($<1 \mu\text{g/ml}$) were discovered in plasma, while for none of the other compounds deglycination products could be detected.

Kidney Model

A physiologically based pharmacokinetic model was used to quantify the processes that are involved in the renal excretion of the benzoylglycines. The model is composed of a series of lumped compartments representing the central plasma pool, the peripheral tissues and the kidney. The kidney is divided further into a renal plasma, tubular cell and tubular urine compartment. A schematic representation and detailed description of the model was given in the foregoing paper. Since the renal extraction of the 4-amino- and hydroxy-substituted benzoylglycines is virtually complete at low plasma concentrations, the process of tubular secretion was considered to be dependent on the total concentration of compound in renal plasma. Plasma and urinary data of each experiment were simultaneously fitted to the model and the results are given in Table 7.3 and are also represented by the solid lines through the data points in Figs. 7.2 and 7.3. The goodness of fit between the observed and model-predicted plasma concentration and renal excretion rate data was in all cases: $R^2_{\text{plasma}} > 0.990$ and $R^2_{\text{urine}} > 0.980$.

Table 7.3 Model parameters characterizing the renal handling of 4-amino- and hydroxy-substituted benzoylglycines.

Substituent	Dog	T_M (mg/min)	K_T (μ g/ml)	CL_{NR} (ml/min)	k_{43} (min ⁻¹)	k_{15} (min ⁻¹)	k_{51} (min ⁻¹)
4-NH ₂	1	144 ^a		10 ± 9	0.14 ± 0.13	0.094 ± 0.023	0.059 ± 0.008
	2	196		10 ± 6	0.23 ± 0.16	0.053 ± 0.007	0.045 ± 0.004
	3	96		7 ± 6	0.31 ± 0.23	0.034 ± 0.004	0.028 ± 0.002
	Mean(SD)	145(50)		9(2)	0.23(0.09)	0.060(0.031)	0.044(0.016)
2-OH	1	5.0 ± 0.9	17 ± 14	20 ± 3	0.07 ± 0.02	0.024 ± 0.005	0.056 ± 0.012
	2	3.3 ± 0.2	20 ± 3	18 ± 2	0.26 ± 0.16	0.042 ± 0.006	0.104 ± 0.014
	3	4.8 ± 0.5	32 ± 9	21 ± 4	0.10 ± 0.03	0.060 ± 0.026	0.143 ± 0.049
	Mean(SD)	4.4(0.9)	23(8)	20(2)	0.14(0.10)	0.042(0.018)	0.101(0.044)
3-OH	1	218 ^a		21 ± 6	0.11 ± 0.07	0.040 ± 0.015	0.060 ± 0.004
	2	179		14 ± 5	0.17 ± 0.11	0.030 ± 0.008	0.056 ± 0.006
	3	186		20 ± 4	0.22 ± 0.07	0.034 ± 0.004	0.058 ± 0.004
	Mean(SD)	194(21)		18(4)	0.17(0.06)	0.035(0.005)	0.058(0.002)
4-OH	1	180 ^a		10 ± 4	0.19 ± 0.14	0.052 ± 0.006	0.047 ± 0.005
	2	143		3 ± 8	0.11 ± 0.06	0.035 ± 0.012	0.040 ± 0.004
	3	137		4 ± 4	0.20 ± 0.06	0.029 ± 0.004	0.038 ± 0.002
	Mean(SD)	153(23)		6(4)	0.17(0.05)	0.039(0.012)	0.042(0.005)

^aSince secretion was not saturated estimates of T_M and K_T were very inaccurate (SD > 200%), therefore only the ratio T_M/K_T (ml/min) is given.

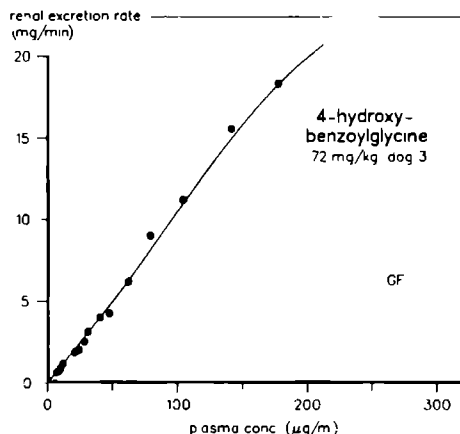
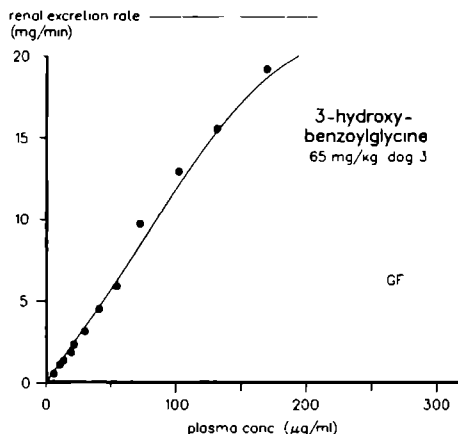
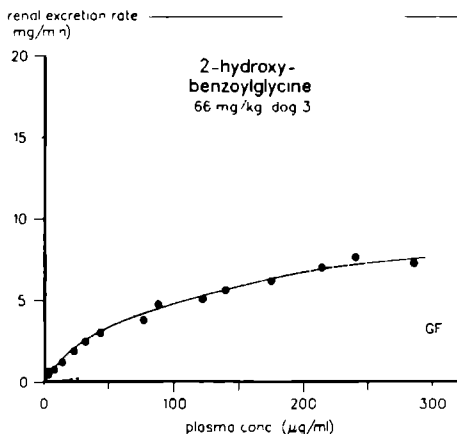
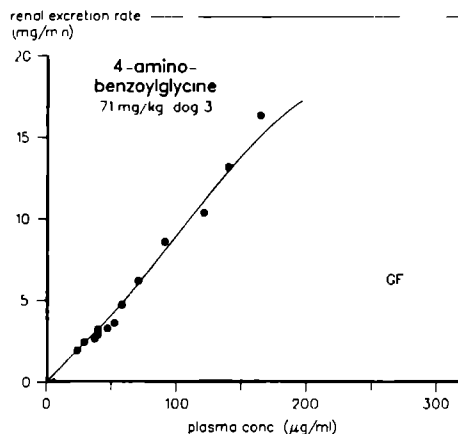


Fig. 7.3 Tubular titration curves representing the relationship between renal excretion rate and plasma concentration of 4-aminobenzoylglycine and hydroxy-substituted benzoylglycines. The solid lines through the data points are calculated according to the kidney model. GF represents the clearance by glomerular filtration.

Fig. 7.3 shows linear plots of the renal excretion rate as a function of the plasma concentration at the midpoint of a urine collection interval. These tubular titration curves indicate that the clearance characteristics of 4-amino-, 3-hydroxy- and 4-hydroxybenzoylglycine were practically the same, whereas the profile of the 2-hydroxy analog was clearly different. At the given doses, saturation of the secretory system was achieved only

for 2-hydroxybenzoylglycine. Renal secretion of the other compounds appeared to be a linear function of the plasma concentration up to levels of at least 150 $\mu\text{g/ml}$. Accordingly, the parameters T_M and K_T , describing the active transport of these compounds, could not be calculated accurately. Therefore only an estimate of the ratio T_M/K_T , the intrinsic secretion clearance (CL_{int}), was given (Table 7.3).

Considering the dissociation constants of the glycine conjugates [Smith et al., 1945; Knoefel et al., 1962], viz., 4-amino- ($\text{pK}_a = 3.8$), 2-hydroxy- ($\text{pK}_a = 3.6$), 3-hydroxy- ($\text{pK}_a = 3.6$) and 4-hydroxybenzoylglycine ($\text{pK}_a = 3.7$), in relation with the experimental conditions, it seems unlikely that reabsorption by non-ionic diffusion played a role of importance in total renal clearance. Although the hydrophobic nature of 2-hydroxybenzoylglycine, due to internal hydrogen bonding, may give rise to passive reabsorption, even when the urinary flow and pH are high [Knoefel et al., 1962], it is clear from the profile of its tubular titration curve, in which the total renal clearance parallels the glomerular filtration at high concentrations, that reabsorption was negligible under the present conditions.

7.4 DISCUSSION

The renal disposition of 4-aminobenzoylglycine and the hydroxy-substituted benzoylglycines can be analyzed in terms of the basic intrarenal processes of glomerular filtration and transtubular secretion. However, the excretory pattern of 2-hydroxybenzoylglycine contrasted clearly with that of the other compounds. Plasma kinetics and renal clearance of the 4-amino and 3- and 4-hydroxy analogs were essentially the same and were characterized by a low plasma protein binding, rapid elimination from plasma and a high renal clearance due to avid tubular secretion. In comparison, the kinetics of the 2-hydroxy analog were characterized by a relatively high protein binding, lower plasma and renal clearance, and limited capacity of the tubular secretory system.

It can be calculated from Table 7.3 that the intrinsic secretion clearance of 2-hydroxybenzoylglycine, $CL_{\text{int}} = T_M/K_T = 203 \pm 19 \text{ ml/min}$, was not less than that of the other compounds, indicating that at low plasma levels

renal clearance was equally efficient and not hindered by the high protein binding. But, at increasing plasma concentrations its renal clearance decreased rapidly and fell toward the level of glomerular filtration, while the renal clearance of the other derivatives remained virtually unaltered. Since passive reabsorption by non-ionic diffusion was negligible under the experimental conditions, the lower renal excretion can be ascribed to the limited capacity of the secretory system (T_M) for 2-hydroxybenzoyl-glycine.

The clearance capacity of the secretory system with respect to 4-amino-, 3-hydroxy- and 4-hydroxybenzoylglycine is apparently so high that up to plasma concentrations of 150 $\mu\text{g/ml}$ saturation was not reached. The almost linear course of the titration curves of these compounds differs clearly from the usual Michaelis-Menten profile and is typical for compounds that are so efficiently excreted that clearance is supply-limited up to levels at which the secretory system begins to be saturated. In this situation the renal plasma flow is the rate-limiting step in clearance. Indeed, the slope of the titration curve is an operational estimate of the effective renal plasma flow. Since the active step in secretion is located at the basolateral membrane of the proximal tubular cells [Møller and Sheikh, 1983], it can be concluded that the cellular uptake of these compounds is in the order of magnitude of the renal plasma flow, i.e., 140 - 170 ml/min. The clearance out of the cells into the tubular lumen ranges from 4 - 9 ml/min, as calculated from the product of the estimated tubular cell volume, being 30 ml [Russel et al., 1988a], and the rate constant k_{43} (Table 7.3). Thus, according to the kidney model, the active secretion of these compounds will be accompanied by a substantial accumulation within the tubular cells. This is in accordance with previously reported in vitro observations [Møller and Sheikh, 1983; Forster and Copenhaver, 1956]

Deconjugation of the glycine group of 4-amino- and 2-hydroxybenzoylglycine has been described to occur in rat kidney [Mályusz et al., 1972; Bekersky et al., 1980]. Apparently, this is not a significant process in dog as we found no metabolic conversion for any of the compounds, except for the small quantities of 4-hydroxybenzoate in plasma in the experiments with 4-hydroxybenzoylglycine. Acetylation of the amino group of 4-aminobenzoylglycine, which is known to occur in liv-

er and kidney of man and many animal species, does not occur in rabbit and dog [Smith et al., 1945; Setchell and Blanch, 1961].

In conclusion, 3- and 4-hydroxybenzoylglycine are very efficiently cleared by the kidney in essentially the same way as 4-aminobenzoylglycine. The excretory pattern of 2-hydroxybenzoylglycine is clearly different and is characterized by a limited transport capacity of the secretory system. It may be suggested that the less efficient interaction of the 2-hydroxy analog with the renal anion transport system is related to its specific property to form an intramolecular hydrogen bond between the hydroxy and carbonyl group.

Acknowledgements

The authors are indebted to Mr. H. van Deelen and Dr. A.J. Beld for the preparation of the glycine conjugates.

7.5 REFERENCES

- Aukland, K. and Løyning, E.W.: Intrarenal blood flow and para-aminohippurate (PAH) extraction. *Acta Physiol. Scand.* **79**, 95-108, 1970.
- Bekersky, I., Colburn, W.A., Fishman, L. and Kaplan, S.A.: Metabolism of salicylic acid in the isolated perfused rat kidney. Interconversion of salicyluric and salicylic acids. *Drug Metab. Dispos.* **8**, 319-324, 1980.
- Forster, R.P. and Copenhaver, J.V.: Intracellular accumulation as an active process in a mammalian renal transport system in vitro. *Am. J. Physiol.* **186**, 167-171, 1956.
- Girndt, J., Mályusz, M., Rumpf, K.W., Neubaur, J. and Sheller, F.: Metabolism of p-aminohippurate and its relevance in man. *Nephron* **13**, 138-144, 1974.
- Knoefel, P.K. and Huang, K.C.: Biochemorphology of renal tubular transport: hippuric acid and related substances. *J. Pharmacol. Exp. Ther.* **126**, 296-303, 1959.

- Knoefel, P K , Huang, K C and Jarboe, C H Renal disposal of salicyluric acid *Am J Physiol* 203, 6-10, 1962
- Lote, C J , McVicar, A J and Yardley, C P Renal extraction and clearance of p-aminohippurate during saline and dextrose infusion in the rat *J Physiol* 363, 303-313, 1985
- Malyusz, M , Girndt, J , Malyusz, G and Ochwaldt, B Die Metabolisierung von p-Aminohippurat in Nieren von normalen Ratten und Ratten mit experimentellen Goldblatt-Hochdruck *Pflugers Arch* 333, 156-165, 1972
- Møller, J V and Sheikh, M I Renal organic anion transport system pharmacological, physiological, and biochemical aspects *Pharmacol Rev* 34, 315-358, 1983
- Russel, F G M , Wouterse, A C and van Ginneken, C A M Physiologically based pharmacokinetic model for the renal clearance of salicyluric acid and the interaction with phenolsulfonphthalein in the dog *Drug Metab Dispos* 15, 695-701, 1987
- Russel, F G M , Wouterse, A C and van Ginneken, C A M Renal clearance of substituted hippurates in the dog I Benzoylglycine (hippurate) and methyl-substituted benzoylglycines *J Pharmacol Exp Ther* submitted, 1988a
- Russel, F G M , Wouterse, A C and van Ginneken, C A M Renal clearance of substituted hippurates in the dog III Methoxy-substituted benzoylglycines *J Pharmacol Exp Ther* submitted, 1988b
- Setchell, B P and Blanch, E Conjugation of p-aminohippurate by the kidney and effective renal plasma flow *Nature (Lond)* 189, 230-231, 1961
- Smith, H W , Goldring, W and Chasis, H The measurement of the tubular excretory mass, effective blood flow and filtration rate in the normal kidney *J Clin Invest* 17, 263-278, 1938
- Smith, H W , Finkelstein, N , Aluminosa, L , Crawford, B and Graber, M The renal clearances of substituted hippuric acid derivatives and other aromatic acids in dog and man *J Clin Invest* 24, 388-404, 1945
- Van Brussel, W and Van Sumere, C F N-Acylamino acids and peptides VI A simple synthesis of N-acylglycines of the benzoyl and cinnamyl type *Bull Soc Chim Belg* 87, 791-797, 1978

RENAL CLEARANCE OF SUBSTITUTED HIPPURATES.
III. METHOXY-SUBSTITUTED BENZOYLGLYCINES¹

Frans G.M. Russel, Alfons C. Wouterse, and Cees A.M. van Ginneken

Abstract - Plasma kinetics and renal excretion of methoxy-substituted benzoylglycines were studied in three Beagle dogs after rapid intravenous administration of about 1 gram. The methoxybenzoylglycines showed non-linear plasma protein binding varying between 10 and 70% over a concentration range of 5 - 450 µg/ml. The compounds were rapidly cleared from plasma, largely by renal excretion (72 - 84% of the administered dose). Variation between the basic pharmacokinetic parameters was small, except for a higher plasma and total renal clearance of the 4-methoxy isomer. At the given dose, tubular secretion of 2- and 3-methoxybenzoylglycine was saturated, while the clearance capacity of the secretory system for the 4-methoxy isomer was so high that complete saturation was not achieved. The kinetic parameters of tubular secretion, obtained from data analysis according to a physiologically based kidney model, were: 2-methoxybenzoylglycine $T_M = 11.7 \pm 4.9$ mg/min, $K_T = 42 \pm 9$ µg/ml, and 3-methoxybenzoylglycine $T_M = 8.8 \pm 1.0$ mg/min, $K_T = 27 \pm 20$ µg/ml. Since secretion of 4-methoxybenzoylglycine was not saturated only the ratio $T_M/K_T = 201 \pm 47$ ml/min could be calculated. The 4-methoxy isomer was metabolized to some extent by deconjugation of the glycine moiety and the resulting benzoate was found in plasma but not in urine.

¹J. Pharmacol. Exp. Ther., submitted

8.1 INTRODUCTION

This paper is the last in a series of three on the influence of ring substitution on renal clearance of benzoylglycine (hippurate). In the preceding papers the excretory characteristics of benzoylglycine, 4-aminobenzoylglycine (p-aminohippurate), methyl-substituted and hydroxy-substituted benzoylglycines were studied [Russel et al, 1988a,b]. The most efficient renal excretion was found with the 3- and 4-hydroxy-substituted benzoylglycines, and the model compound 4-aminobenzoylglycine, which were cleared equally well. The renal disposition of the other benzoylglycines varied considerably as a result of differences in their intrarenal as well as extrarenal behavior. Plasma kinetics and renal excretion rate of all compounds could be adequately analyzed with the same physiologically based kinetic model, which comprises the functional characteristics of the kidney that determine the excretion of the benzoylglycines, i.e., renal plasma flow, urine flow, nonlinear protein binding, glomerular filtration and transtubular secretion.

The present study is concerned with the renal clearance of methoxy-substituted benzoylglycines. The renal transport of the 2-methoxy isomer has been described previously by Knoefel and Huang [1959] in a study in the dog. They found a protein binding of about 40% at a plasma concentration of 250 $\mu\text{g/ml}$ and net tubular secretion of about 10 mg/min at a concentration of 140 $\mu\text{g/ml}$. The extent of secretion was in the same range as was found for benzoylglycine. As far as we know, there have been no reports on the renal clearance of the 3- and 4-methoxy isomers.

8.2 MATERIALS AND METHODS

Chemicals

The methoxy-substituted benzoylglycines were prepared according to the Schotten-Baumann method from the corresponding acylchlorides as described elsewhere [Russel et al, 1988a]. The identity and purity were checked by comparing melting points with available literature values [Quick, 1932, Selheim and Sheline, 1973, ApSimon et al, 1978] and by TLC and HPLC. o-, m-, and p-Anisoylchloride (methoxybenzoylchloride)

were obtained from Aldrich (Brussel, Belgium) All other chemicals are described elsewhere [Russel et al , 1988a]

Clearance Experiments

The experiments were done in the same three male Beagle dogs that were used in the preceding studies, under exactly the same conditions [Russel et al , 1988a,b] Each dog received as a rapid intravenous injection a sterile solution of about 1 gram of 2-, 3- or 4-methoxybenzoylglycine dissolved in about 15 ml water containing an equimolar amount of sodium bicarbonate At regular times throughout the experiment blood samples were taken and urine was collected quantitatively At the end of each experiment the glomerular filtration rate was estimated by measuring the steady-state [^3H]inulin clearance

Analytical Methods

The methoxy-substituted benzoylglycines were determined in plasma and urine according to the elsewhere described HPLC method [Russel et al , 1988a], with slight modifications The mobile phase consisted of a mixture of methanol and twice-distilled water (30/70) containing 0.01 M citrate (pH 2.6) Operating values of the wavelength detector (λ), retention times (t_R) and internal standards (I.S.) were 2-methoxybenzoylglycine $\lambda = 235$ nm, $t_R = 7.2$ min, I.S. = benzoylglycine ($t_R = 4.1$ min), 3-methoxybenzoylglycine $\lambda = 238$ nm, $t_R = 6.0$ min, I.S. = 3-methylbenzoylglycine ($t_R = 8.3$ min), 4-methoxybenzoylglycine $\lambda = 240$ nm, $t_R = 5.2$ min, I.S. = 4-methylbenzoylglycine ($t_R = 7.9$ min)

Plasma and urine samples were checked for the presence of the corresponding acid derivative In the experiments with 4-methoxybenzoylglycine, 4-methoxybenzoic acid ($t_R = 13.8$, methanol/water 35/65, 0.01 M citrate pH 2.6, $\lambda = 254$ nm) was found in plasma and concentrations were quantified

The determination of plasma protein binding and [^3H]inulin concentrations in plasma and urine were the same as described in the foregoing paper

Kinetic Analysis

Plasma concentration and renal excretion rate curves were analyzed separately by statistical moment theory and basic pharmacokinetic parameters were calculated. Plasma curves could be fitted well to the sum of two exponentials, while the nonlinear semilogarithmic renal excretion rate curves were analyzed using a cubic spline interpolation method in combination with extrapolation of the terminal phase of the curve to infinity.

In order to come to a comprehensive analysis of the processes that determine the renal excretion of the methoxy-substituted benzoylglycines, plasma concentration and renal excretion rate data of each experiment were analyzed simultaneously according to a physiologically based kidney model. Equations, calculation methods and computer programs are described in detail elsewhere [Russel et al., 1988a]. Average values are expressed as means \pm SD.

Table 8.1 Experimental conditions of the clearance studies with methoxy-substituted benzoylglycines.

Dog	Weight (kg)	Substituent	Dose (mg)	Q_{GF} (ml/min)	Q_{ur} (ml/min)	pH_{ur}
1	12.8	2-OCH ₃	1000	30 \pm 2	0.97 \pm 0.45	7.18 \pm 0.26
	13.0	3-OCH ₃	1010	32 \pm 2	1.02 \pm 0.29	7.33 \pm 0.12
	12.5	4-OCH ₃	980	31 \pm 5	0.69 \pm 0.25	7.53 \pm 0.11
2	11.5	2-OCH ₃	1010	26 \pm 1	0.64 \pm 0.11	6.43 \pm 0.42
	11.5	3-OCH ₃	990	28 \pm 1	0.70 \pm 0.27	7.20 \pm 0.07
	11.5	4-OCH ₃	980	19 \pm 1	0.76 \pm 0.13	7.34 \pm 0.09
3	13.0	2-OCH ₃	1010	33 \pm 1	0.87 \pm 0.31	7.06 \pm 0.15
	14.5	3-OCH ₃	1000	30 \pm 3	0.99 \pm 0.18	7.18 \pm 0.16
	14.0	4-OCH ₃	990	28 \pm 1	0.95 \pm 0.28	7.44 \pm 0.12

8.3 RESULTS

Experimental Conditions and Protein Binding

The experimental conditions of the clearance studies with the methoxy-substituted benzoylglycines are given in Table 8.1. The glomerular filtration rate (Q_{GF}), measured by steady state [3H]inulin clearance, ranged from 19 - 33 ml/min, the urine flow (Q_{ur}) varied from 0.6 - 1.0 ml/min and the urinary pH from 6.4 - 7.5.

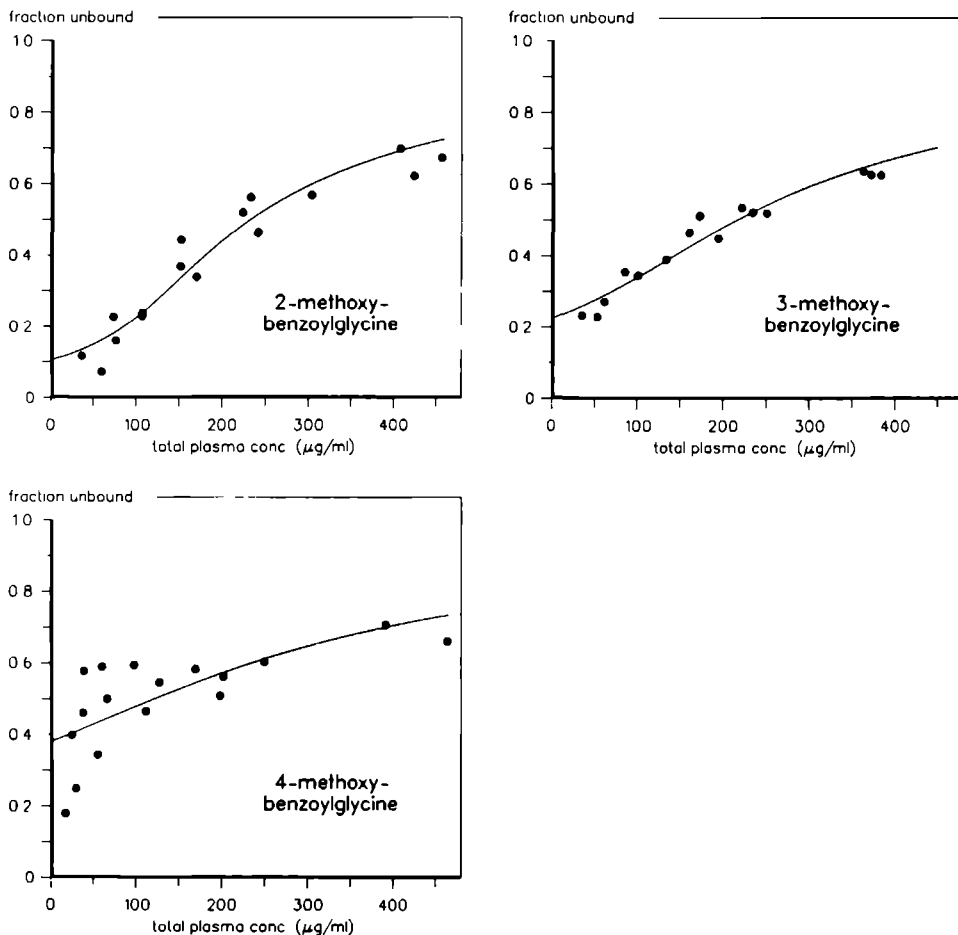


Fig. 8.1 Plasma protein binding of methoxy-substituted benzoylglycines.

Concentration-dependent plasma protein binding was observed for each of the methoxy isomers, the fraction unbound ranging from 10 - 70% (Fig. 8.1). Because interindividual variation was small, data of all experiments were pooled for each compound and analyzed according to a one site binding model as described in the foregoing paper [Russel et al., 1988a]. The results of these fits are given in Table 8.2.

Table 8.2 Plasma protein binding of methoxy-substituted benzoylglycines.

Substituent	n	P ($\mu\text{g/ml}$)	K_d ($\mu\text{g/ml}$)
2-OCH ₃	16	132 \pm 9	16 \pm 4
3-OCH ₃	15	152 \pm 9	44 \pm 6
4-OCH ₃	17	158 \pm 44	97 \pm 41

Pharmacokinetic Analysis

Representative examples of plasma disappearance and renal excretion rate after intravenous administration of the methoxybenzoylglycines are shown in Fig. 8.2. Plasma and urinary data were analyzed separately by statistical moment theory. The results of these calculations are summarized in Table 8.3. There was little variation between the basic pharmacokinetic parameters of the methoxy isomers. Only the plasma clearance (CL) and total renal clearance (CL_R) of the 4-methoxy isomer was higher than the values for the other compounds. The methoxybenzoylglycines are rapidly removed from the body, as can be derived from their short mean residence time (MRT_R) and half-lives in plasma ($t_{1/2,p}$) and urine ($t_{1/2,ur}$). Taking the protein binding of the compounds into consideration it is obvious that the contribution of glomerular filtration was only small, demonstrating that active tubular secretion was the major route of renal excretion.

In the experiments with 4-methoxybenzoylglycine, its deglycination product 4-methoxybenzoate was found in plasma but not in urine (Fig. 8.2). This situation is similar to that observed with 4-methylbenzoylglycine [Russel et al., 1988a]. Plasma concentration data

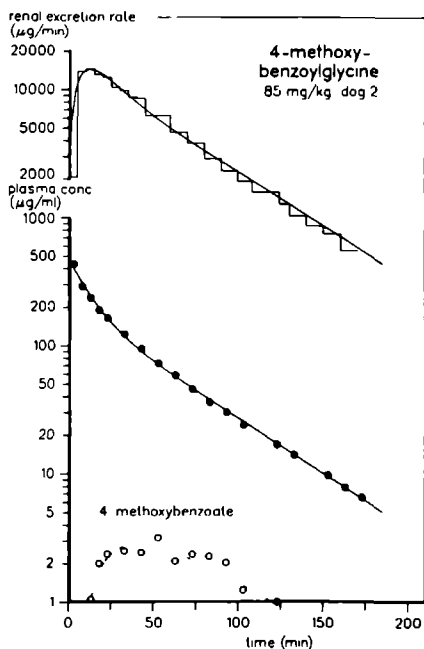
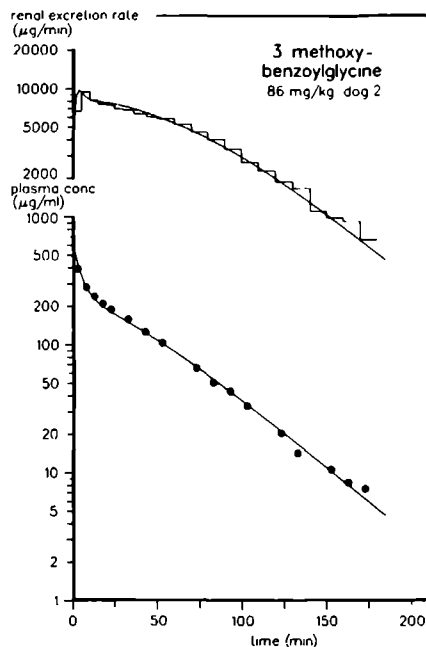
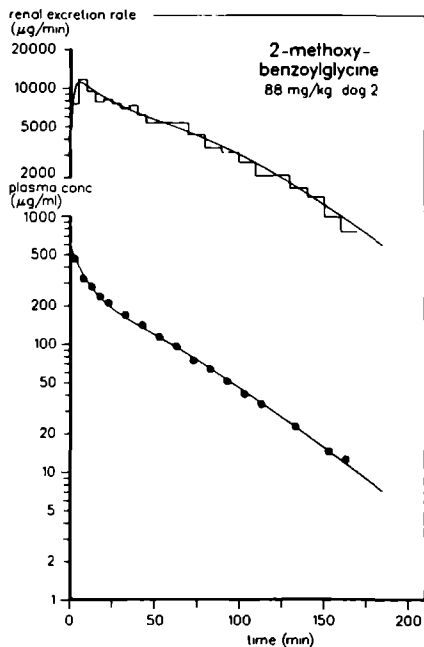


Fig. 8.2 Renal excretion rate and plasma concentration of methoxy-substituted benzoylglycines. The solid lines through the data points represent the results of data analysis according to the kidney model.

Table 8.3 Basic pharmacokinetic parameters of methoxy-substituted benzoylglycines after rapid intravenous injection.

Substituent	Dog	plasma			urine			
		$t_{\frac{1}{2},P}$ (min)	CL (ml/min)	V_1 (l)	$t_{\frac{1}{2},ur}$ (min)	MRT _R (min)	CL _R (ml/min)	D _{ur} (%)
2-OCH ₃	1	26	101	2.20	23	37	77	76
	2	34	57	1.61	41	64	42	74
	3	32	82	2.17	32	48	59	72
	Mean(SD)	31(4)	80(22)	1.99(0.33)	32(9)	50(14)	59(18)	74(2)
3-OCH ₃	1	25	94	2.61	31	52	79	84
	2	31	66	1.51	43	66	49	74
	3	53	84	2.82	36	55	60	72
	Mean(SD)	36(15)	81(14)	2.31(0.70)	37(6)	58(7)	63(15)	77(6)
4-OCH ₃	1	38	120	2.36	39	33	101	84
	2	35	75	2.07	32	49	62	82
	3	43	104	2.65	45	41	85	82
	Mean(SD)	39(4)	100(23)	2.36(0.29)	39(7)	41(8)	83(20)	83(1)

of 4-methoxybenzoate were fitted to two exponentials: the half-life of the ascending phase was 9 ± 5 min, and of the descending phase 63 ± 25 min. The maximum plasma concentration (± 3 $\mu\text{g/ml}$) was reached after 30 - 40 min. In the descending phase of the curve plasma levels up to 7% of the parent compound were found. In case of the 2- and 3-methoxy isomers no deglycination products were found, neither in plasma nor in urine.

Kidney Model

In order to account for the relevant processes that determine the renal clearance of the methoxy-substituted benzoylglycines, plasma concentration and renal excretion rate data of each experiment were analyzed simultaneously with the aid of a physiologically based kidney model. A detailed description of the model is given elsewhere [Russel et al., 1988a]. The results of the model calculations are listed in Table 8.4 and are also represented by the solid lines through the data points in Figs. 8.2 and 8.3. The goodness of fit between the observed and model-predicted plasma concentration and renal excretion rate data was in all cases: $R^2_{\text{plasma}} > 0.990$ and $R^2_{\text{urine}} > 0.983$. Despite their considerable protein binding, renal clearance of the methoxybenzoylglycines approached the renal plasma flow at low plasma levels indicating that the process of tubular secretion was dependent on the total drug concentration in renal plasma.

It appears from the tubular titration curves in Fig. 8.3 that renal excretion of 2- and 3-methoxybenzoylglycine was saturated over the concentration range measured. The kinetic parameters describing the renal handling of both compounds were about the same value (Table 8.4). In the experiments with 4-methoxybenzoylglycine the level at which saturation begins was hardly reached (Fig. 8.3). As a result, individual estimates of T_M and K_T were very inaccurate and only the intrinsic secretion clearance $CL_{\text{int}} = T_M/K_T$ was calculated (Table 8.4). The profiles of the tubular titration curves (Fig. 8.3) gave no reason to suggest that active or passive reabsorption occurred. Non-ionic back-diffusion is very unlikely in view of the experimental conditions and physicochemical properties of the compounds.

Table 8.4 Model parameters characterizing the renal handling of methoxy-substituted benzoylglycines.

Substituent	Dog	T_M (mg/min)	K_T ($\mu\text{g/ml}$)	CL_{NR} (ml/min)	k_{43} (min^{-1})	k_{15} (min^{-1})	k_{51} (min^{-1})
2-OCH ₃	1	17.0 \pm 4.0	32 \pm 28	20 \pm 5	0.23 \pm 0.17	0.017 \pm 0.004	0.042 \pm 0.002
	2	7.2 \pm 1.0	45 \pm 19	11 \pm 3	0.16 \pm 0.06	0.056 \pm 0.006	0.011 \pm 0.003
	3	11.0 \pm 1.5	50 \pm 19	21 \pm 2	0.20 \pm 0.07	0.025 \pm 0.003	0.021 \pm 0.002
	Mean(SD)	11.7(4.9)	42(9)	17(6)	0.20(0.03)	0.033(0.021)	0.025(0.016)
3-OCH ₃	1	9.6 \pm 0.4	6 \pm 2	19 \pm 4	0.27 \pm 0.06	0.025 \pm 0.004	0.050 \pm 0.005
	2	7.7 \pm 1.3	45 \pm 19	16 \pm 4	0.10 \pm 0.04	0.125 \pm 0.022	0.016 \pm 0.004
	3	9.0 \pm 0.8	30 \pm 10	21 \pm 3	0.26 \pm 0.07	0.010 \pm 0.002	0.025 \pm 0.002
	Mean(SD)	8.8(1.0)	27(20)	19(3)	0.21(0.09)	0.053(0.063)	0.030(0.018)
4-OCH ₃	1	250 ^a		20 \pm 9	0.19 \pm 0.08	0.013 \pm 0.003	0.026 \pm 0.003
	2	157		11 \pm 2	0.15 \pm 0.04	0.026 \pm 0.003	0.044 \pm 0.003
	3	195		18 \pm 4	0.32 \pm 0.08	0.013 \pm 0.002	0.026 \pm 0.002
	Mean(SD)	201(47)		16(8)	0.22(0.09)	0.017(0.008)	0.032(0.010)

^aSince secretion was not saturated estimates of T_M and K_T were very inaccurate (SD > 200%), therefore only the ratio T_M/K_T (ml/min) is given.

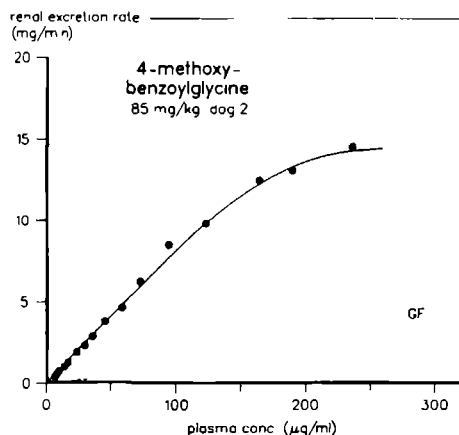
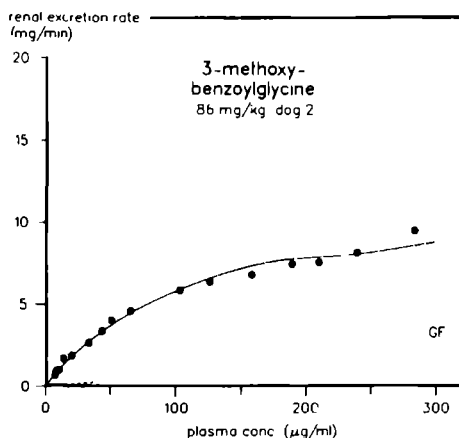
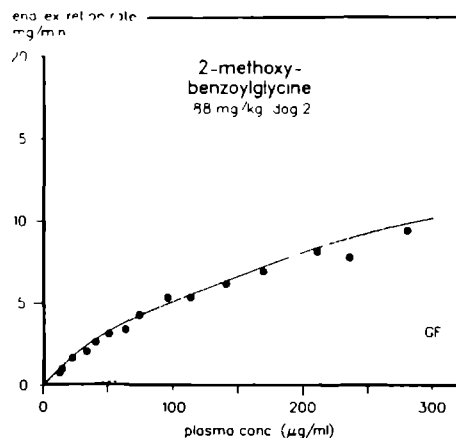


Fig. 8.3 Tubular titration curves representing the relationship between renal excretion rate and plasma concentration of methoxy-substituted benzoylglycines. The solid lines through the data points are calculated according to the kidney model. GF represents the clearance by glomerular filtration.

8.4 DISCUSSION

Compared to the previously studied benzoylglycines, the methoxy-substituted derivatives are cleared reasonably well by the kidney. The variation in excretory patterns between the isomers was considerably less

than that observed with the corresponding methyl and hydroxy analogs [Russel et al., 1988a,b].

The protein binding, plasma kinetics and renal handling of the 2- and 3-methoxy isomers were practically the same. Tubular secretion of both compounds was clearly saturated at the given dose and was not impeded by the high binding to plasma proteins. The tubular secretion of 4-methoxybenzoylglycine was also not influenced by protein binding, but it differed from that of the 2- and 3-methoxy isomers by a much higher clearance capacity. Saturation of the secretory system was not observed until plasma concentrations of about 200 $\mu\text{g/ml}$ were reached. Up to that level, renal clearance was perfusion-rate limited as a result of the high intrinsic secretion clearance (Fig. 8.3, Table 8.4).

Similar to its 4-methyl and 4-hydroxy analogs, 4-methoxybenzoylglycine was metabolized to some extent by deconjugation of the glycine group and the resulting benzoate was found in plasma and not in urine. It seems that substitution in the para position favors such a deconjugation reaction. The nature of the substituent must be also of influence, considering the variation in metabolite concentrations and the absence of deconjugation of 4-aminobenzoylglycine. Taking the area under the metabolite plasma concentration curve as a relative measure of conversion, the extent of metabolite formation was in the order of 4-amino- < 4-hydroxy- < 4-methoxy- < 4-methylbenzoylglycine. This qualitative order corresponded well with the electron-donating properties of the substituents as predicted by the Hammett relation, viz., $\sigma_{4\text{-amino}} = -0.66$, $\sigma_{4\text{-hydroxy}} = -0.37$, $\sigma_{4\text{-methoxy}} = -0.27$, and $\sigma_{4\text{-methyl}} = -0.17$ [Hansch, 1973]. The more strongly a substituent donates electrons, the more negative is its σ value.

However, it should be emphasized that the metabolite concentration in plasma is the resultant of its rate of formation and elimination. Therefore, the influence of a substituent with a lower σ value may just as well be explained by a lower metabolic conversion as a faster elimination of the metabolite.

The presence of the deconjugation product in plasma as well as its probable intrarenal metabolism may have consequences for the renal clearance of the parent compound as has been discussed elsewhere [Russel et al., 1988a].

Taking the findings of the present and the two preceding studies together it can be concluded that introduction of a substituent in the ring of benzoylglycine results in general in a substance for which the renal secretory system has a higher clearance capacity. The most extensive tubular secretion was found for the 4-amino, 3-hydroxy, and 4-hydroxy substitutes, while the extent of secretion of 2-hydroxybenzoylglycine was even less than that of benzoylglycine. In between, a large diversity in excretory characteristics were observed. In spite of these variations, plasma concentration and renal excretion rate curves could be described consistently with a physiologically based kidney model. This type of kinetic modeling may serve to understand and quantify more comprehensively the complexity of processes that determine the renal excretion of drugs.

Acknowledgements

The authors are indebted to Mr. H. van Deelen and Dr. A. J. Beld for the preparation of the glycine conjugates.

8.5 REFERENCES

- ApSimon, J. W., Durham, D. G. and Rees, A. H. Synthesis of some 2-phenylpyrrole derivatives. *J. Chem. Soc. Perkin Trans. 1* 12, 1588-1594, 1978.
- Hansch, C. Quantitative approaches to pharmacological structure-activity relationships. In *Structure-Activity Relationships Vol. I*, ed. by G. Peters and C. J. Cavallito, pp. 75-165, Pergamon Press, Oxford, 1973.
- Knoefel, P. K. and Huang, K. C. Biochemorphology of renal tubular transport: hippuric acid and related substances. *J. Pharmacol. Exp. Ther.* 126, 296-303, 1959.
- Quick, A. J. The relationship between chemical structure and physiological response. II. The conjugation of hydroxy- and methoxy-benzoic acids. *J. Biol. Chem.* 97, 403-419, 1932.

- Russel, F G M , Wouterse, A C and van Ginneken, C A M Renal clearance of substituted hippurates in the dog I Benzoylglycine (hippurate) and methyl-substituted benzoylglycines J Pharmacol Exp Ther submitted, 1988a
- Russel, F G M , Wouterse, A C and van Ginneken, C A M Renal clearance of substituted hippurates in the dog II 4-Aminobenzoylglycine and hydroxy-substituted benzoylglycines J Pharmacol Exp Ther submitted , 1988b
- Selheim, E and Sheline, R R Metabolism of alkene benzene derivatives in the rat I p-Methoxyallylbenzene (estragole) and p-methoxypropenylbenzene (anethole) Xenobiotica 3, 493-510, 1973

PART IV

ISOLATED MEMBRANE VESICLES

Everything should be made as
simple as possible but not simpler

Albert Einstein

Na^+ AND H^+ GRADIENT-DEPENDENT TRANSPORT OF p-AMINOHIPPURATE IN MEMBRANE VESICLES FROM DOG KIDNEY CORTEX¹

Frans G.M. Russel, Peter E.M. van der Linden, Wim G. Vermeulen, Marc Heijn, Carel H. van Os[‡], and Cees A.M. van Ginneken

Abstract - The transport of p-aminohippurate (PAH) was studied in basolateral (BLMV) and brush border membrane vesicles (BBMV) isolated from dog kidney cortex. Imposition of an inwardly directed 100 mM Na^+ gradient stimulated the uptake of 50 μM [^3H]PAH into BLMV, whereas a pH gradient ($\text{pH}_{\text{out}} = 6.0$, $\text{pH}_{\text{in}} = 7.4$) only slightly enhanced uptake. The Na^+ gradient-dependent uptake of PAH was electroneutral, saturable and sensitive to inhibition by probenecid and several anionic drugs, with (apparent) $K_m = 0.79 \pm 0.16$ mM, $V_{\text{max}} = 0.80 \pm 0.05$ nmol/mg protein, 15 sec and K_i for probenecid = 0.08 ± 0.01 mM. Simultaneous imposition of the pH gradient (outward OH^- gradient) and inward Na^+ gradient stimulated PAH uptake significantly over that with a Na^+ gradient alone. These results are consistent with a Na^+ gradient-stimulated PAH/ OH^- exchange mechanism in the basolateral membrane. In BBMV, PAH uptake could be stimulated by an outwardly directed OH^- gradient as well as an inward Na^+ gradient. Both gradients could drive PAH transport via a mediated probenecid-sensitive pathway. Na^+ gradient-stimulated uptake was electrogenic with a (apparent) $K_m = 4.93 \pm 0.57$ mM, $V_{\text{max}} = 6.71 \pm 0.36$ nmol/mg protein, 15 sec and $K_i, \text{prob} = 0.13 \pm 0.01$ mM. The kinetic parameters for PAH/ OH^- exchange were virtually the same, (apparent) $K_m =$

¹Biochem. Pharmacol., submitted. Partly published as an abstract in: Br. J. Pharmacol. 89, 513P (1986)

[‡]Department of Physiology, University of Nijmegen

5.72 ± 0.49 mM, $V_{\max} = 7.87 \pm 0.33$ nmol/mg protein, 15 sec and $K_{i,\text{prob}} = 0.16 \pm 0.02$ mM. When both the Na^+ and pH (outward OH^-) gradient were simultaneously imposed an almost twofold stimulation in uptake was observed over that with either a Na^+ or pH gradient alone. These results suggested that both gradients stimulate PAH transport in BBMV via the same pathway. However, inhibition experiments with various organic anions showed that the specificities of Na^+ and pH gradient-stimulated PAH uptake do not entirely overlap. Thus, our results are in favor of a simple transport mechanism in BBMV, but it cannot be excluded that two separate pathways are involved.

9.1 INTRODUCTION

Most of our present knowledge about the renal handling of organic anionic drugs comes from studies with p-aminohippurate (PAH). In the mammalian kidney transport of PAH and other organic anions is confined to the proximal tubule. PAH is actively secreted by the tubular cells into the urine against its electrochemical gradient. The active step in the transepithelial transport appears to be the uptake across the basolateral membrane into the cells, since PAH is accumulated to much higher concentrations in the cells than in the extracellular fluid. The high intracellular concentration is probably the main driving force for the mediated movement across the brush border membrane into the lumen [1,2].

In the past ten years the use of isolated membrane vesicles has contributed to a better understanding of the role that each plasma membrane plays in the transcellular transport of PAH. However, despite numerous vesicle studies there is no general agreement on the mechanisms and the driving forces that govern PAH transport across the basolateral and brush border membrane.

Several investigators have demonstrated mediated transport of PAH into basolateral membrane vesicles (BLMV) from rat [3-6], rabbit [6-8] and dog [9], which was stimulated by a Na^+ gradient and sensitive to probenecid inhibition. However, only Sheikh and Møller [7] were able to achieve uptake values above equilibrium, using BLMV from rabbit kidney.

On the other hand Tse et al. [10] observed just a minor stimulating effect of Na^+ in rabbit BLMV, while Mg^{2+} and other divalent cations significantly enhanced probenecid-sensitive PAH transport. Berner and Kinne [3] suggested a nonspecific effect of Na^+ by creating an inside positive diffusion potential which stimulated PAH anion uptake, while others observed only a small [4] or no effect [5,7] of the membrane potential on Na^+ -dependent PAH uptake. Taken these results together most studies point to a direct coupling of Na^+ with PAH uptake, but they also suggest that a Na^+ gradient alone may not be the only driving force for the intracellular accumulation of PAH. Kasher et al. [5] found that Na^+ -dependent uptake in rat BLMV could be altered to uphill transport in the presence of an opposing gradient of unlabeled PAH, and they proposed a Na^+ gradient-stimulated anion exchange mechanism. During the preparation of this manuscript a study of Eveloff [11] was published, in which it was shown that in rabbit BLMV an outward OH^- gradient could also provide for concentrative uptake in combination with an inward Na^+ gradient.

With regard to PAH transport across the luminal membrane it has been questioned for some time whether the downhill movement from cell to lumen occurs by unmediated or by mediated diffusion. The first evidence for mediated transport in membrane vesicles was demonstrated by Kinsella et al. [9], using brush border membrane vesicles (BBMV) from dog kidney. In presence of a Na^+ gradient they found saturable and probenecid-sensitive PAH uptake. Na^+ -stimulated transport was also described in BBMV from rabbit [8,12] and rat [4]. Others were unable to observe a stimulation with Na^+ [3,6,13] and it was shown that uptake is stimulated by an inside-positive diffusion potential induced by the Na^+ gradient, rather than by a direct interaction of Na^+ with a PAH transporter [4,12]. Recently, uphill PAH uptake into BBMV from dog [13-15] and rat [16] was demonstrated in presence of an inwardly directed H^+ gradient. Kahn et al. [13,16] showed that stimulation by a pH gradient resulted from carrier-mediated PAH/ OH^- exchange. This anion exchanger also accepts urate, and it can drive uphill transport of PAH and urate by opposing gradients of OH^- , Cl^- and HCO_3^- .

The purpose of the present study was to provide additional information on the effects of a Na^+ or H^+ gradient on PAH transport in isolated mem-

brane vesicles The characteristics and specificity of PAH uptake in BLMV and BBMV from dog kidney cortex were studied

9.2 MATERIALS AND METHODS

Isolation of Membrane Vesicles

Brush border (BBMV) and basolateral membrane vesicles (BLMV) were isolated from the same cortical tissue preparation according to procedures described by Sheikh et al [17] and Windus et al [18] with some modifications Kidneys from Beagle dogs that became available from other, mainly surgical, experiments were used as starting material Immediately after excision, the kidneys were perfused with ice-cold saline to remove residual blood All subsequent steps of the procedure were carried out at 4°C After the kidneys were decapsulated, slices of approximately 5-7 mm thick cortex were cut off, weighed, minced and suspended at 10% w/v in 100 mM mannitol, 5 mM 4-(2-hydroxyethyl)-1-piperazine ethane sulfonic acid (HEPES) buffered to pH 7.4 with Tris and 0.2 mM phenylmethylsulfonylfluoride The mixture was homogenized with a loose-fitting dounce apparatus (30 strokes) and, subsequently, with a Polytron homogenizer on setting 7 for three 30 sec pulses The cortex homogenate was centrifuged at 2,500g for 15 min in a Heraeus Minifuge GL and the supernatant was treated with 10 mM CaCl_2 during 20 min After a second centrifugation step of 2,500g for 15 min the resulting supernatant contained the crude BBMV fraction and the pelleted material contained BLMV and membranes from other cell organelles The crude BBMV fraction was spun at 24,000g for 20 min in an IEC B-60 ultracentrifuge (A-169 rotor) The supernatant was discarded and the upper fluffy layer of the pellet was resuspended in 100 mM mannitol and 5 mM HEPES-Tris pH 7.4, homogenized with a tight-fitting dounce apparatus (30 strokes), and treated again with 10 mM CaCl_2 for 20 min The pellet obtained after centrifugation at 2,500g for 15 min was discarded and the purified BBMV were collected at 30,000g for 20 min The BBMV pellet was washed with the appropriate uptake buffer, generally consisting of 100 mM KCl, 100 mM mannitol and 5 mM HEPES-Tris pH 7.4, to which 0.5 mM ethyleneglycol-bis-(β -aminoethyl ether)N,N'-tetraacetic acid (EGTA) was

added, centrifuged at 30,000g for 20 min and finally resuspended in uptake buffer through a 23-gauge needle to obtain a final protein concentration of 8-12 mg/ml.

The pellet obtained after the first CaCl_2 -precipitation step, containing the BLMV fraction, was resuspended in 250 mM sucrose and 5 mM HEPES-Tris pH 7.4, homogenized using a tight fitting dounce (30 strokes) and spun at 24,000g for 20 min. The fluffy upper layer of the pellet was gently resuspended in the sucrose buffer to a volume of approximately 2 ml/g of initial cortex, homogenized with a tight fitting dounce (30 strokes) and brought to a concentration of 8% v/v Percoll. BLMV were separated from other cellular membranes on the self-orienting Percoll density gradient by centrifugation at 50,000g for 30 min in an SB-283 rotor. A density gradient ranging from 1.020 to 1.050 g/ml as measured by a Bausch and Lomb refractometer was obtained and the purified BLMV were recovered from the second opaque band from the top of the gradient corresponding to a density of approximately 1.034 g/ml. The BLMV suspension was diluted in a ratio of 1 to 4 ml with the appropriate uptake buffer (generally 100 mM KCl, 100 mM mannitol and 5 mM HEPES-Tris pH 7.4) and the Percoll was removed by centrifugation at 96,000g for 30 min. The fluffy layer on top of the glassy Percoll pellet was resuspended in uptake buffer by passing it through a 23-gauge needle. The BLMV were resuspended at a protein concentration of 8-12 mg/ml in uptake buffer.

The purity of the membrane preparations was assessed by assaying the specific activity of the following marker enzymes according to previously published procedures: alkaline phosphatase [19] and maltase [20] for brush border membranes, $(\text{Na}^+ - \text{K}^+) - \text{ATPase}$ [19] for basolateral membranes, succinate dehydrogenase [21] for mitochondria, acid phosphatase [22] for lysosomes and NADPH-dependent cytochrome-c reductase [23] for smooth endoplasmic reticulum. $(\text{Na}^+ - \text{K}^+) - \text{ATPase}$ was determined after detergent treatment with 0.4 mg/ml deoxycholate, followed by freezing-thawing, to disrupt membrane vesicles [18]. Protein was assayed with a commercial coomassie blue kit (BioRad, München, FRG), with bovine plasma globulin as the standard. Compared to the initial homogenate, BLMV were enriched for maltase and alkaline phosphatase 12- to 14-fold, while the enrichment factors for the other marker enzymes were all <0.9. The results of the enzymatic analysis of BLMV showed a 8- to 10-fold enrich-

ment in $(\text{Na}^+ - \text{K}^+)$ -ATPase, 0.8-fold in maltase, 2.5-fold in alkaline phosphatase, 1.2-fold in acid phosphatase and <0.8 -fold in succinate dehydrogenase and NADPH-cytochrome-c reductase.

The membranes were rapidly frozen in liquid nitrogen and stored at -80°C in small aliquots until use. In preliminary experiments, we found no difference in transport of glucose and PAH between frozen and freshly prepared membrane vesicles.

Transport Studies

The uptake of D- $[\text{}^3\text{H}]$ glucose, $[\text{}^3\text{H}]$ glycine and $[\text{}^3\text{H}]$ PAH in BBMV and BLMV was measured at 37°C by a rapid filtration technique [24]. Measurement of solute uptake in membrane vesicles was initiated by the addition of 40 μl of solution to 10 μl of membrane suspension such that the initial content of the extravesicular medium was 100 mM NaCl, 20 mM KCl, 100 mM mannitol, 5 mM HEPES-Tris, pH 7.4 or 5 mM 2-(N-morpholino)-ethanesulfonic acid (MES)-Tris pH 6.0; or 100 mM KCl, 100 mM mannitol, 5 mM HEPES-Tris pH 7.4 or 5mM MES-Tris pH 6.0, and radiolabeled solute. The experimental conditions and the exact composition of the transport buffers are given in the legends. The initial solute concentrations were: glucose 25 μM , glycine 50 μM and PAH 50 μM or 100 μM except in concentration-dependence studies. The uptake of solute was terminated at appropriate time intervals by diluting the incubation mixture with 3 ml ice-cold stop buffer that had the same composition as the incubation medium but without the solute. This sample was immediately filtered under vacuum through a prewetted 0.45 μm cellulose nitrate filter (Schleicher and Schüll, Dassel, FRG) and washed twice with 3 ml of ice-cold stop buffer. The radioactivity remaining on the filters was counted using standard liquid scintillation techniques after dissolution in 10 ml Aqualuma plus (Lumac, Schaesberg, The Netherlands). Corrections were made for the radioactivity bound to the filters in the absence of vesicles.

To ascertain whether PAH uptake by the vesicles represented transport across the membrane into the vesicles rather than binding to the membrane surface, PAH uptake at equilibrium was measured by increasing the extravesicular osmolarity with sucrose. Uptake of PAH was found to decrease linearly with the reciprocal medium osmolarity, and binding was estimated by extrapolating the uptake to infinite osmolarity, which corre-

sponded to approximately 1-3% for BBMV and 10-20% for BLMV of the uptake under standard conditions (\pm 345 mOsm).

Data Analysis and Presentation

Absolute uptake of solute is expressed as picomoles or nanomoles per milligram of protein. All experiments were performed on at least three different membrane preparations. Data are expressed as means \pm SE. The kinetic constants of PAH uptake in BBMV and BLMV were determined from the initial linear uptake values (15 sec) at various substrate concentrations. Total PAH uptake could be described as uptake via a Michaelis-Menten process in parallel with passive diffusion. The carrier-mediated or specific component of uptake was defined as the difference between uptake in the absence and presence of 5 mM probenecid. Inhibition curves of probenecid were analyzed assuming competitive inhibition to a one binding site model. Curve fitting was done by least-squares nonlinear regression analysis using the computer program NONLIN [25]. Student's t-test was used to determine statistical significance. The figures presented in this study were drawn with the DISSPLA computer package [26].

Chemicals

D-[1- 3 H]glucose (15 Ci/mmol) was obtained from New England Nuclear (Dreieich, FRG) and [2- 3 H]glycine (10 Ci/mmol) and p-amino[3 H]hippuric acid (254 mCi/mmol) were from Amersham (Buckinghamshire, UK). Percoll was purchased from Pharmacia Fine Chemicals (Uppsala, Sweden), iodopyracet from Dagra NV (Diemen, The Netherlands) and amiloride was a gift from Merck Sharp & Dohme (Haarlem, The Netherlands). All other chemicals were purchased from either Sigma (St. Louis, MO, USA) or Merck (Darmstadt, FRG) and were of the highest grade available.

9.3 RESULTS

Functionality of the Membrane Vesicles

The isolated membrane vesicles were functionally evaluated by measuring the Na⁺ gradient-dependent glucose and glycine uptake. Fig. 9.1 shows

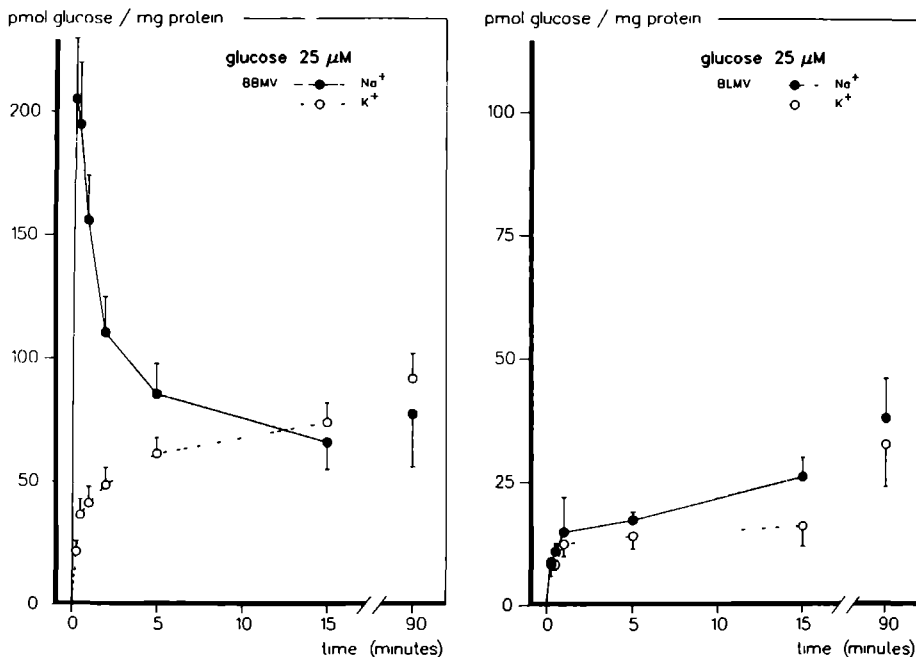


Fig. 9.1 Uptake of 25 μM glucose into BBMV (left panel) and BLMV (right panel) in the presence or absence of a Na^+ gradient. The vesicles were suspended in 100 mM KCl, 100 mM mannitol, 5 mM HEPES-Tris pH 7.4. The initial content of the extravesicular medium was 100 mM mannitol, 5 mM HEPES-Tris pH 7.4 and either 100 mM KCl or 100 mM NaCl and 20 mM KCl. Values are expressed as means \pm SE of four experiments.

the time course of 25 μM glucose uptake into BBMV and BLMV in the presence or absence of an inwardly directed Na^+ gradient. In the presence of a Na^+ gradient an overshoot above the equilibrium value (90 min) of the uptake of glucose into BBMV was observed, while the replacement of NaCl by KCl resulted in the complete disappearance of the overshoot. Uptake at 15 sec in presence of a Na^+ gradient was 9.3-fold enhanced over that observed without Na^+ (205 ± 19 vs. 22 ± 3 pmol/mg protein; $p < 0.001$). BLMV showed no concentrative glucose uptake in presence of a Na^+ gradient and the initial rate of uptake was not different from uptake in a Na^+ -free medium (8.9 ± 0.6 vs. 8.3 ± 2.1 pmol/mg protein, 15 sec; $p > 0.5$). Therefore, contamination of the BLMV preparation by BBMV must be functionally negligible.

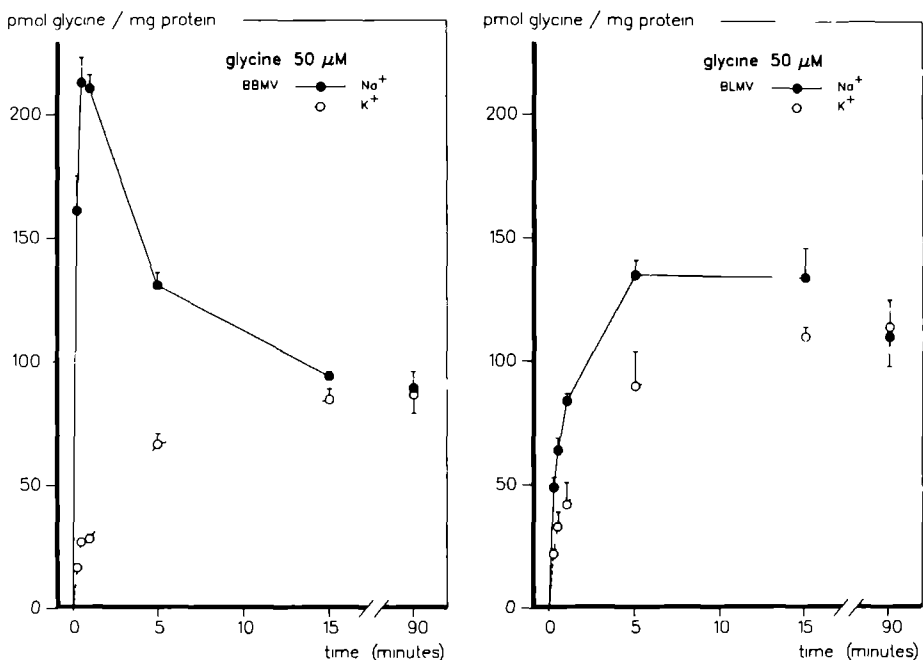


Fig. 9.2 Uptake of 50 μM glycine into BBMVs (left panel) and BLMVs (right panel) in the presence or absence of a Na^+ gradient. The experimental conditions were the same as in Fig. 9.1. Values are expressed as means \pm SE of three experiments.

The functional integrity of the vesicles was further evaluated through the Na^+ gradient-dependent transport of glycine. Fig. 9.2 depicts the uptake of 50 μM glycine into BBMVs and BLMVs as function of time in presence or absence of an inwardly directed Na^+ gradient. The imposition of a Na^+ gradient resulted in a substantial transient accumulation of glycine in BBMVs and to a lesser extent in BLMVs. The initial uptake of glycine measured at 15 sec, as compared with the values measured under Na^+ -free conditions, was 9.8-fold stimulated in BBMVs (161 ± 14 vs. 16.5 ± 1.4 pmol/mg protein; $p < 0.001$) and 2.3-fold in BLMVs (49 ± 4 vs. 21 ± 3 pmol/mg protein; $p < 0.005$). These findings are in good accordance with previously reported observations for glycine transport in dog kidney membrane vesicles [24]. Together with the glucose uptake data these results indicated the transport capability of our membrane vesicles.

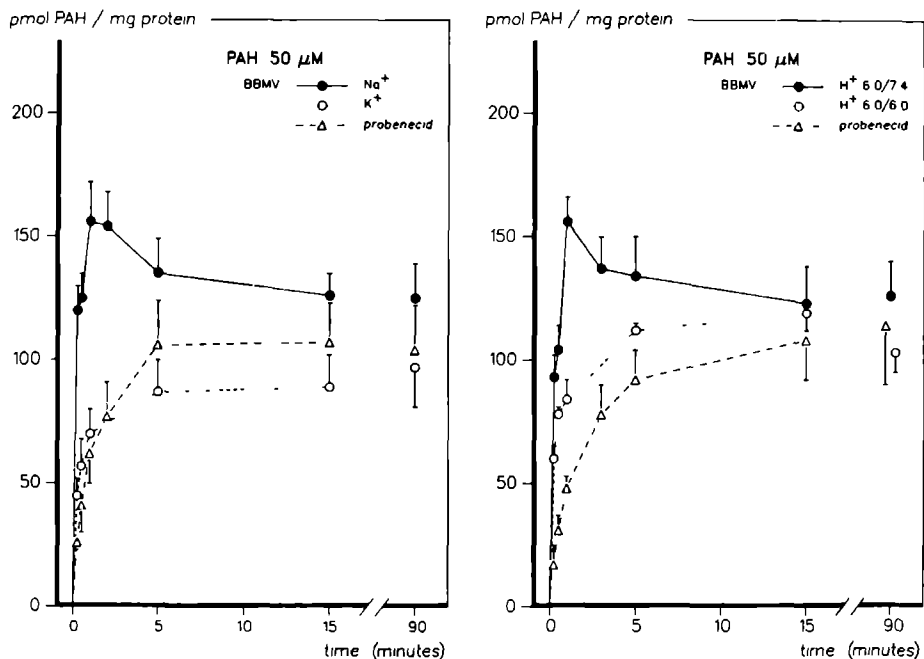


Fig. 9.3 Effect of a Na⁺ gradient (left panel) or a H⁺ gradient (right panel) on the uptake of 50 μ M PAH into BBMVs. Left panel: vesicles were suspended in 100 mM KCl, 100 mM mannitol, 5 mM HEPES-Tris pH 7.4. The initial content of the extravesicular medium was 100 mM mannitol, 5 mM HEPES-Tris pH 7.4 and either 100 mM KCl or 100 mM NaCl and 20 mM KCl with or without 5 mM probenecid. Values are expressed as means \pm SE of five experiments. Right panel: vesicles were suspended in 100 mM KCl, 100 mM mannitol and either 5 mM HEPES-Tris pH 7.4 or 5 mM MES-Tris pH 6.0. The initial content of the extravesicular medium was 100 mM KCl, 100 mM mannitol, 5 mM MES-Tris pH 6.0. Uptake in presence of a H⁺ gradient (H⁺ 6.0/7.4) was measured with or without 5 mM probenecid. Values are expressed as means \pm SE of four experiments.

Na⁺ and H⁺ Gradient-Dependent PAH Uptake

The effect of imposed Na⁺ or H⁺ gradients on the uptake of 50 μ M PAH into BBMVs is illustrated in Fig. 9.3. In the right panel it is shown that when the extravesicular medium was at pH 6.0 and the intravesicular medium at pH 7.4 (6.0/7.4) the uptake of PAH was stimulated and a small transient accumulation over the equilibrium value was observed at 1 min.

The uptake at 6.0/6.0 was slightly faster than at 7.4/7.4 (left panel, open circles), however, uptake rates were clearly decreased compared to the pH gradient situation. To distinguish mediated transport from non-specific uptake by simple diffusion, H^+ -dependent uptake was measured in presence of 5 mM probenecid. This resulted in a marked reduction of the uptake rate, the initial (15 sec) uptake of PAH was inhibited 82% by probenecid (97 ± 7 vs. 17 ± 4 pmol/mg protein; $p < 0.001$). Our results are consistent with previous investigations demonstrating that PAH uptake in BBMV is driven by an outwardly directed OH^- gradient via an anion-exchange transport mechanism [13,14].

However, in contrast with these studies we also observed a stimulation of PAH uptake into BBMV by an inwardly directed Na^+ gradient as is shown in the left panel of Fig. 9.3. Imposition of a Na^+ gradient enhanced PAH uptake above that measured under KCl-equilibrated conditions. Similar to H^+ -stimulated transport, maximum uptake was observed at 1 min slightly exceeding the equilibrium value. Probenecid also clearly interfered with Na^+ -stimulated transport. The PAH uptake measured at 15 sec was inhibited from 103 ± 7 to 26 ± 3 pmol/mg protein (76%, $p < 0.001$).

It has been supposed that Na^+ -stimulated PAH uptake into BBMV is mediated by a non-specific effect on the membrane potential, rather than by transport via a Na^+ -PAH cotransport system [13]. To investigate this, the effect of valinomycin on PAH uptake in presence of a Na^+ gradient was measured (Table 9.1). Due to the outwardly directed K^+ gradient valinomycin renders the intravesicular space more electronegative [27]. This resulted in a significant reduction of PAH uptake into BBMV at 15 sec, confirming that at least an important part of Na^+ -stimulated uptake into BBMV is mediated by an inside-positive membrane potential.

Fig. 9.4 shows the effect of a Na^+ or H^+ gradient on the uptake of 50 μM PAH into BLMV. Uptake conditions were the same as described in Fig. 9.3. An inwardly directed H^+ gradient (6.0/7.4) slightly enhanced PAH uptake over that when the extra- and intravesicular pH were equal at 6.0 (Fig. 9.4, right panel) or at 7.4 (left panel, open circles), and no concentrative uptake was observed. Only a small inhibition was observed in presence of probenecid (27 ± 5 vs. 18 ± 3 pmol/mg protein, 15 sec; $p > 0.10$), indicating that uptake occurred predominantly by simple diffusion.

Table 9.1 Effect of membrane potential on Na^+ gradient-stimulated PAH uptake into BLMV and BBMV.

		PAH uptake (pmol/mg protein)	
	valinomycin	15 sec	90 min
BLMV	-	49 ± 4	71 ± 5
	+	41 ± 2	68 ± 6
BBMV	-	94 ± 5	117 ± 10
	+	$70 \pm 7^*$	110 ± 12

Uptake of 50 μM PAH was measured. The vesicles were suspended in 100 mM KCl, 100 mM mannitol, 5 mM HEPES-Tris pH 7.4. Valinomycin (10 $\mu\text{g}/\text{mg}$ protein) was added in ethanol (2 $\mu\text{g}/\mu\text{l}$). An equal concentration of ethanol (1 %) was added in the controls. The initial content of the extravesicular medium was 100 mM NaCl, 20 mM KCl, 100 mM mannitol, 5 mM HEPES-Tris pH 7.4. Values are expressed as means \pm SE of three experiments. * $p < 0.05$ vs. control.

In the left panel of Fig. 9.4 it is illustrated that the imposition of a Na^+ gradient resulted in a clear stimulation of PAH uptake into BLMV above that measured when no Na^+ was present. A small transient accumulation over the equilibrium value was observed after 15 min. Probenecid effectively inhibited the Na^+ gradient-stimulated uptake from 48 ± 4 to 20 ± 3 pmol/mg protein, 15 sec (58%, $p < 0.005$). Valinomycin did not affect PAH uptake in the presence or absence of a Na^+ gradient (Table 9.1), suggesting that Na^+ -dependent PAH uptake into BLMV is electroneutral and not influenced by the membrane potential.

Kinetics of PAH Uptake and Probenecid Inhibition

The concept of carrier-mediated PAH transport was further supported by the saturability of Na^+ - or H^+ -dependent uptake into BBMV (Fig. 9.5, left panel) and Na^+ -dependent transport into BLMV (Fig. 9.5, right panel) in the presence of increasing PAH concentrations. In both prepara-

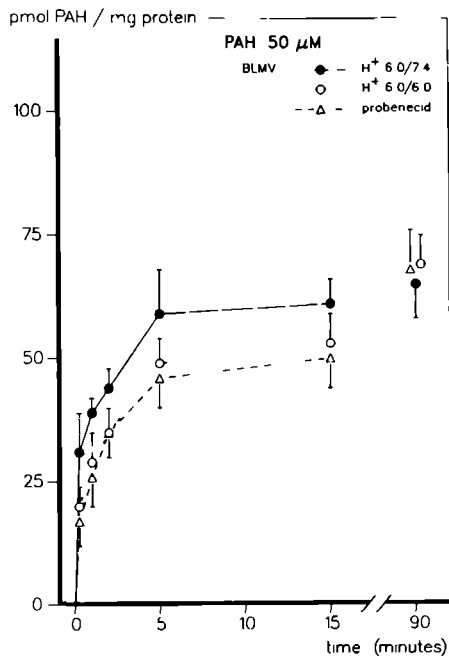
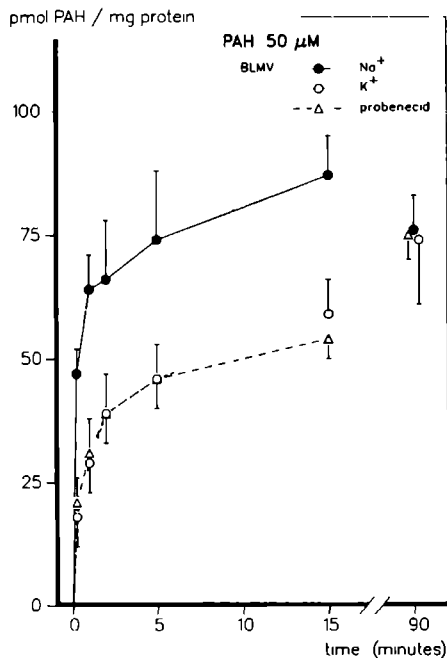


Fig. 9.4 Effect of a Na^+ gradient (left panel) or a H^+ gradient (right panel) on the uptake of $50 \mu\text{M}$ PAH into BLMV. The experimental conditions were the same as in Fig. 9.3. Values are expressed as means \pm SE of four experiments.

tions concentration-dependent uptake could be described by a combination of carrier-mediated uptake following Michaelis-Menten kinetics and nonsaturable simple diffusion. The contribution of the non-specific component to total uptake was estimated from the amount of PAH uptake that could not be inhibited with 5 mM probenecid. The slopes of these linear curves were ($\text{nmol/mg protein, 15 sec per mM}$) 0.811 ± 0.010 for BBMV (Na^+), 0.608 ± 0.007 for BBMV (H^+) and 0.595 ± 0.009 for BLMV (Na^+). The kinetic parameters characterizing the carrier-mediated, probenecid sensitive part of uptake (K_m and V_{max}) were derived from computer-based fit of the individual data and are given in Table 9.2.

The inhibitory effect of increasing probenecid concentrations on carrier-mediated PAH uptake into BLMV and BBMV is shown in Fig. 9.6. The inhibitory constants for probenecid (K_i) were calculated by curve fitting

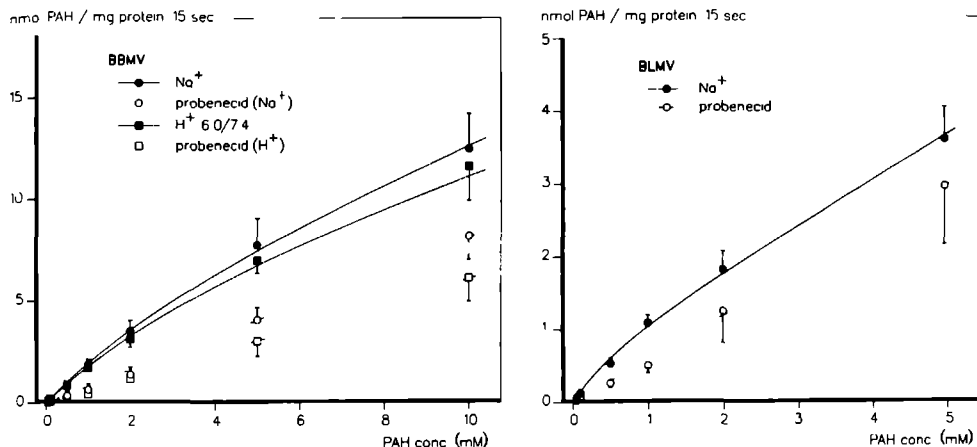


Fig. 9.5 Kinetics of Na⁺ or H⁺ gradient-dependent PAH uptake into BBMV (left panel) and Na⁺ gradient-dependent uptake into BLMV (right panel). The vesicles were suspended in 100 mM KCl, 100 mM mannitol, 5 mM HEPES-Tris pH 7.4. The initial content of the extravesicular medium was either 100 mM NaCl, 20 mM KCl, 100 mM mannitol, 5 mM HEPES-Tris pH 7.4 or 100 mM KCl, 100 mM mannitol, 5 mM MES-Tris pH 6.0, in both cases with or without 5 mM probenecid. Uptake was measured at 15 sec in presence of increasing concentrations of PAH (0.05 - 10 mM). Values are expressed as means \pm SE of three to five experiments.

Table 9.2 Kinetic parameters for Na⁺ gradient-dependent PAH uptake into BLMV and Na⁺ or H⁺ gradient-dependent uptake into BBMV and the interaction with probenecid (prob).

	K_m (mM)	V_{max} (nmol/mg protein, 15 sec)	$K_{i,prob}$ (mM)
BLMV (Na ⁺)	0.79 ± 0.16	0.80 ± 0.05	0.08 ± 0.01
BBMV (Na ⁺)	4.93 ± 0.57	6.71 ± 0.36	0.13 ± 0.01
BBMV (H ⁺)	5.72 ± 0.49	7.87 ± 0.33	0.16 ± 0.02

The experimental conditions were the same as those given in the legends to Figs. 9.5 and 9.6. The results are means \pm SE of three experiments.

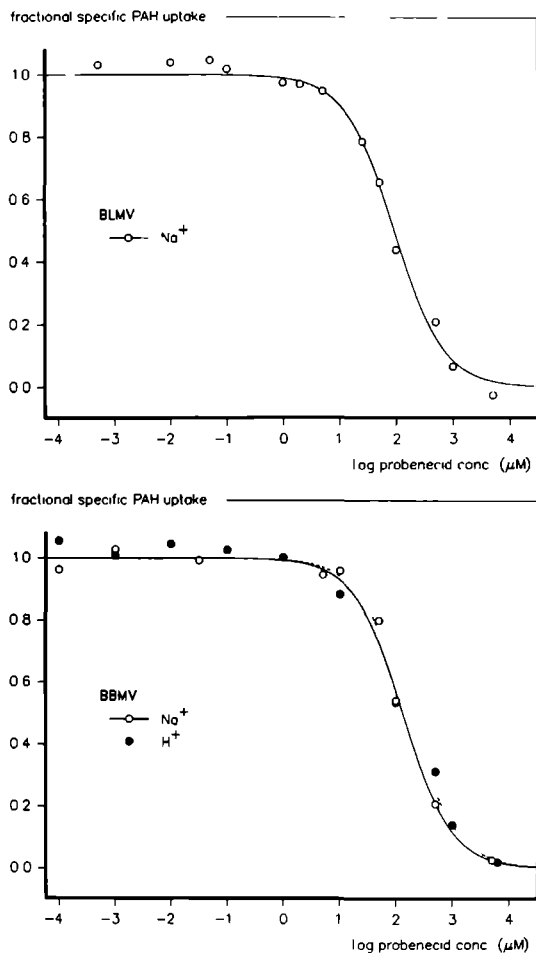


Fig. 9.6 Inhibition of specific Na^+ gradient-dependent PAH uptake into BLMV (upper panel) and Na^+ or H^+ gradient-dependent uptake into BBMV (lower panel) by probenecid. The vesicles were suspended in 100 mM KCl, 100 mM mannitol, 5 mM HEPES-Tris pH 7.4. The initial content of the extravesicular medium was 100 μM PAH and either 100 mM NaCl, 20 mM KCl, 100 mM mannitol, 5 mM HEPES-Tris pH 7.4 or 100 mM KCl, 100 mM mannitol, 5 mM MES-Tris pH 6.0, with varying probenecid concentrations (0.1 nM - 5 mM). Uptake was measured at 15 sec and values are expressed as means of three experiments. SE were less than 10 % for all values.

of individual data according to a one binding site model. Results are listed in Table 9.2. The results show that PAH transport in BBMV has a lower affinity, but a higher capacity than transport into BLMV. The kinetic parameters and probenecid inhibition constants for Na^+ - and H^+ -dependent transport are not significantly different from each other ($p > 0.1$), suggesting that both gradients stimulate PAH uptake via the same transport system.

Effect of Various Organic Anions on PAH Uptake

The substrate specificity of PAH transport into BLMV and BBMV was tested by cisinhibition experiments with various organic anions (Table 9.3). Each organic anion (2.5 or 5 mM) was added to the external medium and its effect on the 15 sec uptake of 100 μM PAH in the presence of an inward Na^+ (BLMV, BBMV) or H^+ gradient (BBMV) was measured. The strongest inhibition in both preparations was found with probenecid.

Because PAH is a glycine conjugate the interaction with glycine was studied. Glycine had no effect on PAH uptake, and conversely we found no effect of concentrations up to 5 mM PAH on Na^+ -dependent uptake of 50 μM glycine (data not shown), indicating that neither in BLMV nor in BBMV PAH and glycine share the same transport system.

In BLMV iodopyracet and salicylate were good inhibitors, while urate only slightly affected PAH uptake. In BBMV some remarkable differences between the inhibitory effect on Na^+ - and H^+ -stimulated PAH uptake were observed. Phenolsulfonphthalein, iodopyracet and urate had no effect and 1-naphthyl-glucuronide had only a small effect on Na^+ -stimulated uptake, whereas they clearly inhibited H^+ -stimulated uptake. The effect of the other anions was virtually the same for both gradients with the exception of hydrochlorothiazide, which inhibited Na^+ -stimulated uptake but did not interfere with uptake in presence of a H^+ gradient. Although the difference in pH may play a role by altering the degree of ionization of phenol-sulfonphthalein ($\text{pK}_a = 7.9$), urate ($\text{pK}_a = 5.8$) and hydrochlorothiazide ($\text{pK}_a = 7.9$), this will hardly be of any influence on the differences in inhibitory effect observed for iodopyracet ($\text{pK}_a = 2.9$) and 1-naphthyl-glucuronide ($\text{pK}_a < 3$). Therefore, these results suggest that the pathways of sodium and H^+ gradient-stimulated PAH uptake into BBMV do not entirely overlap.

Table 9.3 Effect of various organic anions on PAH uptake into BLMV and BBMV.

organic anion	mM	% PAH uptake		
		BLMV (Na ⁺)	BBMV (Na ⁺)	BBMV (H ⁺)
Probenecid	5.0	43 ± 3	29 ± 2	26 ± 9
Glycine	5.0	93 ± 5	101 ± 6	102 ± 7
Hippurate	5.0	69 ± 7	69 ± 9	77 ± 9
Phenolsulfonphthalein	5.0	64 ± 12	99 ± 9	44 ± 11
Iodopyracet	5.0	58 ± 9	92 ± 9	32 ± 8
Salicylate	5.0	54 ± 9	62 ± 3	54 ± 8
Acetylsalicylate	5.0	76 ± 11	78 ± 6	88 ± 12
Urate	2.5	87 ± 9	95 ± 6	70 ± 9
Hydrochlorothiazide	2.5	64 ± 12	69 ± 9	91 ± 13
1-Naphthyl-glucuronide	5.0	65 ± 12	81 ± 6	57 ± 12

The 15 sec uptake of 100 μ M PAH was measured. The experimental conditions were similar to those given in the legend of Fig. 9.5, except for the presence of 2.5 or 5.0 mM organic anion. Results are expressed relative to the respective control uptakes as means \pm SE of three experiments. Control uptakes, measured in presence of 5 mM gluconate, were (pmol/mg protein, 15 sec) 111 ± 4 for BLMV (Na⁺), 224 ± 10 for BBMV (Na⁺) and 210 ± 18 for BBMV (H⁺).

Effect of pH on Na⁺-Dependent PAH Uptake

The effect of a H⁺ gradient ($\text{pH}_{\text{out}} = 6.0$, $\text{pH}_{\text{in}} = 7.4$) on Na⁺-dependent PAH uptake is shown in Table 9.4. When a pH gradient was present alone uptake into BLMV was lower compared to Na⁺ gradient-stimulated uptake, as was also noted in Fig. 9.4. Under pH gradient conditions Na⁺-dependent PAH uptake into BLMV was significantly accelerated compared to the control where extra- and intravesicular were equal at pH 7.4. Valinomycin did not affect pH-stimulated Na⁺-dependent uptake (data not shown). These results are similar to those observed by Eveloff [11] in the rabbit, who showed that PAH transport into BLMV occurs by a Na⁺ gradient-stimulated OH⁻-exchange mechanism.

Table 9.4 Effect of a H^+ gradient on the time course of Na^+ gradient-dependent PAH uptake into BLMV and BBMV.

gradient	PAH uptake ^a (pmol/mg protein)		
	15 sec	1 min	90 min
BLMV			
Na^+ (control) ^b	45 ± 2	66 ± 7	76 ± 4
H^+ ^c	29 ± 3 [*]	44 ± 2 [*]	65 ± 4
Na^+ + H^+ ^d	68 ± 5 [*]	97 ± 6 [*]	82 ± 5
BBMV			
Na^+ (control) ^b	107 ± 5	156 ± 12	125 ± 8
H^+ ^c	93 ± 10	156 ± 7	126 ± 14
Na^+ ^b + amiloride (5 mM)	109 ± 6	149 ± 5	159 ± 14
Na^+ + H^+ ^d	192 ± 6 ^{**}	218 ± 9 ^{**}	139 ± 9

^aUptake of 50 μ M PAH was measured. The vesicles were suspended in 100 mM KCL, 100 mM mannitol, 5 mM HEPES-Tris pH 7.4. Values are expressed as means ± SE of three experiments.

The initial content of the extravesicular medium was:

^b100 mM NaCl, 20 mM KCl, 100 mM mannitol, 5mM HEPES-Tris pH 7.4,

^c100 mM KCl, 100 mM mannitol, 5 mM MES-Tris pH 6.0,

^d100 mM NaCl, 20 mM KCl, 100 mM mannitol, 5 mM MES-Tris pH 6.0.

^{*} $p < 0.05$ and ^{**} $p < 0.01$ vs. respective controls.

Because BBMV are known to contain an active Na^+-H^+ exchange system [28], Na^+ -dependent uptake into BBMV was further evaluated by determining whether an inward directed Na^+ gradient indirectly stimulated PAH transport by generating an outward OH^- -gradient. Uptake in presence of the Na^+-H^+ exchange inhibitor amiloride (5 mM) was not different from the control (Table 9.4), indicating that Na^+-H^+ exchange does not play a role in Na^+ -dependent PAH uptake. Simultaneous imposition of a H^+ and Na^+ gradient resulted in an almost 2-fold enhancement of the initial uptake rate compared to values measured when either a Na^+ or H^+ gradient was

present alone. In presence of valinomycin the 15 sec uptake was significantly decreased to 142 ± 11 pmol/mg protein ($p < 0.05$). Although this value was still higher than the control uptake the difference failed to reach the 5% level of significance. The results suggest that the PAH- OH^- anion-exchanger is stimulated by an inside-positive Na^+ potential. However, an alternative explanation would be that Na^+ -dependent uptake and OH^- -exchange represent two distinct transport pathways.

9.4 DISCUSSION

Basolateral Membrane

Our findings demonstrate that PAH uptake into BLMV is mediated, functionally coupled to a Na^+ gradient across the membrane and insensitive to the membrane potential. These results are consistent with an electroneutral Na^+ /PAH cotransport system in the basolateral membrane. Kinetic analysis demonstrated saturable probenecid-sensitive uptake in presence of a Na^+ gradient. The apparent K_m value determined for PAH was 0.79 mM. This value is in good agreement with previously reported values of 0.56 mM in the dog [9] and 0.54 mM in the rat [3], but considerably higher than the value of 0.054 mM also reported in rat [5]. The value for V_{\max} of 0.80 nmol/mg protein, 15 sec is somewhat high compared to previously reported values of (converted to nmol/mg protein, 15 sec) 0.22 in the dog [9] and 0.11 [3] or 0.06 [5] in the rat. The K_i value for probenecid (0.08 mM) is again in good agreement with values of 0.14 mM [9] and 0.054 mM [3] reported for dog and rat BLMV, respectively.

In accordance with the wide variety of organic anions that are secreted in vivo by the kidney, various compounds showed affinity for Na^+ gradient-stimulated PAH uptake in BLMV (Table 9.3). Only the endogenous anions glycine and urate hardly interfered with PAH transport. The lack of inhibition of urate supports the findings of Kahn et al. [29] in the rat that in contrast to the brush border membrane, the basolateral membrane seems to contain separate transport systems for PAH and urate.

The fact that a large Na^+ gradient is not able to achieve uphill transport in BLMV does not necessarily mean that a Na^+ gradient cannot drive the intracellular accumulation of PAH in vivo. In isolated membrane vesi-

cles an overshoot is only achieved when V_{max} is relatively high compared to the rate of Na^+ gradient dissipation, whereas in vivo the transmembrane Na^+ gradient is permanently present. An alternative pathway for transport across the basolateral membrane might be an anion exchange mechanism like that described for PAH in the brush border membrane [13,16]. However, in presence of an outwardly directed OH^- gradient alone PAH uptake was only slightly stimulated, but when simultaneously an inward Na^+ gradient was imposed uptake was greatly stimulated. Our results provide supporting evidence for the Na^+ gradient-stimulated anion exchanger hypothesized by Kashner et al [5], although we cannot fully exclude the possibility that uptake is the result of additive effects of two separate pathways. Very recently, Eveloff [11] reported Na^+ -dependent PAH/ OH^- exchange in BLMV from rabbit kidney. She concluded that anion exchange is directly coupled to Na^+ , as it was found that PAH counter-transport was also stimulated when Na^+ was equilibrated across the membrane.

What other anions than OH^- and PAH itself might be accepted by this anion exchanger remains to be examined. Low et al [30] proposed a multispecific anion exchanger in the basolateral membrane of the rat that could mediate exchange of sulfate for several inorganic and organic anions including PAH. This common exchanger could additionally be driven by a Na^+ gradient and a pH difference. However, capillary perfusion studies in the rat have indicated that the substrate specificities for PAH and sulfate transport into the tubular cell are clearly distinct [31].

Brush Border Membrane

The results of our transport studies in isolated BBMVs indicate that PAH uptake can be stimulated by a transmembrane pH gradient (outward OH^- gradient) as well as by an inwardly directed Na^+ gradient. It is concluded that both gradients can drive PAH transport via a mediated pathway, since uptake in either case is concentration-dependent, probenecid-sensitive and susceptible to competition by other organic anions. Stimulation by an outwardly directed OH^- gradient is consistent with PAH/ OH^- exchange mediated by the well recognized anion exchange mechanism in the brush border membrane that is also shared by urate [13-16]. Which transport system is involved in Na^+ -stimulated uptake is less well under-

stood, although it is generally accepted that Na^+ stimulation is not achieved via a cotransport mechanism but strictly by electrochemical effects [4,12]. Hori et al. [4] proposed a gated channel through which PAH is transported in its anionic form driven by the transmembrane potential.

The question that arises from our experiments is whether an outward OH^- gradient and a Na^+ -induced potential difference stimulate PAH uptake via the same carrier system or via separate carriers. The extra stimulation of PAH uptake by simultaneous imposition of both a Na^+ and a pH gradient provides little additional information. These results are as much consistent with additive effects of uptake via two distinct pathways as with stimulation of the PAH/ OH^- exchanger by a Na^+ -induced inside positive membrane potential. However, some evidence in favor of the latter mechanism comes from a study by Kahn et al. [16], who found a decrease in PAH/ OH^- exchange when the intravesicular space was rendered more electronegative.

The fact that the kinetic parameters (K_m and V_{\max}) and probenecid inhibition constant (K_i) for sodium- and pH-dependent transport are virtually the same argues for a simple transport pathway. The parameters we found are, except for a higher V_{\max} value, in good agreement with those observed by Kinsella et al. [9] for sodium-stimulated PAH uptake in dog BBMVs. They reported a K_m (apparent) of 3.87 mM, a V_{\max} of 1.3 nmol/mg protein, 15 sec and a K_i for probenecid of 0.30 mM. Surprisingly, this appears to be the only study reporting kinetic data on PAH transport in BBMVs and to our knowledge there are no data available allowing for a comparison of the kinetic parameters obtained in presence of a pH gradient.

On the other hand, the inhibition experiments with various organic anions show a considerable but not a complete overlap in the substrate specificities of Na^+ - and pH-stimulated PAH transport. For some anions, e.g., phenolsulfonphthalein, urate and hydrochlorothiazide, the difference in inhibitory effect may be related with the degree of dissociation of the anion in the incubation medium. For these compounds, raising the pH from 6.0 to 7.4 greatly reduces the concentration of undissociated anion. However, the reduced inhibitory effects of phenolsulfonphthalein and urate at pH 7.4 are opposite to the enhanced inhibitory potency of hydrochlorothiazide.

At present no decisive answer can be given on the precise nature of the system(s) involved in Na^+ - and pH-dependent PAH transport in BBMV, nevertheless our results are in favor of a simple transport pathway. An important question also yet to be answered concerns the physiological relevance of these data. The anion exchanger present in the brush border membrane probably mediates active urate reabsorption in the proximal tubule, driven by anion gradients directed from cell to lumen. These gradients would also favor reabsorption of PAH, still PAH undergoes net secretion. It is presumed that the high intracellular PAH concentration as compared to the luminal concentration can overcome this reabsorptive tendency [32]. On the other hand, transport mediated by a positive membrane potential, either via the anion exchanger a gated channel or a leaky pathway, may very well reflect an important driving force that exists in vivo, as the luminal fluid has a more positive electrical potential than the intracellular compartment.

Acknowledgements

The authors gratefully acknowledge Brigitte van de Camp for excellent technical assistance.

9.5 REFERENCES

1. B.M. Tune, M.B. Burg and C.S. Patlak, *Am. J. Physiol.* **217**, F1057 (1969).
2. E.C. Foulkes, *Am. J. Physiol.* **232**, F424 (1977).
3. W. Berner and R. Kinne, *Pflügers Arch.* **361**, 269 (1976).
4. R. Hori, M. Takano, T. Okano, S. Kitazawa and K. Inui, *Biochem. Biophys. Acta*, **692**, 97 (1982).
5. J.S. Kasher, P.D. Holohan and C.R. Ross, *J. Pharmacol. Exp. Ther.* **227**, 122 (1983).
6. P.D. Williams, M.J.M. Hitchcock and G.H. Hottendorf, *Res. Commun. Chem. Pathol. Pharmacol.* **47**, 357 (1985).
7. M.I. Sheikh and J.V. Møller, *Biochem. J.* **208**, 243 (1982).

8. J.M. Goldinger, B.D.S. Khalsa and S.K. Hong, *Am. J. Physiol.* **247**, C217 (1984).
9. J.L. Kinsella, P.D. Holohan, N.I. Pessah and C.R. Ross, *J. Pharmacol. Exp. Ther.* **209**, 443 (1979).
10. S.S. Tse, C.L. Bildstein, D. Liu and R.D. Mamelok, *J. Pharmacol. Exp. Ther.* **226**, 19 (1983).
11. J. Eveloff, *Biochem. Biophys. Acta* **897**, 474 (1987).
12. I. Kippen, B. Hirayama, J.R. Kleinberg and E.M. Wright, *Biochim. Biophys. Acta* **556**, 161 (1979).
13. A.M. Kahn and P.S. Aronson, *Am. J. Physiol.* **244**, F56 (1983).
14. J.W. Blomstedt and P.S. Aronson, *J. Clin. Invest.* **65**, 931 (1980).
15. P.P. Sokol, P.D. Holohan and C.R. Ross, *Biochem. Biophys. Acta* **862**, 335 (1986).
16. A.M. Kahn, S. Branham and E.J. Weinman, *Am. J. Physiol.* **245**, F151 (1983).
17. M.I. Sheikh, U. Kragh-Hansen, K.E. Jørgensen and H. Røigaard-Petersen, *Biochem. J.* **208**, 377 (1982).
18. D.W. Windus, D.E. Cohn, S. Klahr and M.R. Hammerman, *Am. J. Physiol.* **246**, F78 (1984).
19. A.K. Mircheff and E.M. Wright, *J. Membrane Biol.* **28**, 309 (1976).
20. A. Dahlqvist, *Anal. Biochem.* **7**, 18 (1964).
21. R.J. Pennington, *Biochem. J.* **80**, 659 (1961).
22. G. Hübscher and G.R. West, *Nature (London)* **205**, 799 (1965).
23. G.L. Sottocasa, B. Kuylenstierna, L. Ernster and A. Bergstrand, *J. Cell Biol.* **32**, 415 (1967).
24. S.J. Schwab, S. Klahr and M.R. Hammerman, *Am. J. Physiol.* **246**, F663 (1984).
25. C.M. Metzler, G.L. Elfring and A.J. McEwen, *Biometrics* **30**, 562 (1974).
26. DISSPLA user's manual, Version 9.2, Integrated Software Systems Corporation, San Diego, Ca. (1984).
27. B. Sacktor, in *Current Topics in Bioenergetics* (Ed. R. Sanadi), Vol. **6**, p. 39. Academic Press, New York (1977).
28. D.E. Cohn, K.A. Hruska, S. Klahr and M.R. Hammerman, *Am. J. Physiol.* **243**, F293 (1982).

29. A.M. Kahn, H. Shelat and E.J. Weinman, Am. J. Physiol. **249**, F654 (1985).
30. I. Low, T. Friedrich and G. Burckhardt, Am. J. Physiol. **246**, F334 (1984).
31. K.J. Ullrich, G. Rumrich, G. Fritzch and S. Kloss, Pflugers Arch. **408**, 38 (1987).
32. S.E. Guggino, G.J. Martin and P.S. Aronson, Am. J. Physiol. **244**, F612 (1983).

EFFECT OF SUBSTITUTED BENZOATES ON p-AMINOHIPPURATE
TRANSPORT IN DOG RENAL MEMBRANE VESICLES¹

Frans G M Russel, Marc Heijn, and Cees A M van Ginneken

Abstract - The effect of substituted benzoates on the transport of p-aminohippurate (PAH) was studied in basolateral (BLMV) and brush border membrane vesicles (BBMV) isolated from dog kidney cortex. The probenecid-sensitive part of Na^+ gradient-dependent uptake of $100 \mu\text{M}$ [^3H]PAH into BLMV and Na^+ or pH gradient dependent uptake into BBMV was measured with or without the presence of 5 mM benzoate. Practically all benzoates showed an inhibitory effect on PAH transport in BLMV and BBMV, the strongest inhibitors were 3-Cl- and 4-Cl-benzoate, while the weakest inhibition was found for the 3- NH_2 and 4- NH_2 substitutes. The inhibitory potency, expressed as the apparent inhibition constant (K_i), correlated significantly with the relative hydrophobicity of the ionized benzoates, determined by reversed phase HPLC. This indicates that hydrophobic and electronic properties are the main determinants of affinity for the PAH transport system. It is suggested that the PAH transport system present in the proximal tubules is responsible for the active secretion of benzoates by the mammalian kidney.

¹Biochem Pharmacol, submitted. Partly published as an abstract in Br J Pharmacol 89, 681P (1986)

10.1 INTRODUCTION

The renal organic anion transport system is characterized by a remarkable diversity of compounds that are accepted. A wide variety of xenobiotics and their metabolites as well as numerous endogenous substrates are excreted by the kidney by tubular secretion. p-Aminohippurate (PAH) is generally considered as the model compound representing the renal transport of these organic anions. The active step in renal secretion of PAH occurs at the basolateral membrane of the proximal tubular cell across which the anion is accumulated in the cell by uphill transport. The high intracellular concentration provides a driving force for the movement of PAH from cell, across the brush border membrane, to lumen [1].

Studies with isolated basolateral (BLMV) and brush border membranes (BBMV) have demonstrated that PAH transport across both membranes is carrier-mediated and probenecid-sensitive. PAH uptake into BLMV occurs via a Na^+ gradient-dependent cotransport mechanism, which can be stimulated additionally by an opposing anion gradient [2-4]. PAH transport into BBMV occurs primarily via an anion exchange mechanism driven by opposing gradients of OH^- , Cl^- and HCO_3^- [5], while uptake can also be stimulated by a sodium gradient-induced positive membrane potential [6-8]. At present it is not clear whether this potential-driven transport occurs via the anion exchanger or via another transport system.

For several endogenous anions, e.g., lactate [9,10], di- and tricarboxylic acids [11,12], sulfate [13,14], urate [15,16] and nicotinic acid [17,18], transport systems have been characterized, that are wholly or partially distinct from the PAH transport system. Much work is still needed to define the respective specificities of these transport systems and to understand their functional relationship.

The purpose of the present study was to determine whether benzoic acids have affinity for the PAH transport system in BLMV and BBMV and whether affinity is quantitatively related to the structural properties of this class of compounds. The characteristics of renal transport of benzoate analogs are very difficult to study in vivo because their renal excretion is often modified by concomitant reabsorption [1,19] and extensive metabolism within the tubular cells [20,21]. The technique of isolated membrane vesicles provides the opportunity to study transport pro-

cesses in specific membranes independently and without the disturbing influence of metabolic events.

10.2 MATERIALS AND METHODS

Isolation of Membrane Vesicles

Kidneys from Beagle dogs that became available from other, mainly surgical, experiments were used as starting material. Brush border (BBMV) and basolateral membrane vesicles (BLMV) were prepared from cortical homogenate by CaCl_2 precipitation and Differential Percoll density gradient centrifugation. The method is based on procedures described by Sheikh et al. [22] and Windus et al. [23] with some modifications.

Briefly, cortex was minced and homogenized at 10% w/v in 100 mM mannitol, 5 mM 4-(2-hydroxyethyl)-1-piperazine ethane sulfonic acid (HEPES) buffered to pH 7.4 with Tris and 0.2 mM phenylmethylsulfonylfluoride. The homogenate was centrifuged at 2,500g for 15 min and the supernatant was treated with 10 mM CaCl_2 during 20 min. After a second centrifugation step of 2,500g for 15 min the resulting supernatant contained the crude BBMV fraction and the pellet contained BLMV and membranes from other cell organelles. The crude BBMV fraction was spun at 24,000g for 20 min in an IEC B-60 ultracentrifuge (A-169 rotor), resuspended in 100 mM mannitol and 5 mM HEPES-Tris pH 7.4, and treated again with 10 mM CaCl_2 for 20 min. After centrifugation at 2,500g for 15 min the purified BBMV were collected from the resulting supernatant at 30,000g for 20 min. The BBMV pellet was washed with uptake buffer, consisting of 100 mM KCl, 100 mM mannitol and 5 mM HEPES-Tris pH 7.4, to which 0.5 mM ethyleneglycol-bis-(β -aminoethyl ether)N,N'-tetraacetic acid (EGTA) was added, centrifuged at 30,000g for 20 min and finally resuspended in uptake buffer at a protein concentration of 8-12 mg/ml.

The fraction containing crude BLMV, obtained after the first CaCl_2 -precipitation step, was homogenized in 250 mM sucrose and 5 mM HEPES-Tris pH 7.4 and spun at 24,000g for 20 min. The fluffy upper layer of the pellet was resuspended in the sucrose buffer, brought to a concentration of 8% v/v Percoll and centrifuged at 50,000g for 30 min in an SB-283 rotor. BLMV were recovered from the second opaque band

from the top of the Percoll gradient corresponding to a density of approximately 1.034 g/ml, diluted 1 to 4 with uptake buffer and centrifuged at 96,000g for 30 min. The fluffy layer on top of the glassy Percoll pellet was resuspended in uptake buffer at a protein concentration of 8-12 mg/ml.

The purity of the membrane preparations was evaluated by marker enzyme analysis. $(\text{Na}^+ - \text{K}^+)$ -ATPase was determined after detergent treatment with 0.4 mg/ml deoxycholate, followed by freezing-thawing, to disrupt membrane vesicles [23,24]. Protein was assayed with a commercial coomassie blue kit (BiaRad, München, FRG), with bovine plasma globulin as the standard. Compared to the initial homogenate, BLMV showed a 8- to 10-fold enrichment in $(\text{Na}^+ - \text{K}^+)$ -ATPase, 0.8-fold in maltase [25], 2.5-fold in alkaline phosphatase [24], 1.2-fold in acid phosphatase [26] and <0.8-fold in succinate dehydrogenase [27] and NADPH-cytochrome-c reductase [28]. BBMV were enriched for maltase and alkaline phosphatase 12- to 14-fold, while the enrichment factors for the other marker enzymes were all <0.9.

The membranes were rapidly frozen in liquid nitrogen and stored at -80°C in small aliquots until use. In preliminary experiments, we found no difference in transport activity between frozen and freshly prepared membrane vesicles.

Transport Studies

The uptake of 100 μM [^3H]PAH in BBMV and BLMV was measured at 37°C by a rapid filtration technique [29]. Transport was initiated by the addition of 40 μl solution to 10 μl of membrane suspension. PAH uptake in BLMV was measured in presence of an inwardly directed 100 mM Na^+ gradient, while uptake in BBMV was measured in presence of an inward Na^+ gradient as well as a pH gradient (outward OH^- gradient). The initial content of the extravesicular medium was 100 mM NaCl, 20 mM KCl, 100 mM mannitol, 5 mM HEPES-Tris pH 7.4 or 100 mM KCl, 100 mM mannitol, 5 mM 2-(N-morpholino)-ethanesulfonic acid (MES)-Tris pH 6.0, and 100 μM PAH. In interaction experiments probenecid and benzoates were present in a final concentration of 5 mM. The experimental conditions are given in the legends of the tables. Uptake of PAH was terminated after 15 sec by diluting the incubation mixture with 3 ml ice-cold transport buffer.

This sample was immediately filtered under vacuum through a prewetted 0.45 μm cellulose nitrate filter (Schleicher and Schüll, Dassel, FRG) and washed twice with 3 ml of ice-cold buffer. The radioactivity remaining on the filters was counted using standard liquid scintillation techniques after dissolution in 10 ml Aqualuma plus (Lumac, Schaesberg, The Netherlands). Corrections were made for the radioactivity bound to the filters in the absence of vesicles.

Determination of $\log k_w$

Relative retention times were measured by reversed phase HPLC to characterize the hydrophobic properties of the benzoates, according to the method described by Yamana et al. [30]. In order to obtain a uniform hydrophobic parameter, $\log k_w$, the capacity factor obtained by extrapolation of retention data from binary eluents to 100% water, was determined [31].

A Hewlett-Packard 1084B chromatograph equipped with a 254 nm UV detector, autosampler and terminal (HP7850LC) was used. The stainless-steel column (250 x 4.6 mm I.D.) was packed with CP[®]Spher C18, particle size 10 μm (Chrompack, Middelburg, The Netherlands). The mobile phase consisted of a mixture of methanol and twice-distilled water containing 0.01 M phosphate buffer of either pH 2.9, 5.9 or 7.4. The column temperature was 35°C and the eluent was delivered at a flow rate of 2.0 ml/min. The benzoates were dissolved in methanol at a concentration of 5 mM and 5 μl of the sample was injected into the column. Retention times were measured at varying methanol concentrations of the mobile phase, ranging from 5-50% v/v. Retention is quantitatively described by the capacity factor, k' ,

$$k' = (t_R - t_0)/t_0 \quad (10.1)$$

where t_R is the retention time of the compound and t_0 is the retention time of an unretained reference compound, for which potassium bichromate was used. For each benzoate k' was determined at at least four methanol concentrations, differing 5% or more and lying in a range such that peaks with a reasonable retention time (1.5-25 min) were obtained. A linear relationship was observed between the $\log k'$ and the methanol concentra-

tion of the mobile phase and extrapolation to 100% water (0% methanol) gave the $\log k_w$ value. This procedure was carried out at three different pH values of the mobile phase, viz., 2.9, 5.9 and 7.4. The thus obtained $\log k_w$ values were used as a relative index for the hydrophobicity of the benzoates at each pH.

Data Analysis and Presentation

All experiments were performed on at least three different membrane preparations. Under all given conditions, the initial uptake rate of 100 μM PAH measured at 15 sec was linear with respect to time and concentration. The carrier-mediated or specific component of PAH uptake was defined as the difference between uptake in the absence and presence of 5 mM probenecid. Inhibition was expressed relative to the respective control uptakes as

$$\% \text{inh.} = 100(v - v')/v \% \quad (10.2)$$

where v = probenecid-sensitive part of 100 μM PAH uptake (control) and v' = probenecid-sensitive part of 100 μM PAH uptake in presence of 5 mM benzoate. Assuming that mediated PAH uptake follows Michaelis-Menten kinetics and that inhibition is competitive for a single binding site, the apparent inhibition constant K_i was calculated as

$$K_i = I[v'/(v - v')]/(1 + S/K_m) \quad (10.3)$$

where I = concentration inhibitor (5 mM benzoate), S = PAH concentration (100 μM) and K_m the apparent affinity constant. For K_m previously determined values were taken, viz., 0.8 mM for Na^+ gradient-dependent uptake in BLMV and for Na^+ and pH gradient-dependent uptake in BBMV 4.9 mM and 5.7 mM, respectively [8]. Data are expressed as means \pm SE. Curve fitting was done by least-squares regression analysis of the unweighted data using the computer program NONLIN [32]. Student's t -test was used to evaluate the statistical significance of the coefficient of determination obtained in the regression analysis. The figures presented in this study were drawn with the DISSPLA computer package [33].

Chemicals

p-Amino[³H]hippuric acid (254 mCi/mmol) was from Amersham (Buckinghamshire, UK) and Percoll from Pharmacia Fine Chemicals (Uppsala, Sweden). The benzoates were purchased from either Merck (Darmstadt, FRG), Fluka AG (Buchs, Switzerland) or Janssen Chimica (Beerse, Belgium). All other chemicals were from Sigma (St. Louis, MO, USA) or Merck (Darmstadt, FRG).

Table 10.1 Literature pK_a Values [34] and Capacity Factors ($\log k_w$) Measured at Different pH of the Substituted Benzoates.

substituent	pK_a	$\log k_w$		
		pH 2.9	pH 5.9	pH 7.4
H	4.20	1.96	0.64	0.39
2-CH ₃	3.90	2.34	0.76	0.53
3-CH ₃	4.25	2.53	1.21	0.98
4-CH ₃	4.37	2.49	1.10	0.94
2-OCH ₃	3.90	1.83	0.73	0.44
3-OCH ₃	4.10	2.19	0.95	0.85
4-OCH ₃	4.50	2.26	1.09	0.72
2-OH	2.93	1.98	0.70	0.79
3-OH	4.08	1.41	0.09	-0.05
4-OH	4.67	0.72	0.09	-0.34
2-Cl	2.90	1.75	0.31	0.39
3-Cl	3.84	2.58	1.14	1.11
4-Cl	3.99	2.70	1.20	1.12
2-NO ₂	2.21	1.04	0.10	0.28
3-NO ₂	3.46	1.89	0.74	0.87
4-NO ₂	3.43	1.97	0.64	0.74
2-NH ₂	2.11	1.34	0.18	0.19
3-NH ₂	3.12	1.09	0.12	-0.02
4-NH ₂	2.41	0.78	0.02	-0.18

10.3 RESULTS

Physicochemical Properties

The physicochemical parameters pK_a and $\log k_w$ of the substituted benzoates are listed in Table 10.1. The pK_a values were taken from literature [34], while the $\log k_w$ values were determined by reversed phase HPLC at pH 2.9, 5.9 and 7.4 of the mobile phase. $\log k_w$, the extrapolated capacity factor for an aqueous mobile phase, was used as a parameter to characterize the hydrophobic properties of the benzoates at a given pH. Capacity factors were determined at pH 5.9 and 7.4 because these values correspond with the pH conditions used in the membrane vesicle experiments.

Since all benzoates are weak acids with a pK_a ranging from 2.1-4.7, the $\log k_w$ values determined at pH 5.9 and pH 7.4 depend almost completely on the hydrophobicity of the ionized species. At pH 2.9 most benzoates are largely in their non-ionized form. Under this condition the $\log k_w$ is mainly determined by the hydrophobicity of the undissociated molecule.

Table 10.2 Effect of Probenecid on Na^+ Gradient-Stimulated PAH Uptake into BLMV and Na^+ or pH Gradient-Stimulated Uptake into BBMV.

	BLMV	BBMV	
	Na^+	Na^+	pH
PAH	109 ± 10	204 ± 24	192 ± 13
PAH + probenecid	38 ± 3	25 ± 2	25 ± 6

Uptake of 100 μM PAH at 15 sec was measured in presence of an inwardly directed Na^+ gradient (100 mM) or a pH gradient ($pH_{out} = 6.0$, $pH_{in} = 7.4$) with or without 5 mM probenecid. Uptake values are expressed in pmol PAH/mg protein, 15 sec as means \pm SE of six experiments.

Probenecid-Sensitive PAH Uptake

In Table 10.2 the effect of 5 mM probenecid on Na^+ gradient-dependent PAH uptake in BLMV and on Na^+ - or pH-dependent uptake in BBMV is shown. Since we found no increase in inhibition with higher probenecid concentrations, the difference between uptake in absence and presence of 5 mM probenecid was considered to represent the mediated or specific part of PAH uptake. The probenecid-sensitive part of uptake accounted for 65% of total uptake into BLMV and for 88% of Na^+ -dependent and 87% of pH-dependent uptake into BBMV.

Competition Experiments

The results of the competition experiments of the benzoates with specific PAH uptake into BLMV and BBMV are given in Table 10.3. Control uptakes were measured in presence of 5 mM gluconate and were not different from the uptake values given in Table 10.2. To test whether the benzoates might cause an indirect inhibition of pH-dependent uptake in BBMV by influencing the transmembrane pH gradient, PAH uptake was measured in presence of acetate, an anion that accumulates rapidly into the vesicles by unmediated diffusion [15]. Using concentrations up to 10 mM we were unable to detect inhibition by acetate, indicating that the intravesicular buffering was sufficient.

Practically all benzoates showed an inhibitory effect on PAH uptake in BLMV and BBMV. In both preparations 3-Cl- and 4-Cl-benzoate were the strongest inhibitors, in some cases even approaching the maximum possible probenecid effect. The weakest inhibition was found for the 3- NH_2 and 4- NH_2 analogs. Under the assumption of Michaelis-Menten kinetics and competitive inhibition for a single binding site K_i values were calculated according to Equation 10.3. These values were used to correlate the inhibitory potency of the benzoates with the physicochemical parameters listed in Table 10.1.

Correlation Studies

The most important results of these correlation studies are presented in Table 10.4 and in Figs. 10.1 and 10.2. Logarithmic values of k_w and K_i were used as it may be assumed that these values are linearly related to changes in free energy of the molecule during its interaction with biologi-

Table 10.3 Effect of Substituted Benzoates on Specific PAH Uptake into BLMV and BBMV.^a

substituent	BLMV		Na ⁺		BBMV		pH
	%inh. ^b	K _i ^c	%inh.	K _i	%inh.	K _i	
H	50 ± 2	4.4	69 ± 3	2.2	48 ± 2	5.3	
2-CH ₃	43 ± 6	5.9	41 ± 2	7.0	40 ± 7	7.4	
3-CH ₃	71 ± 2	1.8	79 ± 2	1.3	54 ± 6	4.2	
4-CH ₃	76 ± 5	1.4	60 ± 1	3.3	48 ± 6	5.3	
2-OCH ₃	54 ± 4	3.8	42 ± 4	6.8	33 ± 3	10.0	
3-OCH ₃	67 ± 3	2.2	75 ± 1	1.6	56 ± 3	3.9	
4-OCH ₃	63 ± 5	2.6	62 ± 1	3.0	53 ± 4	4.4	
2-OH	73 ± 4	1.6	50 ± 1	4.9	61 ± 5	3.1	
3-OH	51 ± 6	4.3	49 ± 4	5.1	38 ± 7	8.0	
4-OH	50 ± 4	4.4	10 ± 3	44.1	40 ± 6	7.4	
2-Cl	58 ± 3	3.2	42 ± 8	6.8	53 ± 2	4.4	
3-Cl	88 ± 2	0.6	96 ± 2	<0.5	75 ± 6	1.6	
4-Cl	90 ± 4	0.5	81 ± 2	1.2	71 ± 2	2.0	
2-NO ₂	69 ± 4	2.0	13 ± 2	32.8	49 ± 3	5.1	
3-NO ₂	87 ± 6	0.7	79 ± 2	1.3	70 ± 3	2.1	
4-NO ₂	76 ± 1	1.4	46 ± 2	5.8	69 ± 3	2.2	
2-NH ₂	57 ± 7	3.4	3 ± 5	>50	44 ± 3	6.2	
3-NH ₂	42 ± 6	6.1	8 ± 9	>50	31 ± 3	10.9	
4-NH ₂	38 ± 4	7.2	-6 ± 3	>50	19 ± 2	21.0	

^aThe probenecid-sensitive part of 100 μM PAH uptake at 15 sec was measured. The experimental conditions were similar to those given in Table 10.2, except for the presence of 5.0 mM benzoate. Control uptakes were measured in presence of 5 mM gluconate.

^bInhibition is expressed relative to the respective control uptakes as means ± SE of three to five experiments.

^cInhibition constant calculated according to Eq. 10.3, values are expressed in mM. For %inh. values <10% or >90% estimates of K_i were considered too inaccurate and only the upper or lower limits are given.

cal receptors. Regression analysis revealed a linear relationship between $\log k_w$ and $\log K_i$. All correlations were significant ($p < 0.01$), but highest coefficients of correlation were observed between $\log k_w$ (pH 7.4) and $\log K_i$. The correlation coefficients for these regressions were about 0.8, which means that 64% of the total variation in $\log K_i$ was accounted for by the linear relationship with $\log k_w$.

No significant correlation was observed between pK_a and $\log K_i$ ($r < 0.3$, $p > 0.2$), indicating that electronic properties alone are not responsible for the variance in inhibitory potency. These results showed that the hydrophobic properties of the ionized benzoates were the primary determinants of their inhibitory effect on PAH transport.

Table 10.4 Correlation Between $\log K_i$ and $\log k_w$ of Substituted Benzoates.

$\log k_w$	$\log K_i = a - b \log k_w$		n	r	s
	a	b			
BLMV (Na^+)					
pH 7.4	0.70	0.63	19	0.813	0.21
pH 5.9	0.70	0.52	19	0.647	0.27
pH 2.9	1.01	0.35	19	0.620	0.29
BBMV (Na^+)					
pH 7.4	1.17	0.92	15	0.816	0.31
pH 5.9	1.31	0.96	15	0.780	0.31
pH 2.9	2.06	0.73	15	0.828	0.28
BBMV (pH)					
pH 7.4	0.95	0.51	19	0.798	0.18
pH 5.9	0.95	0.41	19	0.626	0.23
pH 2.9	1.24	0.30	19	0.657	0.22

$\log K_i$ = log inhibition constant, $\log k_w$ = capacity factor, n = number of benzoates studied, r = correlation coefficient and s = standard deviation.

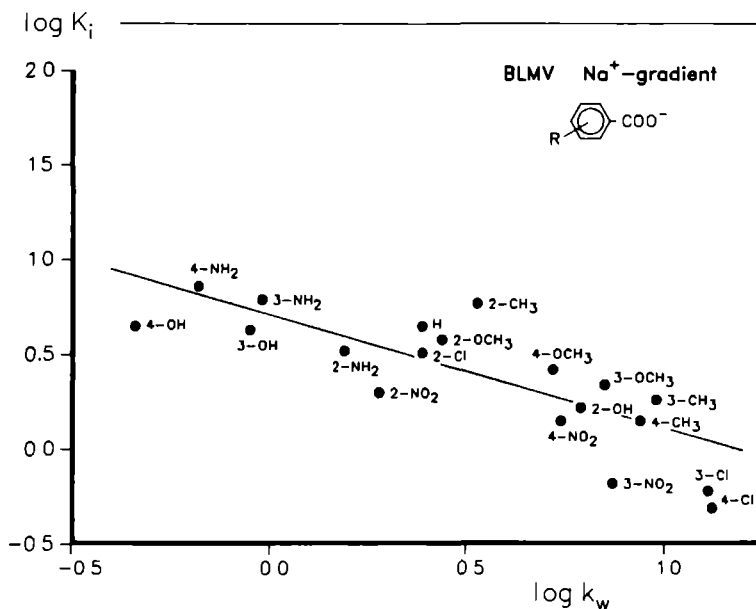


Fig. 10.1 Correlation between the logarithm of the apparent inhibition constant K_i and the capacity factor $\log k_w$ determined at pH 7.4, characterizing the effect of substituted benzoates on sodium gradient-dependent PAH uptake into BLMV.

10.4 DISCUSSION

The results of this study show that substituted benzoates have affinity for the PAH transporter in BLMV and BBMV. The inhibitory potency, expressed as K_i , was predicted best by the relative hydrophobicity of the dissociated benzoates, indicating that hydrophobic as well as electronic properties are the determinants of substrate affinity.

The parameter $\log k_w$, determined by reversed phase HPLC, was used to characterize the hydrophobic properties of the benzoates. The hydrophobicity of a compound is usually expressed by the partition coefficient, $\log P$, derived from distribution studies between *n*-octanol and water. However, the experimental disadvantages of $\log P$ determinations have led to alternative procedures, of which reversed phase HPLC has become the most accepted method. $\log k_w$ is even considered to be a better hydropho-

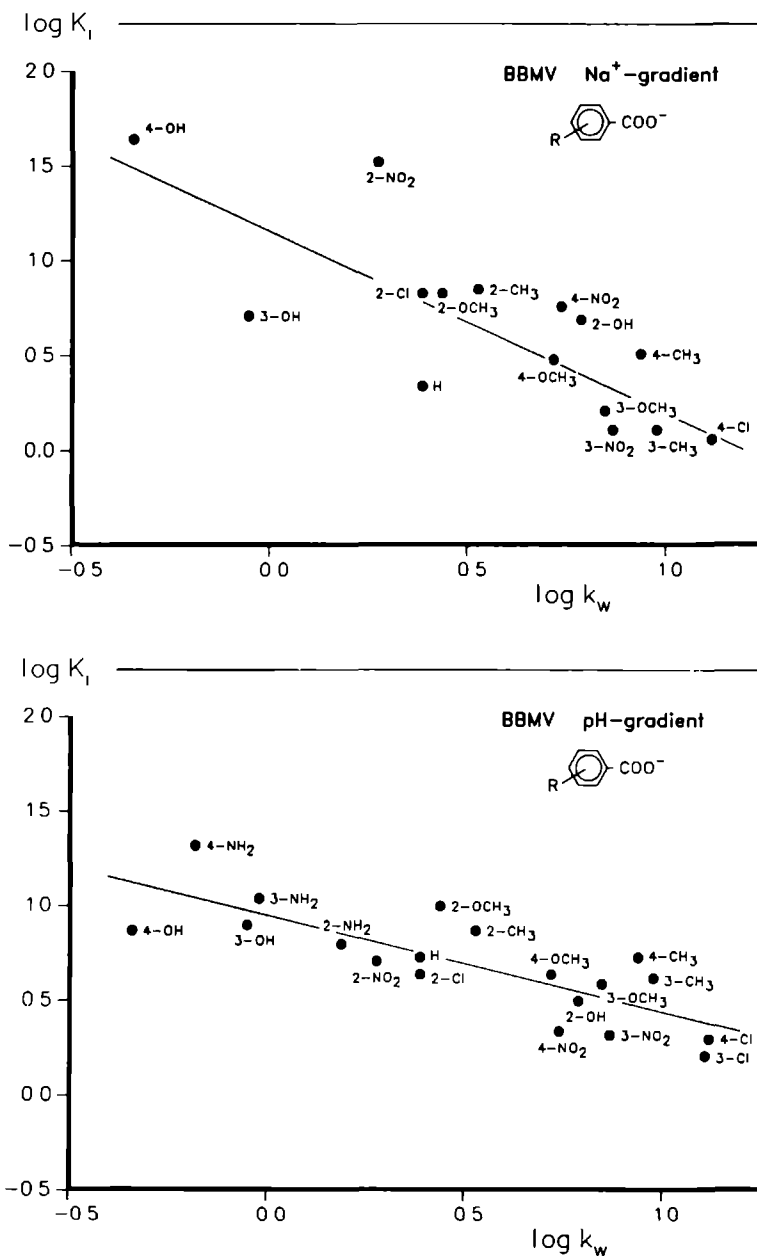


Fig. 10.2 Correlation between the logarithm of the apparent inhibition constant K_i and the capacity factor $\log k_w$ determined at pH 7.4, characterizing the effect of substituted benzoates on sodium gradient-dependent (top) and pH gradient-dependent PAH uptake into BBMV (bottom).

bic parameter than $\log P$, as retention in HPLC is a dynamic process that includes additional information on the steric properties of a compound, which may be also of importance in the interference with biological systems [31].

Although the K_m for PAH transport into BLMV is 7- to 8-fold lower than for uptake into BBMV, most of the K_i values of the benzoates are for both membranes in about the same range. On closer inspection it appears that some benzoates, e.g., 4-OH, 2-NO₂ and 2,3,4-NH₂ analogs, had practically no inhibitory effect on sodium-stimulated PAH uptake in BBMV, whereas they clearly inhibited pH-stimulated uptake in BBMV and Na⁺-dependent uptake in BLMV. This difference in inhibitory effect suggests that Na⁺- and pH-dependent uptake into BBMV represent distinct transport routes with overlapping specificities. Clearly, more detailed studies with varying concentrations of benzoate and PAH are required to obtain conclusive evidence for the existence of separate transport systems.

It can be concluded from the data that active renal secretion of benzoates can occur via the same transport route by which PAH is secreted. However, it should be noticed that inhibition of PAH transport primarily indicates affinity for the PAH transport system and does not necessarily mean that the competitor is actually transported. This can only be determined when transport of the compound itself is directly measured.

In previous *in vivo* studies, it was found that 3-hydroxybenzoate [35], pyrazinoate [36] and nicotinate [17] are not only actively transported by the organic anion secretory mechanism but also actively reabsorbed in the proximal tubule. Ullrich et al. [37] showed that benzoate derivatives inhibit Na⁺-dependent lactate reabsorption in the brush border membrane and they suggested that active reabsorption of benzoates is mediated via the lactate transporter. The relative inhibitory effects on lactate transport are comparable to the effects we observed on PAH transport. A good relationship between interaction with the carrier and the electron density at the carboxylic acid group was observed, but the importance of molecular size and hydrophobicity was also recognized. PAH did not inhibit lactate transport, indicating that the organic anion secretory pathway does not interfere with the reabsorptive lactate system.

Taken these results together, it is proposed that benzoates are actively secreted by the mammalian kidney via the PAH transport system in the basolateral and brush border membrane of the proximal tubules, and actively reabsorbed via the lactate transporter in the brush border membrane.

Acknowledgements

The authors gratefully acknowledge Brigitte van de Camp for skillful determination of the numerous capacity factors.

10.5 REFERENCES

1. I.M. Weiner, in *The Kidney: Physiology and Pathophysiology* (Eds. D.W. Seldin and G. Giebisch), p1703. Raven Press, New York (1985).
2. J.L. Kinsella, P.D. Holohan, N.I. Pessah and C.R. Ross, *J. Pharmacol. Exp. Ther.* **209**, 443 (1979).
3. J.S. Kasher, P.D. Holohan and C.R. Ross, *J. Pharmacol. Exp. Ther.* **227**, 122 (1983).
4. J. Eveloff, *Biochem. Biophys. Acta* **897**, 474 (1987).
5. A.M. Kahn and P.S. Aronson, *Am. J. Physiol.* **244**, F56 (1983).
6. I. Kippen, B. Hirayama, J.R. Kleinberg and E.M. Wright, *Biochim. Biophys. Acta* **556**, 161 (1979).
7. R. Hori, M. Takano, T. Okano, S. Kitazawa and K. Inui, *Biochem. Biophys. Acta*, **692**, 97 (1982).
8. F.G.M. Russel, P.E.M. van der Linden, W.G. Vermeulen and C.A.M. van Ginneken, *Br. J. Pharmacol.* **89**, 513P (1986).
9. M. Barac-Nieto, H. Murer and R. Kinne, *Am. J. Physiol.* **239**, F496 (1980).
10. M. Barac-Nieto, H. Murer and R. Kinne, *Pflügers Arch.* **392**, 366 (1982).
11. I. Kippen, B. Hirayama, J.R. Klinenberg and E.M. Wright, *Proc. Natl. Acad. Sci. USA* **76**, 3397 (1979).
12. K.J. Ullrich, H. Fasold, G. Rumrich and S. Klöss, *Pflügers Arch.* **400**, 241 (1984).
13. C. Bästlein and G. Burckhardt, *Am. J. Physiol.* **250**, F226 (1986).

14. Z. Talor, R.M. Gold, W.C. Yang and J.A.L. Arruda, *Eur. J. Biochem.* **164**, 695 (1987).
15. S.E. Guggino, G.J. Martin and P.S. Aronson, *Am. J. Physiol.* **244**, F612 (1983).
16. A.M. Kahn, H. Shelat and E.J. Weinman, *Am. J. Physiol.* **249**, F654 (1985).
17. P.B. Corr and D.G. May, *J. Pharmacol. Exp. Ther.* **192**, 195 (1975).
18. E.F. Boumendil-Podevin and R.A. Podevin, *Am. J. Physiol.* **240**, F185 (1981).
19. P.K. Knoefel and K.C. Huang, *J. Pharmacol. Exp. Ther.* **117**, 307 (1956).
20. S.H. Wan and S. Riegelman, *J. Pharm. Sci.* **61**, 1278 (1972).
21. S.H. Wan and S. Riegelman, *J. Pharm. Sci.* **61**, 1284 (1972).
22. M.I. Sheikh, U. Kragh-Hansen, K.E. Jørgensen and H. Røigaard-Petersen, *Biochem. J.* **208**, 377 (1982).
23. D.W. Windus, D.E. Cohn, S. Klahr and M.R. Hammerman, *Am. J. Physiol.* **246**, F78 (1984).
24. A.K. Mircheff and E.M. Wright, *J. Membrane Biol.* **28**, 309 (1976).
25. A. Dahlqvist, *Anal. Biochem.* **7**, 18 (1964).
26. G. Hübscher and G.R. West, *Nature (London)* **205**, 799 (1965).
27. R.J. Pennington, *Biochem. J.* **80**, 659 (1961).
28. G.L. Sottocasa, B. Kuylenstierna, L. Ernster and A. Bergstrand, *J. Cell Biol.* **32**, 415 (1967).
29. S.J. Schwab, S. Klahr and M.R. Hammerman, *Am. J. Physiol.* **246**, F663 (1984).
30. T. Yamana, A. Tsuji, E. Miyamoto and O. Kubo, *J. Pharm. Sci.* **66**, 747 (1977).
31. T. Braumann, *J. Chromatogr.* **373**, 191 (1986).
32. C.M. Metzler, G.L. Elfring and A.J. McEwen, *Biometrics* **30**, 562 (1974).
33. DISSPLA user's manual, Version 9.2, Integrated Software Systems Corporation, San Diego, Ca. (1984).
34. E.P. Serjeant and B. Dempsey, *Ionisation Constants of Organic Acids in Aqueous Solution*. Pergamon Press, Oxford (1979).
35. D.G. May and I.M. Weiner, *Am. J. Physiol.* **218**, F430 (1970).

36. I.M. Weiner and J.P. Tinker, J. Pharmacol. Exp. Ther. 180, 411 (1972).
37. K.J. Ullrich, G. Rumrich, S. Klöss and H. Fasold, Pflügers Arch. 395, 227 (1982).

EFFECT OF SUBSTITUTED BENZOYLGLYCINES (HIPPURATES) AND
PHENYLACETYLGLYCINES ON p-AMINOHIPPURATE TRANSPORT IN DOG
RENAL MEMBRANE VESICLES¹

Frans G.M. Russel, Wim G. Vermeulen, and Cees A.M. van Ginneken

Abstract - The effect of substituted benzoylglycines (hippurates) and phenylacetylglucines on the transport of p-aminohippurate (PAH) was studied in basolateral (BLMV) and brush border membrane vesicles (BBMV) isolated from dog kidney cortex. The probenecid-sensitive part of Na^+ gradient-dependent uptake of 100 μM [^3H]PAH into BLMV and Na^+ or pH gradient-dependent uptake into BBMV was measured with or without the presence of 5 mM glycine conjugate. The benzoyl- and phenylacetylglucines studied were unsubstituted or substituted in the 2-, 3-, or 4-position with a CH_3 , OCH_3 or OH group. Benzoylglycines were stronger inhibitors of PAH transport than phenylacetylglucines and the inhibitory potency of the conjugates was in general lower against transport into BBMV than BLMV. The strongest inhibitory effect was found with 2- OCH_3 - and 3- CH_3 -benzoylglycine on BLMV and pH-dependent BBMV transport, while only the 3- CH_3 analog was a strong inhibitor of sodium-dependent BBMV transport. Strikingly, 2-OH-benzoylglycine (salicyluric acid) had no inhibitory potency against PAH transport in BLMV, while it clearly inhibited BBMV transport. It is suggested that intramolecular hydrogen bonding between the hydroxy and carbonyl group hinders the carbonyl from interaction with the carrier, thus preventing transport. The carbonyl group is apparently not essential for transport across the brush border membrane. The inhibitory potency of the glycine conju-

¹Biochem. Pharmacol., submitted

gates, expressed as the apparent inhibition constant (K_i), correlated parabolically with the relative hydrophobicity of the ionized compounds, determined by reversed phase HPLC. This indicates that both hydrophobic and electronic properties are important determinants of affinity for the PAH transport system.

11.1 INTRODUCTION

Glycine conjugation is next to glucuronidation an important metabolic pathway in the elimination of aromatic carboxylic acids [1]. It leads to less toxic compounds that are excellent substrates for the renal organic anion transport system and therefore more readily excreted than the unconjugated molecules [2]. Although aromatic carboxylic acids may be actively secreted by the kidney themselves, the efficiency of their renal clearance is generally low because of extensive passive backdiffusion and/or active reabsorption [3,4]. A classical example is hippurate (benzoyl-glycine), the conjugation product of benzoate and glycine. It is excreted in large amounts in normal urine, depending on the daily intake of benzoate precursors with the diet [5]. The renal clearance of hippurate and related conjugates like p-aminohippurate (PAII) is at low concentrations so efficient, that they are completely extracted from renal plasma in a single pass through the kidney [2,3].

In the past, several studies have been undertaken with the hippurate class of compounds in an attempt to identify the structural properties that are essential for active renal secretion. It was concluded that the carbonyl and carboxylate group play a critical role in the secretion of hippurates [6]. Essig and Taggart [7] studied systematically the influence of ring substitution on the transport properties of hippurate in rabbit kidney cortex slices. The compounds were substituted in the ortho-, meta- or para-position by either a methyl, fluoro, chloro, bromo, iodo or nitro group. Hippurates substituted in the meta-position were better inhibitors of PAH transport than the corresponding para- and ortho-analogs. The capacity to inhibit PAH transport was inversely related to their own transport rates and within the meta- and para-series the inhibitory poten-

cy was related to the weight or bulk of the substituent and not to the electron distribution on the benzene ring. A difficulty in interpreting these results is that slice studies do not allow to differentiate between luminal and basolateral membrane processes [2]. There is now abundant evidence that organic anion transport across both membranes is carrier-mediated and susceptible to inhibition by other anions [2,3,8].

In the present study we used the technique of isolated membrane vesicles to evaluate the specificity of PAH transport across each membrane separately. PAH uptake into basolateral membrane vesicles (BLMV) is Na^+ gradient-dependent and can be stimulated additionally by an opposing anion gradient [9-11]. Uptake into luminal or brush border membrane vesicles (BBMV) occurs primarily via an anion exchange mechanism [12] but can also be driven by a Na^+ gradient-induced positive membrane potential [13-15].

The aim of this study was to characterize the relative affinity of mono-substituted benzoylglycines (hippurates) and phenylacetylglycines for the PAH transport system by measuring their inhibitory effect on PAH uptake into BLMV and BBMV and to determine whether inhibitory potency is quantitatively related to the physicochemical properties of these compounds.

11.2 MATERIALS AND METHODS

Isolation of Membrane Vesicles

Brush border (BBMV) and basolateral membrane vesicles (BLMV) were isolated from Beagle dog kidney cortex using a CaCl_2 precipitation method in combination with differential and Percoll density gradient centrifugation as described previously [16]. The purified membranes were suspended at a protein concentration of 8-12 mg/ml in 100 mM KCl, 100 mM mannitol and 5 mM 4-(2-hydroxyethyl)-1-piperazine ethane sulfonic acid (HEPES) buffered to pH 7.4 with Tris, rapidly frozen in liquid nitrogen and stored at -80°C until use. Compared to the initial homogenate BLMV were enriched about 9-fold as determined by the increase in specific activity of $(\text{Na}^+-\text{K}^+)\text{-ATPase}$ and BBMV about 13-fold as determined by the increase in alkaline phosphatase and maltase activity, while cross contamination was

negligible. Protein and marker enzymes were assayed as previously described [16].

Transport Studies

The 15 sec uptake of 100 μM [^3H]PAH in BBMV and BLMV was measured at 37°C by a rapid filtration technique [17]. Transport was initiated by the addition of 40 μl solution to 10 μl of membrane suspension. The initial content of the extravesicular medium was 100 mM NaCl, 20 mM KCl, 100 mM mannitol, 5 mM HEPES-Tris pH 7.4 (inward Na^+ gradient) or 100 mM KCl, 100 mM mannitol, 5 mM 2-(N-morpholino)-ethanesulfonic acid (MES)-Tris pH 6.0 (outward OH^- gradient), with or without 5 mM probenecid or glycine conjugate. Uptake of PAH was stopped by the addition of 3 ml of the same ice-cold incubation medium. The sample was immediately filtered through a 0.45 μm cellulose nitrate filter (Schleicher and Schüll, Dassel, FRG) and washed twice with 3 ml of ice-cold buffer. The radioactivity remaining on the filters was counted in a liquid scintillation counter and corrections were made for the radioactivity bound to the filters in the absence of vesicles.

Determination of $\log k_w$

In order to study the relative hydrophobicity of the substituted glycine conjugates, the capacity factor $\log k_w$ was determined by reversed phase HPLC as described by Yamana et al. [18]. A Hewlett-Packard 1084B chromatograph equipped with a 254 nm UV detector, autosampler and terminal (HP 7850 LC) was used. The stainless-steel column (250 x 4.6 mm I.D.) was packed with CP[™]Spher C18, particle size 10 μm (Chrompack, Middelburg, The Netherlands). The mobile phase consisted of a mixture of methanol and twice-distilled water containing 0.01 M phosphate buffer of either pH 2.9, 5.9 or 7.4. The column temperature was 35°C and the eluent was delivered at a flow rate of 2.0 ml/min. The compounds were dissolved in methanol (5 mM) and 5 μl was injected into the column. Retention is quantitatively described by the capacity factor $k' = (t_R - t_0)/t_0$, where t_R is the retention time of the compound and t_0 is the retention time of an unretained reference compound, for which potassium bichromate was used. For each compound k' was determined at at least four methanol concentrations ranging from 5-50% v/v and differing

5% or more, such that peaks with a reasonable retention time (1.5-25 min) were obtained. A linear relationship was observed between the $\log k'$ and the methanol concentration of the mobile phase and extrapolation to 100% water (0% methanol) gave the $\log k_w$ value. This procedure was carried out at three different pH values of the mobile phase, e.g., 2.9, 5.9 and 7.4.

Data Analysis and Presentation

All experiments were performed on at least three different membrane preparations. Under all given conditions, the initial uptake rate of 100 μM PAH measured at 15 sec was linear with respect to time and concentration. The carrier-mediated or specific component of PAH uptake was defined as the difference between uptake in the absence and presence of 5 mM probenecid. Inhibition was expressed relative to the respective control uptakes as

$$\% \text{inh.} = 100(v-v')/v \% \quad (11.1)$$

where v = probenecid-sensitive part of 100 μM PAH uptake (control) and v' = probenecid-sensitive part of 100 μM PAH uptake in presence of 5 mM benzoate. Assuming that mediated PAH uptake follows Michaelis-Menten kinetics and that inhibition is competitive for a single binding site, the apparent inhibition constant K_i was calculated as

$$K_i = I[v'/(v-v')]/(1 + S/K_m) \quad (11.2)$$

where I = concentration inhibitor (5 mM), S = PAH concentration (100 μM) and K_m the apparent affinity constant. For K_m previously determined values were taken, e.g., 0.8 mM for Na^+ gradient-dependent uptake in BLMV and for Na^+ and pH gradient-dependent uptake in BBMV 4.9 mM and 5.7 mM, respectively [15]. Data are expressed as means \pm SE. Curve fitting was done by least-squares regression analysis of the unweighted data using the computer program NONLIN [19]. Student's t-test was used to evaluate the statistical significance of the coefficient of determination obtained in the regression analysis. The figures presented in this study were drawn with the DISSPLA computer package [20].

Preparation of the Glycine Conjugates

Benzoylglycine and 2-OH-benzoylglycine were commercially available, the other conjugates were prepared by chemical synthesis. Phenylacetyl-glycine and the benzoyl- and phenylacetyl-glycines with a CH_3 or OCH_3 substituent were prepared according to the Schotten-Baumann method from the corresponding benzoyl and phenylacetyl chlorides by reaction with glycine in the presence of a slight excess of sodium hydroxide [21]. Acyl chlorides were obtained commercially from Aldrich (Brussel, Belgium) or were prepared by reaction of the substituted acid with a slight molar excess of thionyl chloride [22]. The Schotten-Baumann method is not suitable for the preparation of hydroxy-substituted conjugates because the phenolic groups can react with the acylchlorides. For these compounds an activated ester was prepared by reaction of the acid with N-hydroxysuccinimide in presence of N,N'-dicyclohexylcarbodiimide in dry dioxane [23]. The activated ester was separated by filtration and subsequently added to a slightly alkaline glycine solution to yield the hydroxy-substituted glycine conjugate.

The substituted benzoyl- and phenylacetyl-glycines were purified by recrystallization from boiling water. The identity of the compounds was checked by comparing melting points with available literature values [21,23,24-28] and incidently by IR, mass spectrometry and NMR analysis. Purity was checked by TLC and HPLC. TLC was performed on silicagel GF₂₅₄ plates (Merck, Darmstadt, FRG) with a mobile phase of chloroform-methanol-acetic acid (80:20:3). Spots were detected under UV light and by immersing the plates in a saturated iodine solution in carbon tetrachloride. The HPLC method was the same as used for the determination of the $\log k_w$ values.

Chemicals

p-Amino[³H]hippuric acid (440 mCi/mmol) was obtained from Amersham (Buckinghamshire, UK). Unlabelled PAH, benzoylglycine (hippuric acid) and 2-OH-benzoylglycine (salicyluric acid), glycine and thionylchloride were from Merck (Darmstadt, FRG), and N-hydroxysuccinimide and N,N'-dicyclohexylcarbodiimide from Janssen Chimica (Beerse, Belgium). All other chemicals were purchased either from Sigma (St. Louis, MO, USA) or Merck.

Table 11.1 Capacity Factors ($\log k_w$) of the Substituted Benzoylglycines and Phenylacetylglycines Measured at Different pH.

substituent	$\log k_w$		
	pH 2.9	pH 5.9	pH 7.4
benzoylglycines			
H	1.01	0.70	0.90
2-CH ₃	1.35	0.88	1.06
3-CH ₃	1.75	1.29	1.50
4-CH ₃	1.74	1.30	1.45
2-OCH ₃	1.76	1.34	1.54
3-OCH ₃	1.44	1.17	1.39
4-OCH ₃	1.47	0.91	1.35
2-OH	1.54	1.02	1.16
3-OH	0.86	0.46	0.66
4-OH	0.72	0.31	0.47
phenylacetylglycines			
H	1.29	0.88	1.06
2-CH ₃	1.66	1.33	1.51
3-CH ₃	1.89	1.22	1.61
4-CH ₃	1.91	1.23	1.62
2-OCH ₃	1.68	1.38	1.53
3-OCH ₃	1.55	1.31	1.49
4-OCH ₃	1.43	1.29	1.40
2-OH	1.08	0.76	0.95
3-OH	0.83	0.54	0.75
4-OH	0.65	0.39	0.67

11.3 RESULTS

Physicochemical Properties

The capacity factors ($\log k_w$) of the substituted benzoylglycines and phenylacetylglycines, determined by reversed phase HPLC at pH 2.9, 5.9 and 7.4, are given in Table 11.1. $\log k_w$ was obtained by extrapolation of

retention data from methanol-water eluents to 100% water and was used to characterize the relative hydrophobicity of the glycine conjugates at each pH. The pK_a of most compounds is not known, but on theoretical grounds it is reasonable to assume that the values are not much different from the pK_a of benzoylglycine (3.80). This means that $\log k_w$ values determined at pH 2.9 are practically a measure for the hydrophobicity of the unionized molecules, while the values determined at pH 5.9 and 7.4 depend almost completely on the hydrophobicity of the ionized species. Capacity factors at pH 5.9 and 7.4 were chosen because these values correspond to those used in the membrane vesicle experiments.

It was somewhat unexpected to find the $\log k_w$ values determined at pH 7.4 to be higher than the values at pH 5.9. This is probably related to the physicochemical influence of the glycine moiety as we did not observe such a behavior for the corresponding benzoic acids under identical conditions [29]. However, we do not have an explanation for the exact mechanism of this phenomenon.

Table 11.2 Probenecid-Sensitive Part of Na^+ Gradient-Stimulated PAH Uptake into BLMV and Na^+ or pH Gradient-Stimulated Uptake into BBMV.

	BLMV	BBMV	
	Na^+	Na^+	pH
PAH	108 ± 4	164 ± 9	150 ± 10
PAH + probenecid	30 ± 3	33 ± 1	30 ± 5

Uptake of 100 μM PAH at 15 sec was measured in presence of an inwardly directed Na^+ gradient (100 mM) or a pH gradient ($pH_{out} = 6.0$, $pH_{in} = 7.4$) with or without 5 mM probenecid. Uptake values are expressed in pmol PAH/mg protein, 15 sec as means \pm SE of eight experiments.

Probenecid-Sensitive PAH Uptake

The effect of 5 mM probenecid on the 15 sec uptake of 100 μM PAH into BLMV and BBMV is shown in Table 11.2. Uptake into BLMV was measured in presence of a Na^+ gradient and uptake into BBMV in presence of

a Na^+ as well as a pH gradient as it is currently uncertain whether both gradients drive PAH transport via the same or via distinct carrier systems. Uptake in presence of probenecid was measured in order to distinguish carrier-mediated PAH transport from unmediated processes. The probenecid-sensitive part of uptake accounted for 72% of total uptake into BLMV and for 80% of both Na^+ - and pH-dependent uptake into BBMV.

Competition Experiments

The inhibitory effect of the substituted benzoylglycines and phenylacetylglycines on probenecid-sensitive PAH uptake into BLMV and BBMV is shown in Table 11.3. Control uptakes were measured in presence of 5 mM gluconate and were not different from the uptake values given in Table 11.2. Under the assumption of Michaelis-Menten kinetics and competitive inhibition for a single binding site K_i values were calculated according to Equation 11.2.

All glycine conjugates inhibited PAH uptake into BLMV, with one remarkable exception. To our surprise, 2-OH-benzoylglycine had absolutely no inhibitory effect on BLMV transport, whereas it clearly inhibited PAH uptake into BBMV. Furthermore, the inhibitory potency against BLMV was restored in the corresponding 2-OH substitute of phenylacetylglycine. The inhibitory potency of the glycine conjugates was in general lower against transport into BBMV than BLMV. The strongest inhibitory effect was found with 2-OCH₃- and 3-CH₃-benzoylglycine in BLMV and pH-dependent transport in BBMV. Only the 3-CH₃ analog had a strong inhibitory effect on sodium-dependent BBMV transport, while the 2-OCH₃ analog was one of the weakest inhibitors. For most glycine conjugates the inhibitory pattern on Na^+ gradient-dependent PAH uptake in BBMV was comparable to that on pH gradient-dependent uptake, although absolute values were different. Phenylacetylglycines showed both in BLMV (except for the 2-OH substitute) and BBMV a lower and much less differentiated inhibitory effect, as compared to the corresponding benzoylglycines.

Correlation Studies

The logarithm of the apparent inhibition constant ($\log K_i$) was used to correlate the inhibitory potency of the glycine conjugates with the physicochemical parameters listed in Table 11.1. Linear and parabolic regression

Table 11.3 Effect of Substituted Benzoylglycines and Phenylacetylglycines on Specific PAH Uptake into BLMV and BBMV.^a

substituent	BLMV		Na ⁺	BBMV	pH	
	%inh. ^b	K _i ^c	%inh.	K _i	%inh.	K _i
benzoylglycines						
H	50 ± 5	4.4	45 ± 7	6.0	30 ± 5	11.5
2-CH ₃	39 ± 6	6.9	25 ± 5	14.7	26 ± 6	14.0
3-CH ₃	74 ± 6	1.6	83 ± 5	1.0	54 ± 7	4.2
4-CH ₃	56 ± 6	3.5	62 ± 5	3.0	43 ± 3	6.5
2-OCH ₃	76 ± 5	1.4	29 ± 9	12.0	56 ± 4	3.9
3-OCH ₃	63 ± 6	2.6	67 ± 3	2.4	47 ± 7	5.5
4-OCH ₃	51 ± 7	4.3	29 ± 7	7.7	37 ± 3	8.4
2-OH	-5 ± 9	>50	47 ± 6	5.5	52 ± 4	4.5
3-OH	46 ± 6	5.2	36 ± 5	8.7	43 ± 2	6.5
4-OH	56 ± 6	3.5	43 ± 5	6.5	50 ± 3	4.9
phenylacetylglycines						
H	47 ± 4	5.0	22 ± 1	17.4	25 ± 3	14.7
2-CH ₃	47 ± 4	5.0	16 ± 4	25.7	33 ± 3	10.0
3-CH ₃	45 ± 4	5.4	35 ± 4	9.1	34 ± 4	9.5
4-CH ₃	44 ± 4	5.6	27 ± 2	13.2	40 ± 5	7.4
2-OCH ₃	51 ± 5	4.3	2 ± 2	>50	29 ± 2	12.0
3-OCH ₃	49 ± 5	4.6	11 ± 4	39.6	29 ± 1	12.0
4-OCH ₃	56 ± 3	3.5	6 ± 3	>50	30 ± 1	11.5
2-OH	61 ± 4	2.8	3 ± 5	>50	20 ± 6	19.7
3-OH	38 ± 5	7.2	2 ± 3	>50	30 ± 4	11.5
4-OH	36 ± 4	7.9	8 ± 8	>50	26 ± 2	14.0

^aThe probenecid-sensitive part of 100 μM PAH uptake at 15 sec was measured. The experimental conditions were similar to those given in Table 11.2, except for the presence of 5.0 mM inhibitor. Control uptakes were measured in presence of 5 mM gluconate.

^bInhibition is expressed relative to the respective control uptakes as means ± SE of three to five experiments.

^cInhibition constant calculated according to Eq. 11.2, values are expressed in mM. For %inh. values <10% or >90% estimates of K_i were considered too inaccurate and only the upper or lower limits are given.

Table 11.4 Correlation Between $\log K_i$ and $\log k_w$ of Substituted Benzoylglycines and Phenylacetylglycines.

$\log K_i = a + b \log k_w - c(\log k_w)^2$							
$\log k_w$		a	b	c	n	r	s
benzoylglycines							
BLMV	pH 7.4	-0.44	2.72	1.49	9	0.894	0.12
(Na ⁺)	pH 5.9	0.14	1.73	1.24	9	0.852	0.14
	pH 2.9	-0.68	2.53	1.13	9	0.793	0.16
BBMV	pH 7.4	-0.23	2.89	1.71	9	0.801	0.24
(Na ⁺)	pH 5.9	0.21	2.42	1.86	9	0.855	0.21
	pH 2.9	-0.97	3.61	1.66	9	0.750	0.27
BBMV	pH 7.4	-0.54	3.29	1.66	9	0.942	0.07
(pH)	pH 5.9	0.08	2.38	1.48	9	0.886	0.10
	pH 2.9	-0.91	3.17	1.30	9	0.800	0.13
phenylacetylglycines ^a							
BLMV	pH 7.4	2.42	-3.12	-1.29	10	0.806	0.09
(Na ⁺)	pH 5.9	1.37	-1.48	-0.72	10	0.636	0.12
	pH 2.9	1.74	-1.69	-0.61	10	0.770	0.10
BBMV	pH 7.4	0.34	1.68	0.81	10	0.852	0.07
(pH)	pH 5.9	1.03	0.40	0.31	10	0.569	0.11
	pH 2.9	0.78	0.76	0.36	10	0.828	0.07

$\log K_i$ = log inhibition constant, $\log k_w$ = capacity factor, n = number of compounds studied, r = correlation coefficient and s = standard deviation.

^aIn BBMV (Na⁺) practically no inhibition was observed (Table 11.3), as a result data were insufficient for correlation analysis.

analysis was performed and in all cases a quadratic equation described the relationship between $\log k_w$ and $\log K_i$ better than a linear equation. Relevant results of these correlation studies are presented in Table 11.4 and Figs. 11.1 and 11.2. Except for the relation between $\log k_w$ (pH 5.9) and $\log K_i$ of the phenylacetylglycines, all correlations were significant ($p < 0.05$), but on the whole highest coefficients of correlation were observed between $\log k_w$ (pH 7.4) and $\log K_i$. It should be noticed that in case of the benzoylglycines significant correlations were only obtained after exclusion of the 2-OH analog from BLMV and BBMV(pH) and the

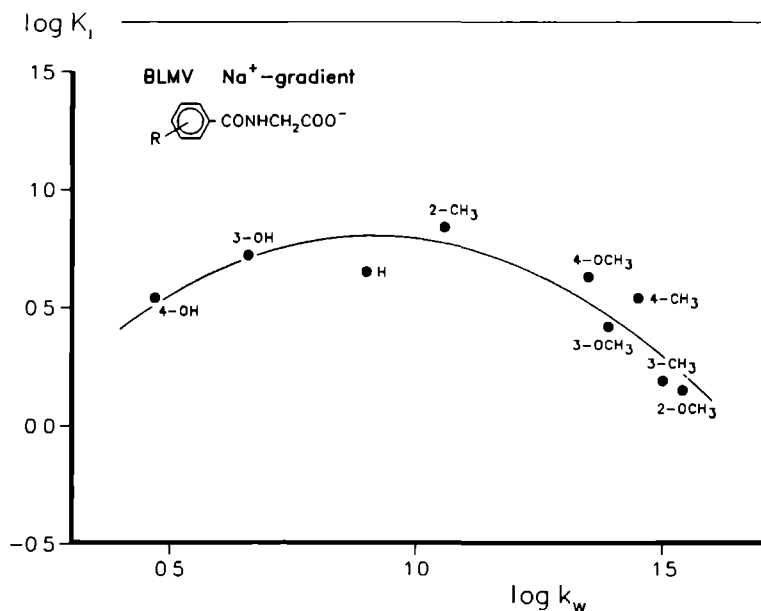


Fig. 11.1 Correlation between the logarithm of the apparent inhibition constant K_i and the capacity factor $\log k_w$ determined at pH 7.4, characterizing the effect of substituted benzoylglycines on sodium gradient-dependent PAH uptake into BLMV.

2-OCH₃ analog from BBMV(Na^+). The correlation coefficients in the regressions with $\log k_w$ (pH 7.4) ranged between 0.80 and 0.94, which means that 64-88% of the total variation in $\log K_i$ was due to the hydrophobicity of the compounds at pH 7.4.

11.4 DISCUSSION

A considerable effort has been made to identify the structural properties that determine whether an anion is secreted by the renal organic anion transport system. Sophisticated models have been proposed to rationalize the vast structural diversity in compounds transported [2,6]. However, recently Ullrich et al. [30,31] showed in a series of elaborate microperfusion experiments in the rat that a monocarboxylic or aldehyde

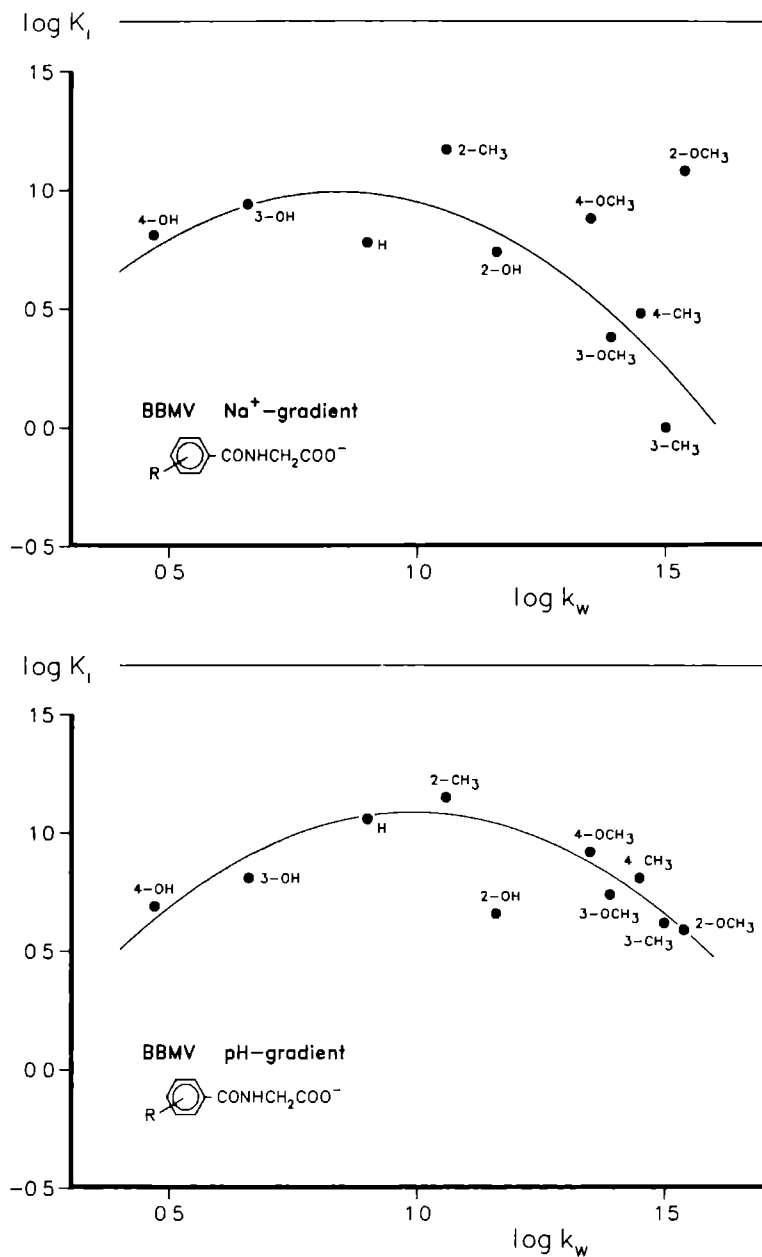


Fig. 11.2 Correlation between the logarithm of the apparent inhibition constant K_i and the capacity factor $\log k_w$ determined at pH 7.4, characterizing the effect of substituted benzoylglycines on sodium gradient-dependent (top) and pH gradient-dependent PAH uptake into BBMV (bottom).

group in combination with a hydrophobic moiety are in fact sufficient to meet the requirements for interaction with the PAH transporter in the basolateral membrane.

In the present study the substrate specificity of PAH transport across basolateral and brush border membranes was tested with a series of closely related hippurate derivatives, and an attempt was made to correlate the affinity of the compounds with their physicochemical properties. The relative hydrophobicity of the glycine conjugates was determined by reversed phase HPLC. It is now well established that retention parameters, in particular the extrapolated capacity factor for an aqueous eluent ($\log k_w$), are very useful for the assessment of the hydrophobic nature of drugs [32]. An important advantage of $\log k_w$ over the classic *n*-octanol-water partition coefficient is the possibility of accurately determining the hydrophobicity of ionized solutes.

The results of the present study show that, apart from two outliers (2-OH- and 2-OCH₃-benzoylglycine), the hydrophobic properties of the ionized glycine conjugates are the primary determinants of their inhibitory effect on PAH transport in BLMV and BBMV. This indicates that hydrophobic as well as electronic properties are decisive for substrate affinity. Benzoylglycines were better inhibitors than phenylacetyl-glycines, indicating that insertion of a CH₂-group between the ring and the carbonyl reduces the influence of the ring and its substituent on the inhibitory potency.

It was very remarkable that we could not observe an inhibitory effect of 2-OH-benzoylglycine on PAH transport in BLMV, all the more since it is well-known that this compound is actively secreted by the kidney in vivo [33]. An explanation for this unexpected behavior may be related with the unique capacity of this compound to form an intramolecular hydrogen bond between the hydroxy and carbonyl group. Fixation of the carbonyl in an intramolecular hydrogen bond may hinder the interaction with the carrier, thus preventing the compound from being transported. A similar mechanism has been suggested for 2-acetamidohippurate, to explain why this compound is not or practically not actively secreted by the kidney [6]. However, it remains unclear why in vivo 2-OH-benzoylglycine is readily excreted by tubular secretion. It is conceivable that under in vivo conditions intramolecular hydrogen bonding is

less favourable. Another explanation, however more tentative, may be that 2-OH-benzoylglycine is also in vivo not transported by the PAH carrier but by a distinct transport system (urate carrier?) in the basolateral membrane. The inhibitory potency of 2-OH-benzoylglycine against PAH transport in BBMV was apparently not affected by intramolecular hydrogen bonding. On the contrary, pH-dependent PAH uptake was even stronger inhibited than predicted from the relation with $\log k_w$.

The inhibitory pattern of the glycine conjugates on sodium- and pH-dependent PAH uptake in BBMV was comparable, except for 2-OCH₃-benzoylglycine. This compound clearly inhibited pH-dependent transport in accordance with its hydrophobicity, while it had an unexpected weak inhibitory effect on Na⁺-dependent transport. Steric hindrance of the bulky 2-methoxy group may be involved, indicating a difference in substrate specificity between Na⁺- and pH-dependent PAH transport. This would support the hypothesis that Na⁺- and pH-dependent PAH transport across the brush border membrane are separate transport routes.

Acknowledgements

The authors are indebted to Mr. H. van Deelen and Dr. A.J. Beld for the preparation of the glycine conjugates and to Mrs. B. van de Camp for the determination of the numerous capacity factors.

11.5 REFERENCES

1. J. Caldwell, in *Metabolic Basis of Detoxication* (Eds. W.B. Jakoby, J.R. Bend and J. Caldwell), p271. Academic Press, New York (1982).
2. J.V. Møller and M.I. Sheikh, *Pharmacol. Rev.* **34**, 315 (1983).
3. I.M. Weiner, in *The Kidney: Physiology and Pathophysiology* (Eds. D.W. Seldin and G. Giebisch), p1703. Raven Press, New York (1985).
4. P.K. Knoefel and K.C. Huang, *J. Pharmacol. Exp. Ther.* **117**, 307 (1956).
5. J.J. Grantham and A.M. Chenko, in *The Kidney* (Eds. B.M. Brenner and F.C. Recktor), p663. W.B. Saunders Company, Philadelphia (1986).

6. A. Despopoulos, J. Theoret. Biol. 8, 163 (1965).
7. A. Essig and J.V. Taggart, Am. J. Physiol. 199, 509 (1960).
8. C.R. Ross and P.D. Holohan, Ann. Rev. Pharmacol. Toxicol. 23, 65 (1983).
9. J.L. Kinsella, P.D. Holohan, N.I. Pessah and C.R. Ross, J. Pharmacol. Exp. Ther. 209, 443 (1979).
10. J.S. Kashner, P.D. Holohan and C.R. Ross, J. Pharmacol. Exp. Ther. 227, 122 (1983).
11. J. Eveloff, Biochem. Biophys. Acta 897, 474 (1987).
12. A.M. Kahn and P.S. Aronson, Am. J. Physiol. 244, F56 (1983).
13. I. Kippen, B. Hirayama, J.R. Kleinberg and E.M. Wright, Biochim. Biophys. Acta 556, 161 (1979).
14. R. Hori, M. Takano, T. Okano, S. Kitazawa and K. Inui, Biochem. Biophys. Acta, 692, 97 (1982).
15. F.G.M. Russel, P.E.M. van der Linden, W.G. Vermeulen and C.A.M. van Ginneken, Br. J. Pharmacol. 89, 513P (1986).
16. F.G.M. Russel, P.E.M. van der Linden, W.G. Vermeulen, M. Heijn, C.H. van Os and C.A.M. van Ginneken, submitted for publication.
17. S.J. Schwab, S. Klahr and M.R. Hammerman, Am. J. Physiol. 246, F663 (1984).
18. T. Yamana, A. Tsuji, E. Miyamoto and O. Kubo, J. Pharm. Sci. 66, 747 (1977).
19. C.M. Metzler, G.L. Elfring and A.J. McEwen, Biometrics 30, 562 (1974).
20. DISSPLA user's manual, Version 9.2, Integrated Software Systems Corporation, San Diego, Ca. (1984).
21. A. Vogel, Vogel's Practical Organic Chemistry, p885. Longman, London (1978).
22. S.M. McElvain and T.P. Carney, J. Am. Chem. Soc. 68, 2592 (1946).
23. W. van Brussel and C.F. van Sumere, Bull. Soc. Chim. Belg. 87, 791 (1978).
24. E. Solheim and R.R. Scheline, Xenobiotica 3, 493 (1973).
25. J.W. ApSimon, D.G. Durham and A.H. Rees, J. Chem. Soc., Perkin Trans. 1 12, 1588 (1978).
26. Beilstein's Handbuch der Organischen Chemie, Vierte Auflage, Band IX, p465, 477, 487. Julius Springer, Berlin (1926).
27. A.J. Quick, J. Biol. Chem. 97, 403 (1932).

28. E. Salkowski and H. Salkowski, *Berichte* **12**, 653 (1879).
29. F.G.M. Russel, M. Heijn, and C.A.M. van Ginneken, submitted for publication.
30. K.J. Ullrich, G. Rummrich, G. Fritsch and S. Klöss, *Pflügers Arch.* **408**, 38 (1987).
31. K.J. Ullrich, G. Rummrich, and S. Klöss, *Pflügers Arch.* **409**, 547 (1987).
32. T. Braumann, *J. Chromatogr.* **373**, 191 (1986).
33. F.G.M. Russel, A.C. Wouterse and C.A.M. van Ginneken, *Drug Metab. Dispos.* **15**, 695 (1987).

The renal organic anion transport system is responsible for the facilitated elimination of endogenous metabolites and foreign substances, which are not easily degraded by the body. Many of these substances are drugs, and the mode of their renal secretion largely determines their disposition and consequently, their pharmacological response. Since carrier-mediated processes are involved, the potential problem of saturation and competition may be the basis for a variety of clinical implications. Therefore, knowledge of the basic processes that determine the active tubular secretion of anionic drugs is of great practical importance.

The investigations described in this thesis were focused on the mechanisms and interactions of organic anion transport in the dog kidney. After a general introduction, the thesis is organized around three major themes, i.e., a new physiologically based modeling approach to describe the excretion kinetics of anionic drugs and their interactions, the substrate specificity of organic anion secretion for a series of closely related substituted hippurates, and the mechanisms of organic anion transport at a subcellular level.

Introduction

In Chapter 1 an introduction into the present state of knowledge of the renal handling of organic anions is given. The proximal tubular cells of the kidney are the main anatomical site of the carrier-mediated secretion of anionic drugs. Organic anions are actively transported at the basolateral membrane, concentrated intracellularly, and subsequently transported from the cell into the tubular lumen by mediated diffusion. One of the remarkable features of the organic anion secretory system is that it accepts a wide variety of substances which may compete with each other for transport. The clinical implications of anionic drug secretion are discussed briefly.

Chapter 2 describes a technique for the quantitative collection of urine in renal clearance studies in the dog. Quantitative urine collection is of crucial importance for accurately assessing the urinary excretion of a drug. A double-walled urinary catheter has been developed which allows

rapid and quantitative urine collection at short time intervals down to 5 min. The catheter consists of a polyurethane outer cannula in which a small Teflon cannula is inserted. The essential of the catheter is that at the end of a collection period residual urine in the bladder is collected completely via the outer cannula by flushing the bladder with physiological saline through the inner cannula. The use of the catheter was demonstrated in a study on the renal clearance of hippurate.

Physiologically Based Kidney Model

In this part a physiologically based pharmacokinetic model of the kidney is proposed, as accurate but also as simple as possible, that is able to describe and quantify the relevant processes of tubular secretion and competition. The model incorporates the functional characteristics of the kidney that determine the excretion of many anionic drugs, i.e., renal plasma flow, urine flow, nonlinear protein binding, glomerular filtration, tubular secretion, and tubular accumulation.

In Chapter 3 the plasma kinetics and renal excretion of intravenous phenolsulfonphthalein (PSP, 1.0 g), with and without concomitant infusion of probenecid or salicylic acid (SUA) are studied in 6 male beagle dogs. Tubular secretion is an important route of PSP excretion, and secretion is inhibited by probenecid as well as SUA. The kidney model enabled an accurate description of the measured plasma levels and renal excretion rates of PSP. The average values of the parameters characterizing the tubular transport maximum (T_M) and the apparent affinity for the secretory system (K_T) were: $T_M = 6.6 \pm 1.6$ mg/min and $K_T = 16 \pm 4$ μ g/ml. The interaction with probenecid and SUA could be adequately accounted for by inhibition of the carrier-mediated uptake of PSP into the tubular cells. But both compounds differed clearly in their inhibitory action. Whereas probenecid showed simple competitive inhibition ($K_I = 7 \pm 6$ μ g/ml), for SUA a considerably more complex interaction (two-site competitive system) had to be taken into consideration ($K_I = 24 \pm 6$ μ g/ml). Especially in the interaction experiments, only satisfactory fits to the model were obtained when secretion was assumed to be dependent on unbound PSP concentrations. Model calculations predicted a pronounced accumulation of PSP within the proximal tubular cells, which was clearly diminished in presence of probenecid or SUA.

Chapter 4 reports on the renal clearance of SUA (0.8 g, i.v.) and the interaction with PSP in 4 dogs. Despite its considerable binding to plasma proteins, SUA is almost completely extracted from the renal plasma at low concentrations, indicating that protein binding does not limit the extent of its tubular secretion. Analysis with the kidney model revealed that PSP inhibited the active uptake of SUA into the tubular cells in a noncompetitive fashion ($T_M = 4.3 \pm 0.6$ vs. 3.3 ± 0.7 mg/min; paired t-test $p < 0.05$, $K_T = 31 \pm 5$ vs. 32 ± 12 μ g/ml; $p > 0.3$). Furthermore, a small but significant reduction in nonrenal SUA clearance was observed (14 ± 3 vs. 11 ± 3 ml/min; $p < 0.05$). The model-predicted cellular accumulation ratios were in accordance with previously reported in vitro values, and were decreased considerably in presence of PSP.

The last chapter of Part II (Chapter 5) is concerned with the renal handling of iodopyracet and the influence of probenecid in 4 dogs. Iodopyracet is weakly bound to plasma proteins and its renal clearance is characterized by supply-limited elimination at low plasma concentrations and, just as the foregoing compounds, capacity-limited elimination at high plasma levels ($T_M = 32 \pm 6$ mg/min, $K_T = 36 \pm 8$ μ g/ml). Also for iodopyracet, model calculations showed a substantial tubular accumulation, which was reduced by probenecid as a result of competitive inhibition of the active cellular uptake ($K_I = 8 \pm 3$ μ g/ml).

Substituted Hippurates

The renal clearance of a series of mono-substituted benzoylglycines (hippurates) was investigated, in order to determine systematically the influence of ring substitution on the excretory characteristics of benzoylglycine. The physiologically based kidney model was applied to analyze the plasma and renal excretion kinetics of the benzoylglycines. The compounds were administered in a dose of about 1 gram (i.v.) to 3 beagle dogs.

Chapter 6 describes the renal handling of benzoylglycine (hippurate) and methyl-substituted benzoylglycines. Benzoylglycine and the 3- and 4-methyl analogs showed nonlinear plasma protein binding varying between 20 and 80% over a concentration range of 5 - 450 μ g/ml. For 2-methylbenzoylglycine an extremely high protein binding of almost 100% was observed at low plasma concentrations (< 50 μ g/ml). All conjugates

were largely excreted via the kidney (>80% of the dose) and tubular secretion appeared to be a function of the total drug concentration in renal plasma, except for the 2-methyl analog, presumably due to its tight protein binding. The average values of the kinetic parameters characterizing tubular secretion were: benzoylglycine $T_M = 5.5 \pm 0.8$ mg/min, $K_T = 40 \pm 5$ μ g/ml; 3-methylbenzoylglycine $T_M = 7.1 \pm 3.3$ mg/min, $K_T = 49 \pm 1$ μ g/ml; 4-methylbenzoylglycine $T_M = 8.0 \pm 1.6$ mg/min, $K_T = 14 \pm 6$ μ g/ml. Tubular secretion of 2-methylbenzoylglycine was not saturated. Accordingly, only the intrinsic secretion clearance (CL_{int}) $T_M/K_T = 163 \pm 54$ ml/min could be calculated. An interesting observation was the partial deconjugation of 4-methylbenzoylglycine to its corresponding benzoate. 4-Methylbenzoate was only found in plasma and not in urine, indicating that the benzoate was either cleared extrarenally, or completely metabolized during transfer through the kidney.

In Chapter 7 the plasma kinetics and renal excretion of 4-aminobenzoylglycine (p-aminohippurate) and hydroxy-substituted benzoylglycines were studied. Plasma protein binding of 4-amino-, 3-hydroxy-, and 4-hydroxybenzoylglycine was low and constant (<15%), while the 2-hydroxy analog showed concentration-dependent protein binding ranging from 40 - 80%. The excretory patterns of the 4-amino, 3- and 4-hydroxy analogs were essentially the same; rapid elimination from plasma into urine (>80% of the dose), mainly by very efficient supply-limited tubular secretion. Conversely, the excretion of 2-hydroxybenzoylglycine was characterized by a lower plasma clearance and total renal excretion (64% of the dose), and a limited capacity of the tubular secretory system. The kinetic parameters characterizing its tubular secretion were, $T_M = 4.4 \pm 0.9$ mg/min and $K_T = 23 \pm 8$ μ g/ml. Since secretion of the other compounds was not saturated, only the CL_{int} was estimated: 4-amino- $CL_{int} = 145 \pm 50$ ml/min, 3-hydroxy- $CL_{int} = 194 \pm 21$ ml/min, and 4-hydroxybenzoylglycine $CL_{int} = 153 \pm 23$ ml/min.

Finally, in Chapter 8 the renal clearance of methoxy-substituted benzoylglycines is characterized. Their plasma protein binding varied between 10 and 70%. The methoxybenzoylglycines were rapidly cleared from plasma, largely by renal excretion (72 -84% of the dose). Tubular secretion of 2- and 3-methoxybenzoylglycine was saturated, while the clearance capacity of the secretory system for the 4-methoxy analog was

so high that complete saturation was not achieved. The kinetic parameters were: 2-methoxy- $T_M = 11.7 \pm 4.9$ mg/min, $K_T = 42 \pm 9$ μ g/ml; 3-methoxy- $T_M = 8.8 \pm 1.0$ mg/min, $K_T = 27 \pm 20$ μ g/ml; 4-methoxybenzoylglycine $CL_{int} = 201 \pm 47$ ml/min. The 4-methoxy analog was metabolized to some extent by deconjugation of the glycine moiety and the resulting benzoate was found in plasma but not in urine.

Taking the results of Part III together, it can be concluded that introduction of a substituent in the ring of benzoylglycine results in general in a substance for which the renal secretory system has a higher clearance capacity. The most extensive tubular secretion was found for the 4-amino, 3-hydroxy, and 4-hydroxy substitutes, while the extent of secretion of 2-hydroxybenzoylglycine was small, even less than that of benzoylglycine. In between, a large diversity in excretory characteristics exists.

Isolated Membrane Vesicles

The carrier systems which control the transtubular transport of organic anions are confined to the plasma membranes of the proximal tubular cells, i.e., the basolateral and brush border membrane. Isolation of these membranes provides an important tool for studies directed at the molecular mechanisms of transport at specific membrane sites.

Chapter 9 describes a technique for the isolation of basolateral (BLMV) and brush border membrane vesicles (BBMV) from dog kidney cortex. The transport of p-aminohippurate (PAH) was studied in these vesicles. Imposition of an inwardly directed sodium gradient (100 mM) stimulated the uptake of 50 μ M [3 H]PAH into BLMV, whereas a pH gradient ($pH_{out} = 6.0$, $pH_{in} = 7.4$) only slightly enhanced uptake. The sodium gradient-dependent uptake of PAH was electroneutral, saturable, and sensitive to inhibition by probenecid and several anionic drugs, with (apparent) $K_m = 0.79 \pm 0.16$ mM, $V_{max} = 0.80 \pm 0.05$ nmol/mg protein, 15 sec, and $K_{i,prob} = 0.08 \pm 0.01$ mM. Simultaneous imposition of the pH gradient (outward hydroxyl gradient) and inward sodium gradient stimulated PAH uptake significantly over that with a sodium gradient alone, suggesting a sodium gradient-stimulated PAH/ OH^- exchange mechanism.

In BBMV, PAH uptake could be stimulated by an outwardly directed hydroxyl gradient as well as an inward sodium gradient. Both gradients

could drive PAH transport via a mediated probenecid-sensitive pathway. Sodium-gradient stimulated uptake was electrogenic with a (apparent) $K_m = 4.93 \pm 0.57$ mM, $V_{max} = 6.71 \pm 0.36$ nmol/mg protein, 15 sec, and $K_{i,prob} = 0.13 \pm 0.01$ mM. The kinetic parameters for PAH/hydroxyl exchange were virtually the same, (apparent) $K_m = 5.72 \pm 0.49$ mM, $V_{max} = 7.87 \pm 0.33$ nmol/mg protein, 15 sec, and $K_{i,prob} = 0.16 \pm 0.02$ mM. Imposition of both the sodium and pH gradient stimulated uptake almost twofold over that with either a sodium or pH gradient alone. These results suggested that both gradients stimulate PAH transport in BBMV via the same pathway. However, inhibition experiments with various organic anions showed that the specificities of sodium and pH gradient-stimulated uptake did not entirely overlap. Thus, it may be possible that two separate pathways are involved.

In Chapter 10 the substrate specificity of the organic anion secretory system was studied by looking at the effect of substituted benzoates on the sodium-dependent PAH uptake into BLMV and the sodium- or pH-dependent uptake into BBMV. Practically all benzoates showed an inhibitory effect on PAH transport in BLMV and BBMV; the strongest inhibitors were 3-Cl- and 4-Cl-benzoate, while the weakest inhibition was found for the 3-NH₂ and 4-NH₂ substitutes. The apparent inhibition constant (K_i) correlated significantly with the relative hydrophobicity of the ionized benzoates (determined by HPLC), indicating that hydrophobic and electronic properties are the main determinants of affinity for the PAH transport system.

The final chapter (Chapter 11) deals with the effect of substituted benzoylglycines (hippurates) and phenylacetylglucines on PAH transport in BLMV and BBMV. Benzoylglycines were stronger inhibitors of PAH transport than phenylacetylglucines and the inhibitory potency of the conjugates was in general lower against transport into BBMV than BLMV. The strongest inhibitory effect was found with 2-OCH₃- and 3-CH₃-benzoylglycine on BLMV and pH-dependent BBMV transport, while only the 3-CH₃ analog was a strong inhibitor of sodium-dependent BBMV transport. Strikingly, 2-OH-benzoylglycine did not inhibit PAH transport in BLMV, while it clearly inhibited BBMV transport. It is suggested that intramolecular hydrogen bonding hinders the carbonyl from interaction with the carrier, thus preventing transport. Apparently, the carbonyl

group is not essential for transport into BBMV. The K_i values of the glycine conjugates correlated parabolically with the relative hydrophobicity of the ionized compounds. This indicates that also for the glycine conjugates, hydrophobic and electronic properties are important determinants of affinity for the PAH transport system.

Concluding Remarks

In this thesis a physiologically based pharmacokinetic model of the kidney has been presented, that was used to analyze the renal clearance of organic anions. In combination with an accurate and frequent urine sampling technique, the model appeared to be a useful tool for the quantitative assessment of the mechanisms that govern the renal excretion of anionic drugs. Furthermore, the model enabled a comprehensive characterization of drug interactions at the level of tubular secretion. Future work has to be aimed at incorporating the mechanisms of active and passive reabsorption to make it applicable to a broader range of compounds. Of course, scaling-up the model to the human situation will be the ultimate goal.

The different types of interactions that were observed in the clearance experiments with PSP and SUA are clearly in favor of the concept of a functional heterogeneity of the renal organic anion secretion system. The studies with the isolated membrane vesicles also provided supporting evidence for this hypothesis. At least for the brush border membrane there were strong indications to suggest separate transport systems with overlapping specificities. To solve the intriguing puzzle of transport multiplicity, more detailed membrane vesicle studies on the interaction between systems which may influence organic anion transport are required, in combination with a greater emphasis on cell and tubule preparations to examine the various pathways under physiological conditions, and to translate these findings to the *in vivo* situation.

Een van de belangrijke functies die de nier in het lichaam vervult is de selectieve verwijdering van afbraakproducten en lichaamsvreemde stoffen. Voor deze veelomvattende taak beschikt het orgaan over een aantal transportsystemen die elk een bepaalde stof of een groep van stoffen kunnen herkennen. Onderwerp van dit proefschrift is het organisch-aniontransportsysteem in de nier. Naast de uitscheiding van enkele endogene substanties zorgt dit systeem er voor dat lichaamsvreemde anionen, waaronder vele geneesmiddelen en metabolieten, op efficiënte wijze uit het lichaam worden verwijderd. De mate van actieve renale uitscheiding zal sterk bepalend zijn voor de duur en intensiteit van werking en bijwerkingen van deze geneesmiddelen. Bovendien zijn er bij dit transport carrier-gemedieerde processen betrokken waardoor er kans op verzadiging en competitie bestaat, wat niet zelden leidt tot een noodzakelijke aanpassing van de farmacotherapie. Een grondige kennis van de processen die een rol spelen bij de actieve uitscheiding van anionische-geneesmiddelen is derhalve van eminent belang.

De experimenten beschreven in dit proefschrift zijn gewijd aan de mechanismen en interacties van het organisch-aniontransport in de nier van de hond. Na een algemene inleiding is het geheel opgebouwd rond een drietal thema's namelijk, fysiologisch-farmacokinetisch modelleren van transport in de nier, specificiteit van anionsecretie voor een reeks van gesubstitueerde hippuraten en mechanismen en interacties van organisch-aniontransport op subcellulair niveau.

Inleiding

Hoofdstuk 1 geeft een overzicht van de huidige stand van zaken op het gebied van de renale klaring van organische anionen. Het aniontransportsysteem is gelocaliseerd in de cellen van de proximale tubulus. Organische anionen worden actief opgenomen aan de basolaterale membraan waarbij hoge intracellulaire concentraties worden bereikt. Vervolgens worden ze in het tubulaire lumen getransporteerd via gefaciliteerde diffusie door de brush-border membraan. Een opmerkelijke eigenschap van het organisch-aniontransportsysteem is dat het een enorme

verscheidenheid aan verbindingen accepteert die met elkaar kunnen competieren voor transport. De klinische implicaties van de tubulaire secretie van geneesmiddelen worden in het kort besproken.

Hoofdstuk 2 beschrijft een methode voor de kwantitatieve monsterring van urine bij renale klaringstudies in de hond. Het kwantitatief verzamelen van urine is van doorslaggevend belang voor een nauwkeurige analyse van de renale excretie van een geneesmiddel. Voor dit doel is een dubbelwandige blaascatheter ontworpen waarmee urine, snel en kwantitatief, in tijdsintervallen van 5 min kan worden verzameld. De catheter bestaat uit een buitencanule van polyurethaan waarin zich een dunne Teflon-canule bevindt. Het principe van de catheter is dat urine, die aan het eind van een verzamelperiode in de blaas is achtergebleven, volledig verzameld kan worden via de buitencanule door de blaas via de binnencanule te spoelen met een fysiologische-zoutoplossing. Aan de hand van een studie naar de renale klaring van hippuursuur is het gebruik van de catheter gedemonstreerd.

Semifysiologisch Niermodel

In Deel II van het proefschrift wordt een farmacokinetisch model van de nier beschreven dat is gebaseerd op fysiologische overwegingen en waarmee het mogelijk is de processen die van belang zijn voor tubulaire secretie en competitie te kwantificeren. Het model bevat de functionele eigenschappen van de nier die van invloed zijn op de excretie van vele anionische-geneesmiddelen dwz., de renale-plasmaflow, de urineflow, niet-lineaire eiwitbinding, glomerulaire filtratie, tubulaire secretie en tubulaire accumulatie.

In Hoofdstuk 3 is het verloop van de plasmaconcentratie en renale excretie van phenolsulfonphthaleïne (PSP, 1.0 g i.v.) in 6 mannelijke honden (beagles) bestudeerd. Tevens is gekeken naar het effect van gelijktijdige infusie van probenecide of salicylzuur (SUA). Tubulaire secretie is voor PSP een belangrijke excretieroute en probenecide en SUA remmen beide dit transportproces. Met het niermodel bleek het mogelijk een nauwkeurige beschrijving te verkrijgen van de experimentele plasma- en urinegegevens van PSP. De gemiddelde waarden van de parameters die het tubulaire-transportmaximum (T_M) en de schijnbare affiniteit voor het secretoire systeem (K_T) weergeven waren, $T_M = 6.6 \pm 1.6$ mg/min en $K_T =$

16 ± 4 µg/ml De interactie met probenecide en SUA kon adequaat worden beschreven door een remming te veronderstellen van de carrier-gemedieerde opname in de tubuluscel. Beide verbindingen verschilden echter duidelijk in hun remmende werking. Probenecide vertoonde een eenvoudige competitieve interactie ($K_I = 7 \pm 6 \mu\text{g/ml}$), terwijl voor SUA een aanmerkelijk gecompliceerder mechanisme (een competitief systeem met twee bindingsplaatsen) noodzakelijk was om de interactie te verklaren ($K_I = 24 \pm 6 \mu\text{g/ml}$). Met name in de interactie-experimenten konden alleen bevredigende fits worden verkregen wanneer werd aangenomen dat de tubulaire secretie een functie van de vrije PSP-plasmaconcentratie is. Modelberekeningen voorspelden een uitgesproken accumulatie van PSP in de proximale-tubuluscellen, die duidelijk verminderde in aanwezigheid van probenecide of SUA.

Hoofdstuk 4 rapporteert over de renale klaring van SUA (0.8 g, i.v.) en de interactie met PSP in 4 honden. Ondanks een aanzienlijke binding aan plasmaeiwitten wordt SUA bij lage concentraties vrijwel volledig door de nier geklaard. Dit betekent dat eiwitbinding geen beperking vormt voor de tubulaire secretie van SUA. Analyse van de interactie met PSP leverde een non-competitieve remming van de actieve opname van SUA in de tubuluscel op ($T_M = 4.3 \pm 0.6$ vs 3.3 ± 0.7 mg/min, gepaarde t-test $p < 0.05$, $K_T = 31 \pm 5$ vs $32 \pm 12 \mu\text{g/ml}$, $p > 0.3$). Daarnaast werd een kleine maar significante daling van de niet-renale klaring van SUA gevonden (14 ± 3 vs 11 ± 3 ml/min, $p < 0.05$). De met het model berekende cellulaire accumulatie-ratio's komen goed overeen met eerder in de literatuur beschreven in-vitro waarden. De ratio's waren aanzienlijk verlaagd in aanwezigheid van PSP.

Het laatste hoofdstuk van Deel II (Hoofdstuk 5) is gewijd aan de renale klaring van iodopyracet en de interactie met probenecide in 4 honden. Iodopyracet heeft een zwakke eiwitbinding en een renale klaring die wordt gekenmerkt door een flow-beperkte eliminatie bij lage plasmaconcentraties en, net als PSP en SUA, een capaciteits-beperkte eliminatie bij hoge concentraties ($T_M = 32 \pm 6$ mg/min, $K_T = 36 \pm 8 \mu\text{g/ml}$). Ook voor iodopyracet voorspelden de modelberekeningen een aanzienlijke tubulaire accumulatie, die wordt gereduceerd door probenecide als gevolg van een competitieve remming van de cellulaire opname van iodopyracet ($K_I = 8 \pm 3 \mu\text{g/ml}$).

Gesubstitueerde Hippuraten

In een systematisch onderzoek naar de invloed van de ringsubstituent op de excretiekenmerken van benzoylglycine (hippuurzuur) is de renale klaring van een reeks mono-gesubstitueerde benzoylglycines bestudeerd. Het eerder beschreven semifysiologische niermodel werd gebruikt om de experimentele plasma- en urinegegevens te analyseren. De benzoylglycines werden in een dosis van 1 gram intraveneus toegediend aan 3 honden.

Hoofdstuk 6 beschrijft de renale klaring van benzoylglycine en de methyl-gesubstitueerde benzoylglycines. Benzoylglycine en de 3- en 4-methyl-analoga vertoonden niet-lineaire plasma-eiwitbinding die varieerde van 20 tot 80% over een concentratiegebied van 5 - 450 µg/ml. In het geval van 2-methylbenzoylglycine werd bij lage plasmaconcentraties (<50 µg/ml) een extreem hoge eiwitbinding van bijna 100% gevonden. Alle glycineconjugaten werden voor het grootste deel via de nieren uitgescheiden (>80% van de dosis). Tubulaire secretie bleek een functie te zijn van de totale plasmaconcentratie met uitzondering van 2-methylbenzoylglycine, hetgeen mogelijk te wijten is aan de sterke eiwitbinding van deze stof. De gemiddelde waarden van de kinetische parameters voor tubulaire secretie waren: benzoylglycine $T_M = 5.5 \pm 0.8$ mg/min, $K_T = 40 \pm 5$ µg/ml, 3-methylbenzoylglycine $T_M = 7.1 \pm 3.3$ mg/min, $K_T = 49 \pm 1$ µg/ml, 4-methylbenzoylglycine $T_M = 8.0 \pm 1.6$ mg/min, $K_T = 14 \pm 6$ µg/ml. Omdat de tubulaire secretie van 2-methylbenzoylglycine niet verzadigd was, kon voor deze verbinding alleen de intrinsieke secretieklaring (CL_{int}) $T_M/K_T = 163 \pm 54$ ml/min worden berekend. Een interessante waarneming was de gedeeltelijke deconjugatie van 4-methylbenzoylglycine tot het corresponderende benzoaat. 4-Methylbenzoaat werd alleen in plasma aangetroffen en niet in urine, hetgeen erop duidt dat het benzoaat ofwel extra-renaal geklaard wordt of volledig gemetaboliseerd wordt tijdens het transport door de nier.

In Hoofdstuk 7 zijn de plasmakinetiek en renale excretie van 4-aminobenzoylglycine (p-aminhippuurzuur) en de hydroxy-gesubstitueerde benzoylglycines bestudeerd. De plasma-eiwitbinding van 4-amino-, 3-hydroxy- en 4-hydroxybenzoylglycine was laag en constant (<15%), terwijl voor 2-hydroxybenzoylglycine concentratie-afhankelijke eiwitbinding (40 - 80%) werd gevonden. Het uitscheidingspatroon van de

4-amino-, 3- en 4-hydroxy-analoga was vrijwel hetzelfde een snelle klaring vanuit het plasma naar de urine (>80% van de dosis), voornamelijk door zeer efficiënte flow-beperkte tubulaire secretie. Daarentegen kenmerkte de excretie van 2-hydroxybenzoylglycine zich door een lagere plasmaklaring, een lagere totale renale excretie (64% van de dosis) en een beperkte capaciteit van het tubulaire-secretoire systeem. De kinetische parameters van de tubulaire secretie van 2-hydroxybenzoylglycine waren, $T_M = 4.4 \pm 0.9$ mg/min en $K_T = 23 \pm 8$ µg/ml. Omdat de tubulaire secretie van de andere glycines niet verzadigd was kon alleen de CL_{int} worden berekend: 4-amino- $CL_{int} = 145 \pm 50$ ml/min, 3-hydroxy- $CL_{int} = 194 \pm 21$ ml/min en 4-hydroxybenzoylglycine $CL_{int} = 153 \pm 23$ ml/min.

In Hoofdstuk 8 is tenslotte de renale klaring van de methoxy-gesubstitueerde benzoylglycines gemeten. Plasma-eiwitbinding was niet-lineair en varieerde van 10 tot 70% en de klaring uit het plasma was snel, voor het grootste deel via renale excretie (72 - 84% van de dosis). De tubulaire secretie van 2- en 3-methoxybenzoylglycine was verzadigd, terwijl de klaringscapaciteit van het tubulaire systeem voor 4-methoxybenzoylglycine te groot was om volledige verzadiging te bereiken. De kinetische parameters waren: 2-methoxy- $T_M = 11.7 \pm 4.9$ mg/min, $K_T = 42 \pm 9$ µg/ml, 3-methoxy- $T_M = 8.8 \pm 1.0$ mg/min, $K_T = 27 \pm 20$ µg/ml en 4-methoxybenzoylglycine $CL_{int} = 201 \pm 47$ ml/min. 4-Methoxybenzoylglycine werd voor een deel gemetaboliseerd door deconjugatie van de glycinegroep. Ook hier werd het gevormde benzoaat alleen in plasma gevonden en niet in de urine.

De resultaten van Deel III samenvattend kan worden geconcludeerd dat introductie van een substituent in de benzeenring van benzoylglycine in het algemeen leidt tot een substantie waarvoor het tubulaire-secretoire systeem een grotere klaringscapaciteit heeft. De meest efficiënte tubulaire secretie werd gevonden voor de 4-amino-, 3-hydroxy- en 4-hydroxy-analoga, terwijl de mate van tubulaire secretie voor 2-hydroxybenzoylglycine zelfs geringer was dan die voor benzoylglycine. Tussen deze uitersten bestaat er een grote verscheidenheid aan klaringskarakteristieken.

Geïsoleerde Membraanvesicles

De carriersystemen die het transtubulair transport van organische anionen controleren bevinden zich in de plasmamembranen van de proximale-tubuluscel te weten, de basolaterale membraan en de brush-border membraan. Isolatie van deze membranen maakt het mogelijk om de moleculaire mechanismen van het transport in elk van de membranen afzonderlijk te bestuderen.

Hoofdstuk 9 beschrijft een methode voor de isolatie van basolaterale (BLMV) en brush-border membraanvesicles (BBMV) uit de cortex van de hondenier. Met behulp van deze vesicles werden de transporteigenschappen van p-aminohippuurzuur (PAH) bestudeerd. De aanwezigheid van een naar binnen gerichte natriumgradient (100 mM) stimuleerde de opname van 50 μM [^3H]PAH in BLMV, terwijl een pH-gradient ($\text{pH}_{\text{buiten}} = 6.0$, $\text{pH}_{\text{binnen}} = 7.4$) slechts een geringe verhoging van de opname gaf. De natriumafhankelijke opname van PAH was electroneutraal, verzadigbaar en gevoelig voor competitie met probenecide en verschillende andere organische anionen. De kinetische parameters van transport waren (schijnbare) $K_m = 0.79 \pm 0.16$ mM, $V_{\text{max}} = 0.80 \pm 0.05$ nmol/mg eiwit, 15 sec en $K_{i,\text{prob}} = 0.08 \pm 0.01$ mM. De gelijktijdige aanwezigheid van de pH-gradient (naar buiten gerichte hydroxylgradient) en een inwaartse natriumgradient stimuleerde de PAH-opname tot significant hogere waarden dan die in aanwezigheid van alleen een natriumgradient. Deze bevindingen suggereerden de aanwezigheid van een natriumgekoppeld-PAH/ OH^- -uitwisselingsmechanisme in de basolaterale membraan.

In de BBMV kon de PAH opname met zowel een uitwaarts-gerichte hydroxylgradient als een inwaartse natriumgradient worden gestimuleerd. Het transport van PAH vertoonde onder invloed van beide gradienten de kenmerken van carrier-gemedieerd en probenecide-gevoelig transport. Natriumgradient-gestimuleerd transport was electrogeen en de kinetische parameters waren: (schijnbare) $K_m = 4.93 \pm 0.57$ mM, $V_{\text{max}} = 6.71 \pm 0.36$ nmol/mg eiwit, 15 sec en $K_{i,\text{prob}} = 0.13 \pm 0.01$ mM. De parameters voor het pH-gradient-gestimuleerde transport waren vrijwel hetzelfde: (schijnbare) $K_m = 5.72 \pm 0.49$ mM, $V_{\text{max}} = 7.87 \pm 0.33$ nmol/mg eiwit, 15 sec en $K_{i,\text{prob}} = 0.16 \pm 0.02$ mM. De gelijktijdige aanwezigheid van een natrium- en pH-gradient resulteerde in een tweemaal zo hoge opname van

PAH in vergelijking met de situatie waarin alleen een natrium- of pH-gradient aanwezig was. Deze resultaten suggereren dat beide gradienten het PAH-transport stimuleren via hetzelfde carriersysteem. Competitie-experimenten met verschillende organische anionen toonden echter aan dat de substraatspecificiteiten van natrium- en pH-afhankelijk transport niet geheel met elkaar in overeenstemming zijn. Dit wijst erop dat er zich mogelijk twee afzonderlijke transportsystemen in de brush-border membraan bevinden.

In Hoofdstuk 10 is de substraatspecificiteit van het organisch-aniontransportsysteem onderzocht door te kijken naar het effect van een reeks gesubstitueerde benzoaten op het natriumafhankelijke PAH-transport in BLMV en het natrium- of pH-afhankelijke transport in BBMV. Vrijwel alle benzoaten remden de opname van PAH in BLMV en BBMV. De sterkste remmers waren 3-Cl- en 4-Cl-benzoeaat, terwijl de zwakste remming werd gevonden voor 3-NH₂- en 4-NH₂-benzoeaat. De schijnbare inhibitieconstante (K_i) correleerde significant met de relatieve hydrofobiciteit van de geioniseerde benzoaten (bepaald m.b.v. HPLC). Dit geeft aan dat hydrofobe en electronische eigenschappen beide belangrijke factoren zijn die de affiniteit voor het PAH-transportsysteem bepalen.

Het laatste hoofdstuk (Hoofdstuk 11) behandelt het effect van gesubstitueerde benzoylglycines (hippuraten) en fenylacetylglycines op het transport van PAH in BLMV en BBMV. Benzoylglycines zijn sterkere remmers van het PAH-transport dan fenylacetylglycines en het remmend effect van de glycineconjugaten was in het algemeen minder in BBMV dan BLMV. De sterkste remming werd gevonden voor 2-OCH₃- en 3-CH₃-benzoylglycine op BLMV-transport en pH-afhankelijk BBMV-transport, terwijl alleen 3-CH₃-benzoylglycine een sterk remmend effect op het natriumafhankelijke BBMV-transport had. Het was opmerkelijk dat 2-OH-benzoylglycine helemaal geen remming van het PAH-transport in de BLMV gaf, terwijl de stof wel een duidelijk effect had op het BBMV-transport. Het is mogelijk dat intramoleculaire waterstof-brugvorming de carbonylgroep afschermt waardoor er geen interactie met de carrier in de basolaterale membraan mogelijk is. Kennelijk is de carbonylgroep niet essentieel voor transport door de brush-border membraan. De gevonden K_i -waarden correleerden parabolisch met de relatieve hydrofobiciteit van de geioniseerde

glycineconjugaten. Dit wijst erop dat ook voor deze groep van verbindingen hydrofobe en electronische eigenschappen van belang zijn voor interactie met het PAH-transportstelsel.

Slotopmerkingen

In dit proefschrift is een semifysiologisch niermodel ontwikkeld voor de analyse van de renale klaring van organische anionen. Gecombineerd met een techniek voor de nauwkeurige en frequente verzameling van urinemonsters is gebleken dat het model zeer bruikbaar is voor het kwantificeren van de transportprocessen die van belang zijn bij de renale klaring van organische anionen. Bovendien is gebleken dat interacties op het niveau van de tubulaire secretie op consistente wijze kunnen worden beschreven. In de toekomst zal aandacht moeten worden besteed aan het incorporeren van de processen van actieve en passieve terugresorptie, zodat het model voor een nog bredere groep van verbindingen bruikbaar is. Het mag duidelijk zijn dat het uiteindelijke doel is het model toepasbaar te maken op de humane situatie.

De verschillende interacties die werden waargenomen in de klaringsexperimenten met PSP en SUA pleiten voor het concept van een functionele heterogeniteit van het organisch-aniontransportstelsel. Ook de experimenten met de geïsoleerde membraanvesicles hebben aanwijzingen in die richting opgeleverd. Er zullen echter nog veel gedetailleerde membraanexperimenten noodzakelijk zijn alvorens de intrigerende maar complexe specificiteit van het organisch-aniontransportstelsel, met name in relatie tot verwante systemen, volledig in kaart kan worden gebracht. Daarbij is het van belang dat eveneens aandacht wordt besteed aan intacte cel- en tubuluspreparaten, zodat de verschillende systemen ook onder meer fysiologische omstandigheden worden bestudeerd en de resultaten gemakkelijker naar de in-vivo situatie kunnen worden vertaald.

DANKWOORD

Nu het proefschrift voltooid is, kan ik met dankbaarheid terug kijken op een periode waarin velen met toewijding hebben bijgedragen aan het welslagen van dit onderzoek.

De medewerkers van de afdeling farmacologie ben ik erkentelijk voor de prettige en inspirerende sfeer waarin ik met grote vrijheid de onderzoeken heb kunnen uitvoeren.

Op de eerste plaats gaat mijn bijzondere dank uit naar Fons Wouterse, met wie ik met veel plezier en waardering heb samengewerkt. Op deskundige en inventieve wijze heeft hij de vele in-vivo experimenten voor zijn rekening genomen en uit het grote aantal hoofdstukken in dit proefschrift waaraan zijn naam verbonden is mag blijken dat zijn bijdrage van essentieel belang is geweest. Inmiddels heeft hij getoond ook een vaardig experimentator op het gebied van de geïsoleerde membraanvesicles te zijn.

Dan zijn er de analisten Henk van Deelen, Brigitte van de Camp en Peter van der Linden die in het kader van de WVM-regeling (Werkgelegenheidsverruimende maatregel) niet alleen hun eigen werkgelegenheid verruimden, maar dat ook in ruime mate met de mijne deden.

Henk van Deelen heeft onder leiding van dr. A.J. Beld zorg gedragen voor de synthese van de glycineconjugaten.

Brigitte van de Camp heeft, met name door haar hoge en efficiënte werktempo, onmisbare hulp verleend tijdens de moeizame en langdurige beginperiode waarin gezocht werd naar een geschikte procedure voor de isolatie van membraanvesicles uit de hondenier. Bovendien heeft zij met veel geduld de talrijke capaciteitsfactoren van de gesubstitueerde benzoaten en glycineconjugaten bepaald.

Ook Peter van der Linden heeft een essentieel aandeel gehad in de uiteindelijke ontwikkeling van een isolatieprocedure voor membraanvesicles en later in de ontelbare transportstudies met deze vesicles. Zijn vriendschappelijkheid en gevoel voor humor maakten hem tot een gewaardeerd medewerker van het nog maar pas opgerichte Department of Vesicology. Van hem stamt ook de inmiddels gevleugelde uitspraak: "Vesicologists swing it out!".

Met dank vermeld ik tevens de belangrijke bijdrage aan de vesicle-experimenten van drs. Wim Vermeulen en drs. Marc Heijn, die beiden in het kader van hun doctoraalstudie, respectievelijk Chemie en Humane Biologie, veel werk en nog veel meer filters hebben verzet.

Ook de (stagiaire-)analisten Mübeyyen Köse en Ingrid Meuwssen, en de doctoraalstudent Chemie drs.(geneeskunde) Hugo Jansen, die meewerkten aan onderzoek dat niet meer beschreven is in dit proefschrift, dank ik voor hun bijdrage en prettige samenwerking.

Collega dr. Maikel Raghoobar ben ik erkentelijk voor zijn stimulerende wetenschappelijke interesse in dit onderzoek. Ook ik denk met veel plezier terug aan onze "gezamenlijke sociale en sportieve activiteiten".

Drs. Ger(rit!) van Lingen dank ik voor zijn hulp bij het "uit het stof halen" van NONLIN, het ten volle benutten van DISSPLA en voor de verhelderende discussies over de ware betekenis van de MRT.

De heer Yuen Tan was altijd bereid zijn grote deskundigheid op het gebied van de HPLC-analyse te delen. Daarnaast zorgde hij samen met de heer Jan Janssen voor het in topconditie houden van de soms zeer humeurige apparatuur.

Mijn dank gaat tevens uit naar dr. C.H. van Os en zijn medewerkers (afdeling fysiologie), die mij op gastvrije wijze de grondbeginselen van de "vesicologie" hebben bijgebracht.

De medewerkers van het Centraal Dierenlaboratorium, de heren G. Grutters, H. Eikholt en A.M. Peters, verleenden vakkundige assistentie bij het uitvoeren van de in-vivo experimenten en verzorgden de proefdieren. De heren Th. Arts, F. Philipsen en T. Peters, medewerkers van de operatiekamer, zorgden steeds voor een optimale coördinatie bij het beschikbaar komen van hondenieren. In dat verband dient ook de goede samenwerking vermeld te worden met de afdeling kaakchirurgie en in een later stadium met de heer F. Hess en mw. S. Steeghs van de afdeling cyto-histologie.

De tekeningen van hoofdstuk 1, 2 en 3 werden vervaardigd door de medewerkers van de medische tekenkamer. Samen met de vele computertekeningen werden deze op vakkundige wijze op foto en dia gezet door de medewerkers van de afdeling medische fotografie.

Mw. drs. S. Bakker en haar medewerkers (medische bibliotheek) stonden altijd klaar voor het verlenen van hulp bij het doorzoeken en verzamelen van literatuur.

Collega, maar bovenal goede vriend, drs. Arjen Geerts ben ik veel dank verschuldigd voor het kritisch doorlezen van de uiteindelijke versie van het proefschrift en de nauwgezette typografische controle.

Tot slot wil ik graag mijn diepe erkentelijkheid betuigen aan mijn ouders en aan Eeke Faber.

Mijn ouders hebben mij altijd aangemoedigd in de dingen die ik deed, maar zij hebben mij vooral ook geleerd om door te zetten, een eigenschap die van onschatbare waarde is gebleken.

Eeke dank ik voor haar nimmer aflatende liefdevolle ondersteuning, waaruit ik veel kracht en wijsheid heb kunnen putten.

Aan hen draag ik dan ook dit proefschrift op.

CURRICULUM VITAE

Frans Russel werd geboren op 2 juli 1957 te Tegelen. Van 1969-1972 bezocht hij het St. Thomascollege te Venlo en vanaf 1972 het Boschveldcollege te Venray, waar hij in 1975 het diploma VWO-B behaalde. In hetzelfde jaar begon hij met de studie Farmacie aan de Rijksuniversiteit Groningen. Het doctoraalexamen werd in januari 1982 afgelegd met als differentiatierichting farmacologie. In het kader daarvan werd onder leiding van Prof. Dr. D.K.F. Meijer (Afd. Farmacologie en Farmacotherapie) onderzoek verricht naar het levertransport van asialoglycoproteïnen. In de zomermaanden van 1979 en 1980 was hij werkzaam bij de Stichting Ziekenhuisapothek en Klinisch Laboratorium te Venray, waar hij onder leiding van Drs. J.B.G.M. Noten (ziekenhuisapotheker) onderzoek deed naar de bioanalyse en farmacokinetiek van enkele neuroleptica. Van 1980-1981 was hij student-assistent van Prof. Dr. D.A. Doornbos bij de afdeling Farmaceutische en Analytische Chemie van de subfaculteit Farmacie te Groningen. In maart 1983 werd het apothekersexamen afgelegd.

Van april 1983 tot augustus 1986 werkte hij als wetenschappelijk assistent, in dienst van FUNGO(nu MEDIGON)-ZWO, op het Farmacologisch Instituut van de Katholieke Universiteit Nijmegen, waar hij onder leiding van Prof. Dr. C.A.M. van Ginneken een onderzoek startte naar het transport van geneesmiddelen in de nier. De belangrijkste resultaten daarvan zijn beschreven in dit proefschrift. Tijdens deze periode behaalde hij in mei 1984 het diploma Stralingsdeskundige Niveau III. In augustus 1986 trad hij in dienst van de K.U. Nijmegen en verrichtte hij verder onderzoek naar de lotgevallen en effecten van geneesmiddelen in relatie tot de nier. Daarnaast is hij sedert april 1986 als docent farmacologie verbonden aan de Opleiding tot Mondhygienist te Nijmegen. Per 1 januari 1988 is hij aangesteld als universitair docent farmacologie.

- Russel FGM, Weitering JG, Oosting R, Groothuis GMM, Hardonk MJ, Meijer DKF. Influence of taurocholate on hepatic clearance and biliary excretion of asialo intestinal alkaline phosphatase in the rat in vivo and in isolated perfused rat liver. *Gastroenterology* 1983;85:225-34.
- Van Ginneken CAM, Russel FGM. Carrier-mediated transport in the renal handling of drugs. In: *Topics in Pharmaceutical Sciences* (eds. D.D. Breimer and P. Speiser), Elsevier, Amsterdam 1983:155-65.
- Wouterse AC, Russel FGM, Grutters GJ, Van Ginneken CAM. Kwantitatieve urinemonstering bij renale klaringstudies in de hond. *Biotechniek* 1984;6:86-8.
- Hekman P, Russel FGM, Van Ginneken CAM. Renal transport of the glucuronides of paracetamol and p-nitrophenol in the dog. *Drug Metab Dispos* 1986;14:370-1.
- Lentjes EWGM, Russel FGM, Van Ginneken CAM. Renal clearance of sulfinpyrazone in man. *Eur. J. Clin. Pharmacol.* 1986;31:473-8.
- Russel FGM, Wouterse AC, Hekman P, Grutters GJ, Van Ginneken CAM. Quantitative urine collection in renal clearance studies in the dog. *J Pharmacol Methods* 1987;17:125-36.
- Russel FGM, Wouterse AC, Van Ginneken CAM. Physiologically based kidney model for the renal clearance of phenolsulfonphthalein and the interaction with probenecid and salicyluric acid in the dog. *J Pharmacokinet Biopharm* 1987;15:349-68.
- Russel FGM, Wouterse AC, Van Ginneken CAM. Physiologically based kidney model for the renal clearance of salicyluric acid and the interaction with phenolsulfonphthalein in the dog. *Drug Metab Dispos* 1987;15:695-701.
- Russel FGM, Wouterse AC, Van Ginneken CAM. Physiologically based kidney model for the renal clearance of iodopyracet and the interaction with probenecid in the dog. *Biopharm Drug Dispos* in press.
- Russel FGM, Van der Linden PEM, Vermeulen WG, Heijn M, Van Os CH, Van Ginneken CAM. Na^+ and H^+ gradient-dependent transport of p-aminohippurate in membrane vesicles from dog kidney cortex. *Biochem Pharmacol* submitted.

- Russel FGM, Heijn M, Van Ginneken CAM. Effect of substituted benzoates on p-aminohippurate transport in dog renal membrane vesicles. *Biochem Pharmacol* submitted.
- Russel FGM, Vermeulen WG, Van Ginneken CAM. Effect of substituted benzoylglycines (hippurates) and phenylacetylglycines on p-aminohippurate transport in dog renal membrane vesicles. *Biochem Pharmacol* submitted.
- Russel FGM, Wouterse AC, Van Ginneken CAM. Renal clearance of substituted hippurates in the dog. I. Benzoylglycine (hippurate) and methyl-substituted benzoylglycines. *J Pharmacol Exp Ther* submitted.
- Russel FGM, Wouterse AC, Van Ginneken CAM. Renal clearance of substituted hippurates in the dog. II. 4-Aminobenzoylglycine and hydroxy-substituted benzoylglycines. *J Pharmacol Exp Ther* submitted.
- Russel FGM, Wouterse AC, Van Ginneken CAM. Renal clearance of substituted hippurates in the dog. III. Methoxy-substituted benzoylglycines. *J Pharmacol Exp Ther* submitted.
- Russel FGM, Wouterse AC, Van Ginneken CAM. Renal transport of 1-naphthyl-glucuronide and phenolphthalein-glucuronide in the dog. In preparation.

De volgende abstracts zijn het resultaat van bijdragen aan diverse wetenschappelijke congressen:

- Russel FGM, Van der Heiden H, Hardonk MJ, Meijer DKF. The influence of taurocholate and the protease inhibitor leupeptin on the hepatic disposition of the glycoprotein asialo-alkaline phosphatase. *Proc 24th Dutch Fed, Leiden* 1983:346.
- Russel FGM, Wouterse AC, Van Ginneken CAM. Supporting evidence for drug retention in the renal tubular system by pharmacokinetic analysis of plasma and urine data. *Proc 25th Dutch Fed, Rotterdam* 1984:349.
- Russel FGM, Wouterse AC, Van Ginneken CAM. Renal tubular drug retention. *Pharm Weekbl Sci Ed* 1984;6:174.
- Russel FGM, Wouterse AC, Van Ginneken CAM. Renal clearance mechanisms of substituted hippurates. *Proc 26th Dutch Fed, Amsterdam* 1985:293.

- Russel FGM, Wouterse AC, Van Ginneken CAM. Renal handling of hippurate and methyl-substituted hippurates in the dog. *Naunyn-Schmiedeberg's Arch Pharmacol* 1985;330:R32.
- Russel FGM, Van der Linden PEM, Vermeulen WG, Van Ginneken CAM. Isolation and organic anion transport properties of membrane vesicles from dog renal cortex. *Pharm Weekbl Sci Ed* 1985;7:234.
- Vermeulen WG, Russel FGM, Van Ginneken CAM. Effect of substituted glycineconjugates on p-aminohippurate uptake into renal membrane vesicles from dog kidney cortex. *Proc 27th Dutch Fed, Groningen* 1986:418.
- Russel FGM, Van der Linden PEM, Vermeulen WG, Van Ginneken CAM. Mechanisms of p-aminohippurate uptake in isolated membrane vesicles from the dog kidney. *Br J Pharmacol* 1986;89:513P.
- Heijn M, Russel FGM, Van Ginneken CAM. Effect of substituted benzoates on the organic anion transport system in isolated dog kidney membrane vesicles. *Br J Pharmacol* 1986;89:681P.
- Russel FGM, Wouterse AC, Van Ginneken CAM. Renal excretion of glucuronide drug conjugates in the dog. *Acta Pharmacol Toxicol* 1986;59(V):125.
- Russel FGM, Wouterse AC, Van Ginneken CAM. Physiologically based modeling of renal drug clearance. *Proc 28th Dutch Fed, Nijmegen* 1987:414.
- Russel FGM, Wouterse AC, Van Ginneken CAM. Physiologically based modeling of renal tubular drug secretion. *Proc 47th FIP Congress, Amsterdam* 1987:221.

STELLINGEN

- 1 Een ondernemende universiteit verwordt tot een universitaire onderneming wanneer een te groot deel van haar onderzoek gebonden is
- 2 De lagere renale-excretiesnelheid van salicylzuur ten opzichte van die van p-aminohippuurzuur bij hoge plasmaconcentraties is primair het gevolg van een lager tubulair-transportmaximum en niet van passieve terugdiffusie van salicylzuur

Knoefel PK et al , Am J Physiol 1962 203 6-10

Dit proefschrift

- 3 Het is niet aannemelijk dat het effect van kalium op de potentiaalgevoeligheid van het natrium-gekoppelde glutamaattransport in basolaterale membraanvesicles van proximale tubuluscellen ook van toepassing is op het natrium-gekoppelde p-aminohippuurzuurtransport in deze vesicles

Pritchard JB, Biochim Biophys Acta 1987, 906 295-308

Dit proefschrift

- 4 Watari et al gaan er in hun berekeningen ten onrechte van uit dat de tubulaire secretie van nitrofurantoin afhankelijk is van de vrije plasmaconcentratie, aangezien hun resultaten duidelijk laten zien dat de renale klaring van nitrofurantoin bij lage plasmaconcentraties, ondanks de hoge eiwitbinding, vrijwel gelijk is aan de renale plasmaflow

Watari N et al , J Pharm Sci 1985 74 165-170

- 5 De renale klaring van een metaboliet kan niet eenduidig worden vastgesteld wanneer ook de moederverbinding in het plasma aanwezig is
- 6 Bij de interpretatie van het effect van probenecide op het transport van organische anionen dient rekening gehouden te worden met een mogelijk effect op het metabolisme van deze anionen

7. De gemiddelde verblijftijd (mean residence time) is niet altijd een modelonafhankelijke parameter.
8. De verdeling van het vak farmacologie over verschillende grote onderwijsblokken van het curriculum geneeskunde, zoals het geval is aan de Katholieke Universiteit Nijmegen, leidt tot een fragmentarische kennis van de farmacologie en is derhalve geen goede voorbereiding op een van de meest voorkomende en ingrijpende medische handelingen van de arts: het voorschrijven van geneesmiddelen.
9. In het nieuwe functionele budgetteringsstelsel voor ziekenhuizen wordt een fusie tussen een basisziekenhuis en een centrumziekenhuis budgettair aantrekkelijk.
10. Het verdient aanbeveling dat apothekers de bevoegdheid krijgen om een goedkoper identiek en gelijkwaardig geneesmiddel af te leveren indien de arts een node-loos duur geneesmiddel heeft voorgeschreven, tenzij de arts uitdrukkelijk op het recept heeft aangegeven dat alleen het voorgeschreven middel mag worden afgeleverd.
11. De in de nieuwe promotieregeling van de Katholieke Universiteit Nijmegen voorgeschreven tekst op het titelblad van het proefschrift: "een wetenschappelijke proeve op het gebied van", gevolgd door de facultaire indeling, suggereert ten onrechte dat het onderhavige proefschrift geen volwaardig wetenschappelijk werkstuk is en is onduidelijk ten aanzien van het vakgebied waarop het werk betrekking heeft. Deze tekst kan dan ook beter vervallen.
12. De opmerkelijke belangstelling van veel apothekers voor de gastronomie is waarschijnlijk bepaald door het grote aantal "kookboek"-practica die zij tijdens de studie genoten hebben.
13. De aantrekkelijkheid van het toptennis als kijkspeel kan beter worden verhoogd door de lengte van het servicevak te verkleinen dan door de nethoogte te vergroten.

Hoogendoorn D, Ned Tijdschr Geneesk 1986; 130: 2343-4.

Russel FGM, Ned Tijdschr Geneesk 1987; 131: 332.

14. Indien presentator Hans Zoet in het radioprogramma "Für Elise" het jonge muzikale talent wat minder plagerig tegemoet zou treden, zou hij er verstoeld van staan hoeveel jong talent er in werkelijkheid in Nederland is.
15. De stelligheid waarmee sommige stellingen bij promoties worden geponeerd, doet afbreuk aan het academische karakter van deze plechtigheid.

Frans G.M. Russel

Nijmegen, 15 januari 1988.

1